Issue no. 3/2006
RSNA Edition

MAGNETOM FLASH

www.siemens.com/magnetom-world
Price 10 Euro

Content

34

SIEMENS
medical

Dear MAGNETOM User,

Continuous table move holds the potential to replace the step-by-step moving table applications of MR in the same way that spiral CT systems have replaced other CT applications. Key advantages of continuous table move include:

- Better image quality, especially in the whole abdomen and peripheral angiography, since the slice of interest is always at the center of the magnet.
- Faster workflow since exams are now continuous. For example peripheral MR Angiography exams from the aortic arch to the feet are in done one continuous step.

In the special edition of the MAGNETOM Flash enclosed with this issue we are very excited to share with you the first clinical results of *syngo* TimCT (Continuous Table move) from the Universities of Freiburg and Essen. These articles describe the advantages of this promising technology in detail and look at some of the possible future applications.

In this issue of MAGNETOM Flash we also present another analogy between CT and MR. Siemens set the trend as the first company to combine CT and PET. And now we are the first company to combine MR and PET. Starting on page 21 you can see the first ever in-vivo images simultaneously acquired by MR and PET. On page 92 we also showcase *syngo* TWIST, which enables 4D MR Angiography, obtaining multiple arterial and venous phases in one scan and providing robust bilateral MRA. With *syngo* TWIST MRA has reached another level towards becoming the golden diagnostic standard.

Other new *syngo* applications powered by Tim are also finding great acceptance among our customers. On page 11 you will find impressive images with *syngo* SWI and *syngo* SPACE from St. Vincent's Hospital in Melbourne, Australia. And *syngo* REVEAL, with its clarity in diagnosing malignant lesions even in extremely difficult anatomical areas like the neck showing parathyroid carcinoma, is a promising sequence. There are also excellent contributions on *syngo* applications from many other sites.

Besides these stimulating articles, you will find a questionnaire in this MAGNETOM Flash. In order to even further align our customer magazine with your requirements we would very much appreciate if you would kindly take the time to give us feedback.

Thank you very much in advance and we hope that you will enjoy reading the Flash.

Ali-Nejat Bengi

Antje Hellwich

The Editorial Team

We appreciate your comments.
Please contact us at magnetomworld.med@siemens.com

A. Nejat Bengi, M.D.
Editor in Chief

Antje Hellwich
Associate Editor

Dagmar Thomsik-Schröpfer, Ph.D.
MR Marketing-Products, Erlangen

Cécile Mohr, Ph.D
Head of Market Segment Management, Erlangen

Heike Weh,
Clinical Data Manager,
Erlangen

Bernhard Baden,
Clinical Data Manager,
Erlangen

Peter Kreisler, Ph.D.
Collaborations & Applications,
Erlangen

Milind Dhamankar, M.D.
Manager Clinical MR
Research Collaborations, USA

Lisa Reid,
US Installed Base Manager,
Malvern, PA, USA

Gary R. McNeal, MS (BME)
Advanced Application Specialist,
Cardiovascular MR Imaging
Siemens Medical Solutions USA

Dr. Sunil Kumar S.L. Manager
Applications MRI, Siemens
Medical Solutions, India

Tony Enright, Ph.D.
Asia Pacific Collaborations,
Australia

T-class: Get Ready for a New Kind of Workflow. ***Page 6***

BrainPET: The Next Wave in the Evolution of Medical Imaging. ***Page 20***

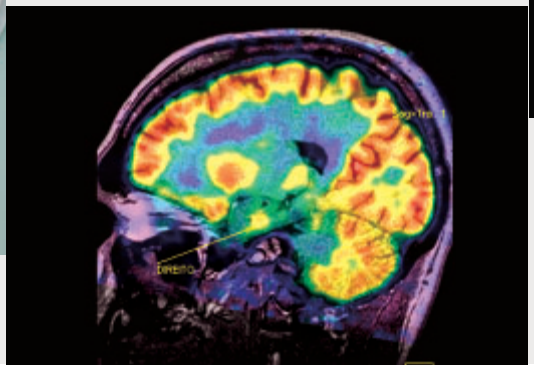

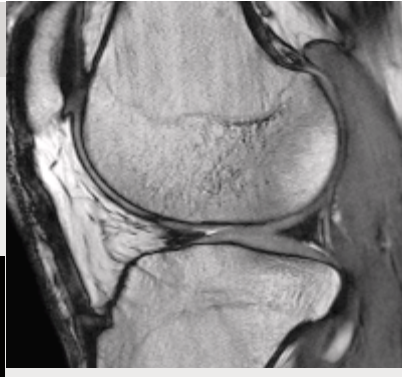

MAGNETOM C!: News with syngo MR A30. ***Page 26***

PRODUCT NEWS

CLINICAL

Pediatric Abdominal MRI in Oncology. ***Page 72***

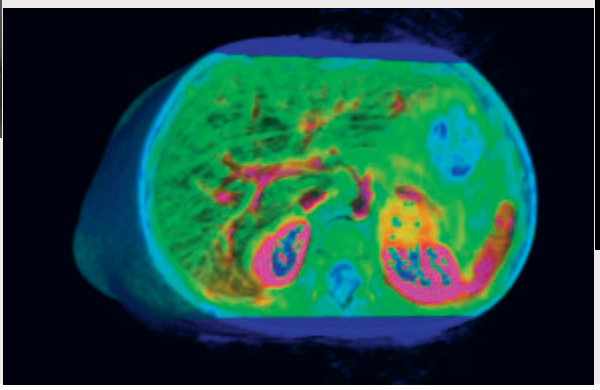

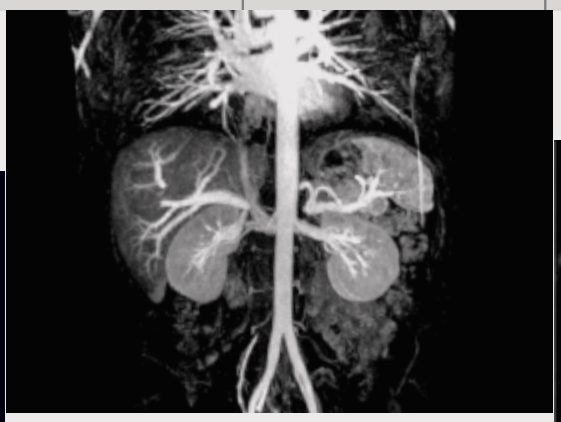

Cardiovascular Whole-Body MRI. ***Page 80***

Coronary MRA at 3T. ***Page 85***

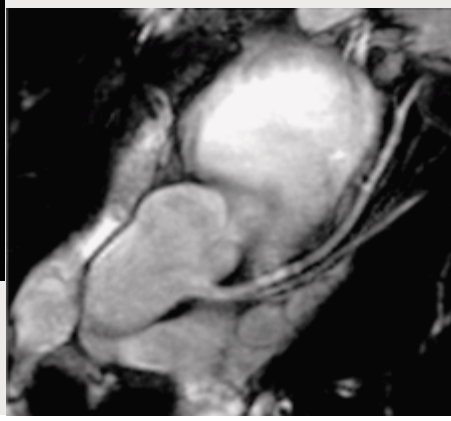

LIFE

T-class
Get Ready for a New Kind of Workflow

Trendsetting applications and trendsetting workflow at and beyond the scanner. The new generation of Tim (Total imaging matrix) systems with T-class allows you to optimize workflow from order entry to billing.

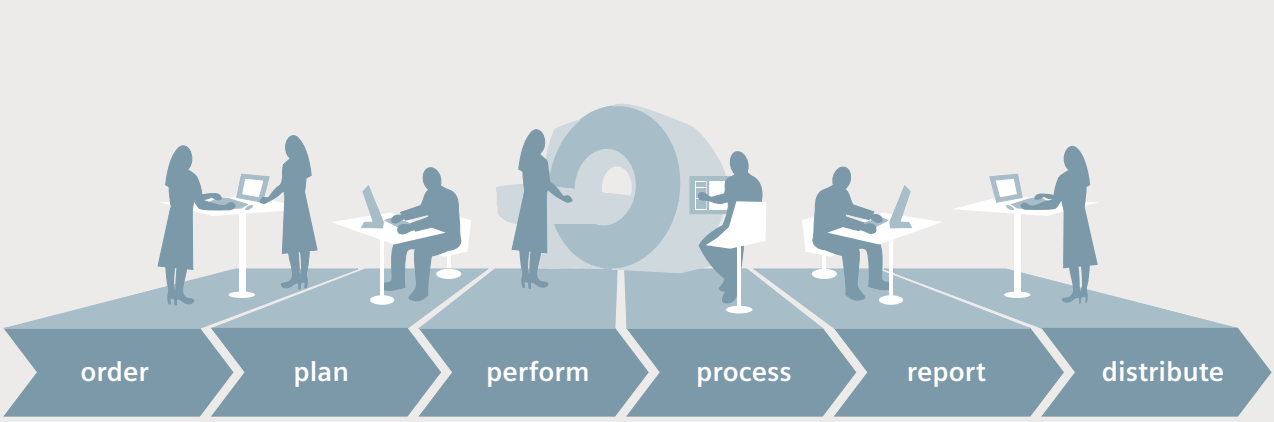

T-class

New Workflow Features

- *syngo* Chorus MR: Integration with a Siemens Radiology Information System (RIS)
  - Protocol Planning
  - Protocol Distribution
  - Inline Follow-up
  - Inline Billing
- AutoAlign Spine
- PhoenixZIP
- Tim Workflow Suite: easier handling
- 3DTaskCard-Study splitting

syngo TimCT (Continuous Table move)

- *syngo* TimCT FastView
- *syngo* TimCT Angiography

New Hardware

- New computer architecture: 64 bit host computer
- 32-channel head coil (3T): higher resolution and higher PAT factors
- 32-channel body coil (1.5T and 3T): High-resolution function in real time and a full cardiac exam in just a few breath-holds.

New Imaging Features

- *syngo* TWIST
- *syngo* DTI-Tractography
- SPAIR: optimal fat saturation
- Advanced Cardiac: coronary improvements
- *syngo* GRACE: breast single voxel spectroscopy
- 32-channel protocols

New Workflow Features

For seamless workflow at your scanner

Tim Workflow Suite

■ **Inline Composing and Inline Filter and Diffusion**

T-class further expands the Inline Technology on your scanner. Whole spine or whole body data acquired in a multi-step scan are combined instantaneously to a seamless image. Immediate calculation of ADC maps is included as is the choice to filter images in no time.

■ **Tim Planning Suite**

Extended Field of View (FoV) scan preparation made efficient and easy. The Tim Planning Suite supports the preparation of MR Angiography or body imaging over several stations in one session with the Set-n-Go protocols. Fully supports scan@center and Phoenix.

***syngo* TimCT (Continuous Table move)**

■ ***syngo* TimCT FastView**

Localizer scans in a single continuous move. Scans the whole body within 40 seconds.

■ ***syngo* TimCT Angiography (optional)**

Easy to set-up, easy to perform. MR Angiography from the aortic arch down to the feet in a single continuous move.

AutoAlign Spine

(optional Workflow feature at the scanner)

Immediate automatic slice positioning to the intervertebral discs. Time saving due to automatic alignment to the vertebral disc space in multiple dimensions.

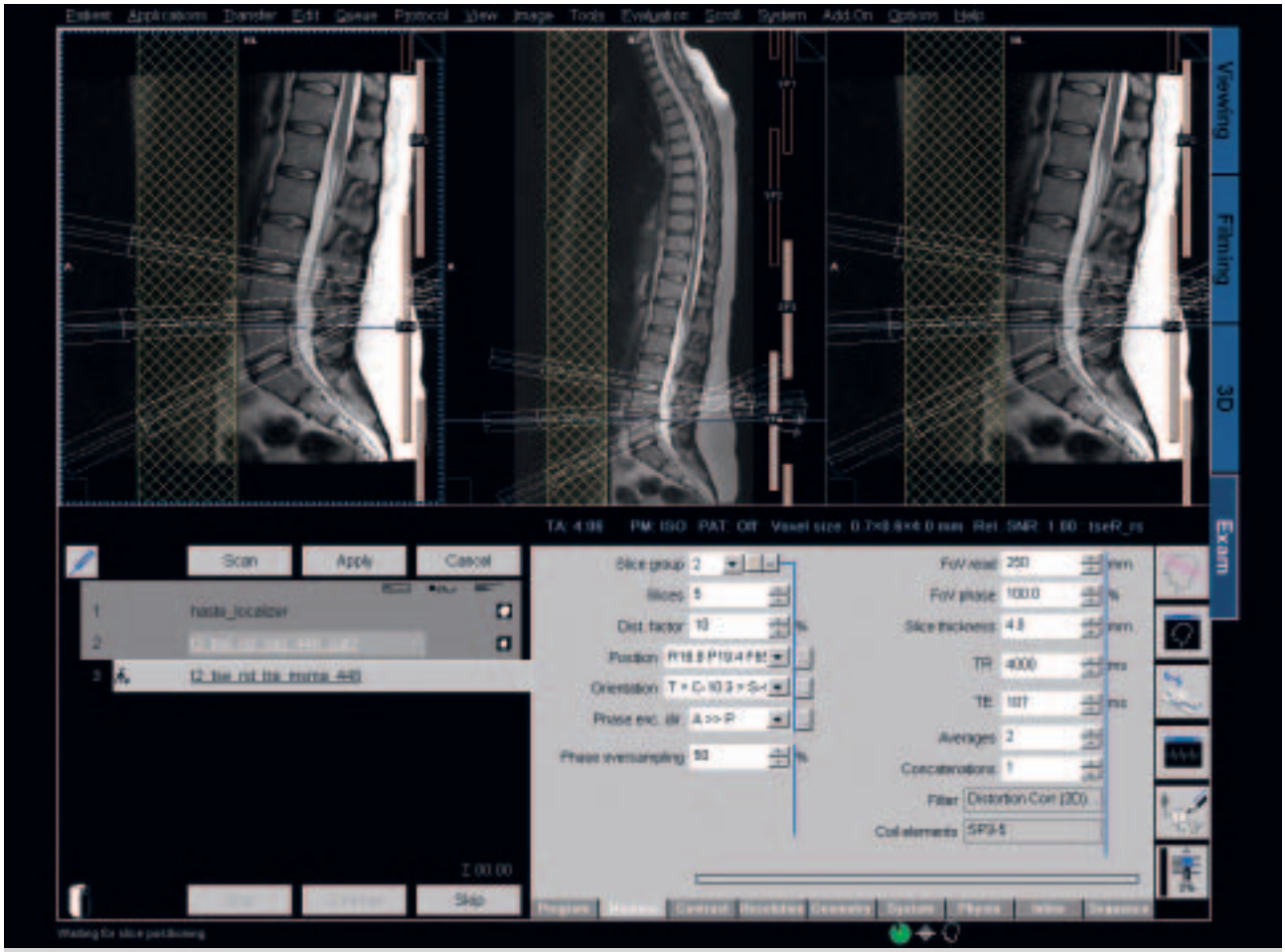

[Figure 1] *AutoAlign Spine: MAGNETOM Avanto.*

PhoenixZIP
PhoenixZIP contains the entire information of an examination and allows direct transfer from the scanner to e.g. a USB stick. PhoenixZIP supports fast and easy protocol sharing.

DICOM Study Split
Separates images according to the different requests.

***syngo* Chorus MR**
For seamless workflow beyond the scanner: *syngo* Chorus MR integrates your scanner with the Siemens Radiology Information System (RIS):

■ **Protocol Distribution**
provides 1-click standardization of protocols on all MR scanners directly from the RIS.

■ **Protocol Planning**
Using Protocol Planning of *syngo* Chorus MR, the radiologist plans the exam in seconds directly in the RIS.

■ **Inline Follow-up**
Using Inline Follow-up of *syngo* Chorus MR, the exact protocol of the previous exam is retrieved. In a matter of seconds it is clear if the previous exam can be run as is or needs changing. The exact protocol is sent to the MRI suite.

■ **Inline Billing / MPPS**
(Modality Performed Procedure Steps)
Inline Billing of *syngo* Chorus MR ensures, with one mouse click and no manual entry, that relevant information is sent for billing purposes.

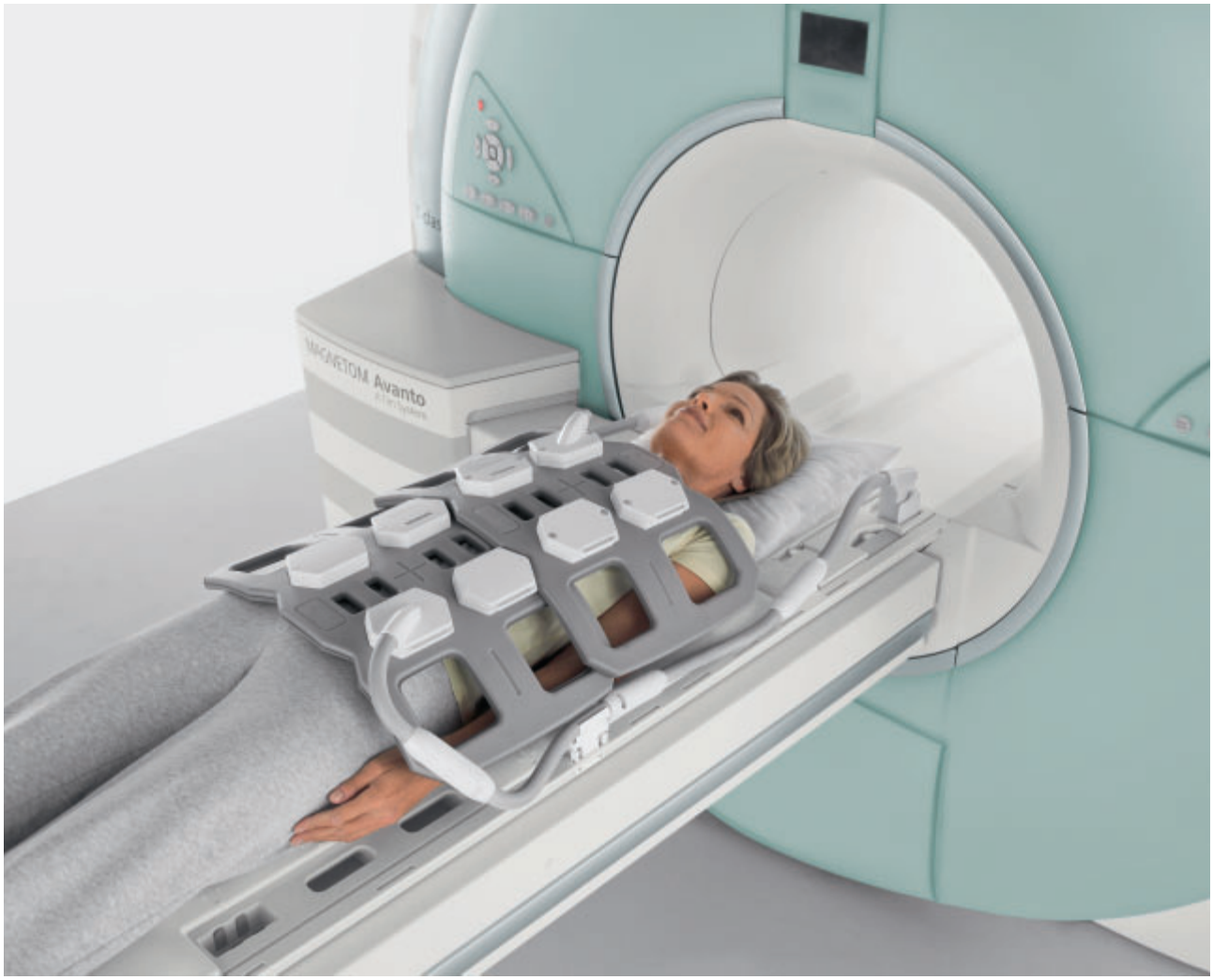

New Applications

DTI-Tractography
Diffusion Tensor Imaging – Tractography allows the visualization of the major white matter tracts of the brain as 3D objects in the context of an anatomical 3D dataset and functional MRI results. This supports e.g. the planning of neuro surgical procedures in brain tumor patients or neuro physiological research.

Improvements in whole-heart coronary MRA
Improved RF-pulses for T2 preparation with less sensitivity to RF field inhomogeneities allow better suppression of myocardial tissue and better delineation of coronary vessels.

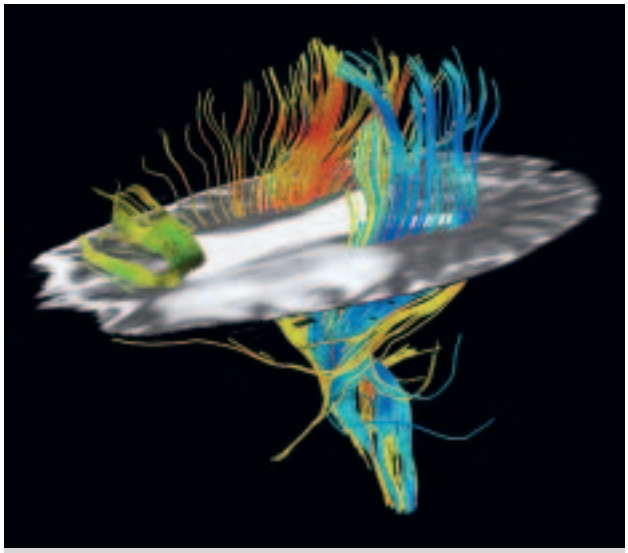

[Figure 2] *DTI Tractography: MAGNETOM Avanto.*

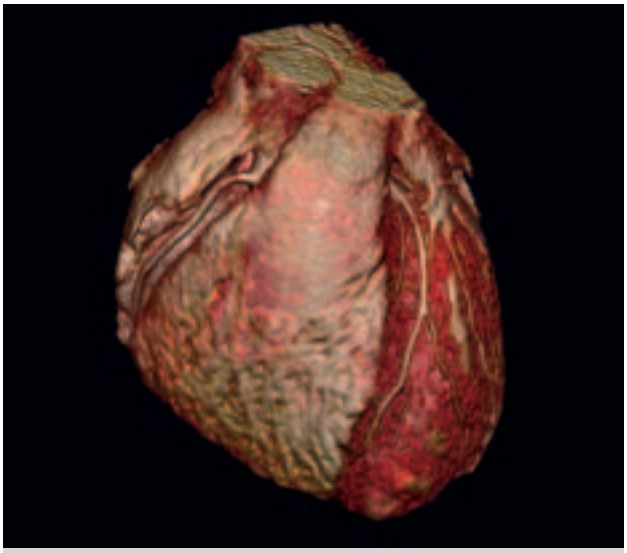

[Figure 3] *Whole-heart coronary MR Angiography: MAGNETOM Avanto*

32-channel protocols
The new protocols support the 32-channel head and -body coils and allow the usage of higher PAT factors.

***syngo* TWIST**
syngo TWIST is our new application powered by Tim: It provides time-resolved MR Angiography in all body regions with small amounts of contrast agent and can be used with iPAT (integrated Parallel Acquistion Techniques) in two directions.

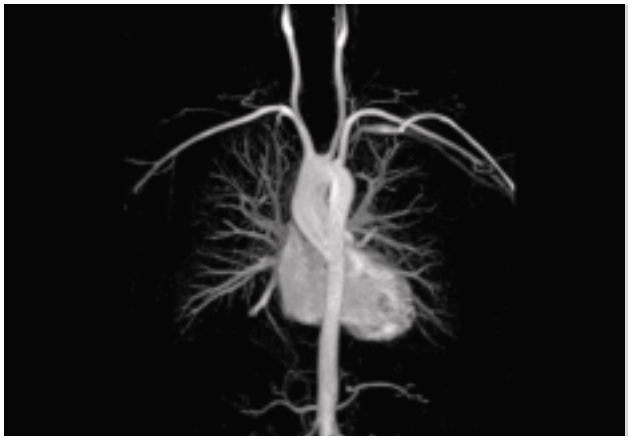

[Figure 4] *syngo TWIST: MAGNETOM Avanto. Angio thoracic, TWIST, 3D FLASH dynamic, maximum intensity projection (MIP), GRAPPA 2.*

TR	*2.8 ms*
TE	*1.1 ms*
TA	*6.42 sec*
eff. SL	*120 mm*
partitions	*72*
matrix	*384*
FoV	*400 mm*

Courtesy of University Hospital Essen, Germany

Software Version *syngo* MR B13 for Tim (Total imaging matrix) Systems

Bradley D. Bolster, Ph.D.; Kevin J. Johnson, BA RT (MR); Brian M. Dale, Ph.D.

Siemens Medical Solutions, Inc., USA

New Applications

***syngo* SWI**

To better visualize susceptibility differences between tissues, *syngo* MR B13 adds a new application known as "susceptibility-weighted imaging" or SWI. SWI is a high resolution, fully flow-compensated 3D sequence that utilizes signal phase information and minimum intensity projections to highlight areas such as hemorrhage and occult vascular disease in the brain.

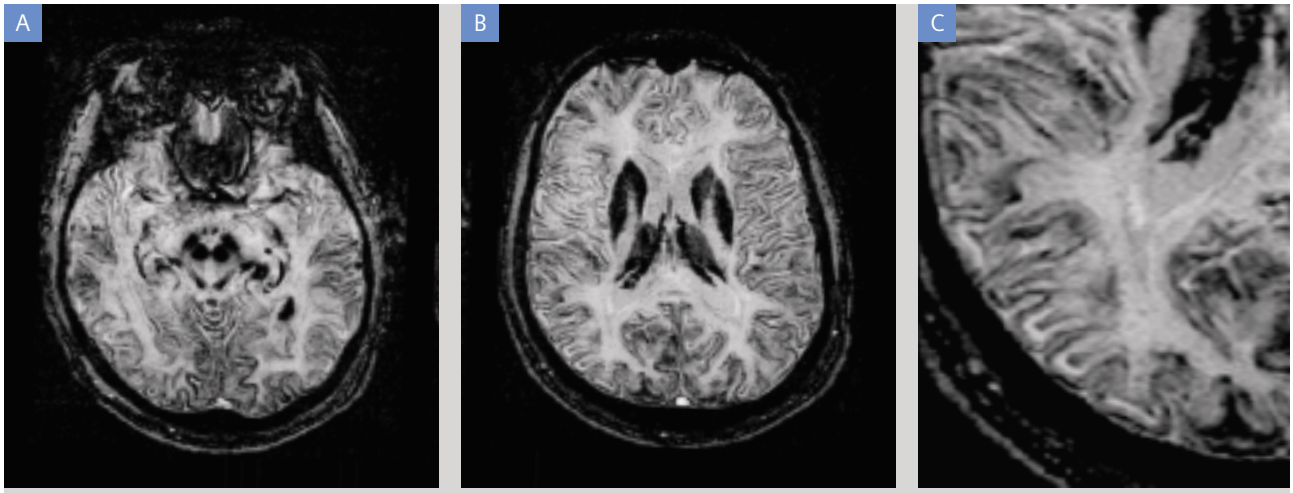

[Figure 1] *Aceruloplasminaemia: deposition of iron in grey matter: deep and cortical.*

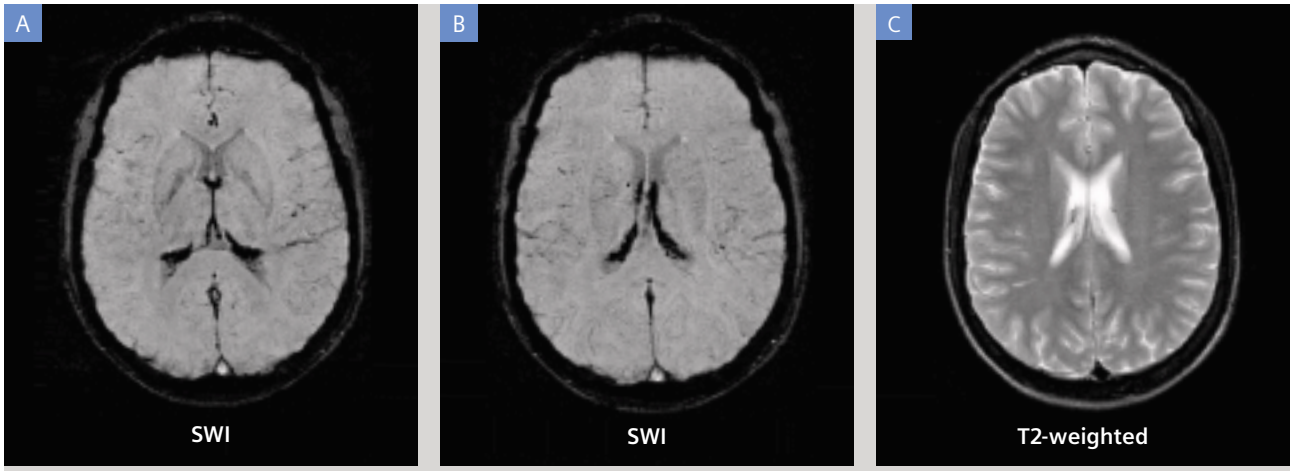

[Figure 2] *Thalassaemia: iron deposition in choroid plexus.*

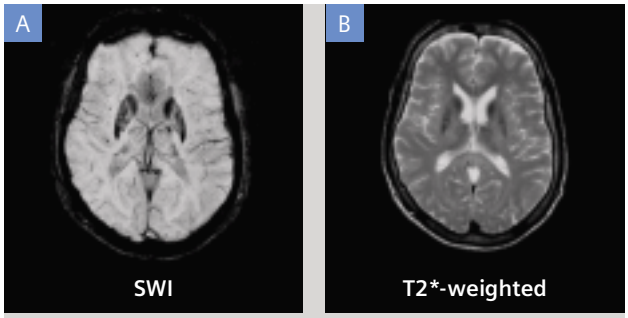

[Figure 3] *Wilson's disease: deposition of copper in deep grey matter.*

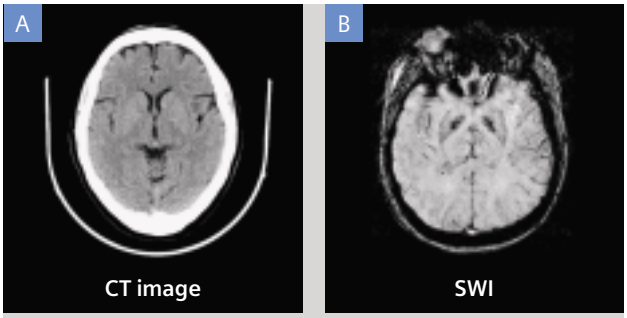

[Figure 4] *Globus pallidum calcification.*

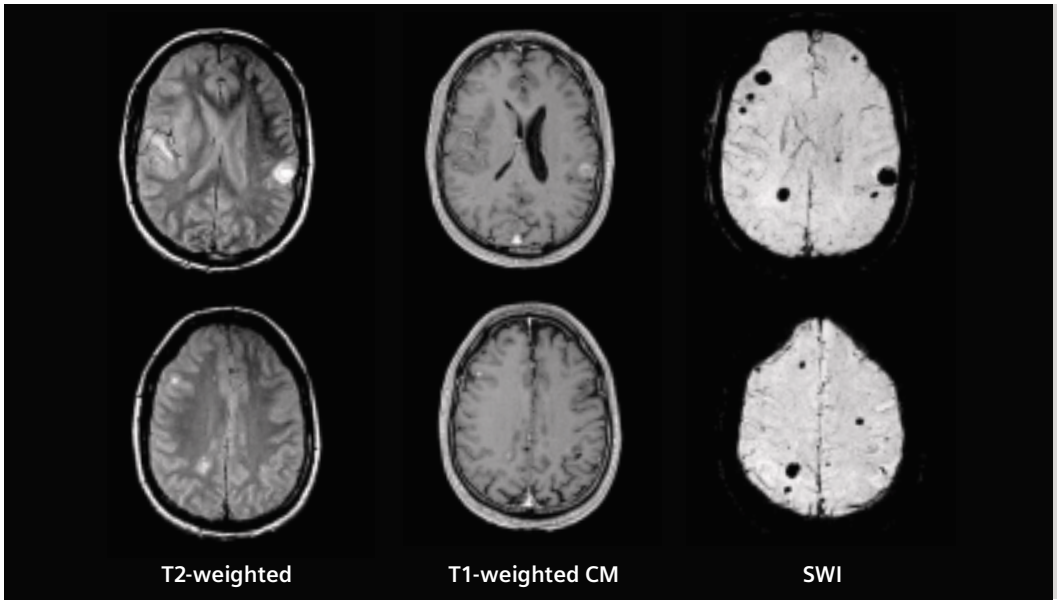

[Figure 5] *Metastatic melanoma.*

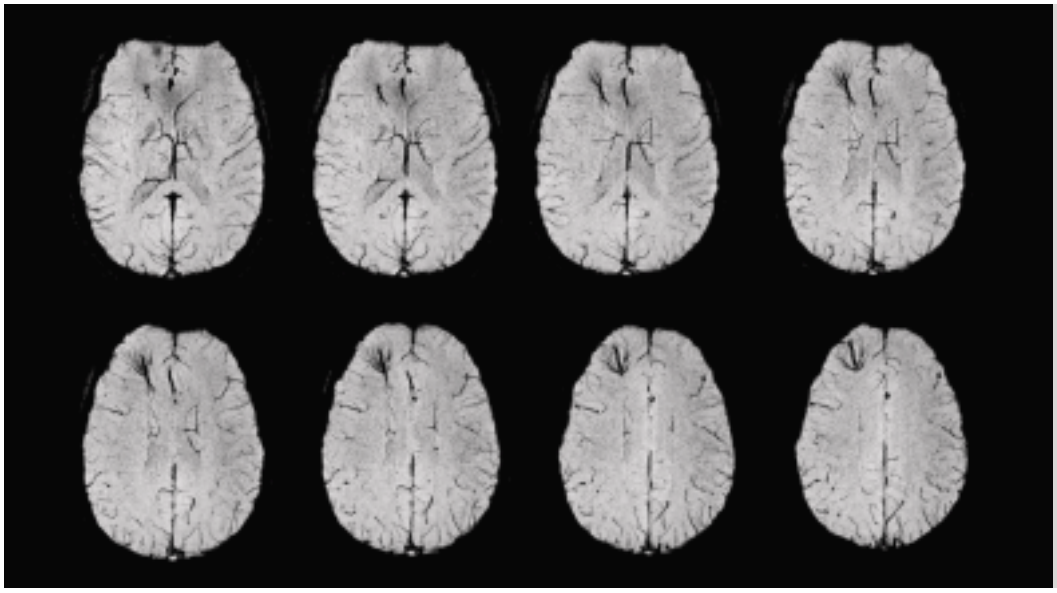

[Figure 6] *Developmental venous anomaly.*

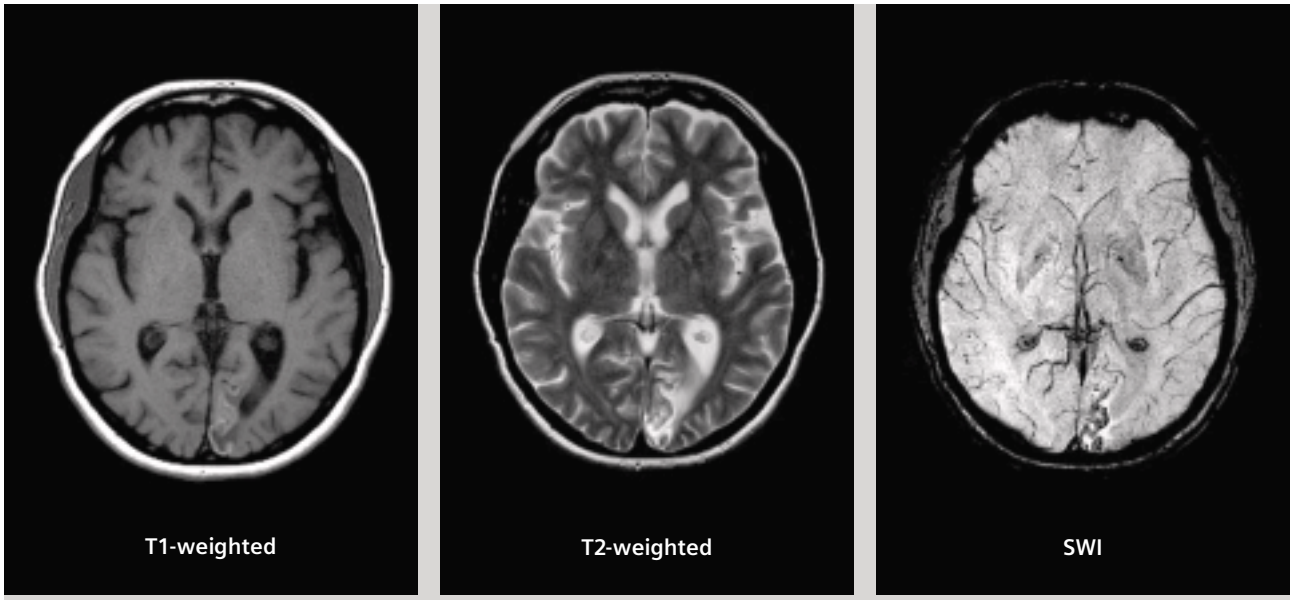

[Figure 7] *Subacute infarct: laminar necrosis and signal change due to free radicals.*

***syngo* SPACE**

syngo SPACE is a contrast-optimized variable flip angle Turbo Spin Echo (TSE) sequence, which can acquire isotropic high-resolution 3D T2-weighted images. Used together with PACE (Prospective Acquisition CorrEction) respiratory navigation, it is perfect for applications such as MRCP (MR Colangiopancreatography). The contrast optimization results in excellent background suppression, the respiratory navigators and high turbo factors reduce motion artifacts, and the high isotropic resolution yields exquisite maximum intensity projection (MIP) images.

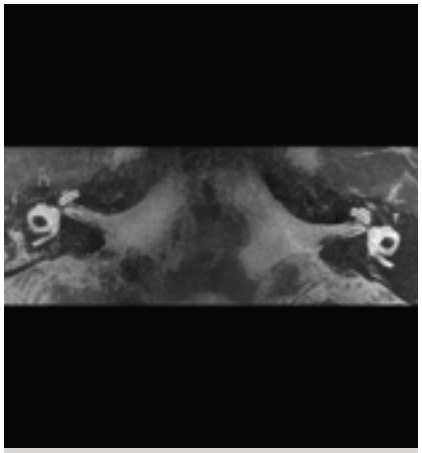

[Figure 8] *MAGNETOM Trio, A Tim System: Head, internal auditory canal (IAC), T2-weighted SPACE 3D, MIP, transversal. TR 1600 ms, TE 156 ms, TA 8:07 min, eff. SL 0.3 mm, partitions 60, matrix 768, FoV 130 mm.*

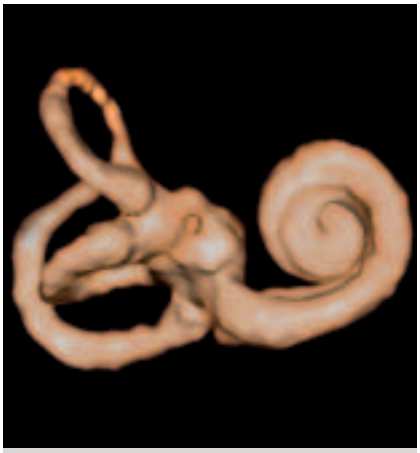

[Figure 9] *MAGNETOM Trio, A Tim System: Head, internal auditory canal (IAC), T2-weighted SPACE 3D, MIP, VRT coloured right, radial. TR 1600 ms, TE 156 ms, TA 8:07 min, eff. SL 0.3 mm, partitions 60, matrix 768, FoV 130 mm.*

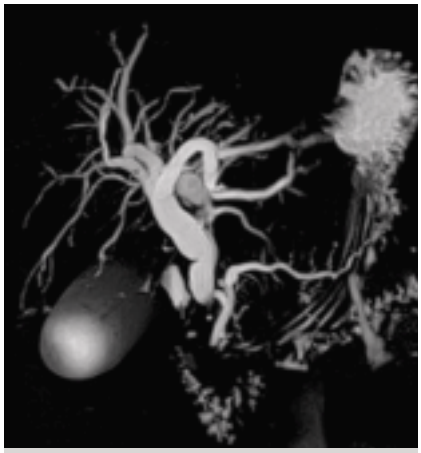

[Figure 10] *MR Colangiopancreatography (MRCP) data acquired using the SPACE sequence with PACE respiratory navigation. The image displayed is a maximum intensity projection (MIP) showing high resolution detail of the branching in the biliary system.*

Courtesy of St. Marien Hospital, Bonn, Germany

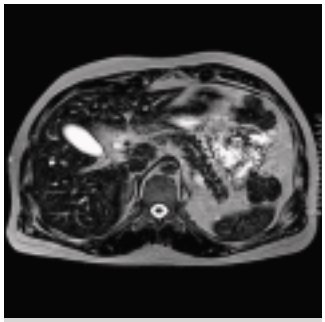

[Figure 11] *High resolution liver imaging with T2-weighted SPACE and PACE free breathing Matrix = 512/100%, 0.7 x 0.7 x 4 mm, TE = 386 ms.*

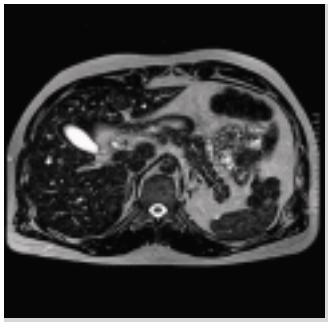

Matrix = 576/100%, 0.65 x 0.7 x SL = 2 mm!

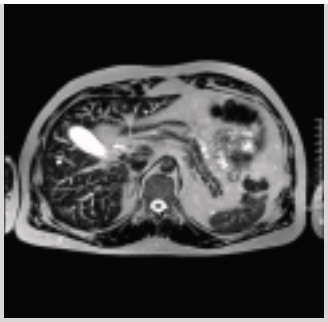

Thin-MIPs

[Figure 12] *High resolution pancreas imaging with T2-weighted SPACE and PACE free breathing.*

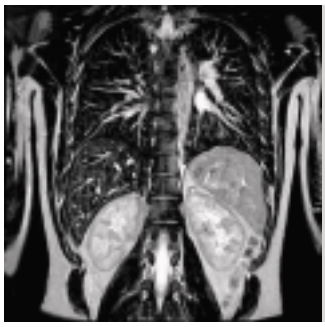

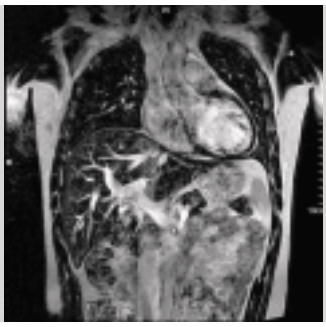

[Figure 13] *Extended field-of-view imaging covering the lung and upper abdomen with T2-weighted SPACE and PACE free breathing Matrix = 512/100%, 0.78 x 0.78 x 4 mm.*

***syngo* BLADE**

The *syngo* BLADE technique incorporates a radial acquisition scheme which oversamples the center of k-space. This additional k-space data is used for motion correction. The technique was initially targeted for pediatrics and uncooperative patients where motion is frequently an issue. Applicable in any imaging plane with several contrast options (T2-weighted, DarkFluid, etc.), the technique has "salvaged" many imaging exams in which motion rendered conventional techniques non-diagnostic.

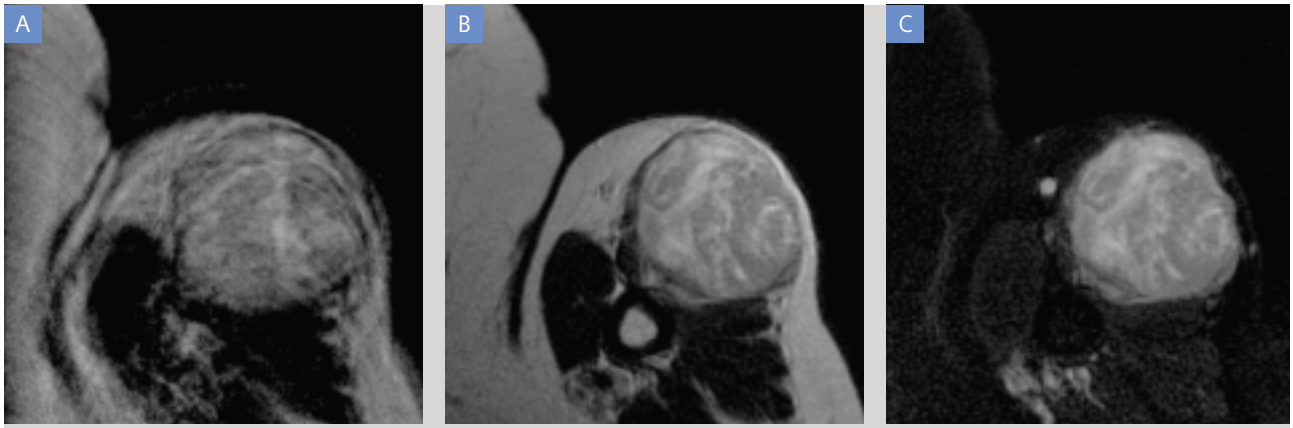

[Figure 14] *A 78-year-old woman with a mass on her upper arm. Immobilization of the arm caused respiratory motion to degrade image quality in conventional T2-weighted imaging (A). BLADE corrected for this motion (B) and also offered a FAT suppression solution (C).*

syngo BLADE can also be used in the body with PACE. Its inherent insensitivity to motion results in high-resolution motion-free body images. Furthermore, *syngo* BLADE is now compatible with iPAT (integrated Parallel Acquisition Technique), applying the power of Tim technology to this useful sequence.

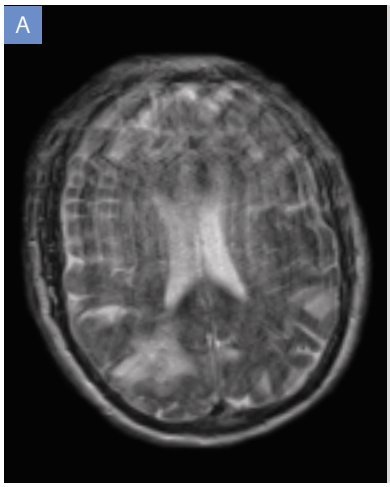

[Figure 15] *MAGNETOM Avanto: Head T2-weighted, TSE, tra, no motion correction. TR 4080 ms, TE 109 ms, TA 24.77 s, SL 5 mm, slices 19, matrix 512, FoV 230 mm.*

Courtesy of Foothills General Hospital, Calgary, Canada

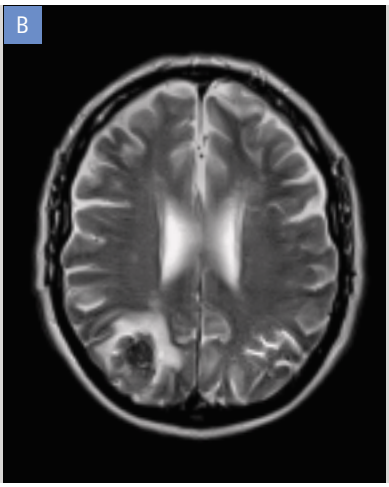

MAGNETOM Avanto: Head, T2-weighted TSE, tra, BLADE. TR 4500 ms, TE 99 ms, TA 1:58 min, SL 5 mm, slices 19, matrix 256, FoV 230 mm.

Courtesy of Foothills General Hospital, Calgary, Canada

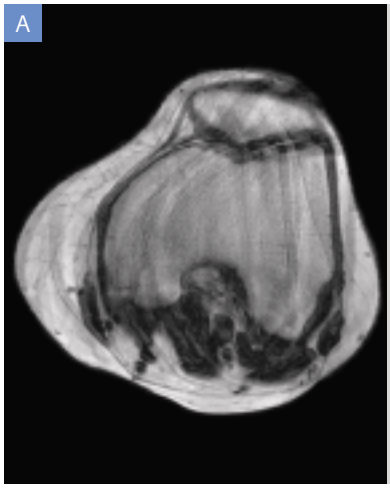

[Figure 16] *MAGNETOM Trio, A Tim System: Knee, T2-weighted TSE, transversal. TR 5000 ms, TE 120 ms, TA 50.42 s, SL 3 mm, slices 19, matrix 320, FoV 150 mm.*

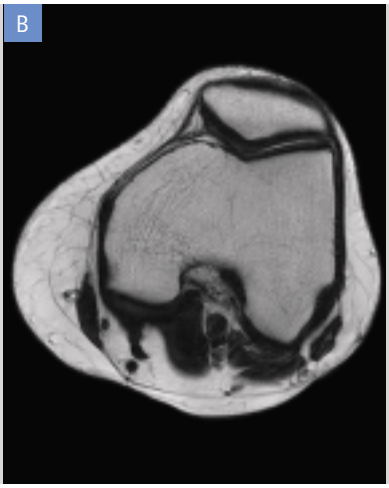

MAGNETOM Trio, A Tim System: Knee, T2-weighted TSE BLADE, transversal. TR 5000 ms, TE 118 ms, TA 1:15 min, SL 3 mm, slices 19, matrix 320, FoV 150 mm.

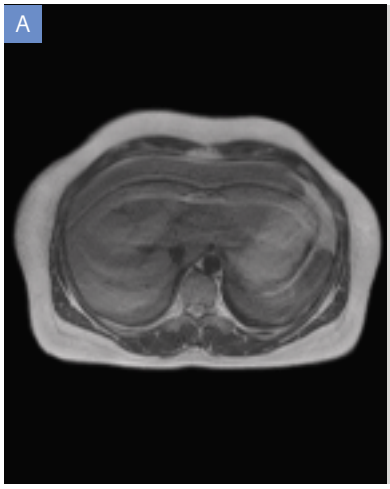

[Figure 17] *MAGNETOM Espree: Liver, T2-weighted TSE, without motion correction, GRAPPA 2. TR 3400 ms, TE 111 ms, TA 42 sec, SL 6 mm, slices 26, matrix 512, FoV 380 mm.*

Courtesy of Klinikum Bremen Mitte, Bremen, Germany

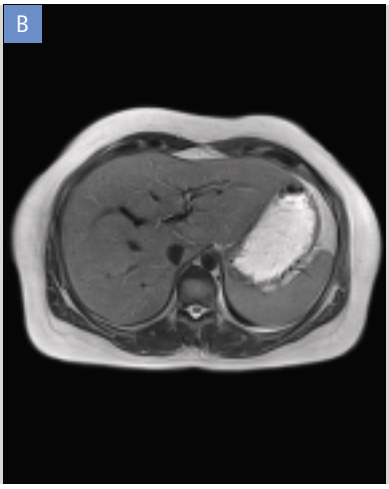

MAGNETOM Espree: Liver, T2-weighted TSE, with BLADE, GRAPPA 2. TR 6365.5 ms, TE 107 ms, TA 1:04 min, SL 5 mm, slices 19, matrix 320, FoV 400 mm.

Courtesy of Klinikum Bremen Mitte, Bremen, Germany

syngo REVEAL

syngo REVEAL brings diffusion-weighted imaging to the body. This contrast mechanism has been used in the brain and now shows tremendous potential for identifying and characterizing tumors in the body as well. The *syngo* REVEAL application, in particular, benefits from the scan@center feature in *syngo* MR B13. This ensures that the images are acquired in the most homogeneous region of the magnet and the most linear region of the gradients for the best possible diffusion results.

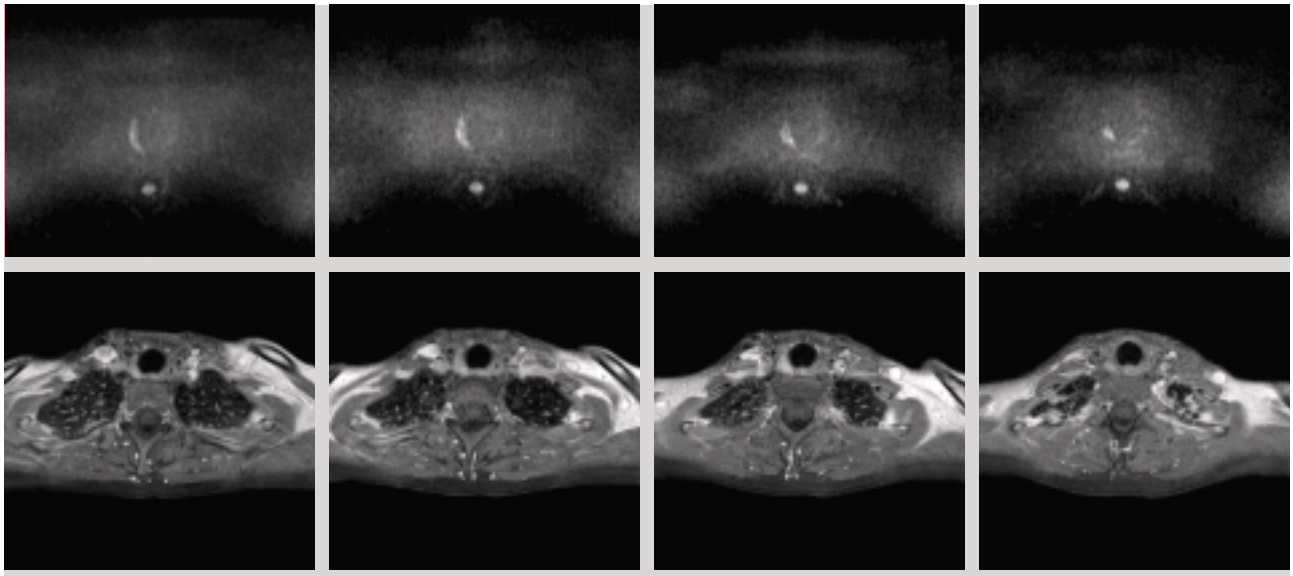

[Figure 18] *syngo REVEAL shows the parathyroid cancer (TI 185 ms, TR 11200 ms, TE 76 ms, TA 0.09 s (= 90 ms), GRAPPA 2, EPI, SL thickness 3 mm, FoV 200, Matrix 256.) The lower row shows the axial T1-weighted post-contrast images of the neck region.*

Courtesy of Kansai Denryoku Hospital, Osaka, Japan

syngo BEAT 3D

syngo BEAT 3D (Fig. 19) is a simple one stop tool to perform a complete cardiac exam. It incorporates 3D and 4D data acquisition, iPAT functionality and the flexibility to adapt the acquisition to the patient in order to rapidly collect data on cardiac morphology, perfusion and viability as well as to easily interrogate valvular function and plan electrophysiology procedures.

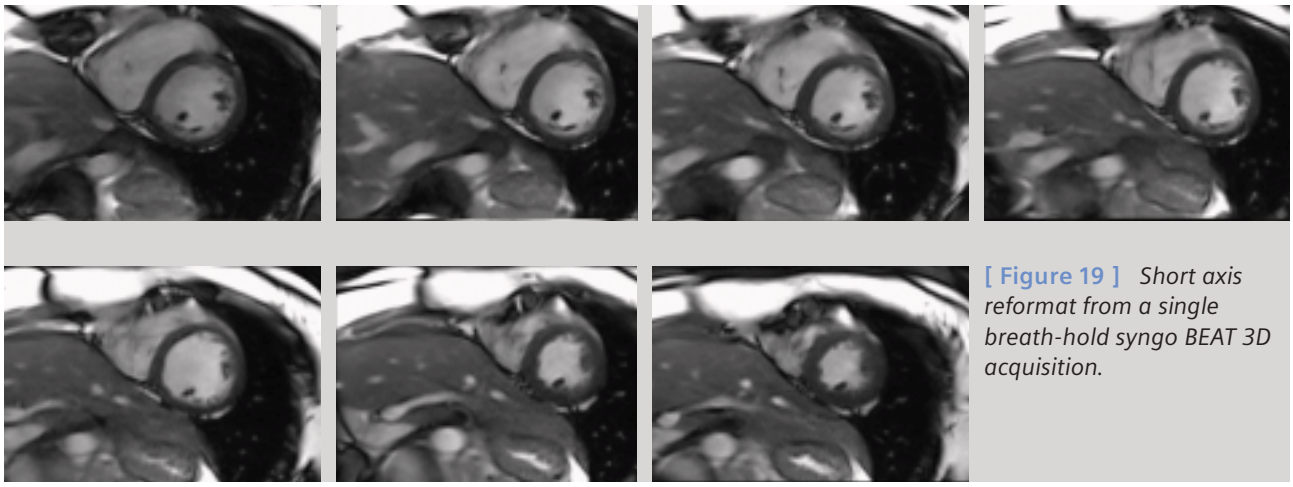

[Figure 19] *Short axis reformat from a single breath-hold syngo BEAT 3D acquisition.*

syngo DTI

The *syngo* Diffusion Tensor Imaging (DTI) capabilities are greatly enhanced under *syngo* MR B13. Not only can the user define and measure up to 256 different directions with up to 16 b-values, but the package also includes inline calculation of FA maps and Trace-weighted images in addition to standard ADC maps. The data from these acquisitions can easily be imported and displayed in the new enhanced 3D Neuro task card. Within this task card it is possible to overlay anatomical information with both functional MRI and DTI data in one volume to allow for more accurate registration and visualization in this multi-parameter data.

[Figure 20] *The Neuro 3D task card with diffusion tensor imaging (DTI) and functional MR imaging (fMRI) data displayed.*

syngo BRACE

syngo BRACE is a non-rigid-body, or warping, registration. Such registration algorithms are only made possible in reasonable amounts of time by using advanced reconstruction hardware and architecture like the *syngo* MR B13 system. It is particularly useful for breast and other soft tissue tumors which can easily be distorted between imaging sessions. However it is also useful for subtraction protocols (Fig. 21), as patients frequently move between pre- and post-contrast acquisitions. This technique can help mitigate such misregistration artifacts.

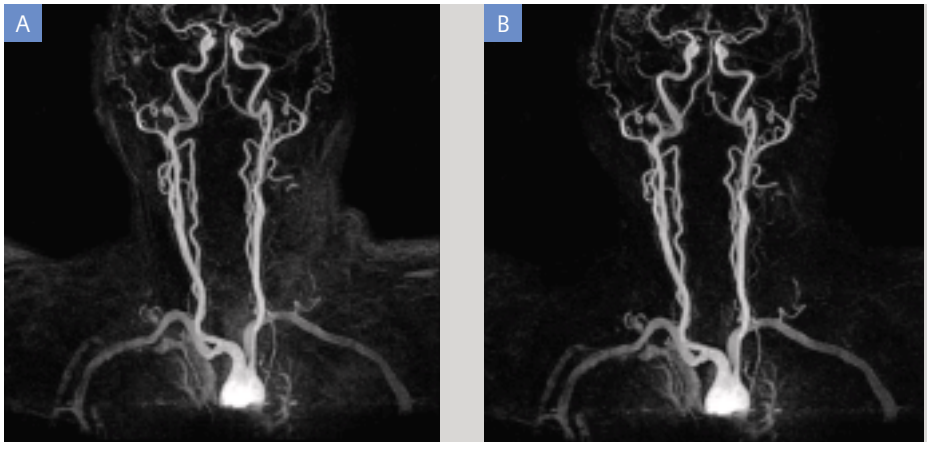

[Figure 21] *Subtraction angiography without (A) and with BRACE (B). As seen in the right hand image, static tissue is greatly suppressed and small vessel detail is enhanced with non-rigid-body registration applied.*

Courtesy of Mayo Clinic, Jacksonville, USA.

***syngo* GRAPPA**

Thanks to the improved reconstruction system, *syngo* MR B13 also contains several further improvements to the industry-leading *syngo* GRAPPA algorithm. The improvements dramatically reduce Parallel Imaging artifacts and therefore allow even higher acceleration factors, particularly for 3D sequences which can be accelerated in both the phase-encode direction and the partition-encode direction. Also, for dynamic scans it is now possible to acquire the reference lines once and then obtain the full acceleration in the dynamic scans. Finally, iPAT averaging can be used to reduce motion artifacts in the same amount of time relative to a non-iPAT single-average sequence.

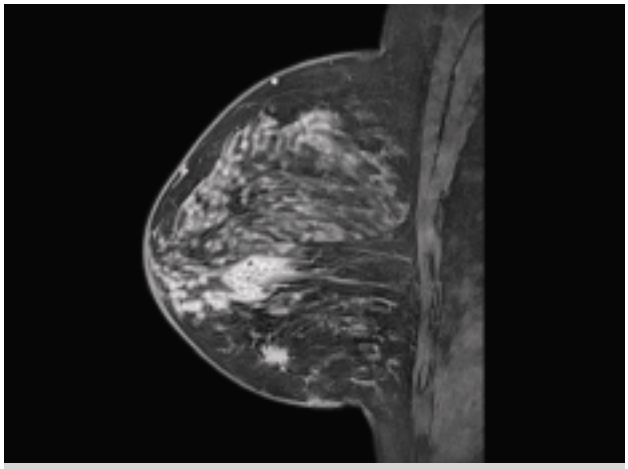

[Figure 22] *MAGNETOM Trio, A Tim System: Breast, T1 FLASH 3D WE, iv., GRAPPA2, sagital, ductal carcinoma in situ TR 8 ms, TE 4 ms, TA 3:34 min, eff. SL 1.5 mm, partitions 224, matrix 320, FoV 200 mm.*
Courtesy of Hong Kong Sanatorium and Hospital.

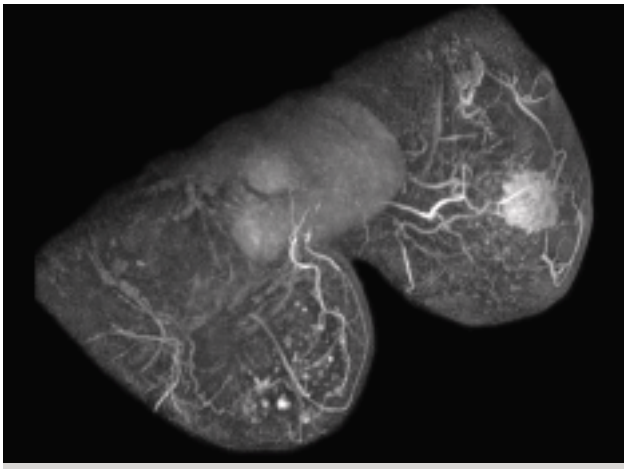

[Figure 23] *MAGNETOM Espree: Breast, ce-MRA, MIP, FatSat, GRAPPA 2, post-contrast, left-anterior, right-anterior, transversal, invasive ductal carcinoma (IDC). TR 4.6 ms, TE 1.6 ms, TA 57 s, eff. SL 0.9 mm, partitions 160, FoV 349 mm.*
Courtesy of HOAG Memorial Hospital, Newport Beach, USA.

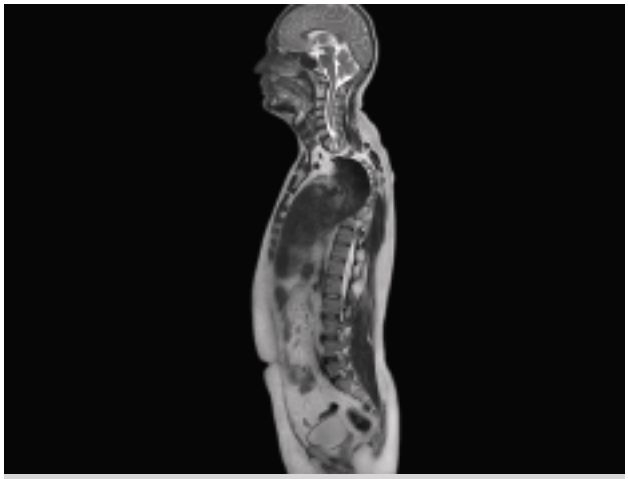

[Figure 24] *MAGNETOM Avanto: whole spine, T2 tse sag, COMPOSED, GRAPPA 2,scoliosis. TR 3870 ms, TE 105 ms, TA 1:33 min, SL 5 mm, FoV 320 mm.*
Courtesy of D.C.R.I., India

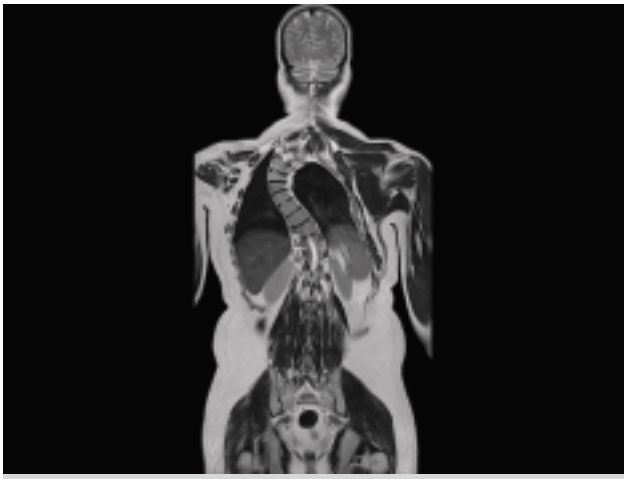

[Figure 25] *MAGNETOM Avanto: whole spine, T2 tse cor, COMPOSED, GRAPPA 2, scoliosis. TR 3870 ms, TE 105 ms, TA 1:33 min, SL 5 mm, FoV 320 mm.*
Courtesy of D.C.R.I., India

Workflow Improvements

Whole-body coordinate system

The whole-body coordinate system creates a virtual field-of-view (FoV) which is much larger than the physical FoV achievable in a single scan (Fig. 26). At the system level, this allows images acquired at different table locations to use the same DICOM (Digital Imaging and Communication in Medicine) frame of reference. In terms of workflow, this enables data from multiple table positions to be "stitched" together and utilized as a single unit for scan planning, prescription, and display. The first series acquired identifies the zero position, and both table position and slice position are displayed on every image.

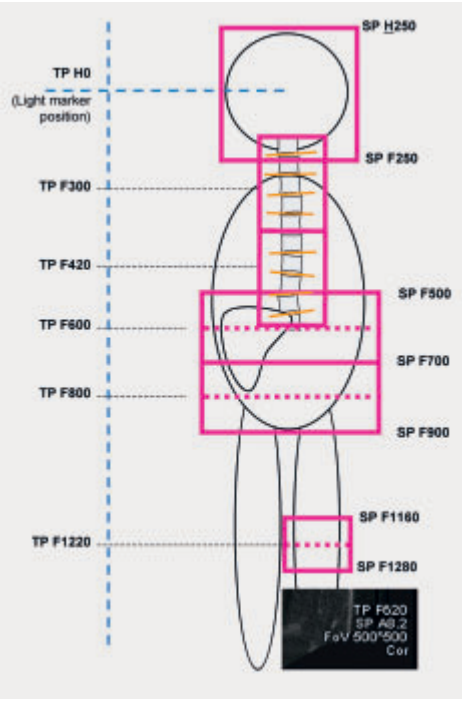

[Figure 26] *Schematic representation of the whole-body coordinate system. The Table Position (TP) and the Slice Position (SP) for all series in the exam share a single origin. As seen in the inset, the TP and SP are both displayed in the image text.*

Scan@center

syngo MR B13 allows scan@center, which is selected by choosing positioning mode "ISO" in the user interface. When activated, the table will move the center of the imaging volume for each acquisition to the magnet/gradient isocenter. Simultaneously, the system will automatically switch to the optimal coil combination for the volume being imaged. This new functionality greatly improves workflow for whole-body or large FoV applications as well as improving the effectiveness of image distortion correction and techniques such as fat saturation that are sensitive to field homogeneity. Coupled with 2D distortion correction, the scan@center mode yields a noticeable improvement in image quality.

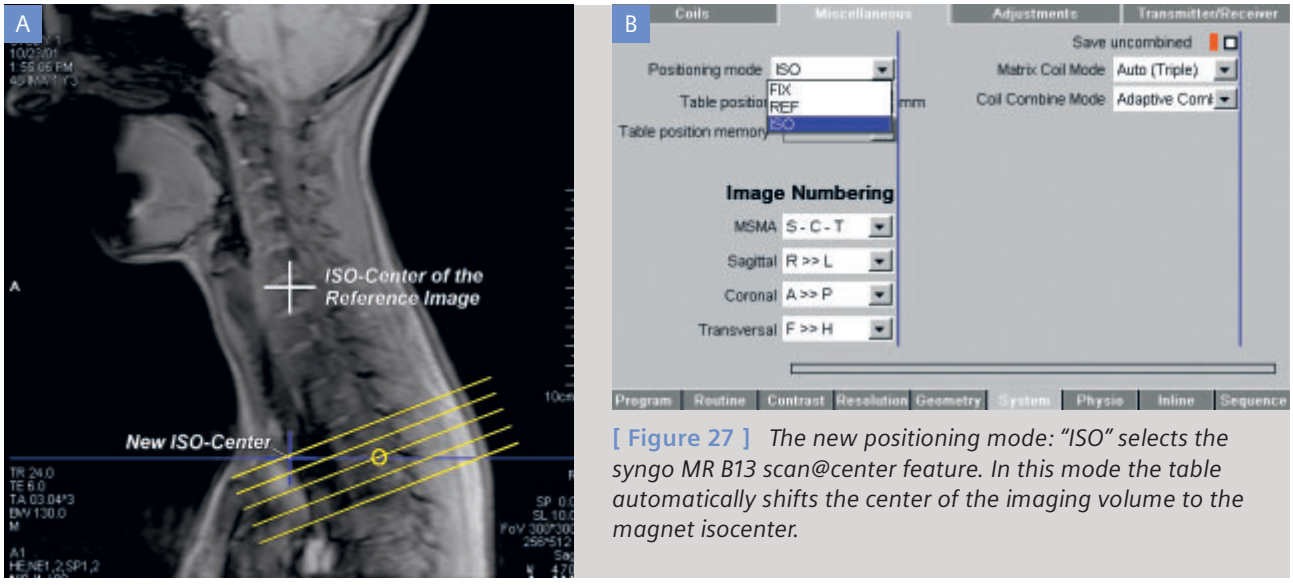

[Figure 27] *The new positioning mode: "ISO" selects the syngo MR B13 scan@center feature. In this mode the table automatically shifts the center of the imaging volume to the magnet isocenter.*

Distortion correction 2D and 3D

The improved reconstruction system opens up the opportunity for improved reconstruction algorithms. One of these new algorithms is a 3D distortion correction (DIS3D), which is simply not possible without the advanced computer hardware introduced by *syngo* MR B13. Not only is the system now able to correct for "Large FOV" effects in-plane (DIS2D), but it can also correct in the through-slice direction with the DIS3D option, as shown with a "grid phantom" in Fig. 28. This is particularly valuable for applications which require a high degree of spatial accuracy and geometric reliability, such as stereotactic planning. In other applications, it allows image composition over large volumes with multiple slices without concerns about through-slice geometric distortions.

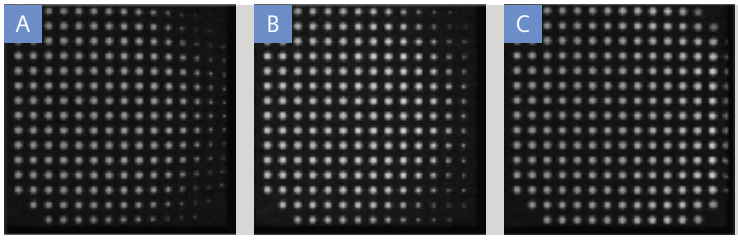

[Figure 28] *Images acquired using a "grid phantom". (A) is the original image without distortion correction. (B) is corrected using the in-plane or "Large FOV" filter. (C) is corrected using the new 3D algorithm.*

Coupled graphics

To further improve workflow, *syngo* MR B13 adds the capability to combine or couple different slice groups together as a single unit. This is obviously helpful in the prescription adjustment of radial slice acquisitions as pictured in Fig. 29, which under previous software versions had to be moved one slice group at a time. However, this functionality is more general than just radial slice acquisitions and is used heavily in the Tim Planning Suite. Here pre-sats can be coupled to slice groups for easy adjustment. Under set-n-go, different protocol steps can be coupled and moved together, adding ease of use to applications such as peripheral angiography. The functionality is also extendable to other applications such as the spectroscopy package which utilizes coupled graphics to connect and move outer volume suppression bands when adjusting the position of the region-of-interest (ROI).

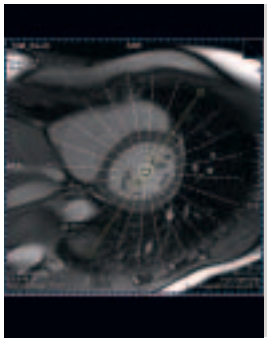

[Figure 29] *An example of a radial slice prescription. Each slice of the prescription represents a different slice group. Prior to coupled graphics adjusting the acquisition center required moving each slice group independently.*

Inline compose

syngo MR B13 now allows building up of one virtual composed FoV from component image sets each acquired in a separate physical FoV to be done "inline" at the time of acquisition. Employing 2D distortion correction to ensure image compatibility results in a large field-of-view image set that can be used to prescribe subsequent acquisitions.

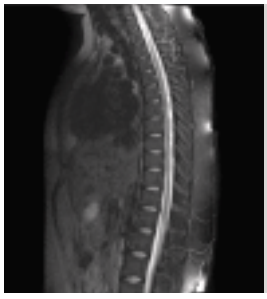

[Figure 30] *An example of an inline compose spine incorporating two overlapping stations. Note the seamless transition between the two stations.*

Tim Planning Suite and Set-n-Go

The Tim Planning Suite is a new, improved-workflow user interface that enables whole-body imaging with efficient utilization of the new scan@center and inline compose capabilities. This interface allows the planning of multi-station exams all at once, realized through a prescription feature called set-n-go (Fig. 31). Set-n-go allows the combination of several acquisitions which differ only by scan position or potentially field-of-view, into a single protocol step.

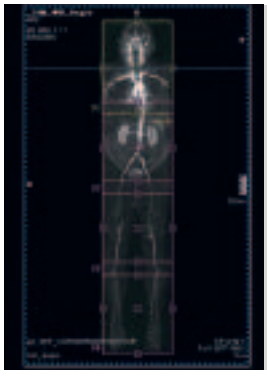

[Figure 31] *The graphical display of a whole-body set-n-go protocol utilizing 4 stations.*

Please note that some of the aforementioned features, e.g. SWI, are optional. Please contact your local Siemens representative for more information.


MAGNETOM Trio

BrainPET*
The Next Wave in the Evolution of Medical Imaging

First to combine CT and PET, now first to combine MR and PET

Siemens has developed a prototype of a new MR-PET solution which enables simultaneous measurements of the same volume without table move or patient repositioning. This is possible with the **IsoVolume Technology**, which is the basis for the development of the first MR-PET system using MR-compatible LSO crystal-based avalanche photodiode detectors instead of the classic photomultiplier tubes for PET signal detection (Fig. 1). Siemens has been the first manufacturer to show a proof-of-principle for this approach at the ISMRM 2006.

While MR focuses more on morphology and functional activities of the human body, PET – Positron Emission Tomography – allows insight into cellular metabolism. Providing MR and PET imaging simultaneously in a hybrid system means we can combine the sensitivity of PET information with the morphologic and functional MR data and thereby achieve new levels of specificity and sensitivity in one exam. Following this path will allow improved differential diagnoses e.g. for dementia, cancer etc. Moreover the radiation exposure of the patient is minimized, which can be important for young and pediatric patients and multiple follow-up studies. In addition, MR-PET-fused data generated with a hybrid system will be acquired at the same time, reducing the total imaging time for the patient significantly and possibly improving cost-efficiency.

Siemens is developing BrainPET, a PET Head Insert for MAGNETOM Trio, A Tim System. BrainPET and Trio with Tim form the first truly integrated MR-PET system – thanks to the **IsoVolume Technology**. BrainPET will serve as a pilot study in order to learn more about the medical use of MR-PET as well as to help develop necessary applications like motion correction, scatter and attenuation correction for PET using MR. In the first step attenuation correction will be done using elliptical models. We are also currently implementing a method that will calculate the effect of the various tissues on the ionizing radiation using MRI. In addition, MR-PET should serve as the breeding ground for a number of new applications such as correlation between metabolic and functional phenomena.

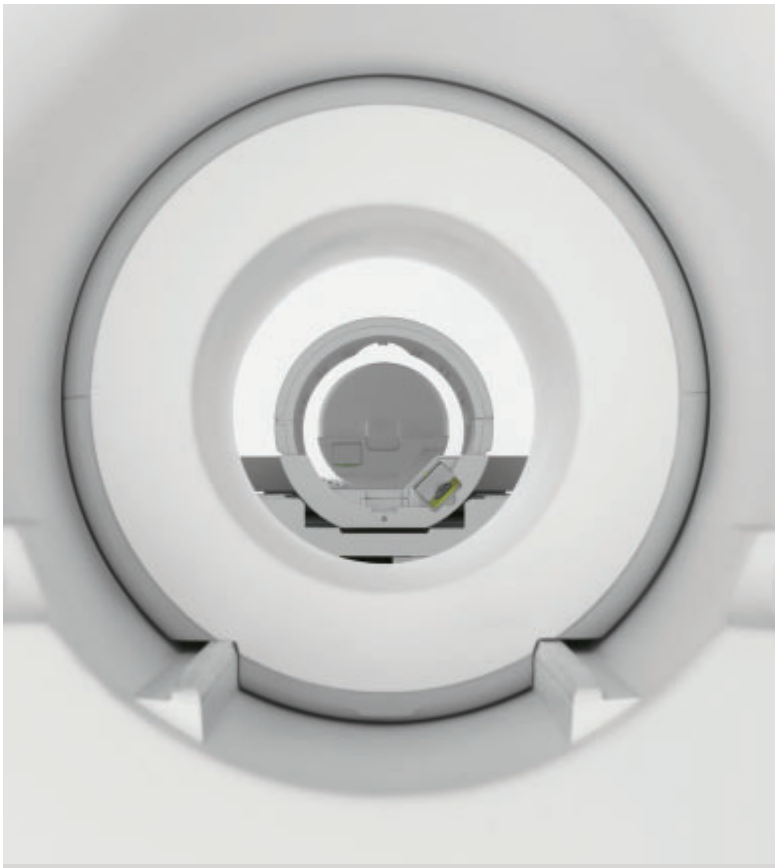

PET Head Insert in the MAGNETOM Trio, A Tim System bore.

Technical Specifications

Set up and removal time for the insert is aimed to be 30 minutes. MR will run at no compromise with or without the insert. Initially separate MRI and PET consoles will be used for acquisition control but the aim is to have a hybrid console in the future. Field of View (FoV) in combined mode is estimated to about 20 cm axial and 24 cm radial. The MR system requires the removable table option and a special table top has been developed to be used with **BrainPET**. A PET compatible Tx/Rx

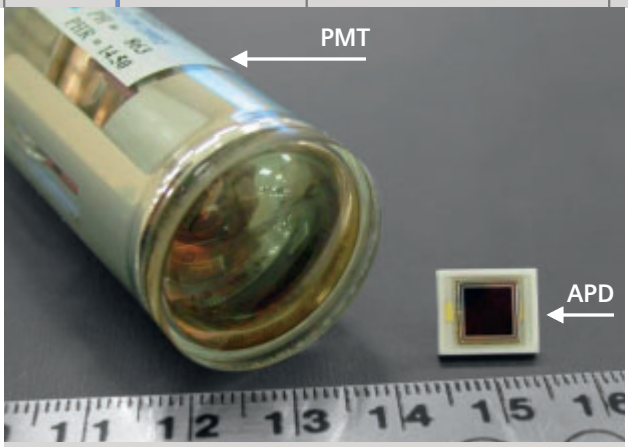

[Figure 1] *Photo Multiplier Tubes (PMT) on the left vs. Avalanche Photo Diodes (APD) on the right.*

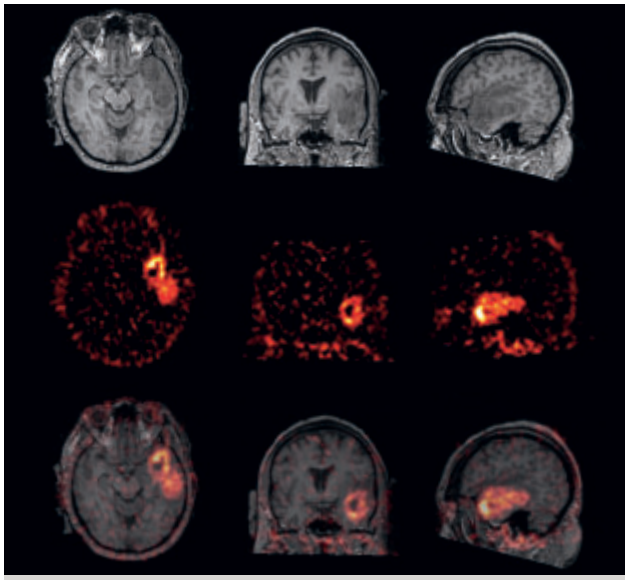

[Figure 2] *Glioma Proliferation. T1-weighted MR image. FLT PET and fused data (FLT = 18F-3'Fluoro-3'-deoxy-L-thymidine).*

Courtesy of Dr. Carpenter, WI, University of Cambridge, UK

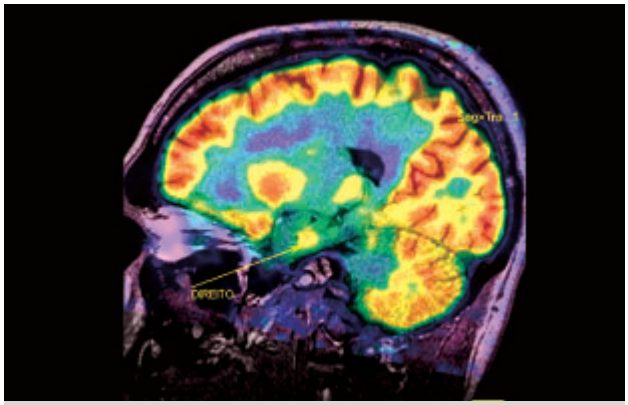

[Figure 3] *The Temporal Lobe epileptic focus is shown with MR-PET.*

Courtesy Dr. Dominguez, CDPI, Rio de Janeiro, Brazil

head coil as well as an 8-channel head coil for high resolution brain imaging are being developed.
Installation requirements involve room shielding for MR and PET (Magnetic field, RF, Radiation) as well as space behind the magnet larger than 1.5 meter. In addition, a radiation license and a room for patient preparation are required.
BrainPET has 192 detector blocks compared to 144 in a conventional 64 slice PET·CT system. For comparison, the HRRT (High Resolution Research Tomograph), which has also 192 detector blocks, achieves a spatial resolution near 3 mm.

Fusion of leading technologies goes beyond fusion of images

MR-PET could potentially assist the physician to better locate, assess, distinguish, monitor and in certain cases predict the outcome of the disease. It is the first major step towards personalized diagnosis considering that it can define the disease status, identify the underlying molecular causes/events and elucidate the disease pathways. Some of the applications are listed below.

BrainPET scientific applications involve:

- Simultaneous activation studies by PET and functional MRI (fMRI: real-time information correlation), PET combination with Diffusion Tensor Imaging, 3D Chemical Shift Imaging and high resolution structural MRI – all benefiting from 3T field strength.
- Precise evaluation of metabolism and function in small brain structures.
- Dynamics of distribution of tracers/drugs in various brain structures.
- Analysis and comparison of radiotracers with dynamic contrast MRI.
- Development and evaluation of cell therapy (stem-cell migration tracking and differentiation).

BrainPET clinical applications involve:

- Neurodegenerative disorders: Parkinson's disease, Alzheimer's disease, Vascular Dementia
- Stroke: Tissue viability
- Neuro-oncology: Tumor viability
- Pediatric neurology: brain development
- Epilepsy: accurate localization.

*Works In Progress – The information about this product is preliminary. The product is under development. It is not commercially available in the US and its future availability cannot be assured.

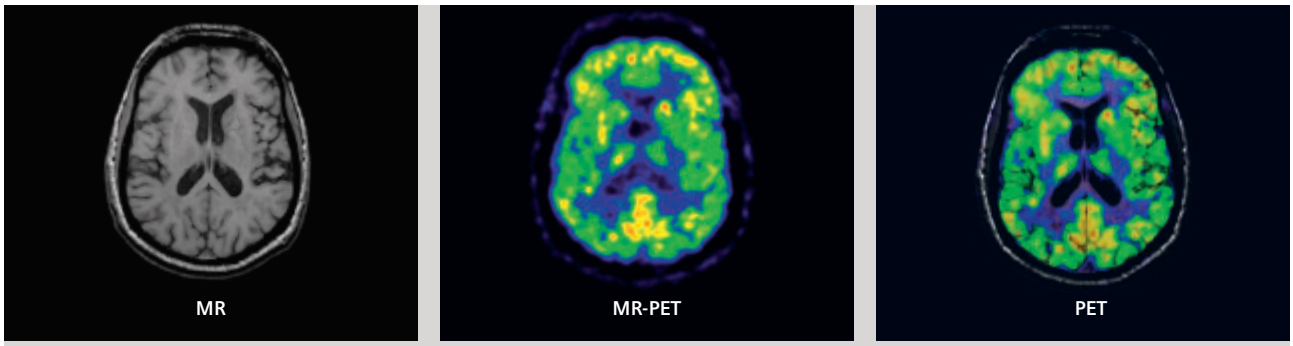

[Figure 4] *First ever in-vivo images simultaneously acquired by MR and PET.*

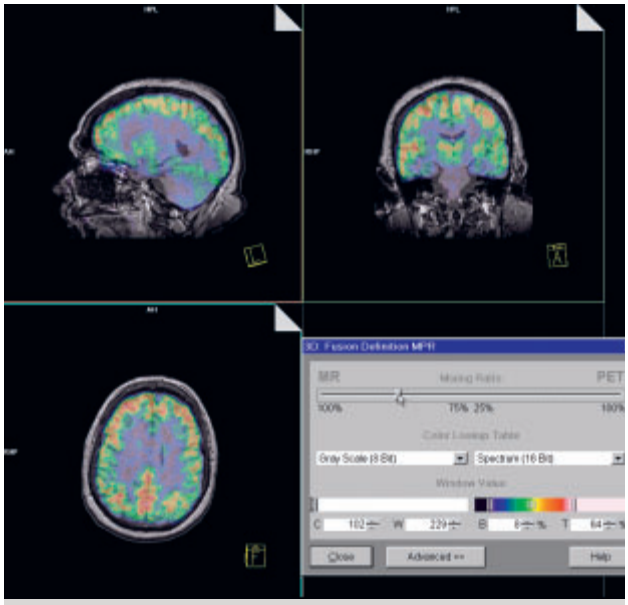

[Figure 5] *1 Examination, 3 Datasets Simultaneously acquired PET (TA 20 min) and T1-weighted 3D FLASH (CP head coil, TA 6 min).*

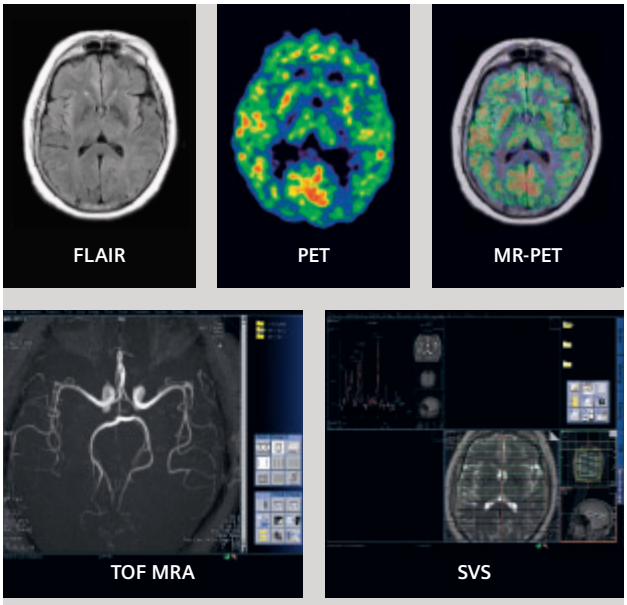

[Figure 6] *FLAIR, TOF and Single Voxel Spectroscopy were applied during the same PET acquisition.*

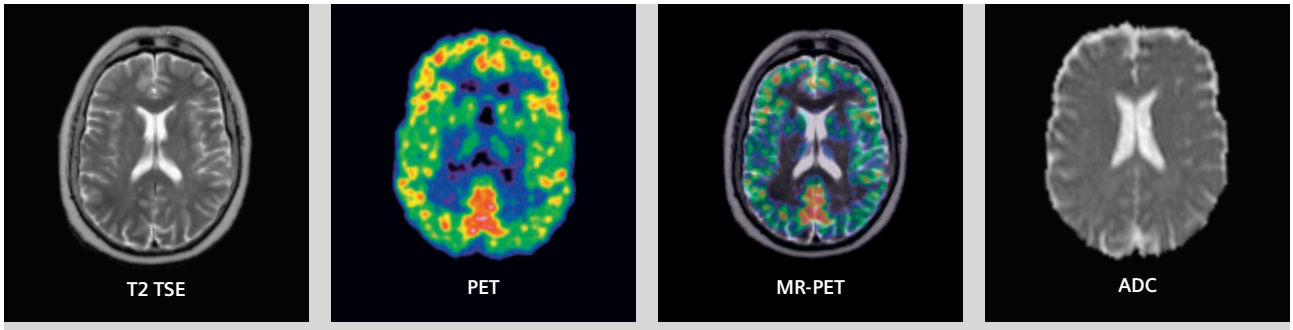

[Figure 7] *Diffusion EPI sequence applied during PET acquisition.*

Images acquired with support of Drs. Townsend and Nahmias, University of Tennessee, USA and Drs. Schlemmer, Pichler and Claussen, Eberhard-Karls-University, Tuebingen, Germany.

syngo BLADE
Motion Correction from Head to Toe

Stuart H. Schmeets

Advanced Specialist Siemens 3T Applications, Siemens Medical Solutions, Inc., Malvern, PA, USA

Introduction

Advances in MRI systems and techniques have continued to push the limits of spatial resolution and acquisition speed leading to an improvement in diagnostic accuracy and increasing MRI's value in patient care. However, as the spatial resolution of MR images is increased the demand on patient cooperation is also increased. Sub-millimeter acquisitions are common, if not routine, and under these conditions even a slight amount of patient motion can degrade the quality of the resulting image. Further complicating the situation is that patient instruction and immobilization techniques do little to reduce the effects of physiologic motion such as peristalsis, respiration, and vascular flow. With this in mind, it's easy to see why motion correcting and motion-insensitive MR sequences such as the new *syngo* BLADE technique are so vital in today's MRI practice.

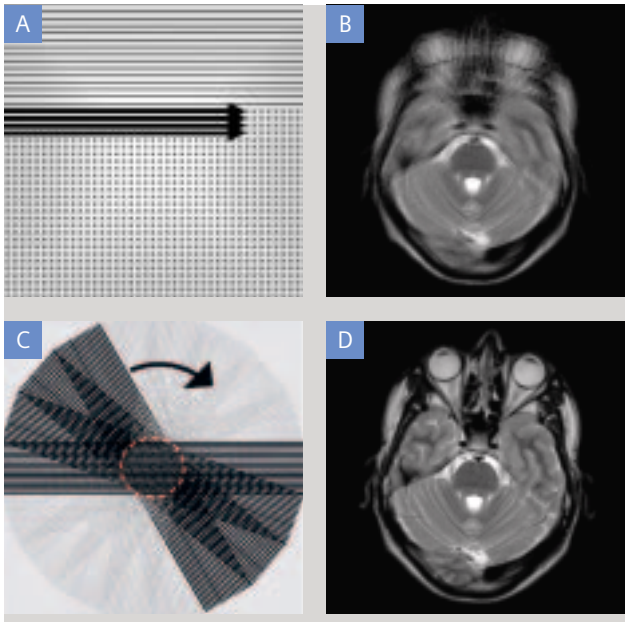

[Figure 1] *syngo BLADE k-space filling sheme.*

Why *syngo* BLADE?

Routine Turbo Spin Echo (TSE) acquisitions fill raw data space (k-space) in a rectilinear or Cartesian fashion meaning that during each TR period data lines equal to the echo train length will fill k-space from top to bottom (Fig. 1A). The center of k-space which contributes the signal and contrast characteristics of the image will only be acquired once (unless multiple averages are used) and patient motions will have a moderate to severe effect on the resulting image depending on the progress of a particular acquisition.

Figure 1B demonstrates the effect patient motion will have on a brain image during a routine TSE acquisition. In this example, a volunteer was asked to move their head in a side-to-side pattern during the acquisition.

The *syngo* BLADE sequence is derived from the radial k-space sampling concept where a set of data lines, or blades, equal to the echo train length are rotated around the center of k-space (Fig. 1C). The most important benefit of this type of sequence design is that each of the acquisition blades re-samples the center of K-space making it possible to generate a low resolution image for each one. This information can then be used to correct for patient motion at the end of the acquisition.

The image in figure 1D depicts the same volunteer experiment as in figure 1B. However, in this test the *syngo* BLADE acquisition technique was employed to eliminate the image artifacts caused by the volunteers' motion.

syngo BLADE in other areas of the body

An additional benefit to *syngo* BLADE is that since each acquisition blade must be corrected for its rotation within k-space the sampling method alone, without motion correction applied, will be significantly less sensitive to motion artifacts than a standard TSE sequence. This intrinsic feature, along with the fact that integrated Parallel Acquisition Techniques (in this case, *syngo* GRAPPA) can be incorporated to reduce imaging times, makes *syngo* BLADE a valuable tool in

all areas of the body including neuro (head and spine), abdominal and orthopedic applications. In addition, it is important to note that *syngo* BLADE works for all orientations, axial, sagittal and coronal.

Abdomen and Pelvis:

Respiration contributes only a portion of the motion artifacts in abdominal and pelvic imaging. Even in cooperative patients that are able to hold their breath well and when motion compensation techniques are employed, flow and peristaltic motion effects can degrade image quality. Furthermore, the increased spatial resolution desired in today's clinical environment often leads to longer breath-hold durations. *syngo* BLADE combined with the PACE (**P**rospective **A**cquisition **C**orr**E**ction) free-breathing respiratory control option provides a solution.

Figure 2A demonstrates how the PACE free-breathing technique minimizes respiratory motion effects in axial abdominal images on a patient who is not able to hold their breath. When used in conjunction with *syngo* BLADE (Figure 2B) motion effects from flowing structures are also minimized.

Figures 2C and 2D further demonstrate how *syngo* BLADE reduces the effects of flow and peristalsis in special pelvic applications such as sagittal MR imaging of the colon.

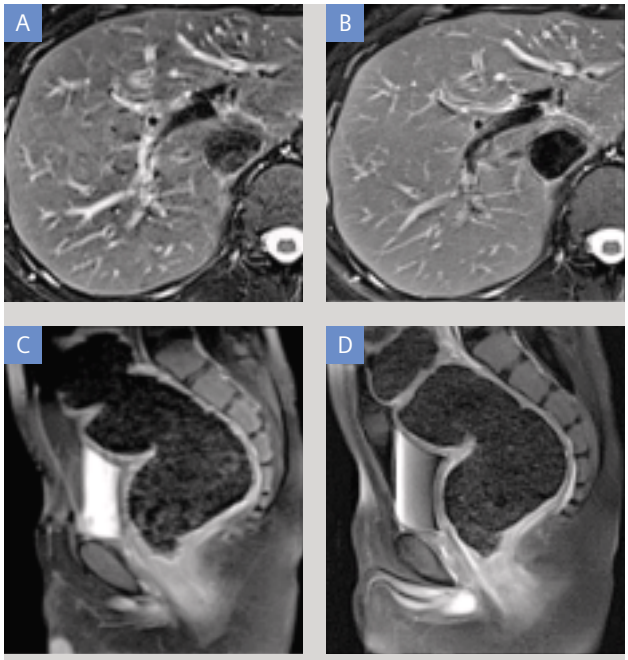

[Figure 2] *The combination of BLADE and PACE minimizes the flow artefacts in liver imaging (B). Note also that bowel peristalsis artefacts are minimized by the combination of these techniques (D).*

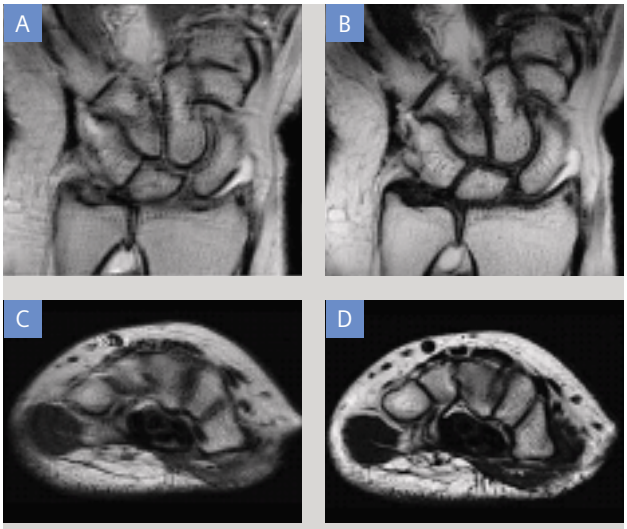

[Figure 3] *syngo BLADE improves the image quality of wrist imaging even with uncooperative patients. Note the detailed visualization of bone and tendons and a small cyst.*

Orthopedic Applications:

Structures of interest in orthopedic MR imaging are often very small. A slight amount of motion can make a difference in the ability to make a diagnosis especially in pediatric applications. *syngo* BLADE has been shown to reduce the effects of patient motion in orthopedic studies on both adult and pediatric patients.

Figures 3A and 3C depict routine coronal and axial TSE images of the wrist with a considerable amount of motion. Applying *syngo* BLADE leads to a noticeable improvement in image quality (Figures 3B and 3D).

Conclusion

One of the best tools for reducing motion artifacts in MRI is careful patient instruction and positioning. However, motion artifacts from sources such as respiration, vascular flow, peristalsis, and general movement e. g. during the pediatric examination can still negatively affect MR image quality. *syngo* BLADE works in all orientations and has been shown to effectively correct for motion effects in the brain, minimize physiologic motion effects in the abdomen and pelvis, and reduce motion artifacts in body and orthopedic examinations.

MAGNETOM C!
News with *syngo* MR A30

Stefan Domalski

Market Segment Manager Open Systems, Siemens Medical Solutions, Erlangen, Germany

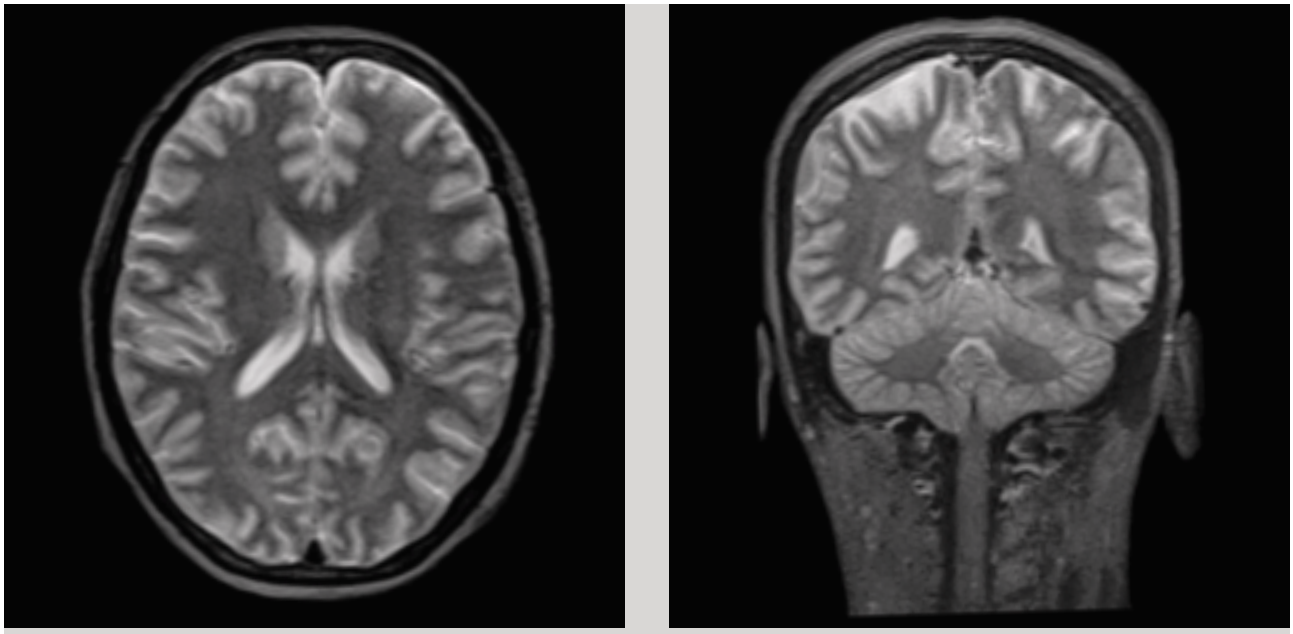

[Figure 1] *syngo SPACE allows isotropic 3D imaging for multi planar reconstruction of data. MAGENTOM C!, 0.35 Tesla open system.*

Currently the next software release for the MAGNETOM C! *syngo* MR A30 is in it's last state of development before it will be rolled out in spring 2007. The software will further exploit the system's unique hardware capabilities with the strongest gradients and the only true multi-channel RF system in mid-field.

The range of Siemens unique applications will be broadened by *syngo* SPACE – the technique for high resolution isotropic 3D imaging. The scan speed required for this technique is based on the unique 24 mT – 55 T/m/s gradient system of the MAGNETOM C!. *syngo* SPACE will be available for spine, head and and orthopedic examinations.

MAGNETOM C!'s capabilities in diffusion imaging will be broadened by adding the unique *syngo* REVEAL body diffusion technique to the scope of applications. *syngo* REVEAL allows multi b-value diffusion imaging in practically all body regions to help differentiate between malignant and benign lesions. For application in the liver *syngo* REVEAL can be used with respiratory gating on the MAGNETOM C!.

Both applications have been introduced to Siemens high-field MAGNETOM systems at the RSNA 2005 and could be made available right away to MAGETOM C! users, because of the common *syngo* software interface of all MAGNETOM systems.

In addition *syngo* GRAPPA parallel acquisition technique for faster scans with higher resolution and larger coverage has been standard on the MAGNETOM C! since it has been released in 2004. *syngo* GRAPPA is based on the four channel receive technology in combination with the family of four element receive coils.

The Neuro Suite in the standard Multi-Channel Application Suite now enables comprehensive neurological examinations with high-resolution and ultra fast sequences with T1, T2, FLAIR

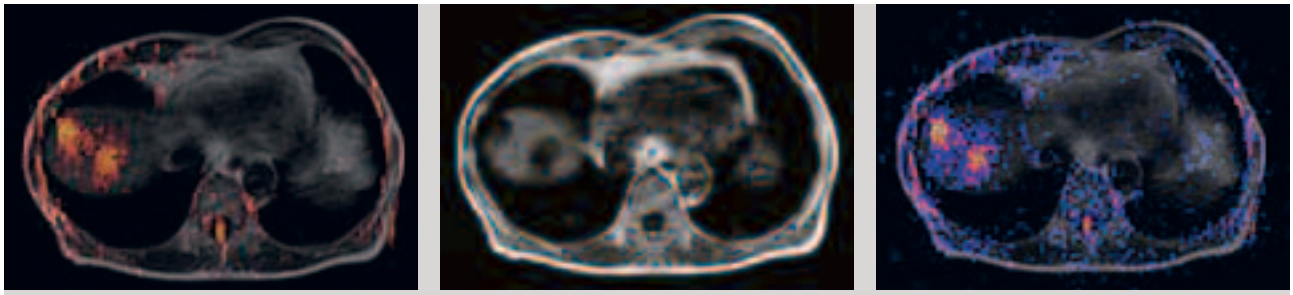

[Figure 2] *syngo REVEAL body diffusion allows the assessment of metastatses, necrotic tumor etc. in various body regions. For application in the liver the technique can be used with respiratory gating. (Data presented using syngo Image Fusion licence.)*

Courtesy of Prof. H.-M. Klein, Jung Stilling Hospital, Siegen, Germany.

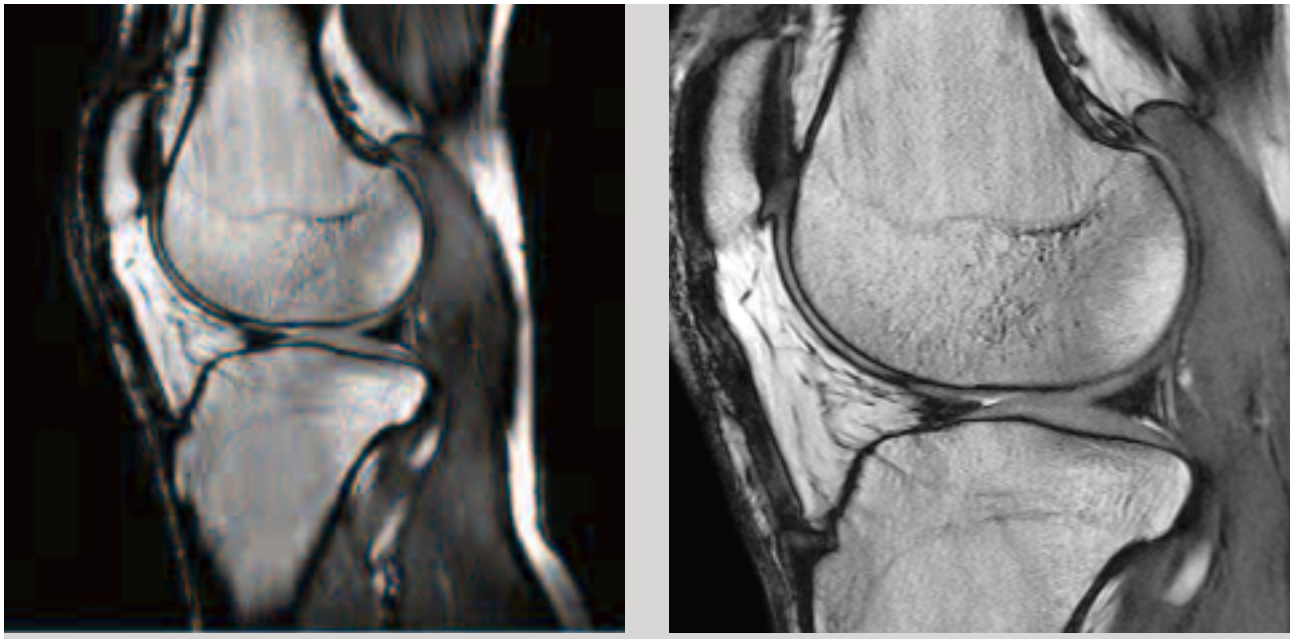

[Figure 3] *New protocols featuring resolution unseen at mid-field. 1024 matrix and 2 mm slices for high resolution T2-weighted imaging with 0.35 Tesla.*

contrasts including various fat saturation techniques and EPI (Echo Planar Imaging) Diffusion and Perfusion techniques without the need of an optional application package.

New protocols focusing on resolution have been developed for the MAGNETOM C!. Thin slices and matrices up to 1024 can be achieved in standard mid-field acquisition times by using the advantages of the strong gradients and the superior signal-to-noise ratio (SNR) of the multi-channel RF system and the unique sequences which are available on the MAGNETOM C!.

These protocols are complemented by throughput oriented protocols which can provide standard mid-field resolution in less than three minutes for applications in every body region. These protocols also make applications like kinematic studies clinically available due to the shorter scan times.

With *syngo* MR A30 the MAGNETOM C! makes another giant step into the world of high-field applications and results which have been unknown to mid-field MRI systems so far and which are unique to the MAGNETOM C! now.

syngo Expert-i, the Interactive Access to MR Examinations

Heinz-Peter Schlemmer, M.D.

Eberhard-Karls-University, Tübingen, Germany

For several months now we have been using *syngo* Expert-i and are very happy with it. It greatly improves our workflow since our MR systems are located in different rooms. Currently we are using this innovative application for four of our systems – MAGNETOM Avanto, Sonata, Symphony Trio, A Tim System. By using *syngo* Expert-i, we are able to select, monitor or access online the current scans running on the other system. This applies to all other MR systems and all other

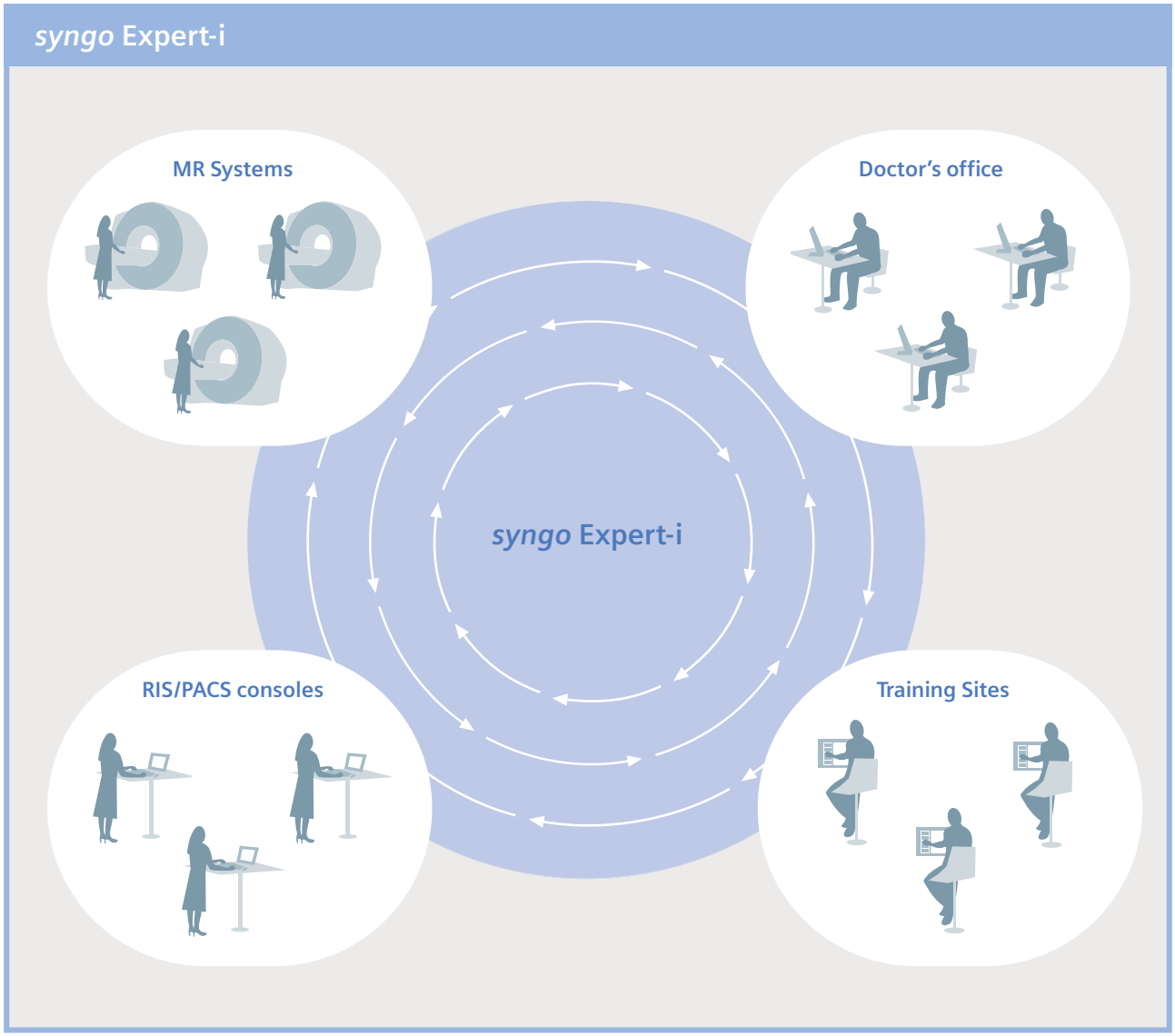

separate reporting stations of the hospital. You don't have to interrupt your work on your own console. All we had to do was to install the software license. As monitors, we use those of the Radiology Information System (RIS) that are installed at every system and every PACS (Picture Archiving and Communication System) reporting station.

Our technologists are very happy with this expansion. Our most experienced technologist is easy to reach and able to give the necessary support. For me, that means additional security: despite the many daily requests I can log in quickly and easily via our hospital network and provide immediate feedback about a particular scan. Our workflow functions smoother and more efficiently with *syngo* Expert-i.

In addition, we are able to improve our communication and cooperation with referring physicians. For example, we can create our reporting documentation directly on the reporting console and transmit it to the lecture room. As a result, we no longer depend on the limited information available on the PACS (Picture Archiving and Communication System).

Product Information

syngo Expert-i is a Siemens-unique solution that lets physicians interact with MR exams in progress from virtually anywhere in a hospital environment. After installation, the expert can simply log on as a remote user with an ID and password. From there they can view the entire patient setup, imaging data, and all sequences performed in real-time. *syngo* Expert-i provides full-screen displays and allows total mouse control. *syngo* Expert-i is available for all MAGNETOM systems: MAGNETOM Avanto, Espree, Trio, Symphony, C!, Concerto, Sonata, Harmony and Allegra.

All of the following software versions support Expert-i: *syngo* MR 2004A, 2004V, 2005E, 2006T, *syngo* MR B13, *syngo* MR A30.

Have real-time access to the MRI suite from anywhere in the network.

"The interactive access to MR examinations is absolutely trendsetting. With *syngo* Expert-i, Siemens offers us once more an innovative technology that considerably improves our processes and positions us as a forward-thinking university hospital."

Heinz-Peter Schlemmer, M.D.,
Eberhard-Karls-University, Tuebingen, Germany

Case 1
Assisting advanced imaging examinations (e.g. cardiac imaging)

Technologist at the MAGNETOM Avanto:
"Generally the cardiac MR exams are made with the help of the chief technologist. On that day, she had to do another difficult exam at the Sonata so I was alone. With cardiac MR I find especially the slice orientation difficult. The patient had aortic stenosis and there was the suspicion of bicuspid valve. After showing the left ventricular outflow tract, I had difficulties to see the aortic valve. I called the chief technologist, she logged on from the second scanner to ours. She performed most of the difficult part of the exam virtually herself. The outcome of the exam was perfect for the radiologist."

Chief technologist at the MAGNETOM Sonata:
"Since we have Expert-i I can log in and control the examination from one scanner to another. I can answer questions immediately without leaving my on-going scan. This technology improves our daily routine work. All technologists are excited about Expert-i."

"With *syngo* Expert-i, we are able to complete many examinations earlier than before, because physicians and technologists do not have to walk from one location to another."

Heinz-Peter Schlemmer, M.D., Eberhard-Karls-University, Tuebingen, Germany

Case 2
Assisting change in protocol following an unsuspected or unclear finding

Technologist at the MAGNETOM Avanto:
"I was doing a routine scan of the whole spine to evaluate scoliosis. After the T1- and T2-weighted scans, I felt that the spinal cord at the thoracic level looked a little bit more bulky. I did not know what to do and I was not sure whether I should inject contrast. I called the responsible radiologist, who was on call. With the help of Expert-i he looked at the images from his office. He made the diagnosis of a syrinx and advised to proceed with axial scanning with T2-weighted sequences at that level without the need of intravenous contrast. Usually in these cases we wait for the doctor to come to the scanner, which might take several minutes depending on the availability of the radiologist. Or even reschedule the patient for another time slot, when we feel that there is too much time pressure due to the waiting patients outside. Expert-i made the work simpler for all of us."

Doctor's office radiologist Professor Schlemmer:
„With the Expert-i technology I can actively access MR examinations in progress without having to interrupt my tasks elsewhere in the hospital."

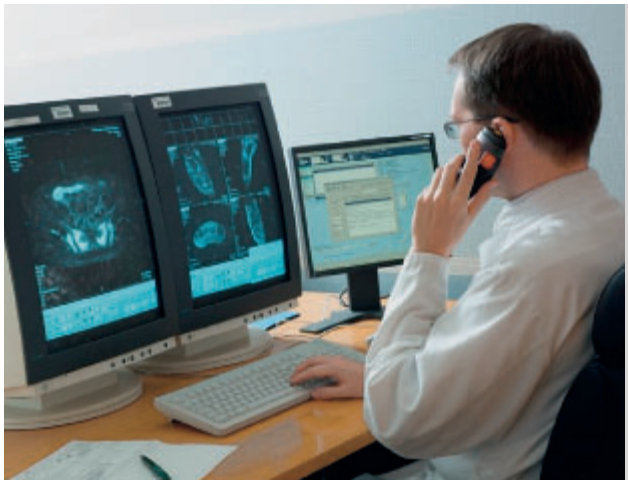

RIS monitor: A radiologist could also answer the question immediately without leaving their working area. syngo Expert-i allows the remote access to any scanner from any RIS (Radiology Information System) console. Prompt answer can be secured.

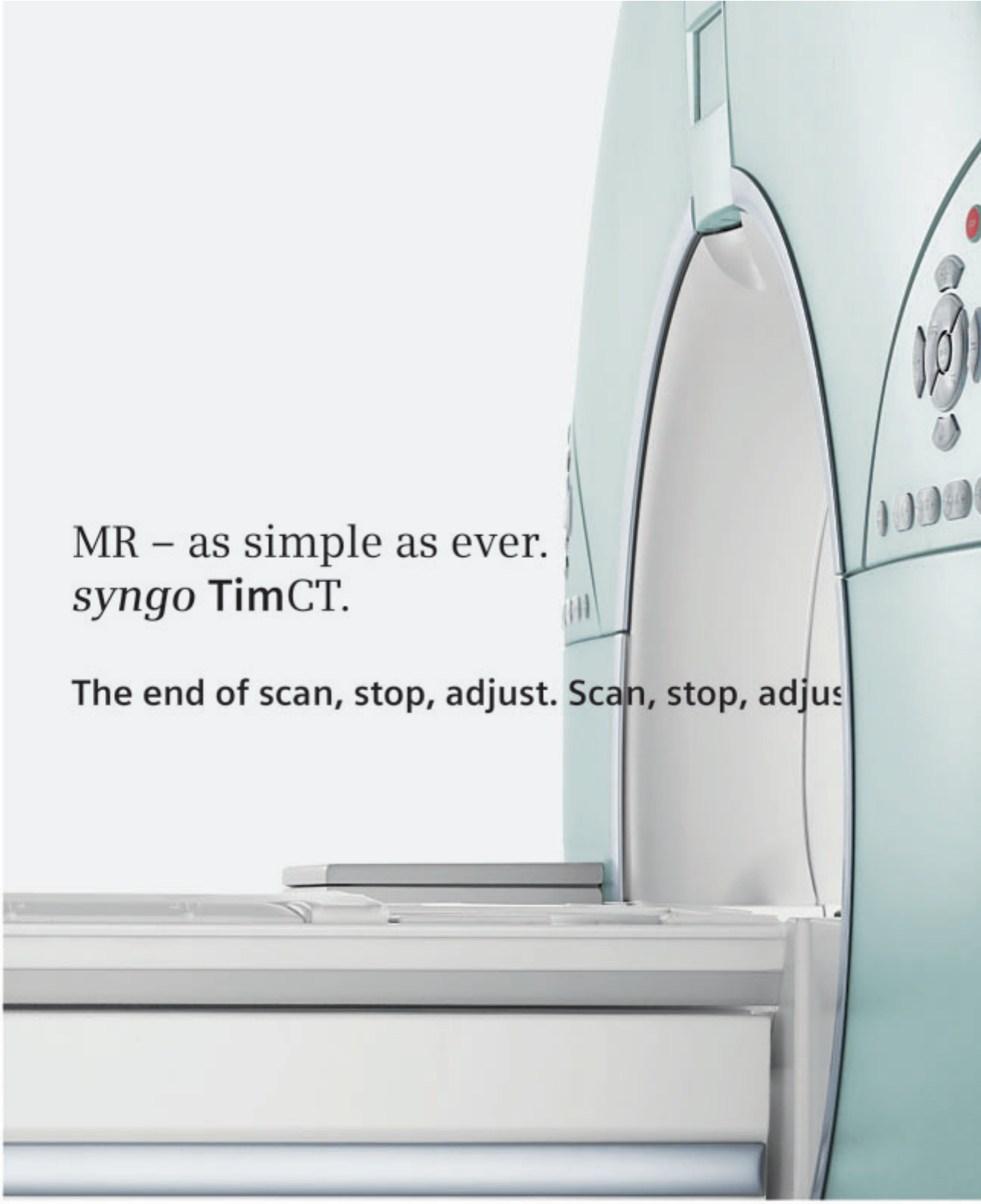

MR – as simple as ever.
syngo **Tim**CT.

The end of scan, stop, adjust. Scan, stop, adjus

Proven Outcomes in Magnetic Resonance.

Get ready for T-class, the next generation of MRI. With *syngo*® TimCT™ – Continuous Table move – the new MAGNETOM® T-class shifts the paradigm to CT-like scanning. No stops. Just continuous scanning. And not a single second wasted. Powered by Tim®, T-class combines increased diagnostic confidence with dramatically increased throughput. Find out more at our website. And see for yourself why at Siemens, the innovation never stops.

www.siemens.com/mr

SIEMENS
medical

MR-Z998-1-7600

Neurology

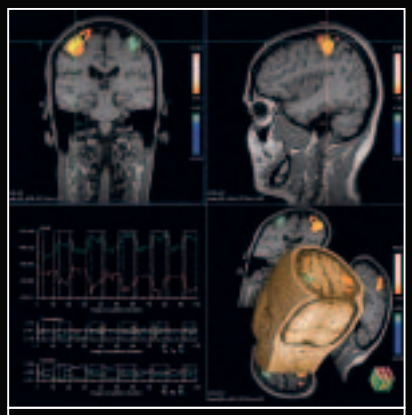

[1] ***MAGNETOM Symphony: Head*** / *functional MRI (fMRI)* / *sagittal* / *morphology with colored activation areas.*

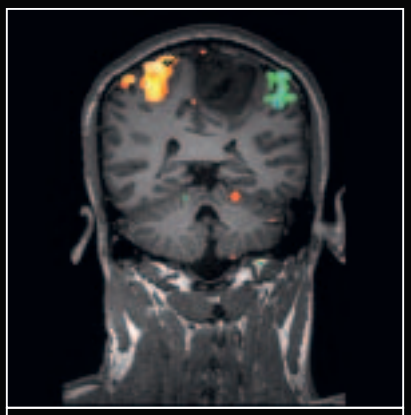

[2] ***MAGNETOM Trio, A Tim System: functional MRI (fMRI)*** / *BOLD* / *coronal* / *meningioma.*
Courtesy of S.Y.S.U.M.#1

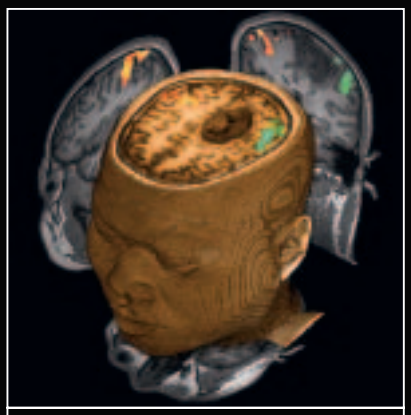

[3] ***MAGNETOM Trio, A Tim System: functional MRI (fMRI)*** / *BOLD* / *Volume Rendering Technique (VRT)* / *meningioma.*
Courtesy of S.Y.S.U.M.#1

[4] ***MAGNETOM Avanto: Head*** / *Fibretracking.*

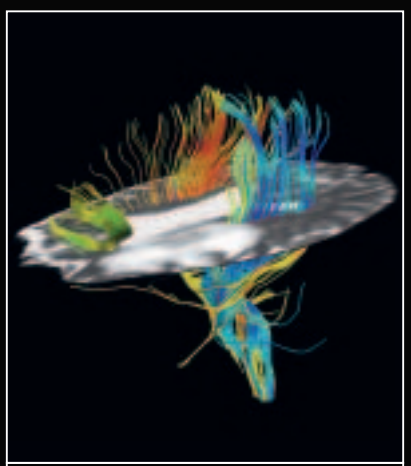

[5] ***MAGNETOM Avanto: Head*** / *Fibretracking.*

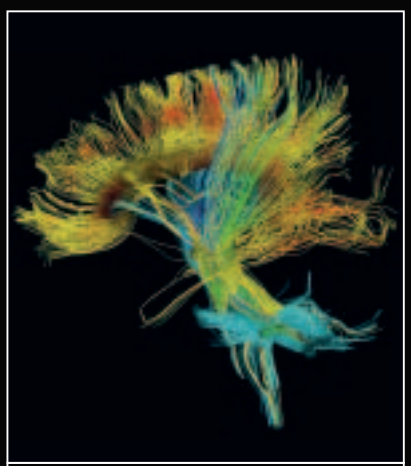

[6] ***MAGNETOM Avanto: Head*** / *Fibretracking.*

SPACE in Head Imaging

Nicholas M. Trost, Mark E. Lourensz

MRI Centre, St Vincent's Hospital Melbourne, Australia

The SPACE (**S**ampling **P**erfection with **A**pplication optimised **C**ontrasts by using different flip angle **E**volutions) series of sequences are single slab 3D TSE (Turbo Spin Echo) acquisitions with large turbo factors and calculated variable flip angles that maintain signal and contrast during the long echo train.

Acquisition time is reduced by combining with Tim (Total imaging matrix) and iPAT (integrated Parallel Acquisition Technique) resulting in measurement times between 4 and 9 minutes.

Isotropic voxels are 0.9 or 1.0 mm^3. These cases were all scanned on a Siemens MAGNETOM Avanto 1.5T unit with 76 coil elements and 32 independent RF channels.

Case 1

Follow up of an oligodendroglioma with the T2-weighted SPACE sequence acquired in the coronal plane at 1 mm slice thickness. The high resolution isotropic voxels allow reformations in any plane resulting in improved evaluation of the extent and relations of the tumour.

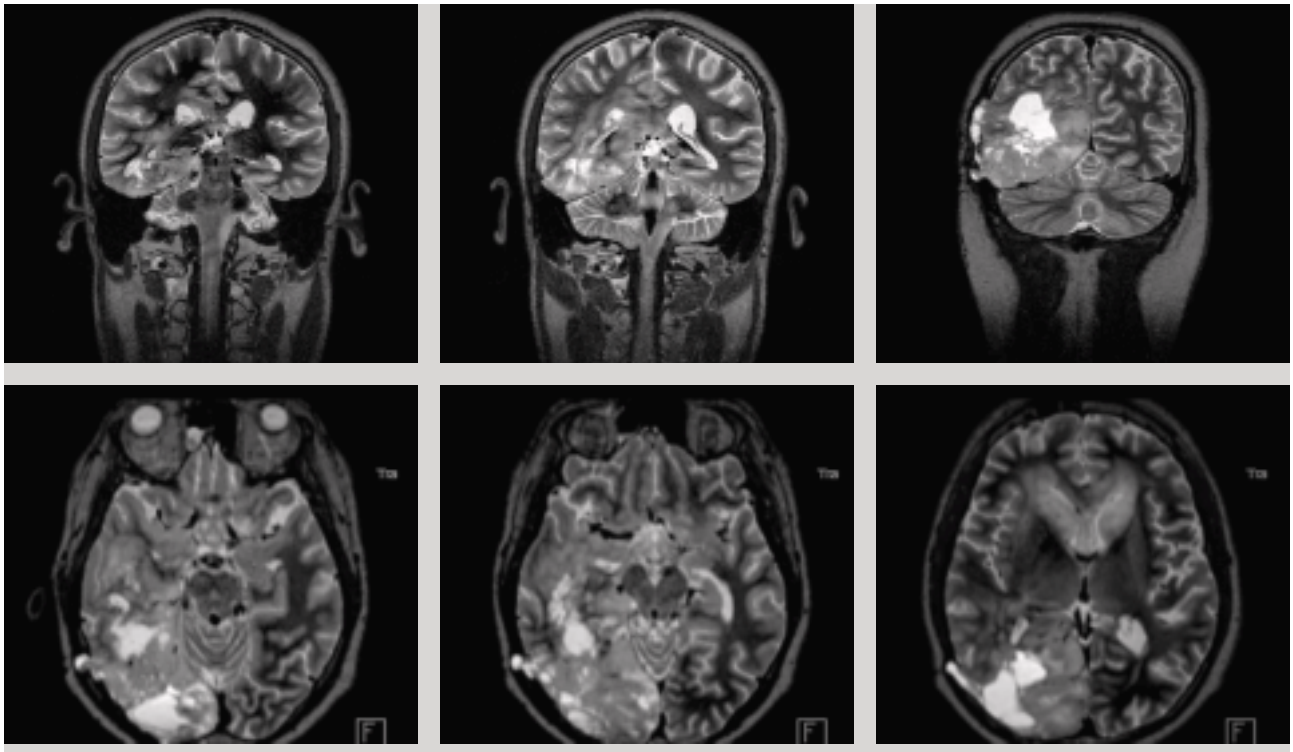

[Figure 1] *T2-weighted SPACE. Oligodendroglioma. Selected slices from coronal acquisition (top row) and axial reformations (bottom row).*

Slice	*1 mm coronal x 160*	***TA***	*8:20**
FoV	*195 x 240*	***NA***	*1*
Steps	*208 x 256*	***TR***	*3500*
Voxel	*1 x 1 x 1 mm^3*	***TE***	*355*

*These sequeces have been measured with a works in progress software version. With software version *syngo* MR B13 acquisition times will be about 50% shorter.

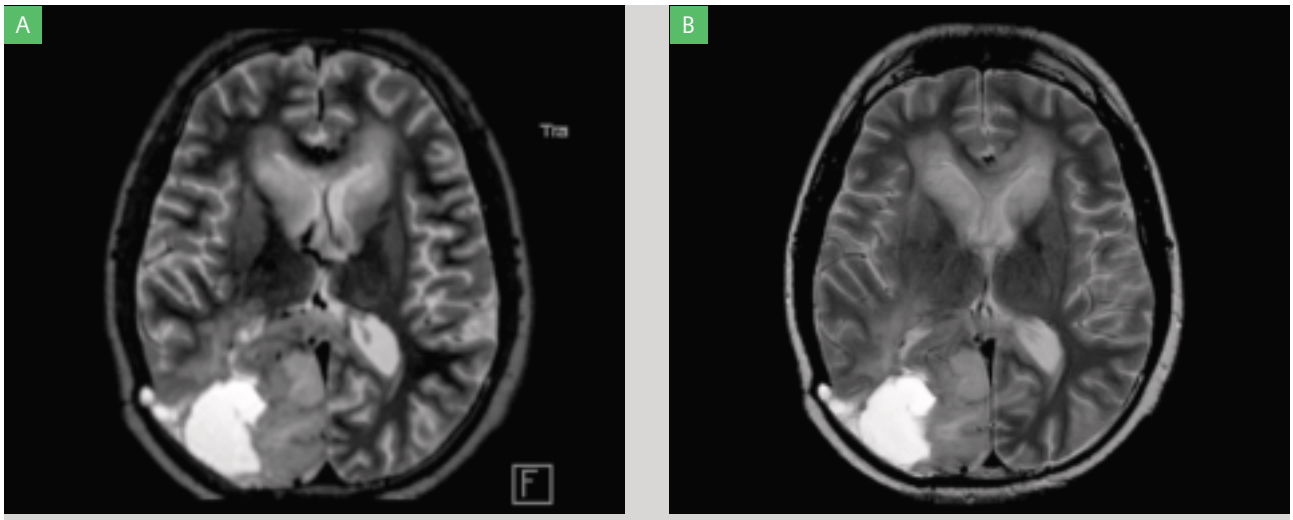

[Figure 2] *The contrast weightings of the T2-weighted SPACE (A) is similar to a standard 2D TSE T2-weighted sequence (B).*

Case 2

The T2-weighted SPACE sequence provides improved resolution of the reformations.
This is another case of an oligodendroglioma acquired in the axial plane with the T2-weighted SPACE sequence.

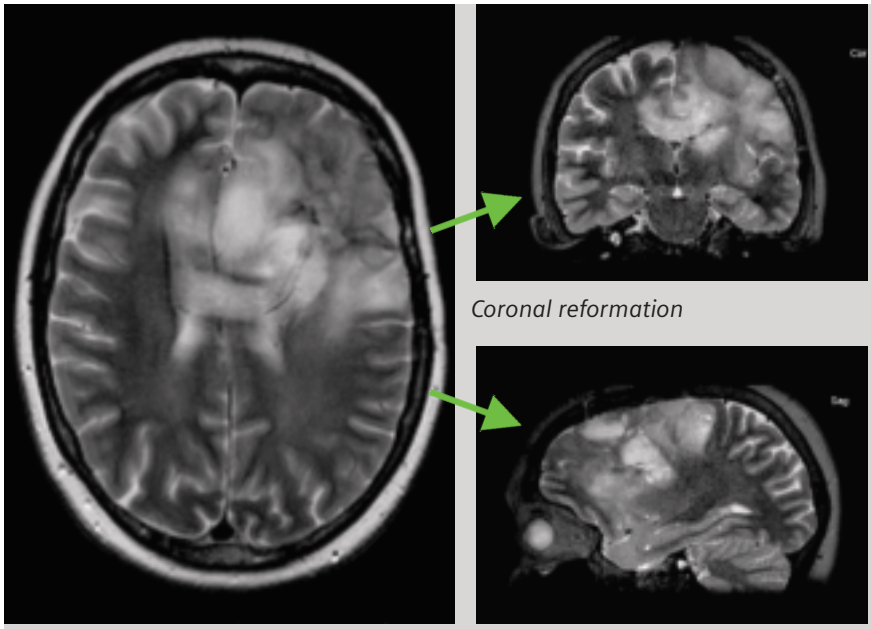

Axial acquisition

Coronal reformation

Sagittal reformation

[Figure 3] *T2-weighted SPACE Oligodendroglioma reformations in the coronal and sagittal planes demonstrate equivalent spatial resolution to the image from the axial acquisition.*

Slice	*0.9 mm axial x 120*
FoV	*173 x 230*
Steps	*190 x 256*
Voxel	*0.9 x 0.9 x 0.9 mm³*
TA	*6:10**
NA	*2*
TR	*3200*
TE	*445*

*These sequeces have been measured with a works in progress software version. With software version *syngo* MR B13 acquisition times will be about 50% shorter.

Case 3

Similarly the SPACE DarkFluid provides equivalent high resolution in the acquisition and reformatted planes:

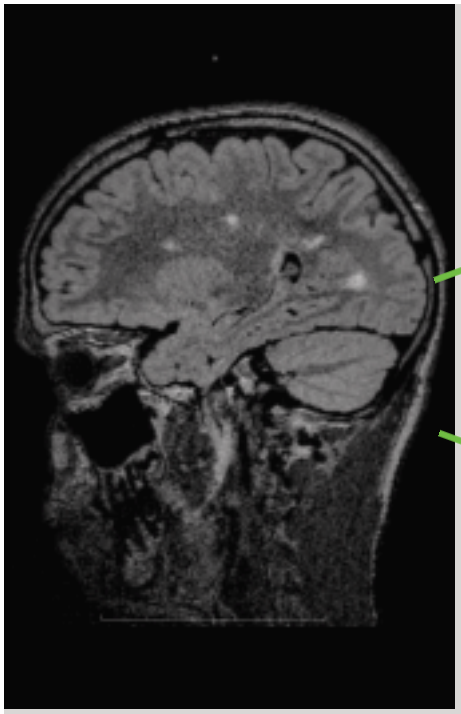

Sagittal acquisition

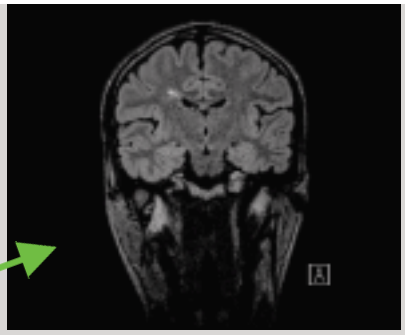

Coronal reformation

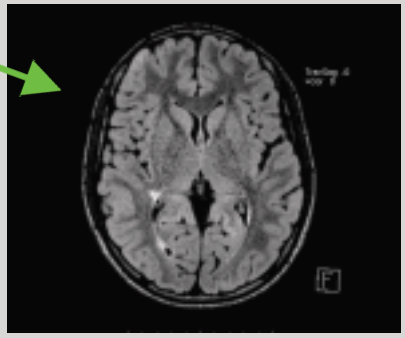

Axial reformation

[Figure 4] *SPACE DarkFluid. Periventricular lesions in multiple sclerosis. Reformations in the coronal and axial planes demonstrate equivalent resolution to the image from the sagittal acquisition.*

Slice	*1.0 mm x 176*
FoV	*224 x 256*
Steps	*222 x 256*
Voxel	*1.0 x 1.0 x 1.0 mm³*
TA	*7:17**
NA	*1*
TR	*5000*
TE	*405*
TI	*1800*

Case 4

The high resolution studies can be used with operative navigation systems that allow localization of lesions that may not be visible on the normally used T1-weighted post-contrast studies. This is a case of a subtle area of cortical dysplasia in the left hemisphere responsible for focal seizures that were poorly controlled with drug therapy. There is a craniotomy due to the recent placement and subsequent removal of grids. Resection of this lesion resulted in clinical improvement.

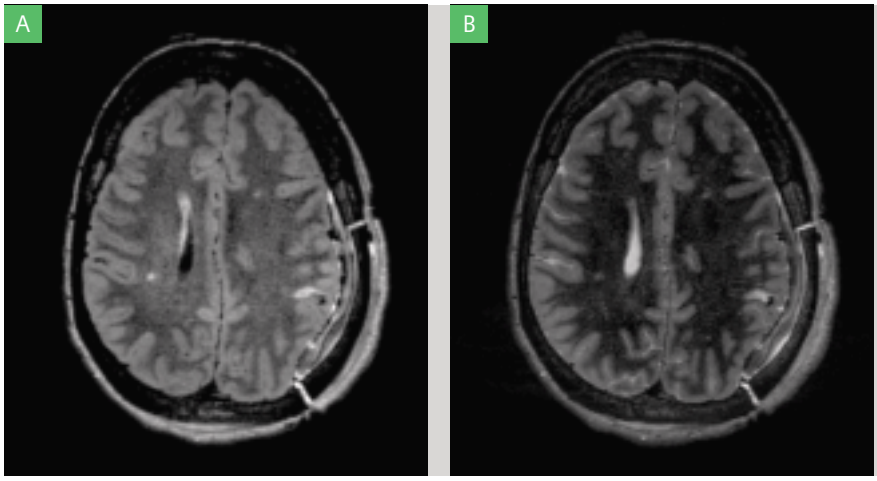

[Figure 5] *Cortical dysplasia. Representative images from each of the volume series. (A) SPACE DarkFluid 1 x 1 x 1mm³, TA 7:46. (B) T2-weighted SPACE 1 x 1 x 1mm³, TA 8:26*.*

*These sequeces have been measured with a works in progress software version. With software version *syngo* MR B13 acquisition times will be about 50% shorter.

Case 5

Follow up studies can be more accurately compared using equivalent slice positions from the high resolution 3D sequences as in this case of breast metastases.

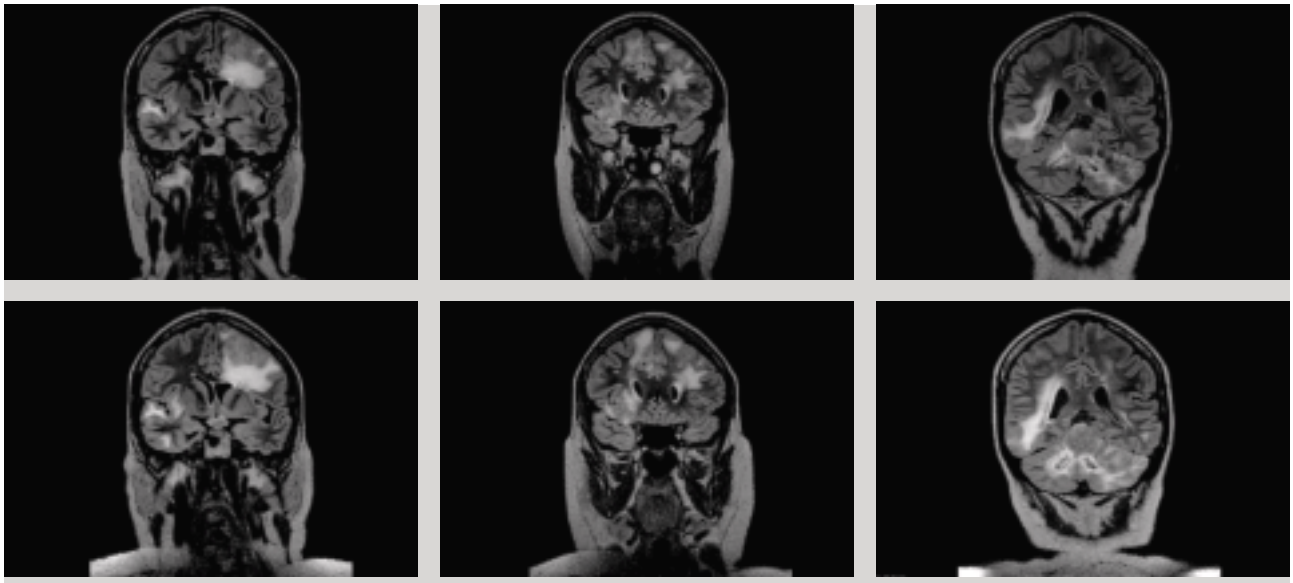

[Figure 6] *T2-weighted SPACE. Cerebral metastases from primary breast carcinoma. 2 series of scans 1 month apart. 19 July (upper row) and 16 August (lower row). The 3D high resolution scans enable accurate comparison.*

Case 6

Sensitivity for detecting small lesions is greater on the 3D sequence compared to standard 2D sequences due to thinner slices even though the in-plane resolution is lower.

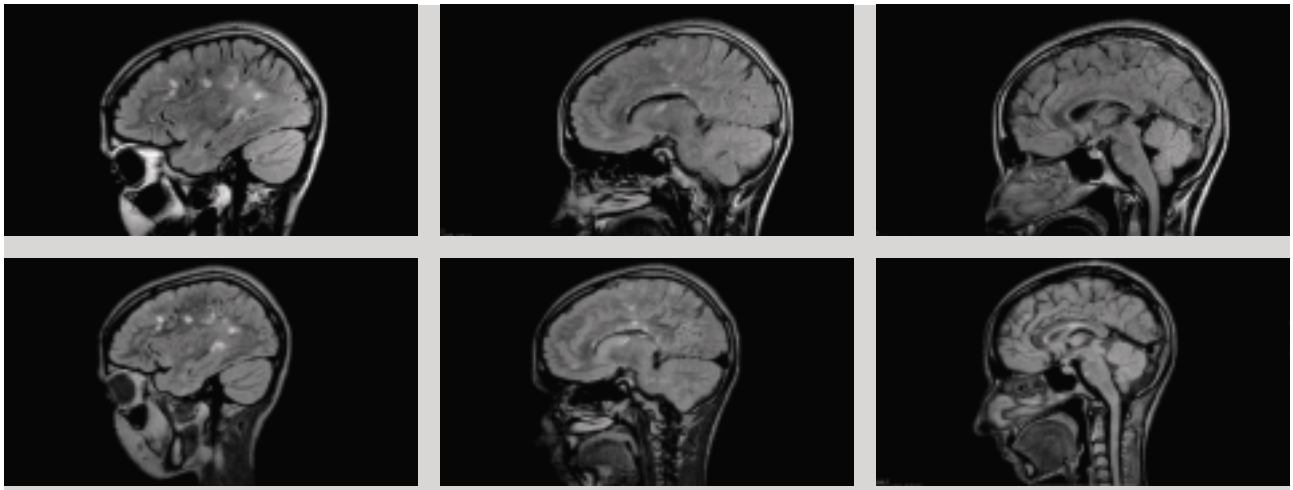

[Figure 7] *2D FLAIR: sagittal acquisition, 0.6 x 0.5 x 4 mm^3 (upper row) and SPACE DarkFluid, sagittal acquisition, 1.0 x 1.0 x 1.0 mm^3, 7:46* (lower row). Multiple sclerosis. A greater number of small lesions are demonstrated on the SPACE sequence. Margins of plaques are also sharper.*

*These sequeces have been measured with a works in progress software version. With software version *syngo* MR B13 acquisition times will be about 50% shorter.

Case 7 and Case 8

There is a version of the SPACE sequences with 3 mm slice thickness. The 3 mm DarkFluid sequence is free from significant flow artifact that often affects 2D FLAIR images and is thus very useful for the evaluation the of the posterior fossa.

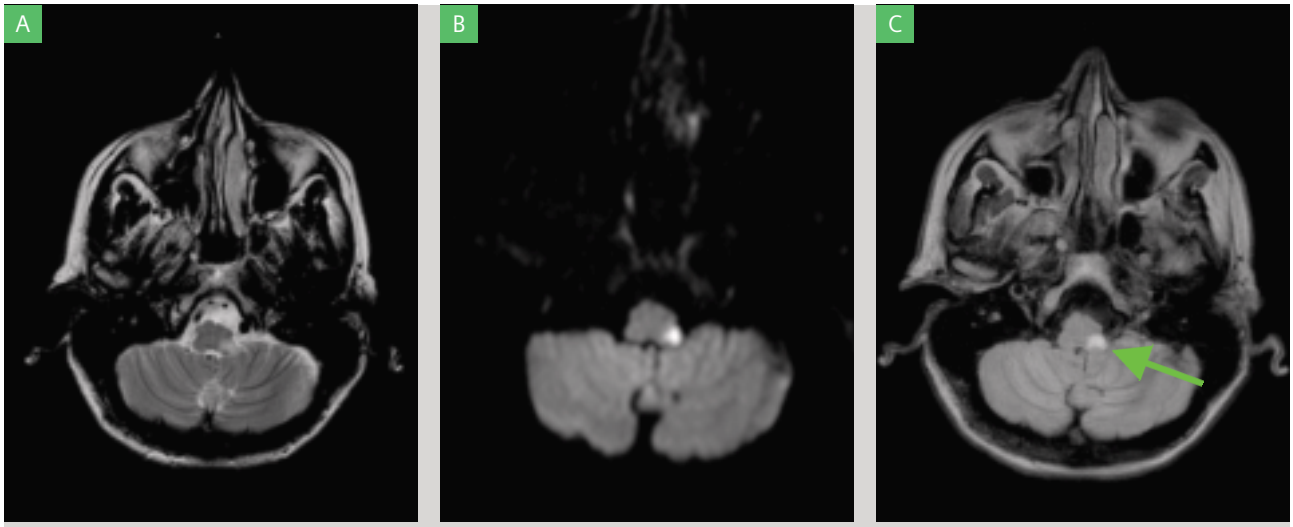

[Figure 8] ***Case 7:*** *Acute lateral medullary infarct clearly demonstrated on the 3 mm SPACE DarkFluid (C). Comparison with 2D T2 TSE (A) and DWI (B).*

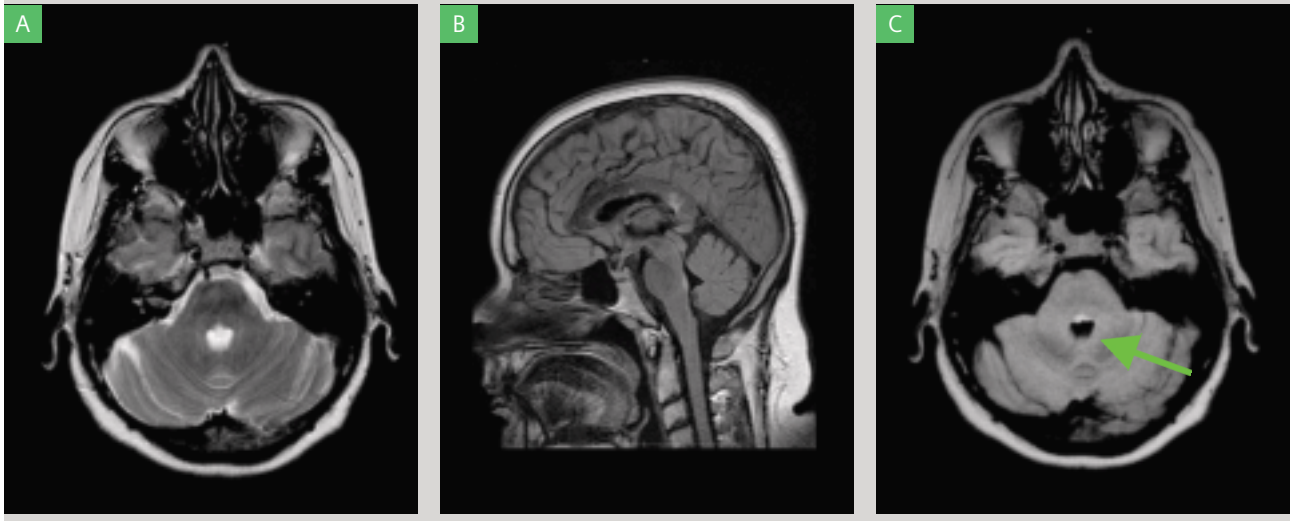

[Figure 9] ***Case 8:*** *Possible demyelination plaque in medial longitudinal fasciculus causing internuclear opthalmaplegia: 2D T2 TSE (A), 2D FLAIR (B) and 3 mm SPACE DarkFluid (C).*

SPACE DarkFluid 3 mm	
Slice	*3.0 mm axial x 36*
FoV	*187 x 230*
Steps	*207 x 256*
Voxel	*0.9 x 0.9 x 3.0 mm³*

TA	*6:32*
NA	*2*
TR	*6000*
TE	*355*
TI	*2100*

*These sequeces have been measured with a works in progress software version. With software version *syngo* MR B13 acquisition times will be about 50% shorter.

Case 9

The inversion recovery T1-weighed SPACE produces high contrast between grey and white matter at 1 mm spatial resolution.

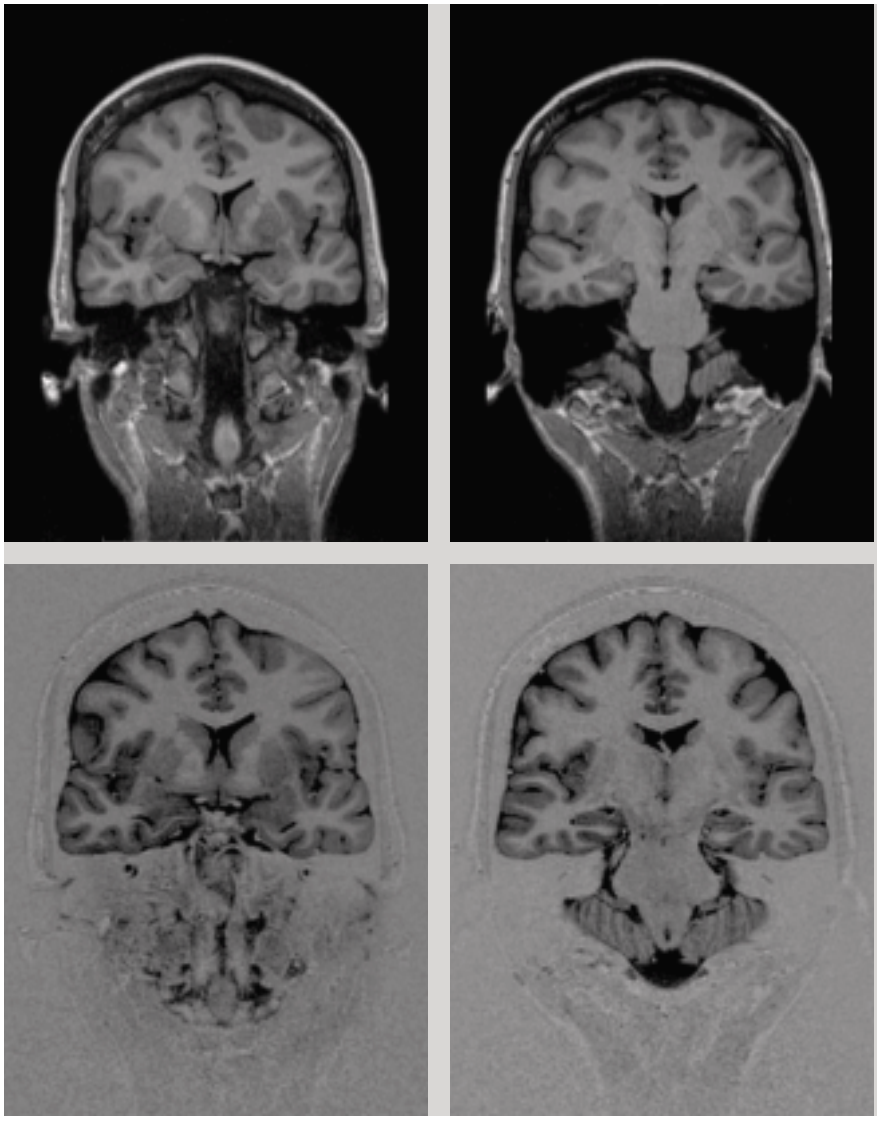

[Figure 10] *Normal hippocampal anatomy well demonstrated on both the MPRAGE [1 x 1 x 1 mm³, TA 6:8] (upper row) and T1-weighed SPACE (lower row).*

T1-weighed SPACE	
Slice	*1.0 mm sagittal x 176*
FoV	*228 x 260*
Steps	*223 x 256*
Voxel	*1 x 1 x 1 mm³*
TA	*8:50**
NA	*1*
TR	*4000*
TE	*354*
TI	*350*

*These sequeces have been measured with a works in progress software version. With software version *syngo* MR B13 acquisition times will be about 50% shorter.

Pre-surgical Evaluation in Seizure Patients with Brain Lesions using Inline BOLD fMRI

B. Thomas[1], C. Kesavadas[1], A. K. Gupta[1], A. Mathew[2], S. Sujesh[3], T. Krishnamoorthy[1], S. Purkayastha[1], V.V. Radhakrishnan[4], K. Radhakrishnan[5]

[1]Departments of Imaging Sciences and Interventional Radiology, [2]Neurosurgery, [3]Biomedical Engineering, [4]Pathology and [5]Neurology, Sree Chitra Tirunal Institute for Medical Sciences and Technology, Trivandrum, Kerala, India

Introduction

Pre-surgical evaluation of patients with seizures due to brain lesions may need mapping of the eloquent cortex so as to minimize deficits after surgery and functional MR imaging (fMRI) has the potential to predict this non-invasively. In this study we analyzed the usefulness of Inline Blood Oxygen Level Dependent (BOLD) imaging in motor-sensory mapping and language lateralization (Fig. 1).

Purpose

To evaluate the effectiveness of fMRI using Inline BOLD in the surgical treatment planning of seizure patients with brain lesions, compared to a standard post-processing tool. Also to compare the results of fMRI with that of intra-operative cortical stimulation and Intra-carotid Amobarbital Test (IAT) in selected cases and the post-operative outcome in all the cases (Fig. 2).

Materials and methods

26 patients were included in the study (14 males, 12 females; mean age 23 years). The inclusion criteria: history of seizures, brain lesion/s, consideration for surgical treatment, and need for defining eloquent brain areas. The pathological substrates included Focal Cortical Dysplasia (FCD), Dysembryoplastic Neuro Epithelial Tumor (DNET), Glial Neoplasms, Gliosis, and Rasmussen's Encephalitis. All the cases were done on a 1.5T MRI unit (MAGNETOM Avanto, SQ-engine, Siemens Medical Solutions, Erlangen, Germany). Paradigms for eloquent areas were tailored according to brain region of suspected seizure focus. The motor and sensory mapping were done in most cases. Language paradigms included verbal fluency and semantic decision tasks. The data were analyzed using the Inline BOLD software provided by the vendor. The first 12 patients were also analyzed with Statistical Parametric Mapping 2 (SPM2, Wellcome Institute of Neurology,

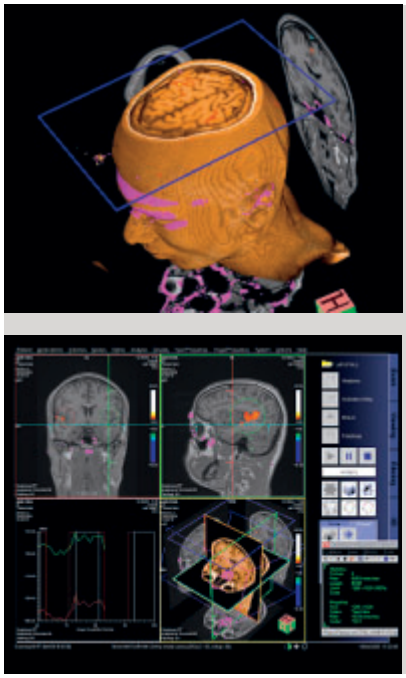

[Figure 1] *Inline BOLD imaging results seen on the syngo user interface.*

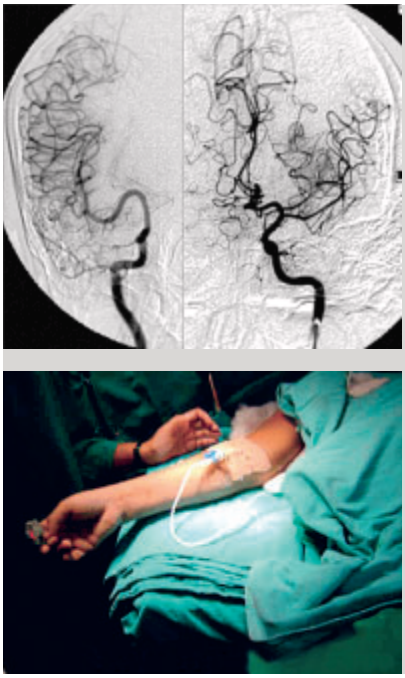

[Figure 2] *Performing the WADA test.*

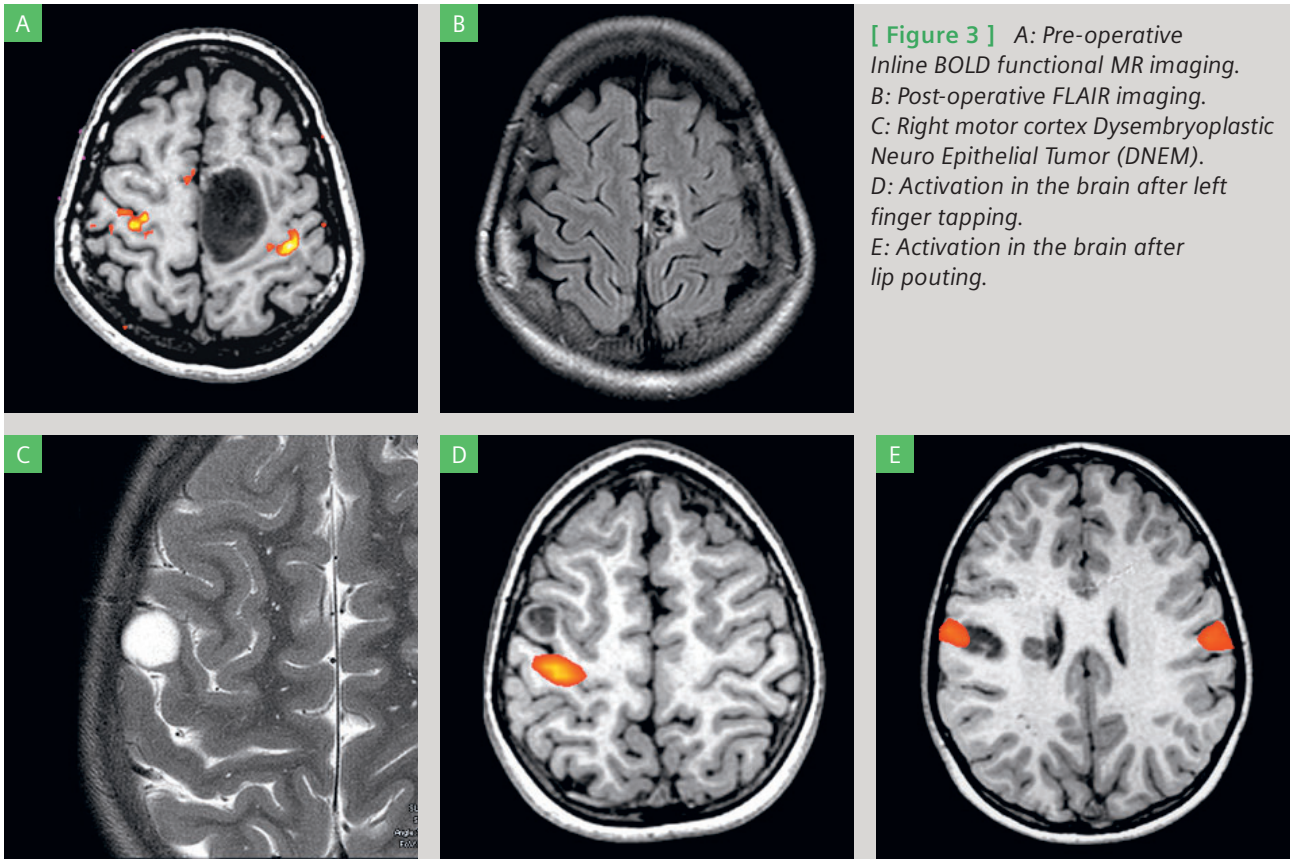

[Figure 3] *A: Pre-operative Inline BOLD functional MR imaging. B: Post-operative FLAIR imaging. C: Right motor cortex Dysembryoplastic Neuro Epithelial Tumor (DNEM). D: Activation in the brain after left finger tapping. E: Activation in the brain after lip pouting.*

London) and the first 3 patients in whom language lateralization was to be studied underwent the IAT. 4 patients underwent intra-operative cortical stimulation. In all patients a detailed post-surgical neurological assessment was done.

Results

In 12 patients language mapping and in 21 sensory-motor mapping were performed. In the initial 12 patients, comparison of Inline BOLD to SPM processing showed perfect correlation in all patients (100%). The IAT gave only hemispheric lateralization whereas fMRI showed the receptive and motor language areas more precisely. In the latter 9 patients, language lateralization was done solely based on the fMRI results. However laterality was determined only by visual assessment and a 'laterality index' could not be calculated. The fMRI results agreed with the results of intra-operative cortical stimulation in all the patients. fMRI predicted the post-surgical neurological deficits in 7 patients in whom the lesions were placed extremely close to eloquent cortex and post-operative follow up confirmed these findings (Fig. 3).

Conclusion

Inline BOLD has made functional MRI an easily performable clinical diagnostic tool for the pre-surgical assessment of patients with seizures. The results of this fMRI technique correlated well with that of standard post-processing methods, intra-operative cortical stimulation, IAT and post-surgical neurological assessment.

Reference

[1] Yetkin FZ, Mueller WM, Morris GL, et al: Functional MR activation correlated with intraoperative cortical mapping. AJNR Am J Neuroradiol 18: 1311–1315, 1997.

[2] Adcock JE, Wise RG, Oxbury JM, et al. Quantitative fMRI assessment of the differences in lateralization.

MRI, ^{1}H MRS and DWI in Cysts and Cyst Like Infective Lesions of the Brain

B. Thomas[1], C. Kesavadas[1], T. Krishnamoorthy[1], A. K. Gupta[1], V. V. Radhakrishnan[2], T. R. Kapilamoorthy[1], N. K. Bodhey[1], S. Purkayastha[1]

[1]Department of Imaging Sciences and Interventional Radiology, [2]Pathology, Sree Chitra Tirunal Institute for Medical Sciences and Technology, Trivandrum, Kerala, India

Introduction

Precise etiological diagnosis of infective lesions of the brain is clinically important and radiologically challenging. The newer imaging methods like Diffusion Weighted Imaging (DWI) and ^{1}H MR Spectroscopy (MRS) are making an impact in the diagnosis of cystic infective lesions of the brain.

Purpose

To evaluate the usefulness of MRI, ^{1}H MRS and DWI in the differential diagnosis of cysts and cyst like infective lesions of the brain.

Materials and methods

28 cases of infective lesions presenting with cysts or cyst like intracranial lesions on MR imaging were selected for the study. There were 16 tuberculomas (Fig. 1), 5 intra parenchymal cysticercosis (Fig. 1), 2 tuberculous abscesses, 2 pyogenic abscesses (Fig. 2), 1 case of chronic sterile abscess (Fig. 3), 1 cryptococcosis and 1 racemose cysticercosis (Fig. 4). All the cases were done on a 1.5T MRI unit (MAGNETOM Avanto, SQ-engine, Siemens Medical Solutions, Erlangen, Germany). MR imaging including T1- and T2-weighted sequences and post contrast fat saturated images were obtained. 3D con-

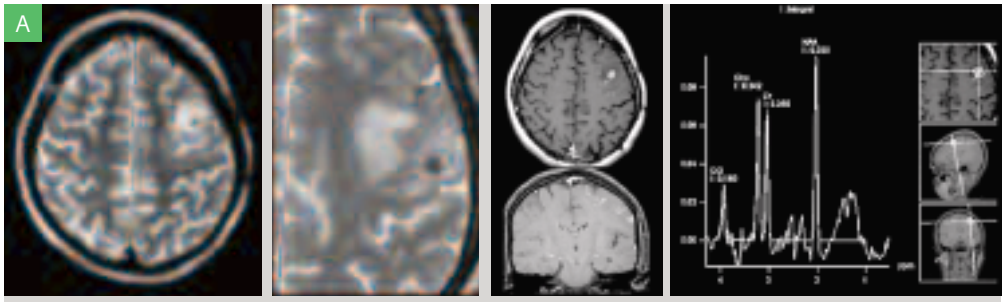

[Figure 1A] *Images showing a patient with intracranial tubercolomas. Spectroscopy measurement indicated a lipid peak.*

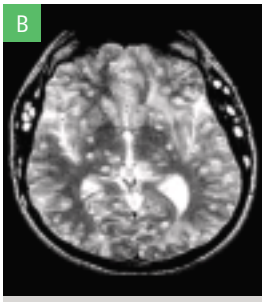

[Figure 1B] *A case of parenchymal cysticercosis.*

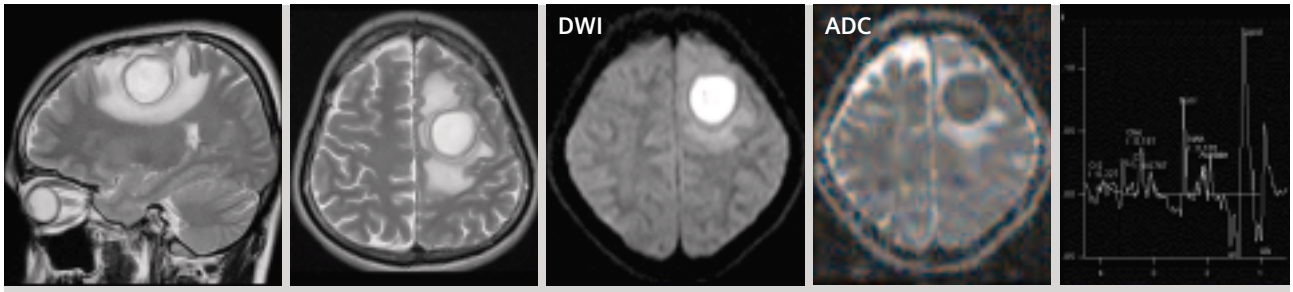

[Figure 2] *Pyogenic abscess. Note the presence of aminoacids in the spectroscopy results.*

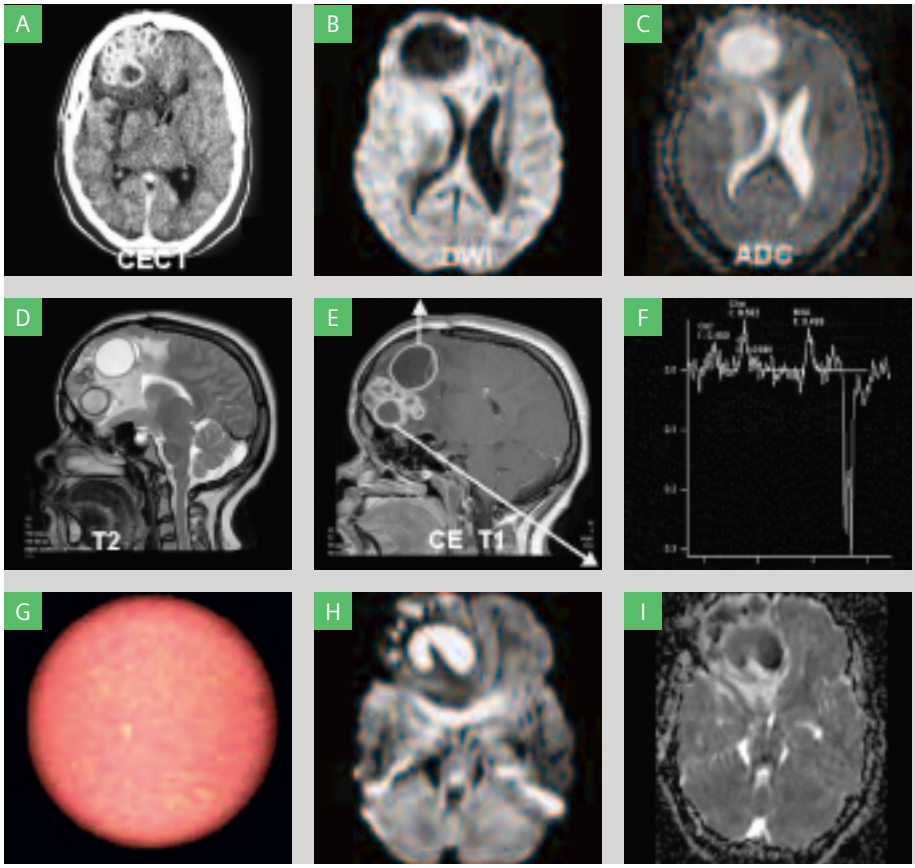

[Figure 3] *Chronic brain abscess. Upper frontal lobe lesion shows increased ADC contrary to the other lesions with restricted ADC. This finding is an important differentiator for chronic abscesses, as other pyogenic infections show restricted ADC.*

structive interference at steady state (CISS) imaging was done in the racemose cysticercosis case (Fig. 4). In addition DWI, Inline ADC maps, MRS at TE 30, 135 and 270 ms using a PRESS sequence were obtained. Histopathological correlation was obtained whenever possible except in the cases of tuberculomas and parenchymal cysticercosis, where therapeutic response was noticed.

Results

The granulomas showed a hyperintense rim on T1-weighted images, which was hypointense on T2, (90% of the cases) with variable perilesional edema. The presence of a 'scolex' was characteristic of parenchymal cysticercosis, but was seen in 3 of the 5 cases (60%). CISS images demonstrated the racemose cysticercosis best (Fig. 4). The abscesses showed

restricted diffusion except in a portion of the chronic sterile abscess (Figs. 2 and 3). The tuberculomas and tuberculous abscesses showed a prominent lipid peak (0.9 and 1.3 ppm) (16/18 cases, 88.9%) (Fig. 1). The cysticerci, especially the racemose cyst showed no restriction on diffusion and the presence of lactate (1.33 ppm), alanine (1.47 ppm), acetate (1.92 ppm) and succinate (2.4 ppm) on MRS (Fig. 4). The pyogenic abscesses were characterized by cytosolic aminoacids (0.9 ppm), lactate, alanine, acetate, succinate and glycine (3.56 ppm) (Fig. 2).

Conclusion

It is possible to differentiate between the various causes of cysts and cyst like infective lesions of the brain using MR imaging, ^{1}H MRS and Diffusion-weighted imaging (DWI). This differentiation is therapeutically very important.

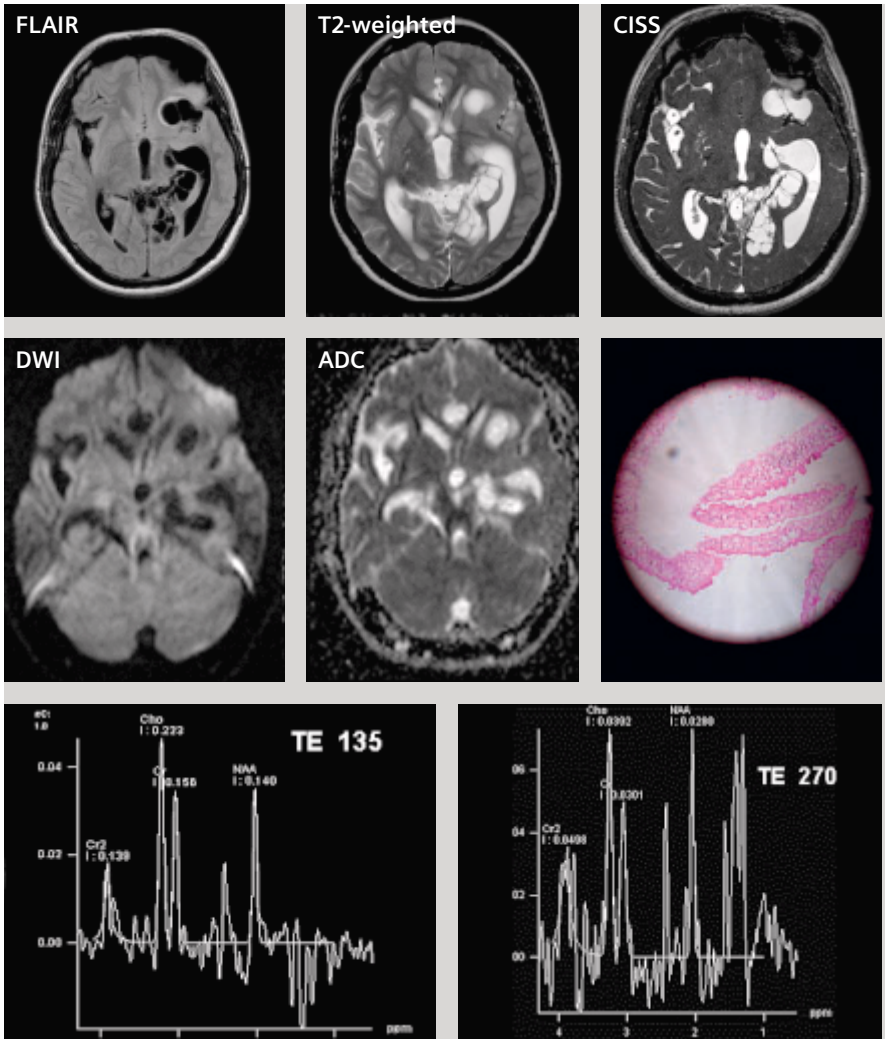

[Figure 4] *MR imaging and MR spectroscopy of cerebral cysticercosis. Note that there is no restricted diffusion.*

References

[1] Gupta RK, Prakash M, Mishra AM, Husain M, Prasad KN, Husain N. Role of diffusion weighted imaging in differentiation of intracranial tuberculoma and tuberculous abscess from cysticercus granulomas-a report of more than 100 lesions. Eur J Radiol. 2005; 55: 384–92.

[2] Garg M, Gupta RK, Husain M, Chawla S, Chawla J, Kumar R, Rao SB, Misra MK, Prasad KN. Brain abscesses: etiologic categorization with in vivo proton MR spectroscopy. Radiology. 2004; 230: 519–27.

Proton MR Spectroscopic Imaging of the Mesial Temporal Lobe

C. Kesavadas, B. Thomas, A. K. Gupta, T. Krishnamoorthy, T.R. Kapilamoorthy, N. Bodhey

Sree Chitra Tirunal Institute for Medical Sciences and Technology, Trivandrum, Kerala, India

Purpose

To evaluate variations in regional metabolite concentrations in the mesial temporal lobe (MTL) using Proton MR Spectroscopic Imaging (MRSI) in normal individuals and in patients with mesial temporal sclerosis (MTS).

Materials and methods

Metabolite concentrations and ratios were measured in 10 healthy people and in 10 patients with MTS using the 12-channel Head Matrix coil (phased array) on a 1.5T MR unit (Siemens MAGNETOM Avanto [76 x 18], SQ-engine, Erlangen,

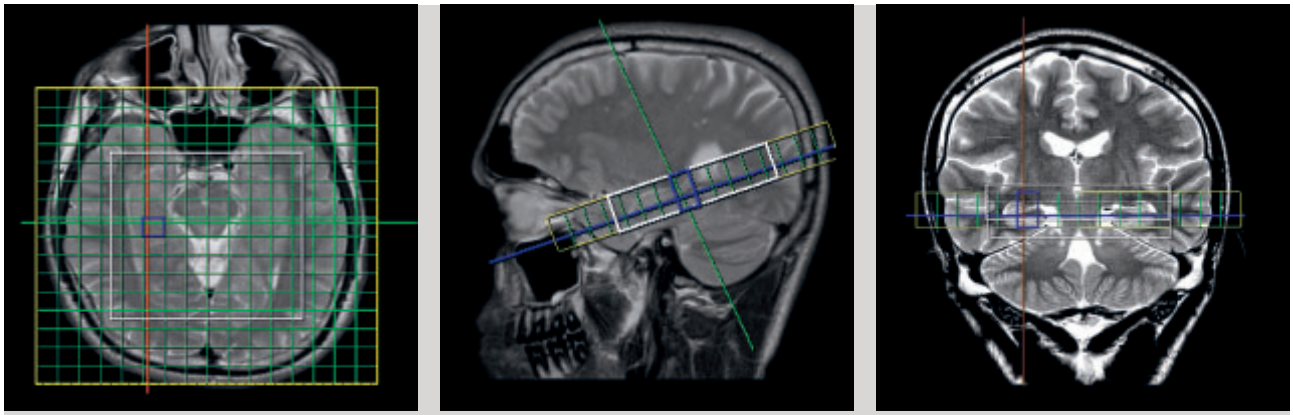

[Figure 1] *Plane of acquisition was along the hippocampus.*

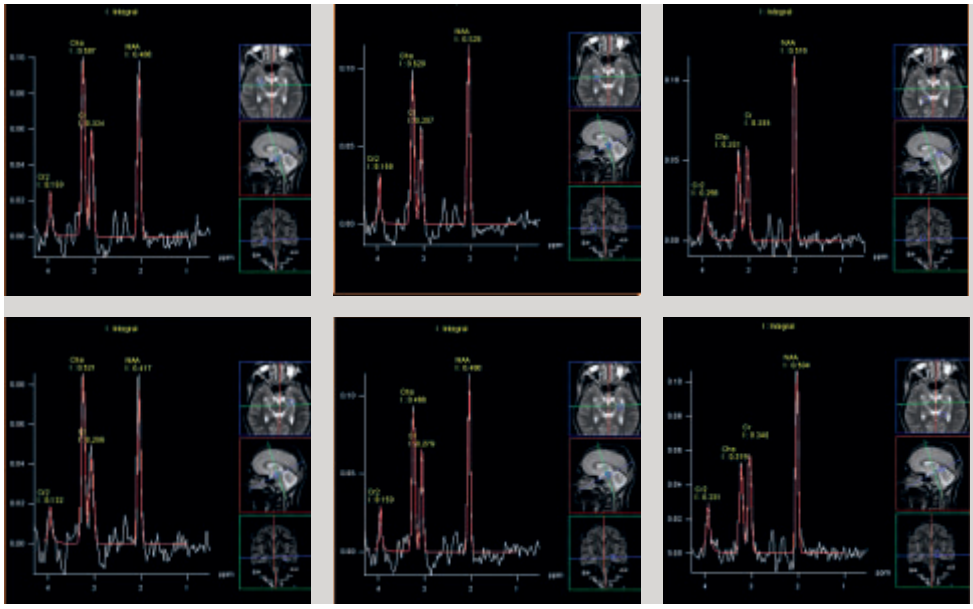

[Figure 2] *Spectra from the anterior, middle and posterior hippocampus show gradual decrease in choline from the anterior to the posterior hippocampus.*

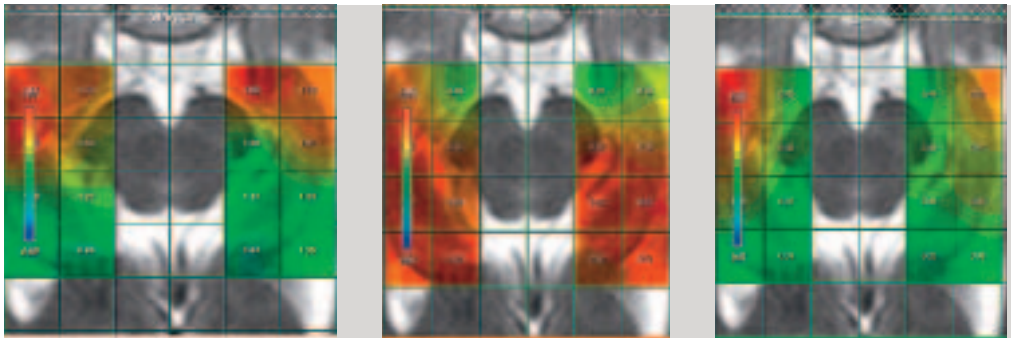

[Figure 3] *The color metabolite maps of the Cho/Cr ratio, the NAA and Cho maps allow easy interpretation of the spectroscopy data.*

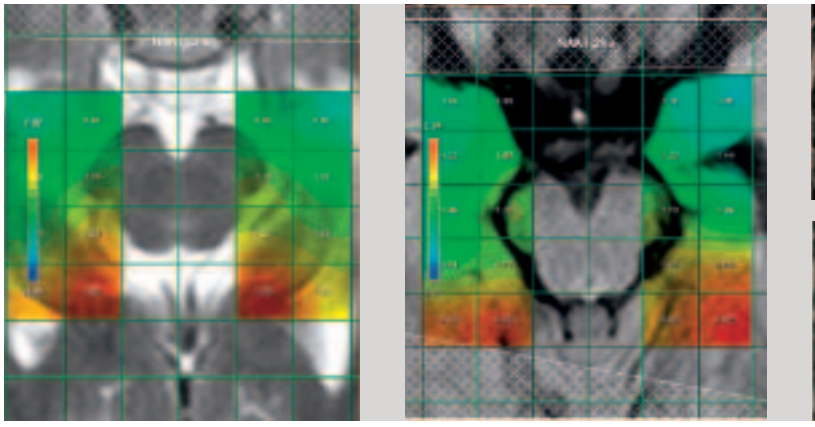

[Figure 4] *Decrease in NAA in the anterior hippocampus on the side of MTS. The normal MRI is given as a reference.*

Germany). In all the ten patients the clinical criteria, MRI with conventional seizure protocol and video EEG data lateralized the TLE (Temporal Lobe Epilepsy) to the same side. We used PRESS sequences with a TR of 1500 ms and TE of 30 ms and 135 ms. The acquisition was planned along the hippocampal plane (Fig. 1). Since the mesial temporal lobe is a difficult region of the brain for spectroscopy, we used 6 saturation bands and third order shimming to avoid magnetic field inhomogeneity. A spectral map and a metabolite image were created for the hippocampus on both sides.

Results

In the normal individuals the highest choline concentration was found in the Anterior Mesial Temporal Lobe (AMTL) than MMTL (Middle Mesial Temporal Lobe) and PMTL (Posterior Mesial Temporal Lobe) (Fig. 2). The N-Acetylaspartate (NAA) concentration was just the reverse. The Anterior Mesial Temporal Lobe also had a higher Cho/Cr ratio compared to the middle and posterior mesial temporal lobe (Fig. 3).

In patients with MTS the NAA map showed areas of decrease in NAA in areas of sclerosis. The map obtained from normal individuals served as reference (Fig. 4).

Conclusion

The MTL shows regional metabolite changes along its anteroposterior course. This has to be considered in the interpretation of pathologies involving the MTL.

The MRSI technique used in this study gives good and easily interpretable information about the metabolite concentrations in the normal and diseased hippocampus.

In patients with MTS an assessment of the metabolite image will define the severity and extent of involvement along the hippocampal head, body and tail.

Body

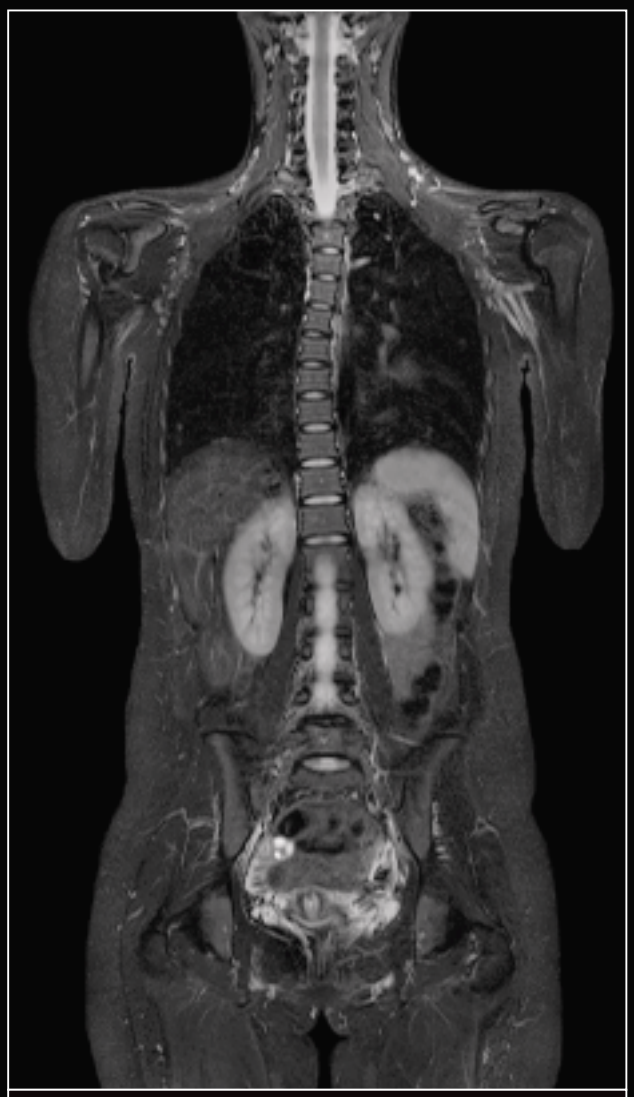

[1] ***MAGNETOM Avanto: Lymph node and bone screening*** / *T2-weighted TIRM / coronal / composed / GRAPPA with PAT factor 2 / invasive breast cancer. / TR 6060 ms / TE 68 ms / TA 5:28 min / SL 5 mm / slices 36.*
Courtesy of First Hill Diagnostic Imaging Center, Seattle, USA

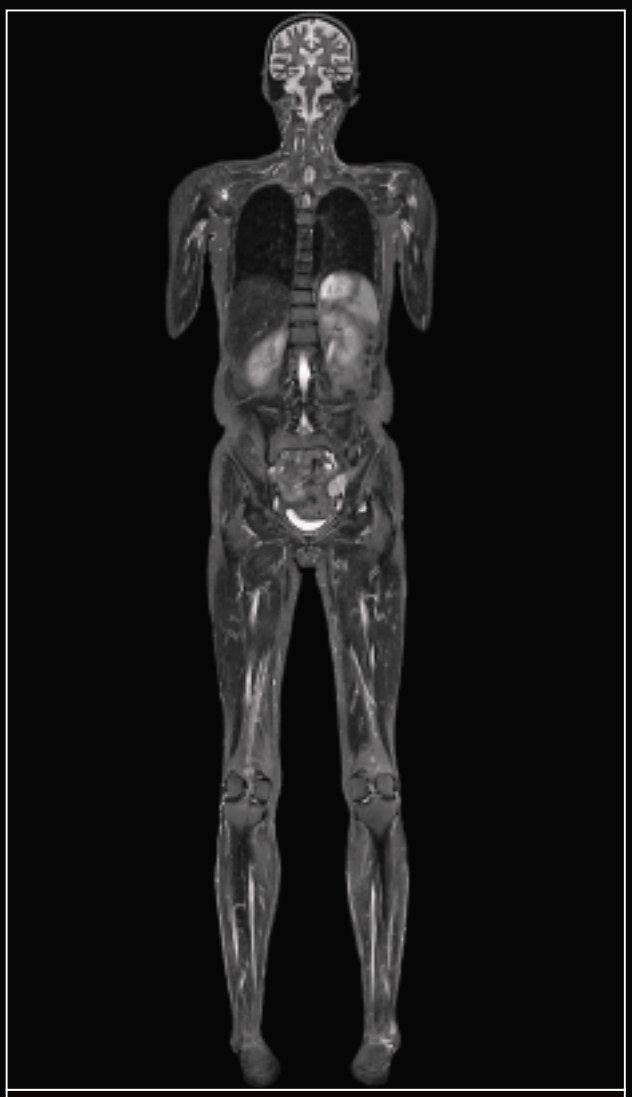

[2] ***MAGNETOM Avanto: Whole-body*** / *T2-weighted TIRM / coronal / 5 steps / GRAPPA 2 / melanoma. / TR 5490 ms / TE 87 ms / TI 150 ms / total TA 11:39 min / SL 5 mm / slices 23 / matrix 384 / FoV 1844 mm.*
Courtesy of Eberhard-Karls-University, Tuebingen, Germany

Comparison of Whole-Body MRI and Whole-Body PET-CT for Staging of Advanced Bronchial Carcinoma

C. Plathow[1], S. Eschmann[2], P. Aschoff[1], V. Heinrich[3], J. Schaefer[1], C. Claussen[1], T. Hehr[3], C. Pfannenberg[1], H-P. Schlemmer[1]

[1]*Department of Radiology, Eberhard-Karls-University Tuebingen, Tuebingen, Germany*
[2]*Department of Nuclear Medicine, Eberhard-Karls-University Tuebingen, Tuebingen, Germany*
[3]*Department of Radiation Oncology, Eberhard-Karls-University Tuebingen, Tuebingen, Germany*

Purpose

To compare whole-body MRI with whole-body PET-CT and thereby correctly evaluate tumor staging in patients with advanced Non-Small-Cell Lung Carcinoma (NSCLC).

Materials and methods

16 patients (11 male / 5 female) ranging in age from 49 to 71 years (mean age 62 years) with stage IIIb to IV NSCLC were examined prior to chemotherapy using whole-body MRI adapted for oncologic staging (Siemens Medical Solutions, MAGNETOM Avanto, 5 subsequent table positions, FLAIR axial (Brain), STIR coronal (whole-body) and axial (Neck), T2-weighted STIR-TSE axial (thorax), T1-weighted SE axial and coronal pre and post contrast (brain), T1-weighted 3D VIBE axial pre and post contrast (thorax), T2-weighted TSE fatsat axial (abdomen), T1-weighted 2D FLASH fatsat axial pre and post contrast (abdomen, neck, pelvis), T2-weighted STIR-TSE axial (pelvis); total acquisition time 60 min).
Within a period of 3 days, whole-body PET-CT was performed (400 MBq F-18-FDG, native CT in low dose technique and after CM application, iterative image reconstruction with CT based attenuation correction, total acquisition time 60 min). This was repeated after 3 weeks for first control. Tumors were staged independently by experienced radiologists and nuclear medicine specialists. In cases of discrepancy of tumor staging between whole-body MRI and PET-CT, the follow-up PET-CT served as a control.

Results

In 14 out of 16 patients, T-staging was identical using whole-body MRI and whole-body PET-CT. In 2 patients, MRI was able to correctly differentiate between tumor infiltration and no tumor infiltration of the chest wall, which was confirmed by the follow-up. In these 2 cases only STIR and T1-weighted 3D VIBE post contrast application sequences were able to correctly perform T-stage, whereas PET-CT over- or under-estimated T-staging. In 13 out of 16 patients N-staging was identical; in 1 patient whole-body MRI was able to correctly define a hilar lymphatic node, whilst in 2 cases PET-CT was able to correctly define ipsi- and contralateral lymphatic nodes. In all patients M-staging was identical.

Conclusion

Whole-body MRI using a dedicated sequence protocol for oncologic staging is able to correctly classify T-stage very accurately in patients with advanced bronchial carcinoma. STIR and T1-weighted 3D VIBE post contrast sequences seem to be particularly suitable for correct T-staging. Whole-body PET-CT seems to have advantages in correct N-staging.

References
[1] Schlemmer et al. 2005, Invest Radiol.
[2] Eschmann et al. 2004, Nucl Med Comm.
[3] Barkhausen et al 2001, Radiology.
[4] Antoch et al. 2003, JAMA Proc. Intl. Soc. Mag. Reson. Med. 14 (2006) 1798.

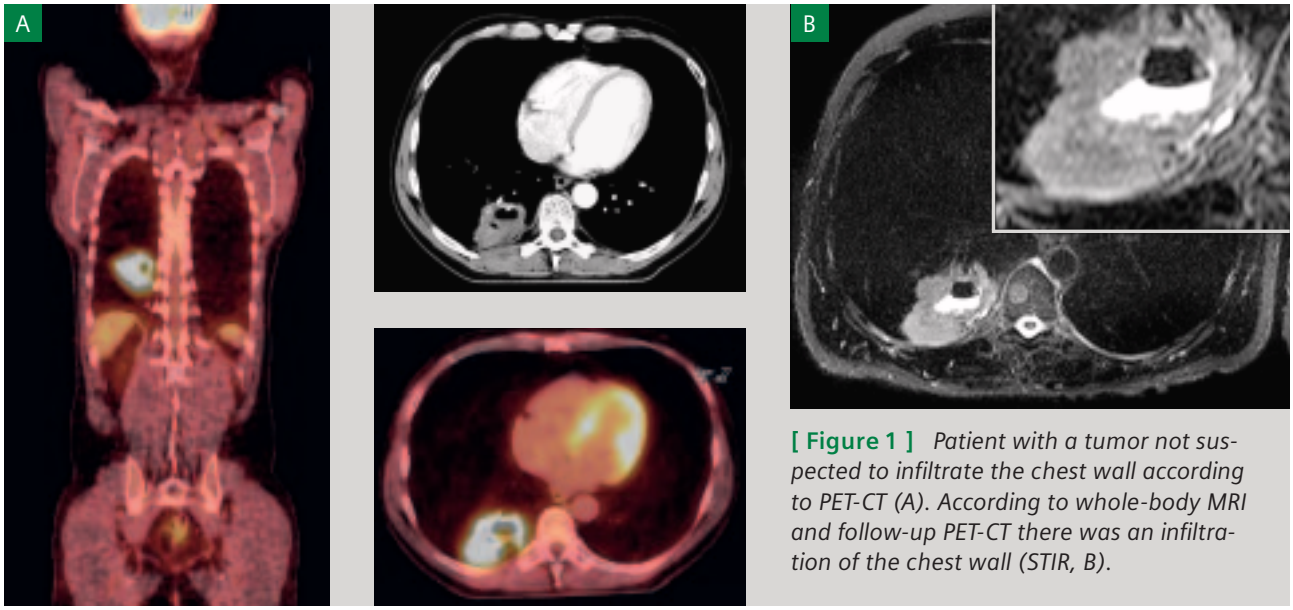

[Figure 1] *Patient with a tumor not suspected to infiltrate the chest wall according to PET-CT (A). According to whole-body MRI and follow-up PET-CT there was an infiltration of the chest wall (STIR, B).*

Table 1: PET-CT whole-body MRI comparison

Patient	I. PET-CT	II. Whole body MRI	T-staging		N-staging		Both	
			I.	II.	I.	II.	I.	II.
1.	T2N3	T4N3	–	+	+	+	–	+
2.	T2N3	T2N3	+	+	+	+	+	+
3.	T4N0	T4N0	+	+	+	+	+	+
4.	T4N0	T4N1	+	+	+	–	+	–
5.	T4N0	T4N0	+	+	+	+	+	+
6.	T2N3	T2N2	+	+	+	–	+	–
7.	T2N3	T2N3	+	+	+	+	+	+
8.	T4N1	T4N0	+	+	–	+	–	+
9.	T4N3	T4N3	+	+	+	+	+	+
10.	T2N2	T2N2	+	+	+	+	+	+
11.	T3N3	T3N3	+	+	+	+	+	+
12.	T4N2	T4N2	+	+	+	+	+	+
13.	T3N3	T3N3	+	+	+	+	+	+
14.	T4N2	T3N2	–	+	+	+	–	+
15.	T3N2	T3N2	+	+	+	+	+	+
16.	T3N2	T3N2	+	+	+	+	+	+

List of all included patients. + correct staging, – incorrect staging, M-staging is not shown, as there was no difference between both techniques.

Rectal Cancer Local Staging. A Review using SPACE

M. K. Seale; M. E. Lourensz; N. M. Trost; P. J. Smith

St Vincent's Hospital Melbourne, Australia

Introduction

Magnetic resonance imaging (MRI) has emerged as an accurate method for local staging of rectal cancer, which is vital in determining appropriate treatment of this disease.

Colorectal cancer is the most common cancer in Australia (excluding non-melanoma skin cancers), and second most common cause of cancer deaths (after lung cancer). Rectal cancers are usually adenocarcinoma, and account for 1/3 of colorectal malignancies. Prognosis is directly related to the extent of local spread [1]. The more locally advanced the tumor, the greater the risk of distant metastases, and of local recurrence, which is often debilitating and incurable.

The main aims of treatment are to control local disease, to optimize survival and quality of life. This requires resection with minimization of the risk of local recurrence.

In the majority of cases, the current preferred surgical approach is "total mesorectal excision" (TME). The rectum is removed 'en bloc' with its surrounding sleeve of fat and visceral fascia (the 'mesorectum'). Embedded within the fat are the draining lymph nodes of the rectum. TME has been shown to markedly reduce the risk of local recurrence, and to increase 5 year survival [3].

Role of staging

The local extent of rectal cancer determines optimum treatment. Patients with early disease (T1, T2) proceed directly to surgical resection, while neoadjuvant chemotherapy and/or radiotherapy is recommended for patients with locally advanced tumors (T3, T4 tumors). This stratification of treatment means a reliable method of pre-operative imaging is required.

Role of MRI

While endorectal ultrasound and endorectal MRI give high resolution images of the layers of the rectal wall, both have limited field of view and hence provide limited assessment of perirectal tissues. Conversely, MRI performed with phased array surface coils demonstrates the layers of the rectal wall, and perirectal tissues. Bowel preparation is not required, and unlike endorectal techniques, imaging is unaffected by size or degree of stenosis caused by the rectal tumor. As well as demonstrating the local extent of the primary tumor, MR of the rectum clearly depicts the mesorectal fascia, which is the desired plane of surgical dissection. This allows the surgeon to visualize the tumor and its relationship to the surgical margin and other structures.

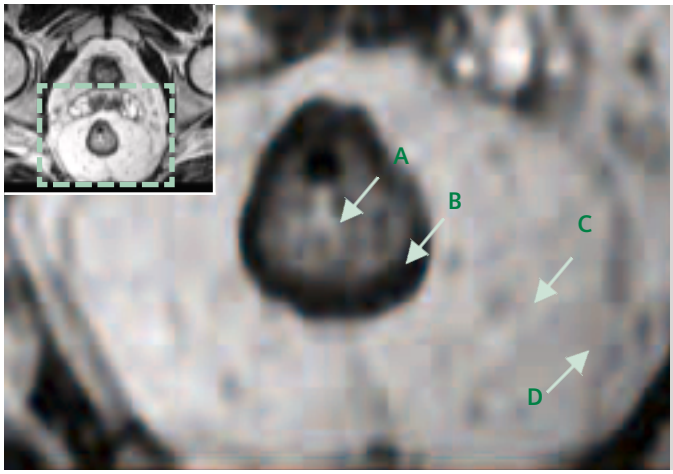

[A] *Hyperintense mucosa & submucosa (no differentiation between layers possible)*
[B] *Hypointense muscularis propria (differentiation between inner circular & outer longitudinal layers sometimes possible)*
[C] *Hyperintense mesorectal fat*
[D] *Thin hypointense layer of mesorectal fascia*

[Figure 1] *Axial T2-weighted sequence showing layers of the rectal wall and surrounding mesorectum.*

Hence, MR is currently the best modality for T staging of rectal cancer. It is also useful for regional nodal staging, but has a limited role in evaluation for distant metastases, for which CT is better suited.

Current standard protocol

Most recent literature describes sequential fast spin echo (FSE) T2-weighted imaging using phased array surface coils. We perform sagittal images of the bony pelvis and axial images of the whole pelvis, using a field of view of 240 mm, slice thickness of 5 mm, and in-plane resolution of 0.9 x 0.5 mm. High resolution axial images perpendicular to the long axis of the tumor are then acquired using 160 mm field of view, 3 mm slice thickness, and in-plane resolution of 0.6 x 0.6 mm. Coronal images are added for low rectal lesions to evaluate tumor relationship to levator ani.

SPACE sequence

In addition to the MR protocol described above, approximately 50 recent cases of rectal cancer from our institution have been imaged with 'SPACE', a Siemens T2-weighted 3D sequence. The 3D variable flip angle T2 turbo spin echo sequence is acquired in the coronal plane, covering the rectal cancer and most of the pelvic contents. This gives isotropic 1 mm voxels, allowing image reconstruction in any plane. It also allows curved reformats to be reconstructed (Fig. 2). The sequence produces contrast similar to conventional T2 FSE 2D sequences, and takes approximately 8 minutes* to acquire.

We use a *syngo* Multi-Modality Work Place (Leonardo 3D workstation) to read the study (Fig. 3). This has the advantages of scrolling through the scanned volume in any plane to evaluate the tumor and evaluate its relationship to adjacent structures. Vessels can be followed, and easily differentiated from lymph nodes (Fig. 4). There is a minor degree of in-plane loss of resolution compared to the high resolution images from the current standard protocol, but we believe this is offset by the ability to scroll.

All MR images in this article are examples of the SPACE sequence.

Staging

Rectal cancer is staged according to the 'TNM' system, which indicates extent of the primary tumor ("**T**"), involvement of regional nodes ("**N**"), and distant metastases ("**M**").

*This examination was carried out using a *syngo* MR 2004V WIP package. With the new *syngo* MR B 13 product sequences examination time decreased to approx. 4 minutes.

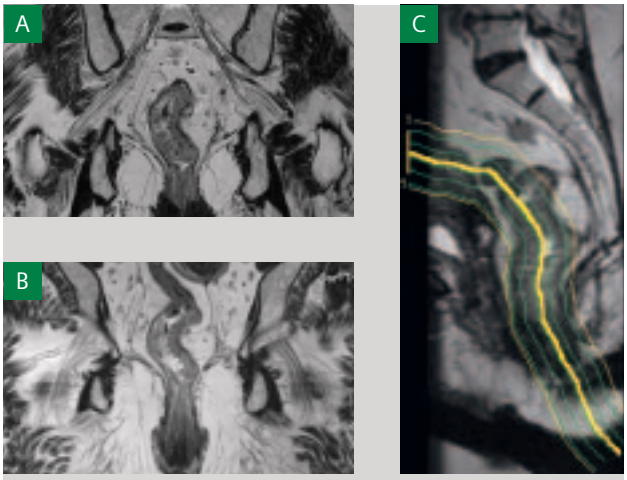

[Figure 2] *A) Coronal image of low rectal cancer in 80-year-old female. B) Curved coronal multiplanar reconstruction (MPR) gives a clearer depiction of tumor extent. C) Scout for planning of curved MPR.*

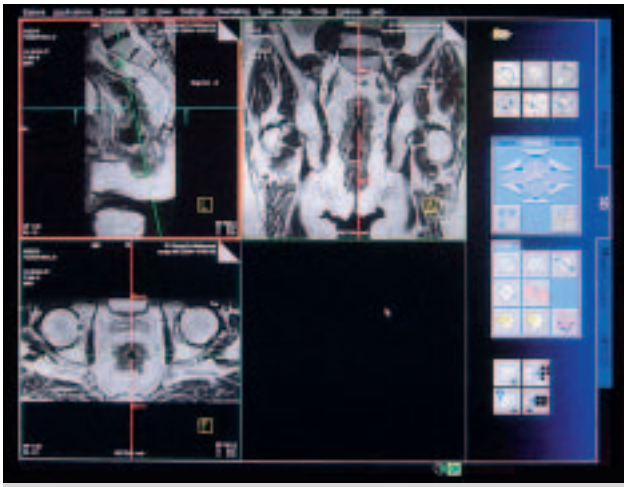

[Figure 3] *syngo Multi-Modality Work Place (Leonardo 3D workstation) used to view 3D volume sequence.*

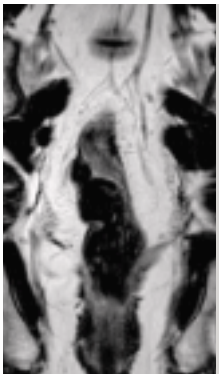

[Figure 4] *Curved coronal MPR in 59-year-old male with a mid-rectal tumor clearly depicts the superior rectal vessels. Lymphatic drainage of mid-upper rectal tumors is along the course of these vessels.*

TNM staging of rectal cancer is summarized below:

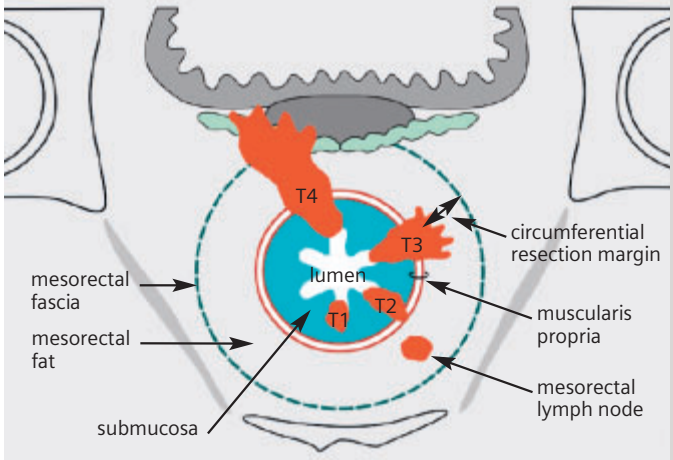

[Figure 5] ***T stage:***
T1 *Tumor invades submucosa*
T2 *Tumor invades muscularis propria*
T3 *Tumor invades through the muscularis propria*
T4 *Tumor directly invades other organs or structures, and/or perforates visceral peritoneum*

Tumor is usually of intermediate (IM) signal intensity (SI), between that of hyperintense mucosa / submucosa, and hypointense muscularis propria

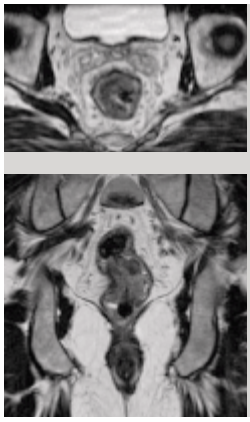

[Figure 6] *IM SI tumor in the mucosal / submucosal layers of the rectum of 53-year-old male patient. Note the tumor does not penetrate the hypointense muscularis propria. This was a T1 tumor at resection.*

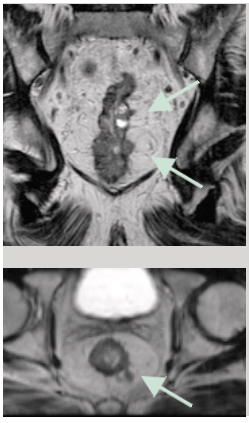

[Figure 8] *Coronal and axial images of a midrectal tumor in a 78-year-old male. Nodular extension of IM SI tumor is seen in both planes in this T3 tumor (arrow heads).*

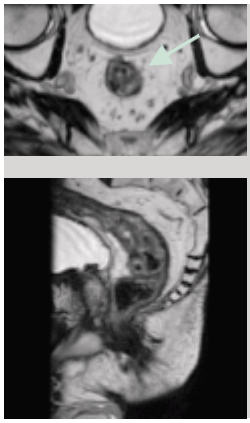

[Figure 7] *83-year-old male. Axial and sagittal images of a mid-rectal tumor, IM SI extending into but not through hypointense muscularis propria at the left lateral aspect of the rectum (arrow head). T2 tumor was confirmed histolgically.*

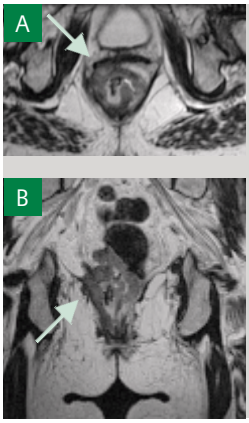

[Figure 9] *Axial and coronal images of a low rectal cancer in a 63-year-old female. Tumor invades the right vaginal fornix (A) and right levator ani (B) (arrow heads). This patient unfortunately had distant metastases. She underwent chemo/radio therapy for control of local disease.*

Micrometastases to normal-size nodes are common in rectal cancer [2], and so unfortunately, size criteria have been found to be neither sensitive nor specific in predicting nodal involvement. (Figs. 10, 11). Some studies suggest irregular border and/or heterogenous signal intensity (SI) may help detect involved nodes. Early studies using ultrasmall superparamagnetic iron oxide particles (USPIO)* are promising – normal nodes take up the particles and appear low in signal, whereas nodes replaced by neoplastic cells do not, and have high SI.

N Stage:
N0 *No regional lymph node metastases*
N1 *Metastasis in 1 to 3 perirectal lymph nodes*
N2 *Metastasis in 4 or more perirectal lymph nodes.*
N3 *Metastasis in node along the course of a named vessel*

M stage:
M0 *No distant metastases*
M1 *Distant metastases*

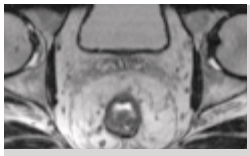

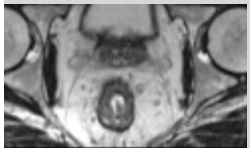

[Figure 10] *Axial images through 2 levels in this 58-year-old male with a mid rectal tumor show numerous small to medium size nodes, suspicious for nodal spread. However, the tumor was T3N0 at resection.*

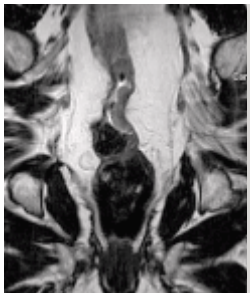

[Figure 11] *Curved coronal MPR in a 59-year-old male showing a representative image of a midrectal tumor and surrounding mesorectum. There were no discernible nodes in the mesorectum on MR. However, histologically, this was a T3N2 tumor.*

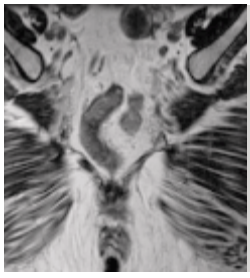

[Figure 12] *Heterogenous nodes in the mesorectum of this 80-year-old female are clearly abnormal. She had a T3N2 tumor.*

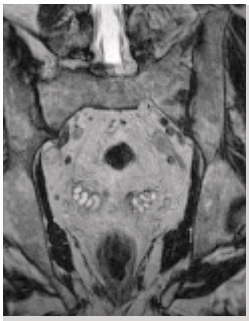

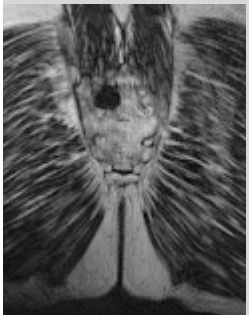

[Figure 13] *Although it is uncommon to see metastases to other structures in the pelvis on MR, a thorough inspection should be made. In this 75-year-old male with past history of rectal cancer, bone lesions in the right sacral promontory and left sacral ala are suspicious for metastases.*

Other Local Prognostic Indicators

1. Circumferential Resection Margin (CRM)

The minimum distance from tumor to the surgical resection plane (the mesorectal fascia) is termed the circumferential resection margin (CRM). Several studies have shown this to be a more powerful predictor for local recurrence than T stage [2] i.e. the smaller the CRM, the greater the risk of local recurrence.

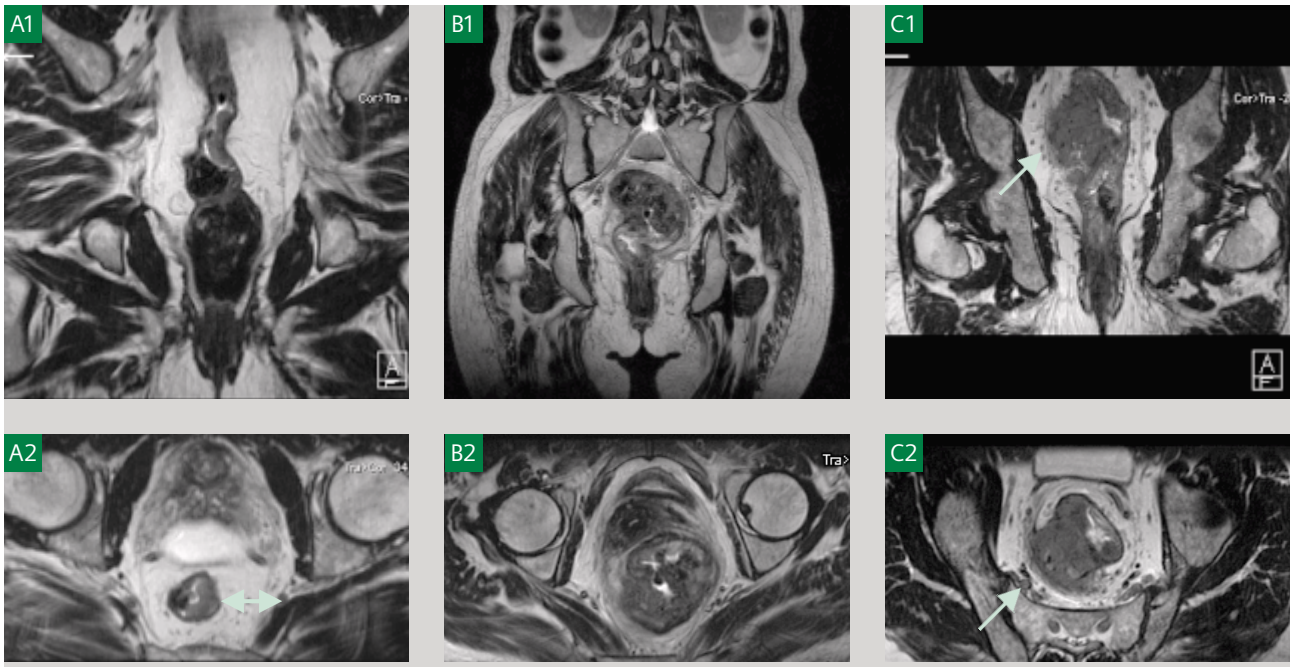

[Figure 14] *3 patients with T3 rectal cancers with variable CRM (coronal and axial image of each case). (A) demonstrates a mid rectal cancer with a wide CRM (double headed arrow); (B) the CRM is very small – 3 mm on histology; in (C) IM SI tumor invades the thin hypointense layer of mesorectal fascia on the right (arrow heads). If this patient underwent TME, the surgical margin would be involved, and residual tumor would remain in situ. Neoadjuvant treatment was given to the patients in (B) and (C) to decrease tumor bulk preoperatively, increase CRM and improve chances of tumor-free resection margin at surgery.*

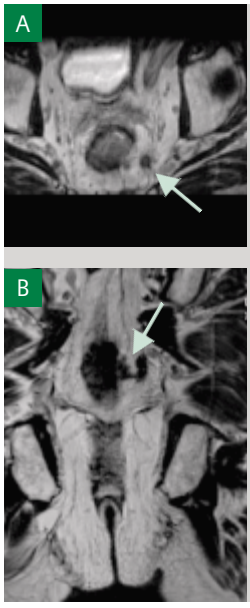

[Figure 15] *Axial image (A) clearly demonstrates T3 tumor in this 90-year-old male. A suspicious nodule in the region of the mesorectal fascia on the left is shown to be part of nodular venous spread on curved coronal MPR (B).*

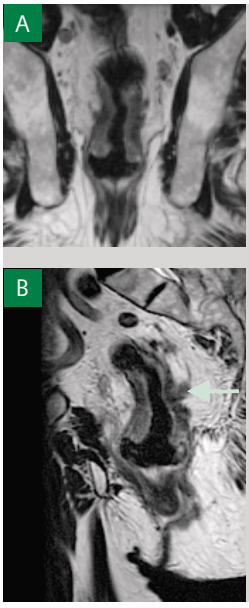

[Figure 16] *A classic 'apple core' stenosing rectal cancer is shown on a curved coronal MPR (A) in this 72-year-old male. Oblique coronal image (B) demonstrates tubular extension of tumor along perirectal vessels.*

2. Extramural venous invasion

Rectal cancer may spread along vessles in perirectal fat, and if present, this is a poor prognostic indicator. On MR, this is seen as discrete tubular projection of tumor along the course of perirectal vessels, and is particularly observed posteriorly along the superior rectal vessels.

3. Peritoneal infiltration

Rectal cancer which has penetrated into the peritoneal cavity may become disseminated via transcoelomic spread. This is of particular concern for tumors of the mid to upper rectum.

Conclusion

Rectal cancer is a major cause of morbidity and mortality in our population. Accurate local staging is required to determine treatment and prognosis. Rectal MRI with phased array surface coils currently gives the best local assessment of rectal cancer, enabling T staging and prediction of CRM. This helps identify patients at increased risk of local recurrence, who would benefit from neoadjuvant therapy. We have found the new T2 3D sequence (SPACE) helpful in increasing the accuracy of MR staging. The SPACE sequence is easy to acquire, allows visualization and "scroll through" of the scanned field in any plane on a 3D workstation, and also allows formation of curved reformats along the entire length of the rectum.

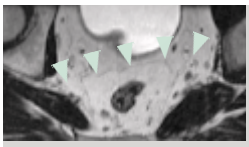

[Figure 17] *Axial image through the upper rectum in this 51-year-old male (with a low rectal tumor) shows the normal peritoneal reflection, which passes from the superior aspect of the bladder posteriorly to the junction between the upper 2/3 and mid 1/3 of the rectum, attaching onto the anterior aspect of the rectum in a V-shape [5].*

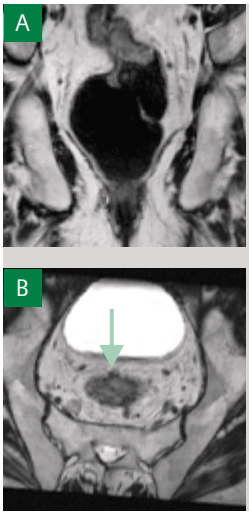

[Figure 18] *This 81-year-old male has a high rectal tumor, seen on curved coronal MPR (A). Axial image at the level of the peritoneal reflection demonstrates IM SI nodule anteriorly, at the site of peritoneal attachment to the rectum. This patient is at increased risk of peritoneal spread. Also note tumor nodule projecting posteriorly into mesorectal fat, and probable involved node on the right.*

Acknowledgements:

Thank you to Dr. Robin Cassumbhoy for original illustration in Figure 5; and for general graphics assistance.

Please note that the above information and images have been presented in poster format at RANZCR Scientific Meeting, Christchurch, New Zealand, October 2006.

*This contast agent is not yet available in Australia.

References

[1] Brown G, Richards CJ, Newcombe RG et al. Rectal Carcinoma: Thin-section Imaging for staging in 28 patients. Radiology 1999; 211: 215–222.

[2] Beets-Tan RGH, Beets GL; Rectal Cancer: Review with Emphasis on MR Imaging. Radiology 2004; 232: 335–346.

[3] Iafrante F, Laghi A, Paolantonio P et al. Preoperative Staging of Rectal Cancer with MR Imaging: Correlation with Surgical and Histopathologic Findings. Radiographics 2006; 26: 701–714.

[4] Brown G, Daniels IR, Richardson C, Revell P, Peppercorn D, Bourne M. Techniques and trouble-shooting in high spatial resolution thin slice MRI for rectal cancer.

[5] Brown G, Kirkham A, Willaims GT et al. High-Resolution MRI of the Anatomy Important in Total Mesorectal Excision of the Rectum. AJR 2004;182: 431–439.

VIBE: Fast Gradient Echo Imaging for Every Part of the Body

Brian M. Dale, Ph.D.; Helmuth Schultze-Haakh, Ph.D.; Agus Priatna, Ph.D.

R&D, Siemens Medical Solutions

Introduction

VIBE (Volume Interpolated Breath-hold Exam) is one of the most important pulse sequences in the industry. It is a fast and reliable spoiled GRE (Gradient Recalled Echo) sequence which can easily acquire high resolution T1-weighted 3D volumes in short acquisition times. Although it was originally designed and intended primarily for abdominal imaging, the VIBE sequence has also found an important role in most other areas of the body. These other applications have been refined and expanded by Siemens and our partners over the course of our many years of clinical experience with VIBE. In addition, VIBE is fully integrated with our industry-leading Tim (Total imaging matrix) technology, which makes it even more powerful thanks to higher resolution and greater acquisition speed than ever before.

Tim Matrix coils and iPAT

One of the chief advantages of the VIBE sequence is its complete integration into the Tim (Total imaging matrix) platform. All Tim Matrix coils are compatible with the VIBE sequence, which allows the acquisition of T1-weighted 3D GRE images at every location in the body with high SNR (signal-to-noise ratio). In addition, under the current software version, the VIBE sequence can utilize iPAT (integrated Parallel Acquisition Techniques) acceleration in both the phase-encode and partition-encode or slice directions for the highest acceleration factors possible (Fig. 1). The iPAT (integrated Parallel Acquisition Technique) algorithms themselves have been improved and refined specifically with the intention to bring these higher acceleration factors into standard clinical use. Our widespread use of integrated reference scans elim-

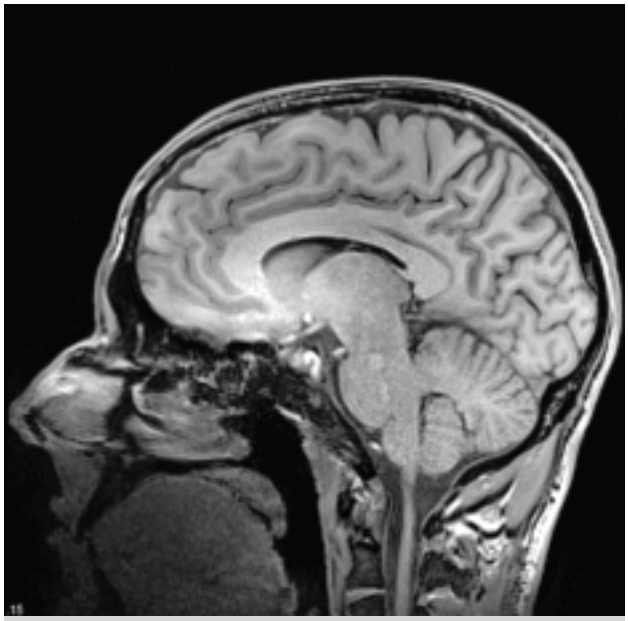

[Figure 1] *Very high temporal resolution using iPAT², at least a factor of 6.*

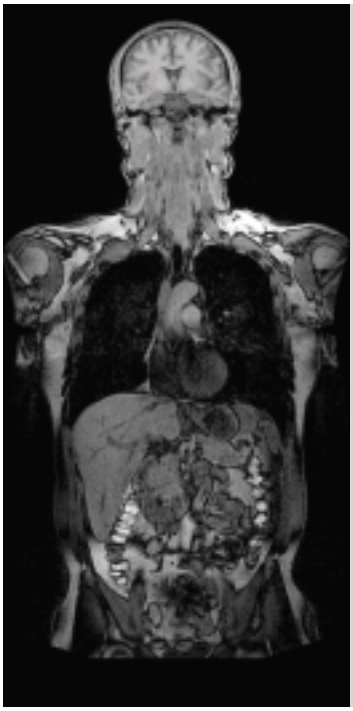

[Figure 2] *A Large FOV and high spatial resolution with inline compose.*

inates artifacts often caused by patient movement between the reference scan and the imaging scan. Finally, the Inline compose feature of Tim allows multiple acquisitions to be concatenated into a single data set. As shown in Fig. 2, this permits the acquisition of large FoV images without compromising spatial resolution.

Contrast-enhanced imaging

With the T1-weighting of VIBE, the use of T1-shortening contrast agents is a natural and effective combination, particularly at ultra-high field strengths where tissue T1 values are lengthened. In addition to the excellent anatomical information inherently provided by T1-weighted VIBE, a wide variety of pathologies can also be clearly depicted with the administration of contrast. When combined with iPAT acceleration, the SNR increase from contrast uptake can be effectively traded for further improvements in spatial or temporal resolution.

Many of the standard Siemens protocols using VIBE also incorporate Inline processing, for example subtractions of a pre-contrast data set from post-contrast ones as well as Maximum Intensity Projections (MIPs) in various orientations.

Abdominal and pelvic imaging

The original uses for VIBE were abdominal and pelvic imaging and they still continue to be the dominant applications. High resolution T1-weighted 3D abdominal images can easily be acquired in a single breath-hold, particularly when using Tim and Parallel Imaging. Even patients with limited breath-holding capability can be accommodated when Parallel Imaging is used. The VIBE 3D encoding scheme ensures that there are no gaps between slices. Time efficient fat suppression is achieved through spectral saturation and centric reordering. The net result is a simple, fast, reliable sequence for generating high-quality anatomical datasets in the abdomen.

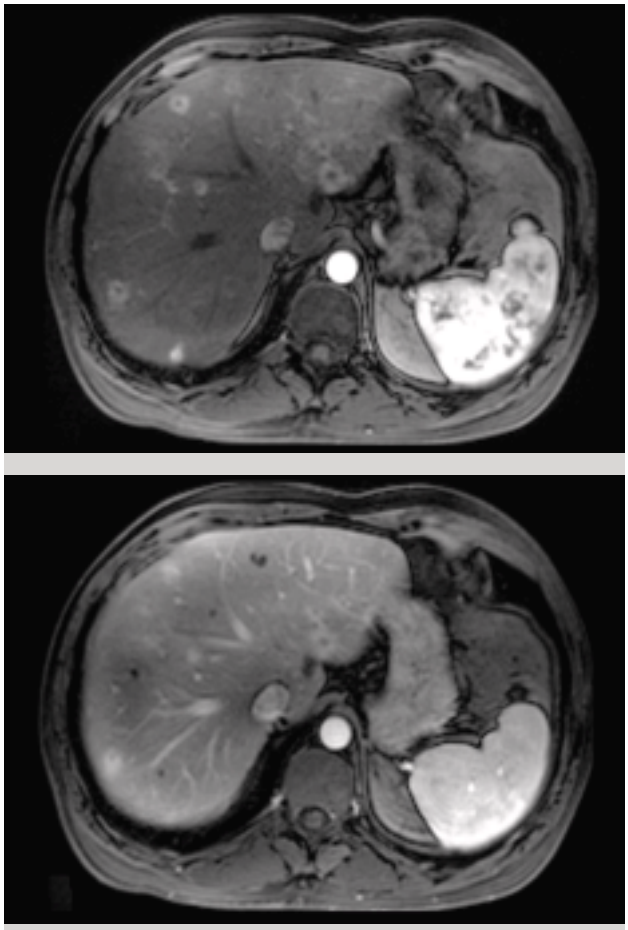

[Figure 3] *Dynamic liver examination showing enhancing lesions.*

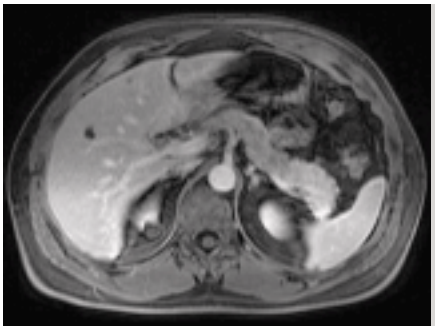

[Figure 4] *Post-contrast liver image.*

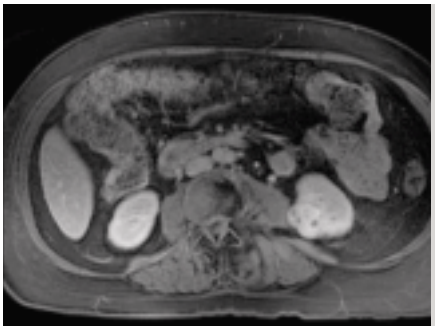

[Figure 5] *Post-contrast kidney image.*

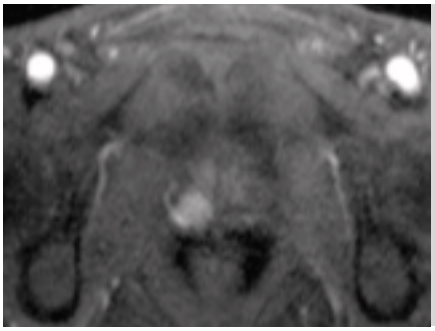

[Figure 6] *Post-contrast prostate image.*

The use of contrast extends VIBE from an anatomical imaging technique to a powerful diagnostic tool. It can be used for dynamic liver exams to image contrast uptake as well as for post-contrast livers (Figs. 3 and 4). In the abdomen the VIBE post-contrast is also useful for renal imaging, while in the pelvis it can be extended to prostate imaging (Figs. 5 and 6).

Whole-body imaging

Whole-body imaging, particularly for screening, requires a series of very rapid exams and an easy transition from one anatomical location to another. The VIBE and HASTE pulse sequences and SENSE or GRAPPA iPAT image reconstruction are the key software components in this approach, while the Matrix coils and other Tim technologies are the key hardware components. With this approach the abdomen, chest, pelvis, and head can be examined in less than 10 minutes of total acquisition time (Figs. 3–5 and 7 and refer to Semelka and Dale: "Whole-Body MRI: Faster with Tim". MAGNETOM Flash, 1/2006: 75–79).

Breast imaging

VIBE is a critically important sequence for breast imaging. It is used both for dynamic acquisitions with both high temporal resolution and high spatial resolution images (Figs. 8 and 9). These 3D T1-weighted breast sequences have become a standard on all Siemens MAGNETOM systems. The optimized breast sequences are named VIEWS, Volume Imaging with Enhanced Water Signal and are based on the principle of VIBE. The 3D dynamic VIEWS sequences acquired in about 1 minute with near isotropic voxels are essential for lesion visualization and characterization and use the quick fat saturation technique described above. A high-resolution data set

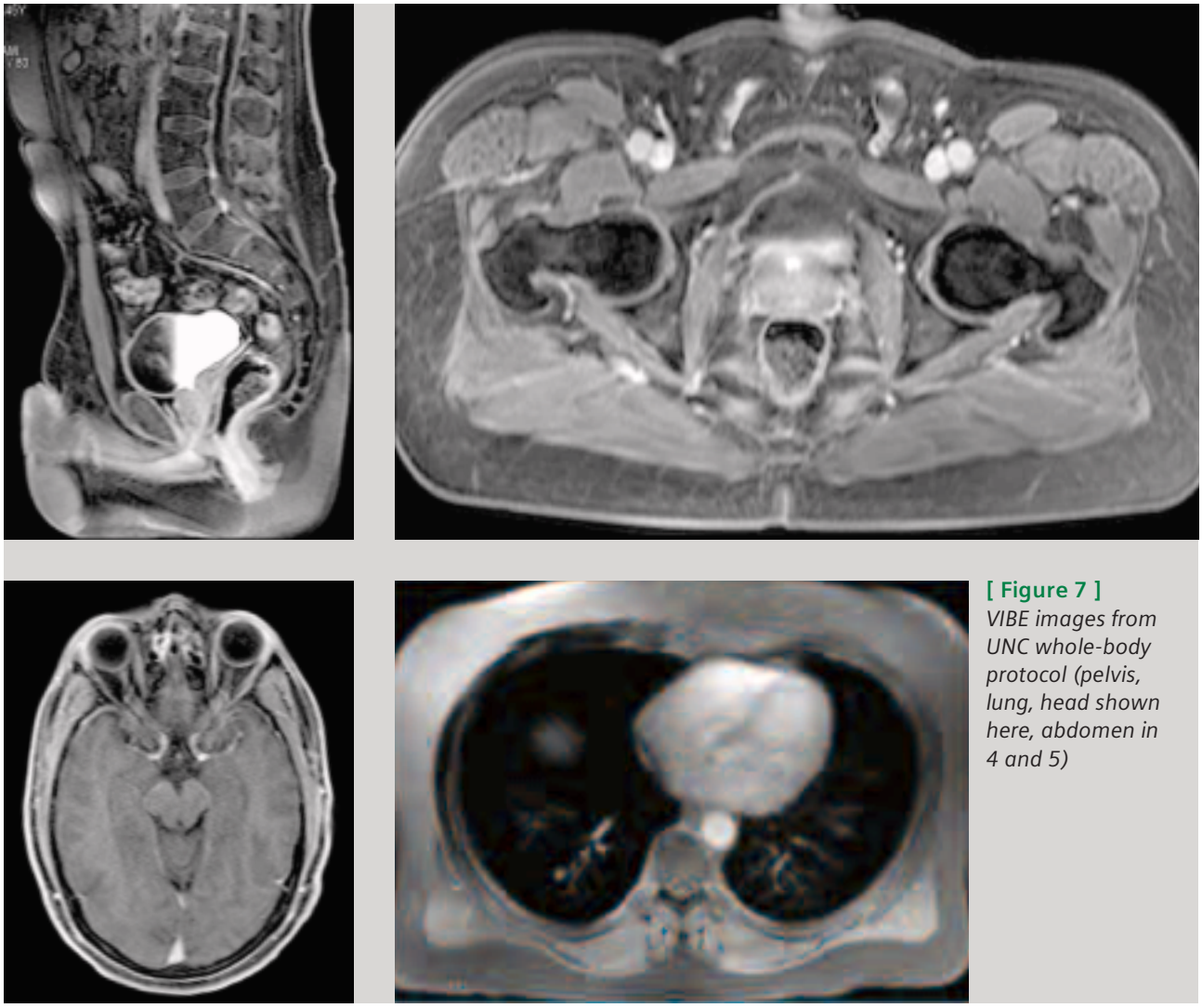

[Figure 7] *VIBE images from UNC whole-body protocol (pelvis, lung, head shown here, abdomen in 4 and 5)*

is important for lesion differentiation based on morphology and uses Water Excitation pulses for superior fat suppression, particularly at ultra-high field strengths. The use of iPAT is essential for acquiring these high-resolution breast datasets in a reasonable amount of time, and with multiplane reformatting a single 3D acquisition can replace up to three separate multislice acquisitions.

Conclusion

VIBE is a key sequence with widespread application throughout the body. Its fast and reliable T1-weighted 3D images provide essential clinical information in a minimal amount of time. Together with the Tim Matrix coils and iPAT algorithms, the VIBE sequence offers unparalleled flexibility and image quality over an unmatched range of applications.

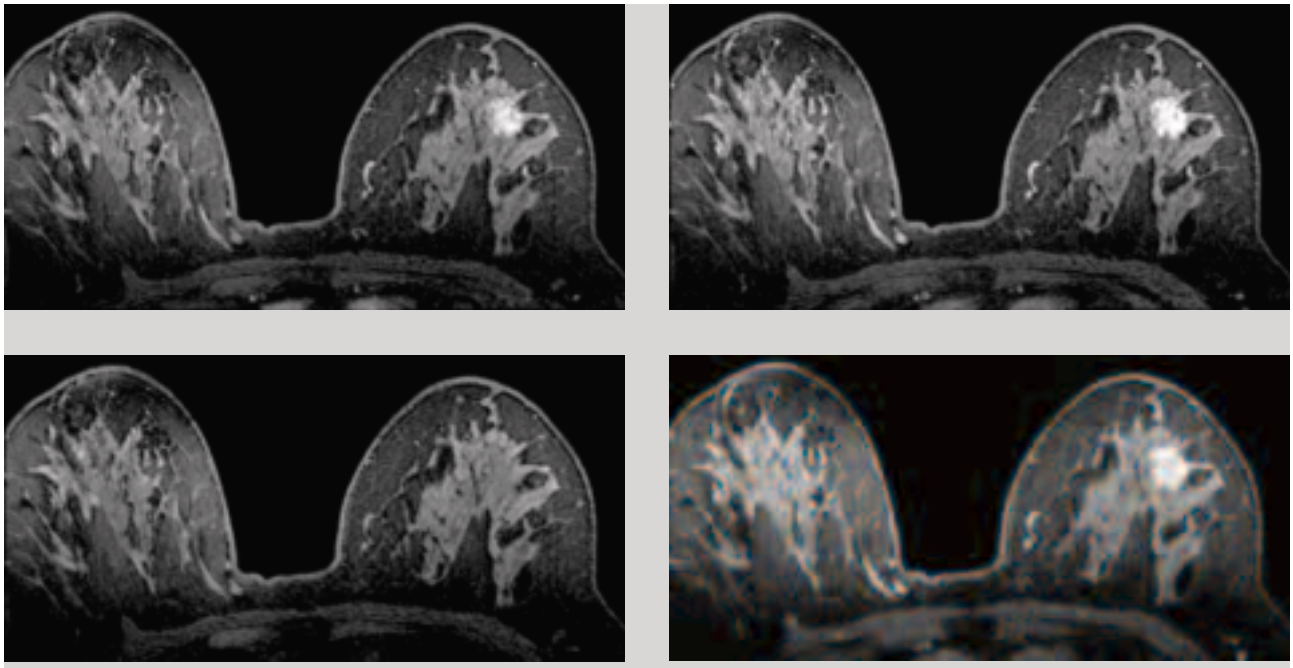

[Figure 8] *Dynamic breast examination with VIEWS.*

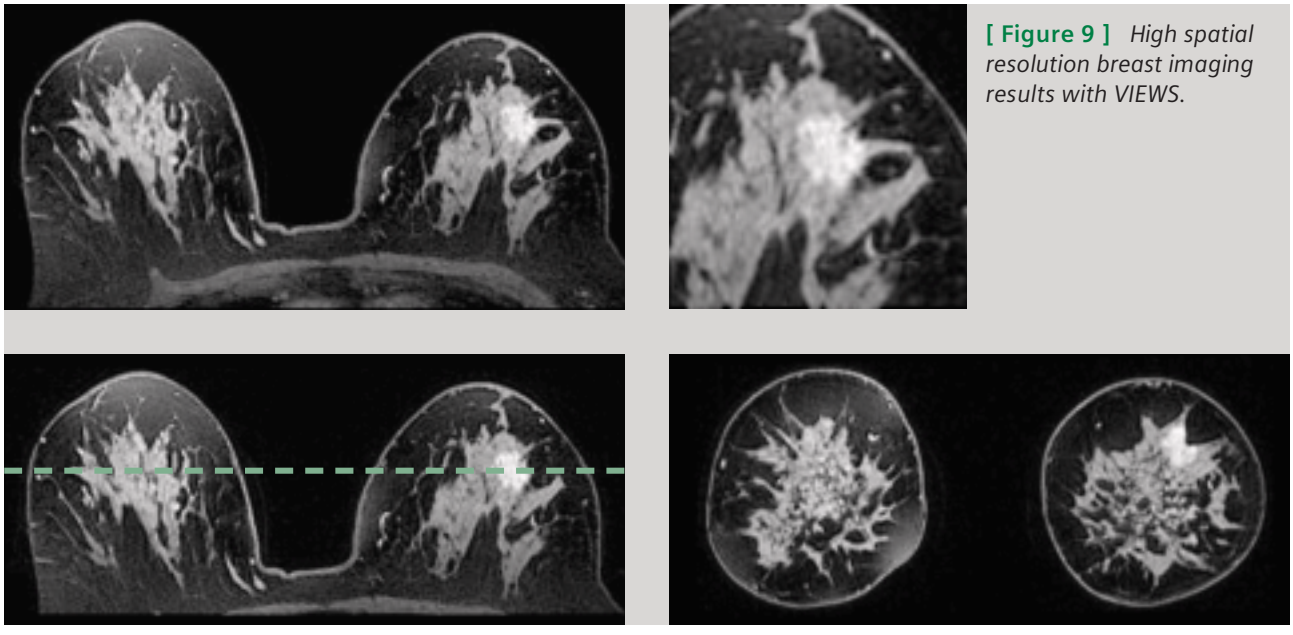

[Figure 9] *High spatial resolution breast imaging results with VIEWS.*

^{1}H Single Voxel Spectroscopy with 2D PACE Motion Correction

Nouha Salibi[1], Jian XU[1], Bachir Taouli[2]

[1]MR R&D, Siemens Medical Solutions USA, Malvern, PA, USA
[2]New York University school of Medicine, New York, NY, USA

Introduction

Proton MR Spectroscopy (MRS) is commonly used in the brain and the prostate for non invasive assessment of metabolite variations that result from disease. There is also a growing interest in abdominal ^{1}H MRS where respiratory motion degrades spectral quality and inhibits accurate evaluation of metabolites. Factors that contribute to deterioration of spectral quality include: difficulty in shimming, non-optimal suppression of unwanted peaks, and spatial misregistration due to significant displacement of tissue in and out of the localized voxel. These effects are seen in the spectrum as noticeably reduced and broad metabolite peaks that cannot be accurately interpreted. Clinical utility of MRS in the body requires improved spectral quality with breath-holding or motion correction techniques.

Methods for motion correction

The use of breath-holding is common in abdominal scanning and does significantly improve image quality. Breath-holding techniques are also useful for certain MR spectroscopic examinations of abdominal organs such as for the evaluation of high signals from water and fat. However, they are not adequate for detection of small metabolite peaks, which require signal averaging and hence longer scan times. Additionally breath-holding techniques are not suitable for patients who are unable to hold their breath and for patients who cannot follow instructions. These patients can benefit from free breathing techniques with motion correction schemes such as respiratory gating or the Siemens 2D PACE* (**P**rospective **A**cquisition **C**orr**E**ction) technique. Respiratory gating requires monitoring of the breathing motion via a belt

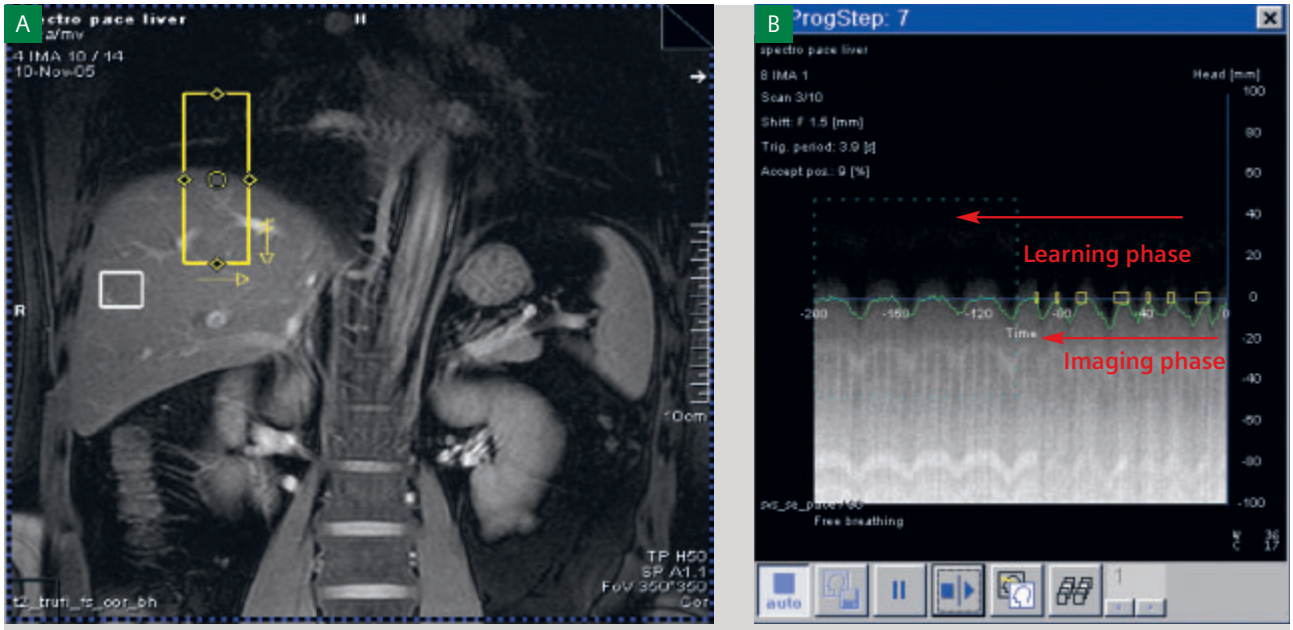

[Figure 1] *(A) Selection of the 2D area (yellow box) used for detection of the diaphragm position, half the rectangle is within the lungs, and the other half is within the liver. The selected SVS voxel is represented by the white box. (B) Online display of the respiratory curve (Green Color). The height of the small yellow boxes shows the accepted motion tolerance.*

wrapped around the patient's abdomen, which is uncomfortable and may not be suitable for some patients; furthermore the clinical workflow is disrupted by the additional time needed for patient preparation prior to the MR examination.

The 2D PACE method consists of acquiring a low resolution coronal gradient echo image. A user defined small box (Fig. 1A) is placed over the diaphragm to track the respiratory motion by monitoring changes in signal intensity within the box. During a learning phase (Fig. 1B), which occurs at the beginning of the measurement and prior to data acquisition, the system acquires preliminary scans, which are used to analyze the patient's breathing pattern and to determine the central position of an acceptance window (Fig. 2). Data acquisition starts when the position of the diaphragm is within the acceptance window as calculated during the learning phase. Since its implementation into the *syngo* MR 2002A software 2D PACE has proven to reliably improve MR image quality in the body** without the use of external monitoring or triggering devices. 2D PACE MRS is now proving to also improve MR spectral quality in the body.

2D PACE ^{1}H single voxel spectroscopy

The Siemens 2D PACE technique has been implemented in the single voxel spectroscopy svs-se sequence† with a learning phase of 5 respiratory cycles. MRS data acquisition starts at the onset of expiration when the diaphragm position is within the acceptance window as determined by real time evaluation of the navigator signal (Fig. 2). The effect of small displacements within the acceptance window is minimized by acquiring only one average within a breathing cycle. In the liver, a measurement with 2D PACE takes 3 to 5 minutes depending on the voxel size, number of averages and TR, which is determined by the breathing cycle. Hence MRS measurement times with PACE are not significantly longer than typical in vivo MRS measurements. Figure 3 illustrates the effect of 2D PACE on the large water peak in the liver of a healthy volunteer. The spectra were acquired on the MAGNETOM Trio with (Fig. 3A) and without (Fig. 3B) 2D PACE using the same parameters, and with breath-hold. The 2D PACE measurement TR (~ 4500 ms) is set by the breathing cycle; the same TR is then used in the free breathing measurement without PACE. Measurement times are 2 minutes 45 seconds for the PACE sequence in figure 3 and 1:12 for the measurement without PACE. The free breathing spectrum without PACE (Fig. 3B) has a lower and slightly broader water peak compared to the PACE spectrum (Fig. 3A) and to the breath-hold spectrum (Fig. 3C). Figure 4 illustrates a case where spectral quality and small peak definition are better in the 2D PACE measurement than in the breath-hold measurement. The spectra are from a fatty liver acquired on the MAGNETOM Sonata, with a TR of 4600 ms, and 32 averages in 5:35 for the 2D PACE, and with 5 averages in 23 sec for the breath-hold measurement. Although the peak amplitudes are almost the same in both spectra, the 2D PACE spectrum has better signal-to-noise ratio (S/N) and better defined peaks especially demonstrated by the small TMA (trimethylamine moiety) peak at 3.2 ppm.

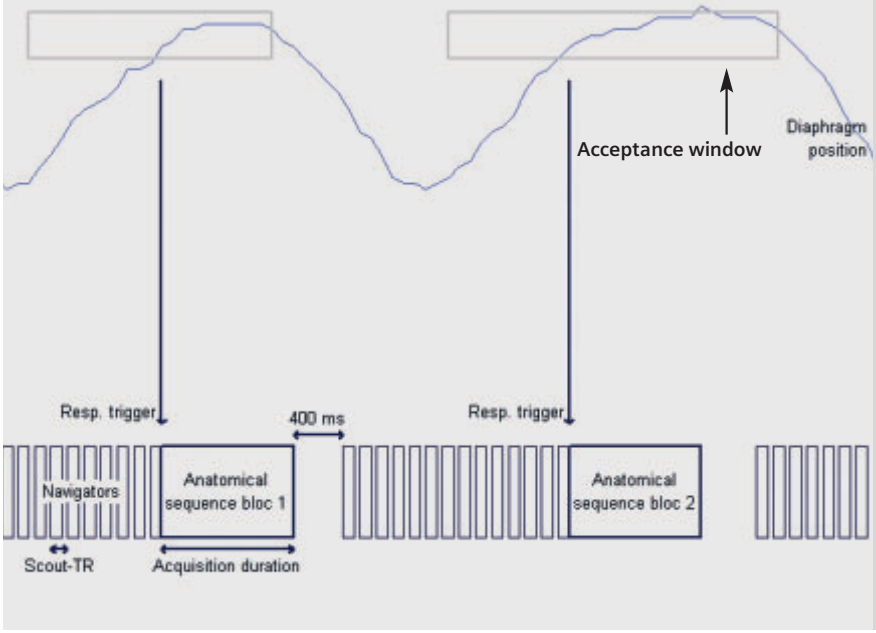

[Figure 2] *The upper blue curve represents the free breathing pattern of a subject with the corresponding acceptance window as defined in the learning phase. Data acquisition is started as the soon as detected position of the diaphragm falls within the acceptance window at the onset of the expiration phase.*

Conclusion

Without motion correction ^{1}H MRS in the abdomen suffers inaccurate localization and degraded spectral quality. Although breath-holding techniques can be used for measuring large metabolite signals, they are not adequate for detection of small metabolite peaks; and they are not suitable for patients suffering from respiratory disorders or from an impaired ability to follow breath-holding instructions. Respiratory gating is uncomfortable for the patient and incompatible with an efficient clinical workflow. Compared to these techniques, free breathing with 2D PACE MRS produces better localization; it improves spectral quality without significantly increasing measurement time and without the need for external monitoring devices. 2D PACE spectral quality is as good as or better than the spectral quality obtained with breath-holding techniques making MRS in the body more reliable and more clinically useful.

* MAGNETOM Flash No. 2, 2002, page 16.
** MRI Hot Topics, Motion under control with prospective acquisition correction (PACE), Siemens Medical Solutions.
† The sequence is a Works-In-Progress (WIP) available only for software version *syngo* MR 2004. It is not commercially available.

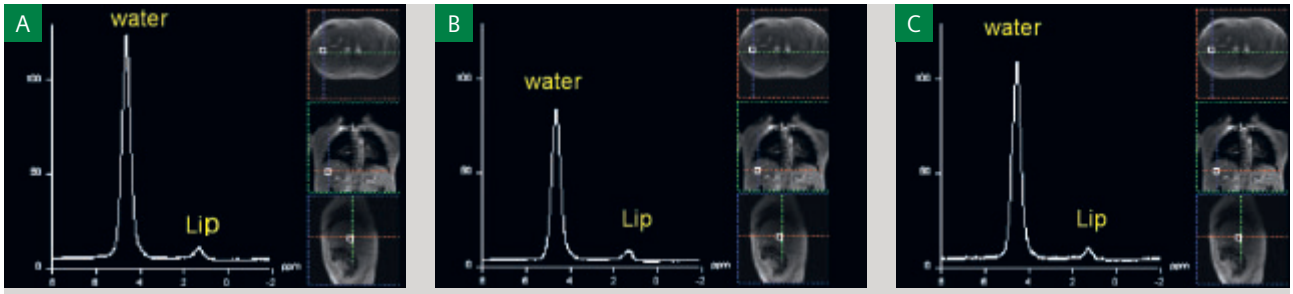

Free breathing with 2D PACE *Free breathing without motion correction* *Breath-hold*

[Figure 3] *Spectra acquired on the MAGNETOM Trio from an 8 cm^3 voxel in the liver of a healthy volunteer to compare the effect of 2D PACE, free breathing without motion correction and breath-hold on the large water peak at 4.7 ppm. A small lipid peak is seen at 1.3 ppm. (A) Spectrum acquired with motion correction, a TR of about 4500 ms, TE = 30 ms, 16 averages, and a measurement time of 2:45. (B) Spectrum acquired without motion correction using the same parameters including TR of 1:12. (C) Spectrum acquired with breath-hold in 22 s using 5 averages and the same TR and TE as in A and B. The free breathing spectrum without PACE has a lower and slightly broader water peak compared to the PACE spectrum and to the breath-hold spectrum.*

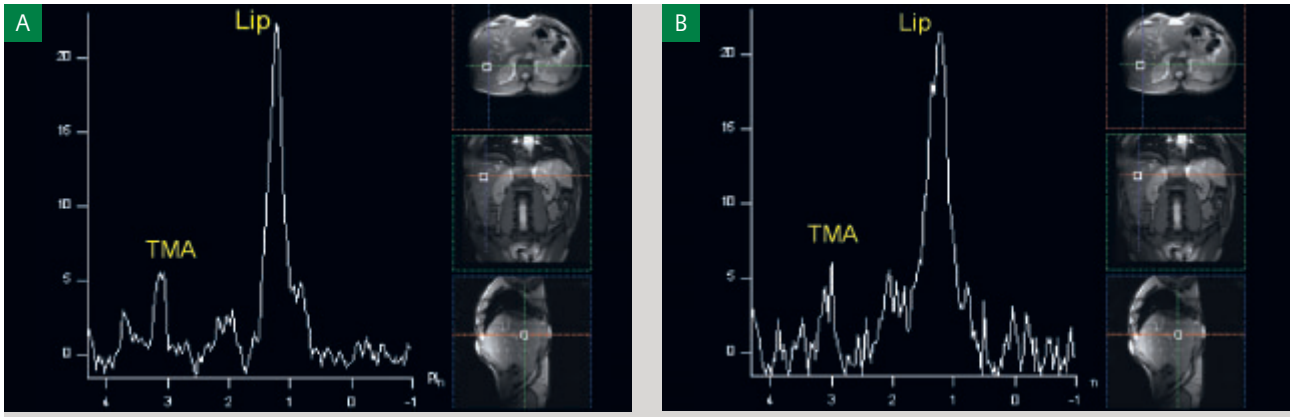

Free breathing with 2D PACE *Breath-hold*

[Figure 4] *Spectra acquired on the MAGNETOM Sonata from an 8 cm^3 voxel in a fatty liver. A: Spectrum with free breathing 2D PACE, a TR of about 4600 ms, TE = 30 ms, 32 averages, and a measurement time of 5:35. B. Spectrum with breath-hold using the same TR with 5 averages and a measurement time of 23 s. The spectra show a large lipid peak at 1.3 ppm and a small TMA (trimethylamine moiety) peak at 3.2 ppm. Although the peak amplitudes are about the same in both spectra, the spectrum in A has higher S/N with narrower and better defined peaks.*

Screening for Bone Metastases: Benefit of Whole-Body MRI using Multi-Channel Systems

Gerwin P. Schmidt, M.D.; Stefan O. Schoenberg, M.D.; Maximilian F. Reiser, M.D. ; Andrea Baur-Melnyk, M.D.

Department of Clinical Radiology, University Hospitals Grosshadern, Ludwig-Maximilians-University Munich, Germany.

Introduction

The skeletal system is a frequent target of metastatic disease, and early detection of bone metastases has an important impact on patient management, disease outcome and the quality of life of the patient. In clinical practise most commonly multi-modality algorithms are used in cases of suspected metastatic bone disease, including conventional x-ray, skeletal scintigraphy, PET (**P**ositron **E**mission **T**omography), CT (**C**omputed **T**omography) and MRI (**M**agnetic **R**esonance **I**maging). At present, ^{99m}Tc-phosphonate-based scintigraphy is the standard method for initial staging. However, at the early stage of disease, lesions may remain invisible in the absence of an osteoblastic response.

Recent studies have indicated that fluorodeoxyglucose-(FDG)-PET increases specificity of bone marrow screening compared to scintigraphy due to tracer uptake directly into malignant cells [1]. Fused PET-CT scanners combine the functional data of PET with the anatomical information of CT scanners in a single examination and have further improved diagnostic accuracy and lesion localization [2, 3]. Also, the CT image data allows assessment of paraosseous tumor expansion and provides information on the extent of osteolysis as well as criteria of bone stability.

However, MRI is the only imaging technique that allows direct visualization of bone marrow and its components. Moreover, the unique soft-tissue contrast of MRI enables precise assessment of tumor infiltration within the bone marrow and adjacent paraosseous structures, such as the spinal canal. It has been reported that up to 40% of skeletal metastases occur outside of the field-of-view (FoV) covered by a routine assessment of the axial skeleton, underlining the importance of whole-body bone marrow imaging [4]. Whole-body MRI (WB-MRI) and FDG-PET-CT represent two imaging modalities that can potentially detect metastatic bone disease at an early stage of growth, before an osteoblastic host reaction occurs. The purpose of a study performed at the Institute of Clinical Radiology in Grosshadern-Munich, Germany, was to compare the diagnostic potential of these whole-body modalities for the detection of bone metastases and to establish an MR protocol covering the entire body from head to toe.

Basic concepts of whole-body bone marrow MRI

The combination of non-contrasted T1-weighted spin echo sequences and fat suppressed short TI inversion recovery (STIR) imaging has proved to be most accurate in the detection of malignant bone marrow disorders, whilst an excellent negative- and positive-predictive value, especially for STIR-imaging, has been described in literature [5, 6]. In the past, different requirements in coil setup, sequence design and slice positioning, as well as time-consuming patient repositioning procedures, have delayed the realization of WB-MRI as a clinical application. Initial experiences with whole-body scanning revealed promising results for WB-MRI with a higher lesion detection rate compared to established bone marrow screening techniques (e.g. skeletal scintigraphy), but with a sequential approach room time far in excess of one hour had to be allowed for [7]. Improvements in hardware and software, including dedicated rolling platforms with integrated surface coils, facilitated WB-MRI and for the first time allowed whole-body coverage within less than one hour. However, with this technique considerable compromises in spatial resolution, especially in peripheral body regions like the head/neck and lower extremities, had to be taken into account [8]. With the introduction of multi-channel MR scanners, using a system of multiple phased-array coils covering the whole body like a matrix, imaging of the total skeletal system without compromises in spatial resolution became possible. The total imaging matrix concept (Tim) makes WB-MRI from head to toe possible without patient repositioning and allows the use of parallel acquisition techniques (PAT) in all 3 dimensions at a total field of view of 205 cm. Especially the combination of free table

Whole-body-MRI protocol at 1.5 Tesla

Sequence	Image plane	Matrix / Resolution (mm^3)	TR (ms) / TE (ms)	PAT	Acquisition time (min)
STIR-WB	coronal	384 / 1.8 x 1.3 x 5.0			
Head/neck			6380 / 92	3	1:55
Thorax/abdomen			3380 / 101	3	2:02
Pelvis			6090 / 84	3	2:02
Thigh			6090 / 84	3	2:02
Calf			5900 / 84	2	2:45
T1w TSE-WB	coronal	484 / 1.3 x 1.1 x 5.0			
Head/neck			797 / 12	3	3:41
Thorax/abdomen			400 / 8.2	3	1:38
Pelvis			797 / 12	3	3:41
Thigh			797 / 12	3	3:41
Calf			767 / 12	2	3:28
T1w TSE-spine	sagittal	384 / 1.0 x 1.0 x 3.0	848 / 11	2	7:46
STIR-spine	sagittal	384 / 1.0 x 1.0 x 3.0	5700 / 59	2	7:24
Total					**43:05**

[Figure 1] *Whole-body MRI bone marrow screening at 1.5 Tesla using Parallel Imaging on a 32-receiver channel scanner (MAGNETOM Avanto, Siemens Medical Solutions).*

movement with PAT have resulted in substantially shorter room time and allow to sensibly integrate potentially time-consuming, but indispensable sequence types (e.g. STIR-sequences), for whole-body bone marrow imaging. Using PAT acceleration, whole-body STIR-imaging is possible within 10 minutes and 46 seconds and T1-weighted-imaging within 16 minutes and 9 seconds at a 1.8 x 1.3 mm and 1.3 x 1.1 mm in-plane-resolution, respectively. The proposed imaging protocol allows for T1-weighted SE- and STIR-imaging from head to toe, combined with dedicated imaging of the complete spine at a total scan time of 43 minutes (Fig. 1).

Discussion

The diagnostic performance of MRI compared to bone scintigraphy for the detection of skeletal metastases has been examined in various studies and a higher specificity and sensitivity for MRI in the early detection of skeletal metastases has been reported [7, 8].

In a recent study at our institute, 30 patients (18 female, 12 male, mean age 58 years, range 24-76 years) with different primary tumors underwent whole-body FDG-PET-CT on a dual-modality-scanner (Gemini, Philips Medical Systems, Cleveland, Ohio) for the work-up of skeletal metastatic disease. These patients also underwent WB-MRI using the above described protocol (MAGNETOM Avanto, Siemens Medical Solutions, Erlangen, Germany). PET-CT was conducted using a low-dose CT for attenuation correction, a PET-emission scan and diagnostic contrast-enhanced CT scan covering the thorax, abdomen and pelvis [9].

In a lesion-by-lesion analysis, 102 malignant and 25 benign bone lesions were confirmed by histology or follow-up. WB-MRI showed a significantly higher overall diagnostic accu-

racy than PET-CT (91% vs. 78%, Fig. 2). WB-MRI showed a superior sensitivity (94% vs. 78%), partly due to the fact that more smaller lesions below 5 mm were depicted by WB-MRI (cut-off size 2 mm) compared to PET-CT (cut off 5 mm). Lesions below double the size of the spatial resolution of the PET-scanner (which usually is 6 mm) can potentially lead to false-negative results. In addition, WB-MRI revealed 10 additional bone metastases in 4 patients in the distal extremities due to the larger field-of-view (the FOV of a routine PET-CT is depending on the diagnostic spiral CT, normally ranging from the skull base to the proximal femora). However, specificity was higher in PET-CT (PET-CT 80% vs. WB-MRI 76%). Here certainly the additional metabolic information of PET plays the most important role to reliably discriminate between malignant and benign lesions (e.g. atypical haemangioma). Still, it is important to remember that FDG is not a tumor-specific tracer and may also accumulate in the presence of inflammation and thus lead to false-positive findings.

Very few comparative studies between WB-MRI and FDG-PET-CT have yet been carried out [10, 11]. Antoch et al. analyzed the accuracy of both modalities in 98 patients with different oncologic diseases in terms of TNM-based tumor staging using the rolling platform approach [11]. Regarding skeletal metastases, the sensitivity was significantly higher when using WB-MRI (85%) than in PET-CT (62%), conforming to our observations.

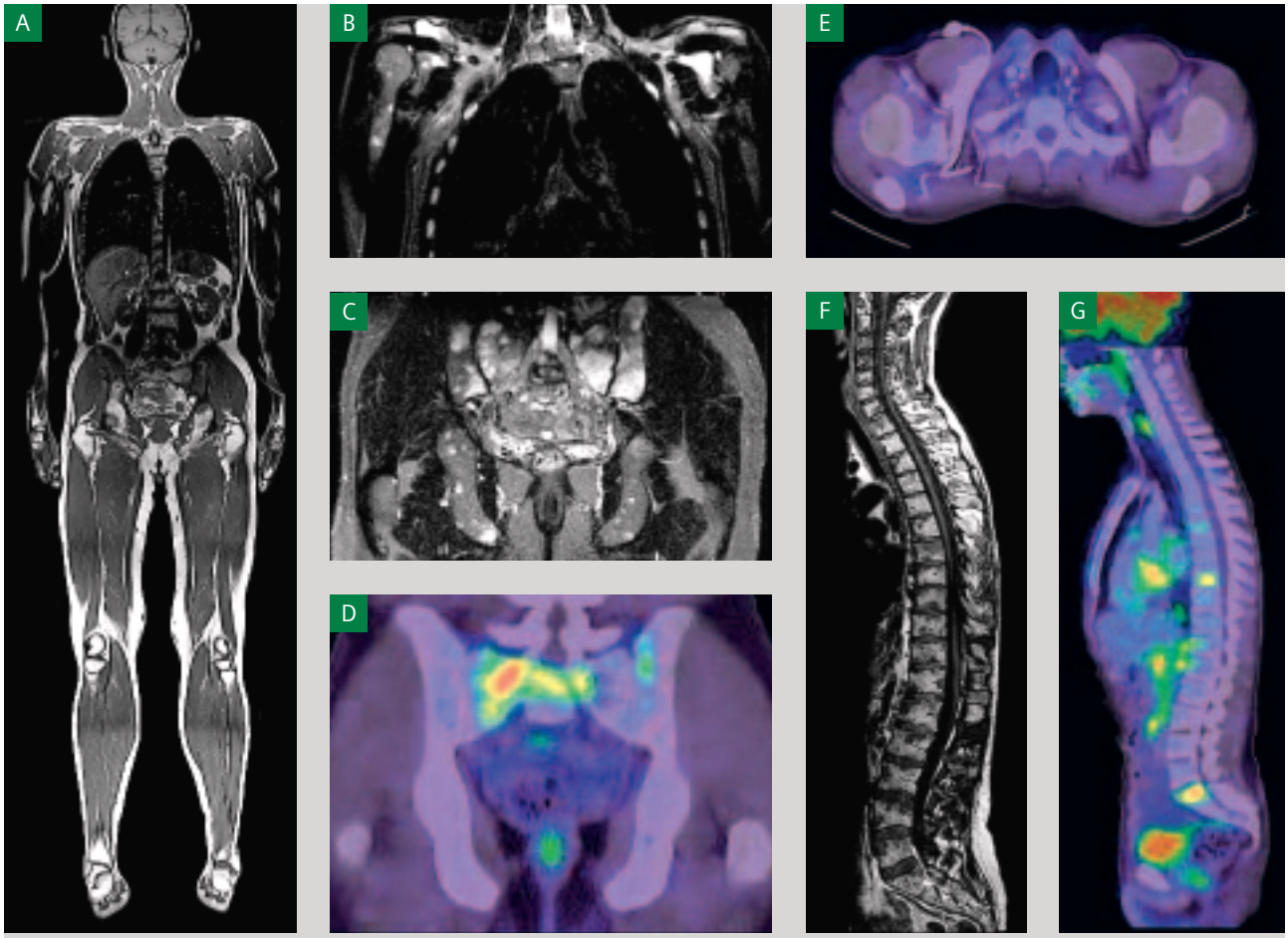

[Figure 2] ***28-year-old male with Non-Hodgkin's lymphoma.***
(A) T1-weighted TSE WB-MRI at 1.5 Tesla. (B + C) WB-STIR imaging reveals multi-focal bony infiltration of the shoulder girdle, humeri, sacral bone and pelvis. (D + E) PET-CT underestimates the extent of infiltration in the pelvis and shows hardly any visible FDG-uptake in the shoulder girdle. (F) T1-weighted TSE imaging of the spine reveals extensive multifocal tumor infiltration. (G) Sagittal PET-CT reconstruction of the spine underestimates infiltration of the spine, especially in the cervical region.

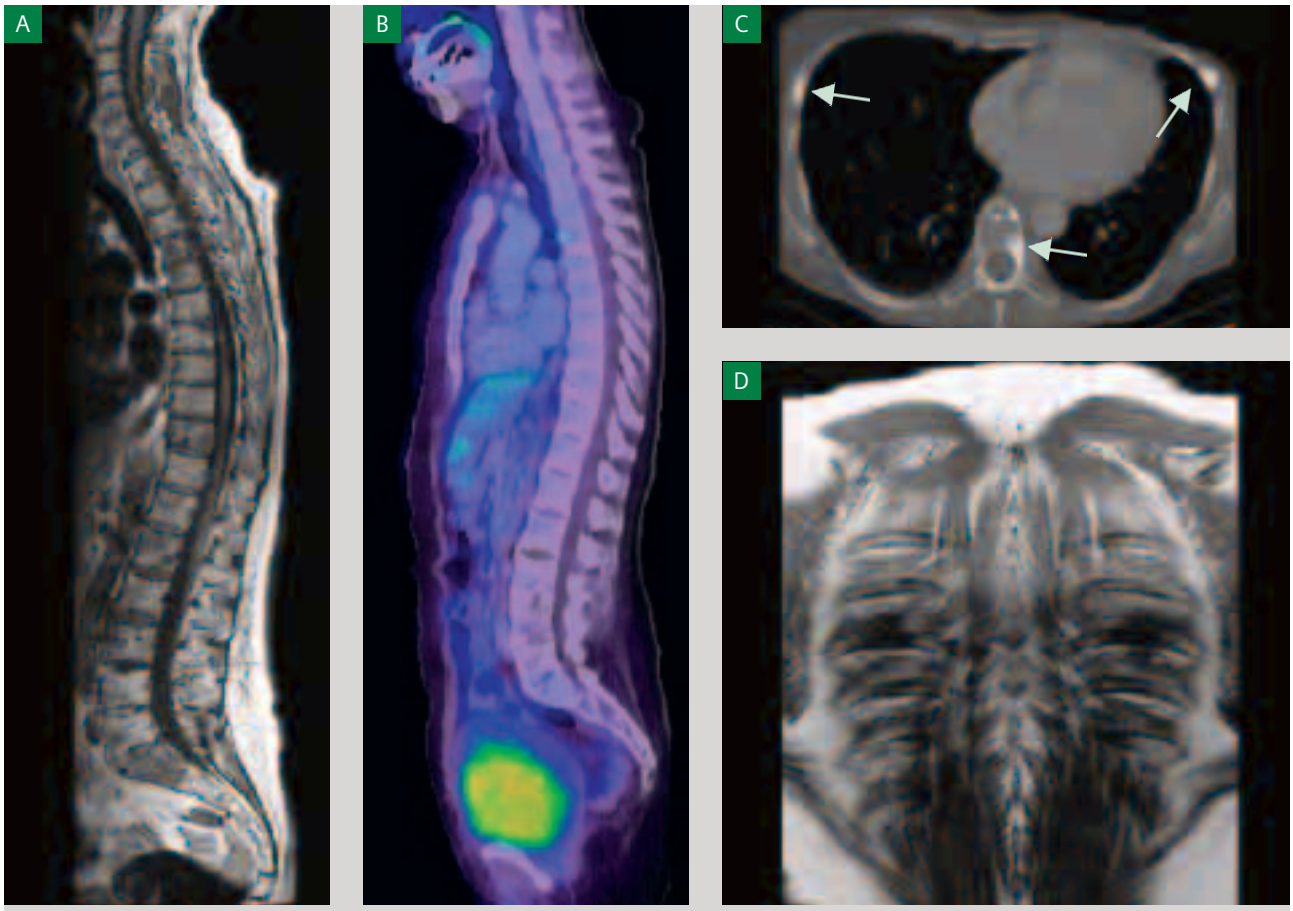

[Figure 3] ***56-year-old female with breast cancer.***
(A) Sagittal TSE-imaging of the spine at 1.5 Tesla depicts multi-focal osteoblastic metastases. (B) PET-CT of the same patient shows no noticeable FDG-uptake of the spinal metastases. (C) Bone window CT depicts larger spinal metastases due to bone sclerosis and reveals more osteoblastic metastases of the rib cage.
(D) Coronal T1-weighted WB-MRI misses the rib metastases.

Another study group used the same multi-channel MR scanner system as previously described and compared the performance of WB-MRI for the detection of organ metastases in different malignancies with CT as a standard staging method. They reported a significantly higher detection of bone lesions in patients suffering from malignant melanoma, plasmocytoma and lymphoma [12].

There have been reports that WB-MRI, especially when performed in coronal orientation, is prone to miss lesions in small curved flat bones, like the rib cage, a problem which is certainly reinforced by motion artefacts of respiration (Figs. 3 and 4) [7]. These might be overcome using fast Turbo Spin Echo sequences for thoracic imaging in combination with axial slicing. However, skull metastases in PET-CT are particularly difficult to identify, because of a high physiological tracer uptake in normal brain. Finally, different patterns of FDG-uptake have been reported between osteoblastic, osteolytic or mixed lesions, indicating that sclerotic lesions may be less FDG-avid (Fig. 3) [13]. Here the additional morphologic component of PET/CT compared to PET alone is certainly of great value to increase diagnostic sensitivity.

An important indication in bone marrow imaging is lesion monitoring after chemotherapy or radiation therapy. It has to be remembered that in MRI avital bone metastases can remain virtually unchanged in morphology or signal, which may complicate evaluation of therapy response. In the CT

image, osteolytic metastases often show a typical sclerotic transformation. In this setting, future studies are needed to show how quickly FDG-PET-CT depicts tumor response to chemotherapy and whether sensitivity is reduced in the first days after initiation of therapy.

Future trends

Recently, approved clinical WB-MRI scanners with a field strength of 3.0 Tesla have become commercially available, equipped with the same technique of multiple phased-array coils and receiver channels. This has opened the way for

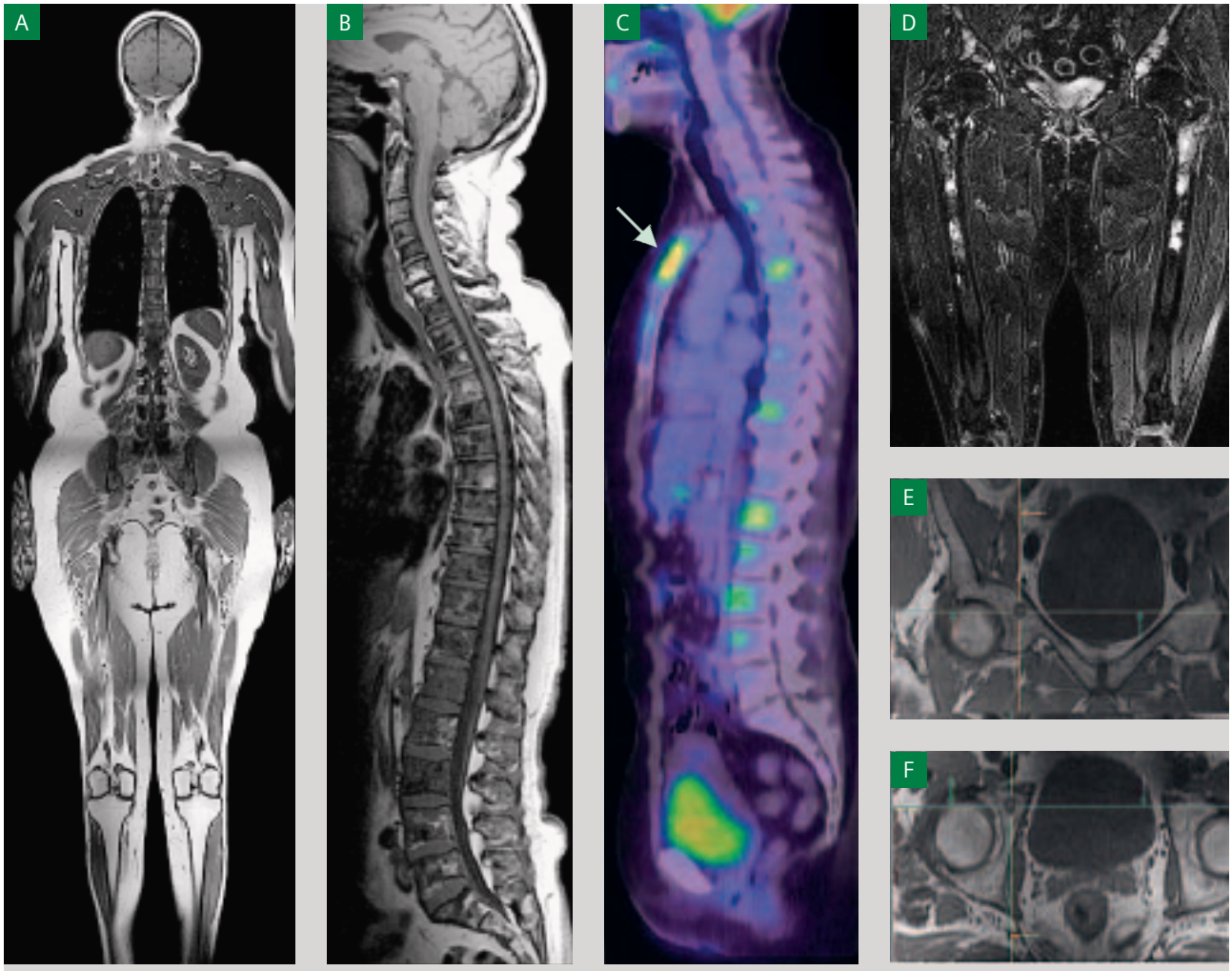

[Figure 4] ***68-year-old female with breast cancer.***
(A) T1-weighted TSE WB-MRI at 3.0 Tesla. (B) Sagittal T1-weighted TSE sequences reveal infiltration of almost the complete spine. A metastasis of the sternum is masked by field saturation and is prone to be missed in coronal WB-MRI. (C) PET-CT shows pathological FDG-uptake in the larger focal metastases only. The sternal metastasis shows high FDG-uptake (arrow). (D) WB-STIR shows multi-focal pelvic metastases and additional infiltration of both femurs, not covered by the field of view of the PET-CT scan. (E+F) T1-weighted isotropic 3D Turbo Spin Echo sequence with high sampling efficiency (SPACE) of the pelvis in a different patient reveals a small focal metastasis (5 mm) of the right acetabulum.

migration of multi-organ- and whole-body applications to higher field strength. The gain of signal-to-noise ratio (SNR) can be used to reduce overall scan time, especially for the acquisition of T2-weighted fat suppressed sequences at a constant image resolution. Alternatively, image resolution can further be increased to potentially gain higher sensitivity. Furthermore, with the use of PAT, the increased SNR allows recording of large, highly resolved isotropic 3D-data sets within short acquisition times, which can further ameliorate diagnosis of bone pathologies in complex anatomic structures, like the pelvis, rib cage or spinal pedicles (Fig. 4). 3D Turbo Spin Echo sequences with high sampling efficiency (SPACE) have recently been developed with T1-weighted-, STIR- and T2-weighted contrast. STIR-SPACE imaging of the whole spine, for example, is possible within a 10-minute scan time at a resolution of 0.8 x 0.8 x 2.0 mm. Finally, initial results for 3D whole-body continuous data acquisition as a new potential strategy for WB-MRI metastases screening, especially for large field-of-view imaging in short bore systems, have been reported [14].

Acknowledgements

The authors acknowledge the work of the entire whole-body MRI team at the Department of Clinical Radiology: Denise Friedrich, RT; Michele Picciolo, RT; Frank Stadie, RT; at the Department of Nuclear Medicine: Rupert Schmidt, MD; Reinhold Tiling, MD and of Siemens Medical Solutions: Wilhelm Horger, PhD. The authors also acknowledge the "Verein zur Förderung der Forschung und Entwicklung der Magnetresonanztomographie e.V.".

References

[1] Cheran SK, Herndon JE, Patz EF. Comparison of whole-body FDG-PET to bone scan for detection of bone metastases in patients with a new diagnosis of lung cancer. Lung cancer 2003; 44: 317–325.
[2] Even-Sapir E, Metser U, Flusser G, Zuriel L, Kollender Y, Lerman H. Assessment of malignant skeletal disease: initial experience with 18F-fluoride PET/CT and comparison between 18F-fluoride PET and 18F-fluoride PET/CT. J Nucl Med 2004; 45: 272–278.
[3] Pelosi E, Messa C, Sironi S, Picchio M, Landoni C, Bettinardi V, et al. Value of integrated PET/CT for lesion localisation in cancer patients: a comparative study. Eur J Nucl Med Mol Imaging 2004; 31: 932–939.
[4] Krishnamurthy GT, Tubis M, Hiss J, Blahd WH. Distribution pattern of metastatic bone disease. JAMA 1977; 237: 837–842.
[5] Mehta RC, Marks MP, Hinks RS, Glover GH, Enzmann DR. MR evaluation of vertebral metatases: T1-weighted short inversion time inversion recovery, fast spin echo, and inversion-recovery fast spin-echo sequences. Am J Neuroradiol 1995; 16: 281–288.
[6] Mahnken A, Wildberger JE, Adam G, Stanzel S, Schmitz-Rode T, Günther R, et al. Is there a need for contrast-enhanced T1-weighted MRI of the spine after inconspicuous short Ù inversion recovery imaging? Eur Radiol 2005, 15: 1387–1392.
[7] Steinborn M, Heuck AF, Tiling R, Bruegel M, Gauger L, Reiser MF (1999) Whole body bone marrow MRI in patients with metastatic disease to the skeletal system. J Comput Assist Tomogr 23: 123–129.
[8] Lauenstein T, Freudenberg L, Goehde S, Ruehm G, Goyen M, Bosk S, et al (2002) Whole body MRI using a rolling table platform for the detection of bone metastases. Eur Radiol 12: 2091–2099.
[9] Schmidt GP, Schoenberg SO, Schmid R, Stahl R, Tiling R, Becker C, et al (2006) Screening for bone metastases: whole-body MRI using a 32-channel system versus dual-modality PET-CT. Eur Radiol (published online).
[10] Schmidt GP, Baur-Melnyk A, Herzog P, Schmid R, Tiling R, Schmidt M, et al (2005) High-resolution whole-body magnetic resonance image tumor staging with the use of parallel imaging versus dual-modality positron emission tomography-computed tomography: experience on a 32-channel system. Invest Radiol 40: 743–753.
[11] Antoch G, Saoudi N, Kuehl H, Dahmen G, Mueller SP, Beyer T, et al. (2004) Accuracy of whole-body dual-modality fluorine-18-2-fluoro-2-deoxy-D-glucose positron emission tomography and computed tomography (FDG-PET/CT) for tumor staging in solid tumors: comparison with CT and PET. J Clin Oncol 22: 4357–68.
[12] Schlemmer HP, Schaefer J, Pfannenberg C, Radny P, Korchidi S, Muller-Horvat C (2005) Fast whole-body assessment of metastatic disease using a novel magnetic resonance imaging system: initial experiences. Invest Radiol 40: 64–71.
[13] Cook GJ, Houston S, Rubens R, et al (1998) Detection of bone metastases in breast cancer by 18-FDG-PET: differing metabolic activity in osteoblastic and osteolytic lesions. J Clin Oncol 16: 3375–3379.
[14] Zenge MO, Ladd ME, Vogt FM, Brauck K, Barkhausen J, Quick HH (2005) Whole-body magnetic resonance imaging featuring moving table continous data acquisition with high-precision position feedback. Magn Reson Med 54: 707–711.

Whole-Body MRI and ^{11}C-Choline PET/CT in Patients with Prostate Cancer

H-P. W. Schlemmer[1], S-M. Eschmann[2], C. Pfannenberg[1], P. Aschoff[1], C. Mueller-Horvat[1], M. Lichy[1], E. Rodegerts[1], A. Anastasiadis[3], A. Stenzl[3], R. Bares[2], C. D. Claussen[1]

[1]*Diagnostic Radiology, Eberhard-Karls-University Tuebingen, Tuebingen, Germany*
[2]*Nuclear Medicine, Eberhard-Karls-University Tuebingen, Tuebingen, Germany*
[3]*Urology, Eberhard-Karls-University Tuebingen, Tuebingen, Germany*

Introduction

Prostate cancer is the most common malignant disease and second-highest cause of deaths from cancer among men in Western Europe and North America. The most favorable outcome that can be achieved is a complete tumor resection. For optimizing therapeutic outcome and avoiding unnecessary complications it is essential to obtain precise information about local tumor extension as well as distant tumor spread particularly to the most common sites, such as bone marrow and lymph nodes. Endorectal MRI (endMRI) and MR Spectroscopy (MRS) have been shown to provide the most

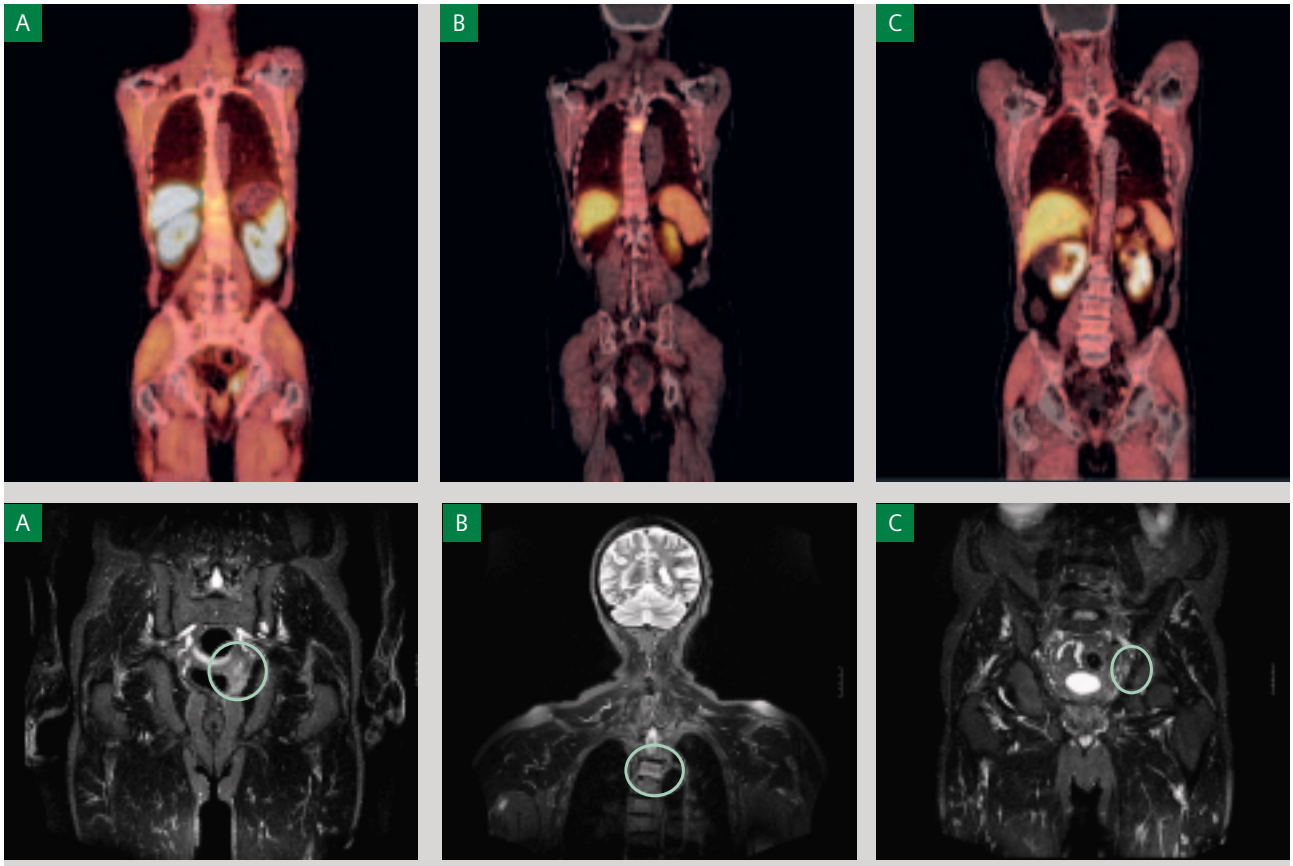

[Figure 1A] *Both PET-CT (top) and STIR images show a residual tumor tissue after prostate ca operation.*

[Figure 1B] *Thoracic vertebra metastasis of prostate ca. seen by PET-CT (top) and MR (bottom).*

[Figure 1C] *Lymph node metastasis is seen clearly with PET-CT and MRI with STIR sequence.*

accurate prediction of pathologic outcome of extracapsular extension and seminal vesicle invasion [1, 2]. However, unexpectedly high failure rates are observed even after intended curative treatment, attributable to unknown systemic progression. High-resolution whole-body MR imaging (wb-MRI) shows great potential for fast assessment of tumor spread in cancer patients [3]. Recently, it has been shown that PET/CT with ^{11}C-choline (Cho-PET/CT) is a feasible method of identifying foci of cancer within the prostate [4, 5]. In this study we have compared the diagnostic potential of wb-MRI and Cho-PET/CT to detect distant tumor spread in patients with prostate cancer.

Materials and methods

We studied 22 patients (average age 69-years-old) with prostate cancer. All patients underwent staging examinations by Cho-PET/CT and wb-MRI following initial diagnosis of prostate cancer (8 patients), increase of serum PSA (Prostate Specific Antigen) either after curative intended therapy (11 patients) or during anti-hormonal treatment (3 patients). Wb-MRI was performed on a 1.5T whole-body MR system equipped with 32 independent receiver-channels (MAGNETOM Avanto, Siemens Medical Solutions, Germany). The patients were placed in supine position with their arms beside the body and five to six surface coils were attached: Head Matrix coil (12 coil elements), Neck Matrix coil (4 coil elements), depending on the size of the patient two or three Body Matrix coils for abdomen/pelvis (12 or 18 coil elements), and Peripheral Angiography Matrix coil for lower extremities (8 coil elements). The Spine Matrix coil with 24 elements is embedded in the patient table. Using automatic table movement in 5 subsequent table positions the whole body was examined in coronal direction and the spine additionally in sagittal direction using STIR- and T1-weighted turbo spin-echo MR sequences with parallel imaging (acceleration factor of 2, GRAPPA reconstruction). Breathhold axial STIR- and VIBE-sequences were additionally acquired for the examination of the ribs. The total examination time was approximately 45 minutes. Cho-PET/CT examinations were performed 0–3 days before wb-MRI using a LSO Hi-REZ Biograph 16 system (Siemens Medical Solutions, Germany). Following contrast-enhanced whole-body CT, PET images were acquired 5 minutes after i.v. administration of 800 MBq ^{11}C-Cholin produced at the own cyclotron facility (7–8 table positions with acquisition time of 3 min each). The interpretation of MRI, CT and PET, and color-coded PET/CT images was first performed separately by experienced specialist for oncologic radiology and nuclear medicine. Consensus reading finally compared all imaging modalities.

Results

In total 58 malignant lesions were detected in 21 out of the 22 patients: local primary or recurrent tumor (11) as well as metastases to bone (33), lymph nodes (8), lung (3) and brain (3). Bone metastases were clearly displayed with high contrast on T1-weighted MR images due to the characteristic osteoblastic behavior. Small vertebral metastases in 3 cases were detected initially only by MRI, but retrospectively also by Cho-PET/CT. Rib metastases were detected by both modalities. Lymph node metastases were better visualized on STIR MR images with high signal compared to surrounding fat tissue. Cho-PET/CT showed in 9 patients small (<1cm), on MRI normal-appearing inguinal and mediastinal lymph nodes with ambiguous choline uptake. In one patient a suspicious colonic polyp was detected only on Cho-PET/CT, but retrospectively also visualized on MRI. Consensus reading showed that lesions were visualized by both modalities, but generally with higher contrast on PET/CT.

Conclusions

Our initial data suggest that wb-MRI is a very promising diagnostic tool for evaluating distant tumor spread in patients with prostate cancer. Particularly bone marrow involvement could be better visualized by wb-MRI than by Cho-PET/CT. The potential of wb-MRI for detecting bone metastases in general has been shown by clinical studies proving that MRI is even more sensitive than conventional skeletal scintigraphy [6]. A further distinct advantage of MRI is its high sensitivity for detecting metastases in parenchymal organs, e.g. the brain. For detecting lymph nodes, however, wb-MRI and Cho-PET/CT are both limited and visualize only relatively large metastases (>1cm). The synopsis of Cho-PET/CT and wb-MRI (PET/MR) turned out to be most favorable for detecting and interpreting tumor suspicious findings. High-resolution MRI after intravenous application of magnetic nanoparticles enables the detection of, even small lymph node metastases with high sensitivity and specificity [7]. For initial and repeated staging, the combination of wb-MRI and MRS may consequently be most advantageous for differentiating patients with localized disease and systemic progression. Prospective clinical studies should now be initiated to justify this diagnostic approach.

References
[1] Nakashima J, et al. Urology. 2004; 64(1): 101–5. [5] Yamaguchi T, et al. Eur J Nucl Med Mol Imaging 2005; 32(7): 742–8.
[2] Kurhanewicz J, et al. J Magn Reson Imaging 2002; 16(4): 451–63 [6] Ghanem, N,et al. Europ Radiol 2005; 55: 41–55.
[3] Schlemmer HP, et al. Invest Radiol 2005; 40(2): 64–71 [7] Harisinghani MG, et al. N Engl J Med 2003; 348(25): 2491–9.
[4] Farsad M, et al. J Nucl Med 2005; 46(10): 1642–9.

Pediatric

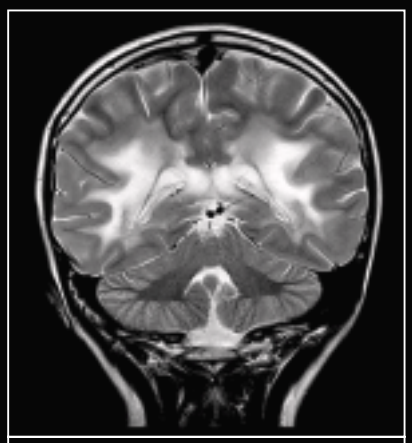

[1] ***MAGNETOM Trio, A Tim System: Head, 8-year-old***
T2 TSE / coronal / leukodystrophy. TR 3190 ms / TE 90 ms / TA 1:49 min / SL 5 mm / slices 23 / matrix 512 / FoV 200 mm.
Courtesy of Hong Kong Sanatorium and Hospital

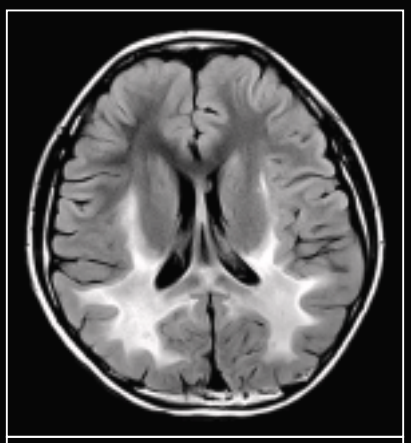

[2] ***MAGNETOM Trio, A Tim System: Head, 8-year-old***
DarkFluid / GRAPPA 2 / transversale / leukodystrophy. / TR 10000 ms / TE 92 ms / TI 2500 ms / TA 2:40 min / SL 5 mm / slices 11 / matrix 320 / FoV 220 mm.
Courtesy of Hong Kong Sanatorium and Hospital

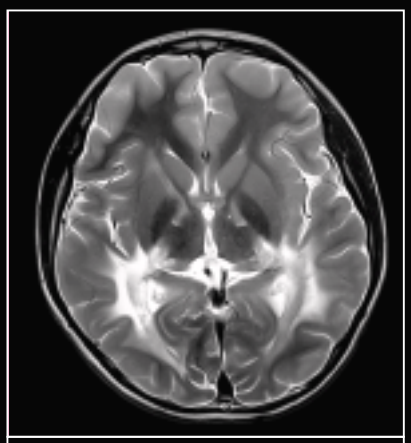

[3] ***MAGNETOM Trio, A Tim System: Head, 8-year-old,***
T2 TSE / GRAPPA 2 / transversale, leukodystrophy. / TR 4400 ms / TE 98 ms / TA 2:25 min / SL 5 mm / slices 22 / matrix 512 / FoV 220 mm.
Courtesy of Hong Kong Sanatorium and Hospital

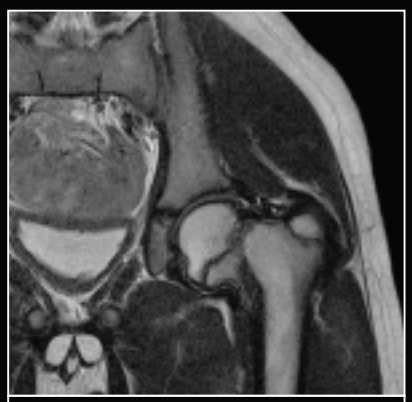

[4] ***MAGNETOM Espree: Hip, T2-weighted Turbo Spin Echo (TSE), 7-year-old male***
coronal / morbus perthes. / TR 3650 ms / TE 79 ms / TA 1:57 min / SL 3 mm / slices 20 / matrix 512 / FoV 160 mm.
Courtesy of Alegent Gold Circle, Omaha, USA

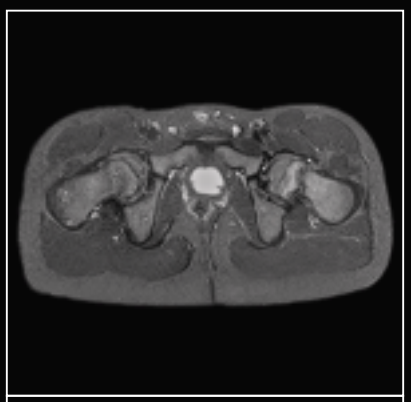

[5] ***MAGNETOM Espree: Hip, T2-weighted Turbo Inversion Recovery (TIR), 7-year-old male***
GRAPPA 2 / transversale / morbus perthes / TR 5170 ms / TE 57 ms / TI 150 ms / TA 1:33 min / SL 3 mm / slices 20 / matrix 512 / FoV 280 mm.
Courtesy of Alegent Gold Circle, Omaha, USA

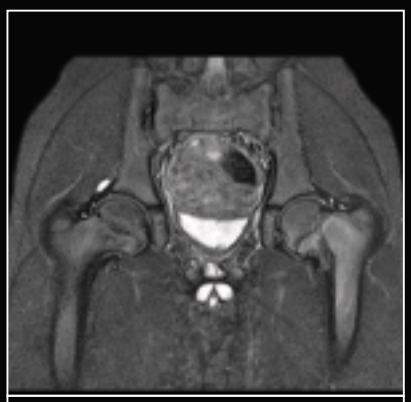

[6] ***T2-weighted Turbo Inversion Recovery (TIR), 7-year-old male***
GRAPPA 2 / coronal / morbus perthes. / TR 5250 ms / TE 57 ms / TI 150 ms / TA 1:34 min / SL 3.5 mm / slices 20 / FoV 280 mm.
Courtesy of Alegent Gold Circle, Omaha, USA

Pediatric* Abdominal MRI in Oncology

Sebastian Ley[1,2], Julia Ley-Zaporozhan[2], Patrick Guenther[3], Stefan Delorme[2], Jens-Peter Schenk[1]

[1]Department of Pediatric Radiology, University Hospital Heidelberg, Heidelberg, Germany
[2]Department of Radiology (E010), German Cancer Research Center, Heidelberg, Germany
[3]Department of Pediatric Surgery, University Hospital Heidelberg, Heidelberg, Germany

Introduction

The potential bioeffects and late effects of radiation in diagnostic procedures in children have long been discussed. Although the radiation dose for single procedures may be low, children are often examined repeatedly, which will result in relatively high cumulative doses. Most importantly, children are considerably more sensitive to the carcinogenic effects of ionizing radiation than adults, and have a longer life expectancy resulting in a larger window of opportunity for suffering the sequelae of radiation damage. Therefore, all diagnostic procedures without ionizing radiation are to be preferred in children, whenever adequate, and the "ALARA" (as low as reasonably achievable) concept applies if radiation can not be entirely avoided [1].

The most common abdominal lesions in children are hepatoblastoma, neuroblastoma, Wilms' tumor, nephroblastomatosis, rhabdomyosarcoma and germ cell tumors. For diagnosis of abdominal masses, ultrasound (US) and magnetic resonance imaging (MRI) are the methods of choice, since they are non-invasive and free of ionizing radiation.

US is widely available, cheap and can be performed bed-side without needing to sedate the child. Nevertheless, US is highly user-dependent and volumetric evaluation of masses, especially of complex geometry, is difficult. Therefore, MRI has several advantages over US, but has challenges of its own in children. Examination times are longer, and children must eventually be sedated or even intubated. The technology is less available and standard examination protocols are not yet established. However, MRI allows for the most comprehensive imaging of the body with a high soft tissue contrast, angiography and 3D volumetry of lesions and organs. Therefore, only MRI permits to comprehensively answer the clinical questions for initial staging and follow-up examinations.

The proposed MR imaging protocol is an attempt to cover most of the numerous clinical demands. Once detected, a lesion must be named, and differential diagnoses considered. A local and general staging is expected. A combination of initial chemotherapy for tumor volume reduction and tumor resection is the basic treatment for solid tumors (non-lymphoma) (for Europe, treatment schemas are developed by the "Society of Pediatric Oncology and Hematology") [2]. Follow-up examinations are performed during chemotherapy, before and after surgery. For the different phases, major clinical issues are:

1. Initial diagnosis: Establishment of diagnosis; rule out differential diagnosis; local infiltration; staging (metastases); 3D tumor volumetry

2. Follow-up during chemotherapy: Local infiltration and current extent of the tumor; 3D tumor volumetry; characterization of tumor tissue (development of necrosis and residual active tumor tissue)

3. Pre-operative planning: 3D tumor volumetry; tumor fragility; vascular feeding of the tumor, display of adjacent organs to be spared during surgery

4. Follow-up examinations: Residual tumor; relapse; re-staging

Using MRI, these clinical questions can be covered, but at a price of an examination time of 45 to 60 minutes, even with a basic imaging protocol.

The examination time is shorter with general anesthesia, but a light sedation of the child is less invasive and easier (on an out-patient basis). Therefore, our examination protocol makes extensive use of respiratory gating (like PACE – Prospective Acquisition CorrEction – technology) for optimal imaging results.

The protocol was developed on a MAGNETOM Avanto (Numaris/4, *syngo* MR 2004 V) with a Body Matrix coil combined with the Spine Matrix coil (phased array, 12 elements).

* The safety of imaging fetuses / infants has not been established.

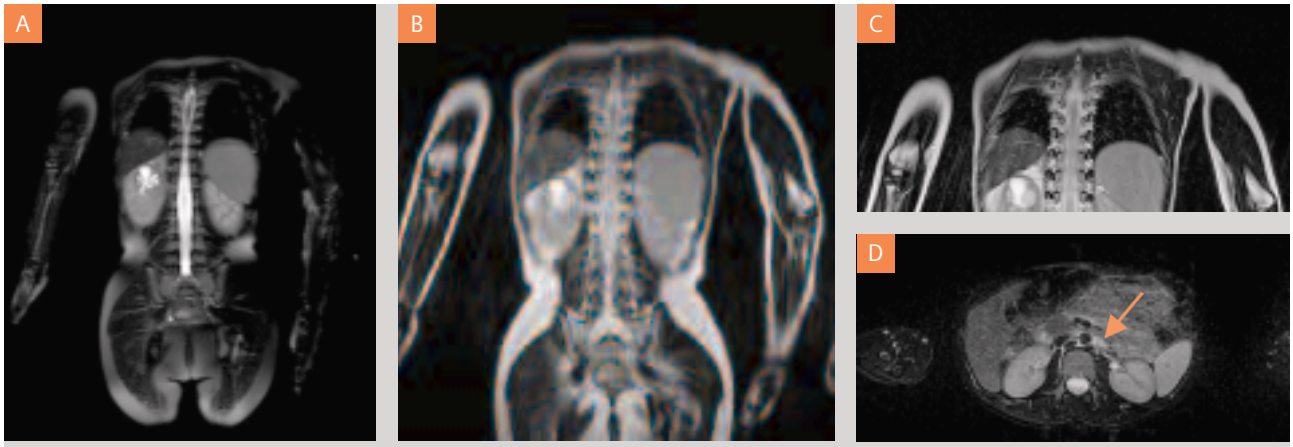

[Figure 1] *4-year-old girl with a Wilms' tumor of the right kidney. The HASTE Cor FS sequence provides a fast anatomical overview of the abdomen (A). The T2 TSE Cor (respiratory gated) has a higher spatial resolution and provides a better delineation between tumor and surrounding tissues (B). 8-year-old girl with a pelvic teratoma. While she tolerated the examination unsedated, she was unable to cooperate and hold her breath. However, the T2 TSE FS images, acquired with respiratory gating (transversal) allowed detailed staging of the liver (C) and showed enlarged paraaortic lymph nodes (D).*

Morphology

As always, two orientations at least should be acquired (such as coronal and transversal orientation). With recent sequence technologies, thin slice isotropic data sets can be acquired, which allow multiplanar reformats (MPR) and possibly obviate additional, second plane sequences, although (due to averaging effects or breathing artifacts) the results of such reformats are not always as good.

For imaging of children a small field-of-view (FOV) and high spatial resolution should be used. For sufficient signal-to-noise ratio, most sequences have to be averaged 3 to 5 times and the bandwidth has to be kept low.

After a basic localizer a TrueFISP sequence with 50% slice overlap is acquired. This allows fast, free breathing image acquisition. Due to the nature of TrueFISP the vessels light up bright and enable a first inspection of the vasculature. Furthermore, the abdominal organs are well displayed. As the organ capsulature is visualized pronounced discontinuity due to tumor break-through the capsule can be visualized easily.

For a fast and more detailed overview, a coronal and transversal HASTE can be used. Due to better tumor delineation a T2-weighted TSE in two orientations (respiratory gated, preferably with FS) is preferable (Fig. 1) [3].

For optimal visualization of the vertebral bodies, long bones and pelvis for staging of the patient a coronal T2-weighted TIRM is suited best (Fig. 2).

For characterizing of the tumor, T1-weighted images are acquired pre- and post-contrast. Post-contrast examinations are done with fat saturation.

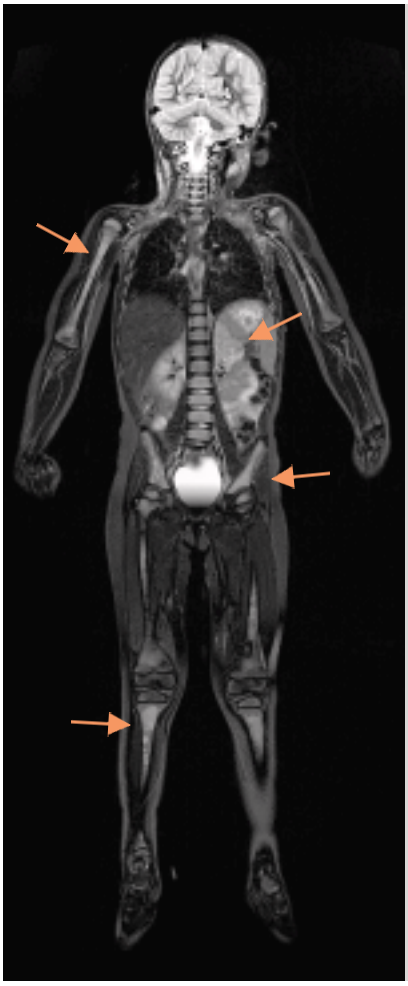

[Figure 2] *3-year-old girl with neuroblastoma of the left adrenal (arrow). This is a composed T2-weigthed TIRM image showing the multiple metastasis of the long bones and pelvis. This combination of high spatial local MR and fast whole body screening makes MRI a valuable tool for the clinicians and will reduce the many single staging procedures as performed today.*

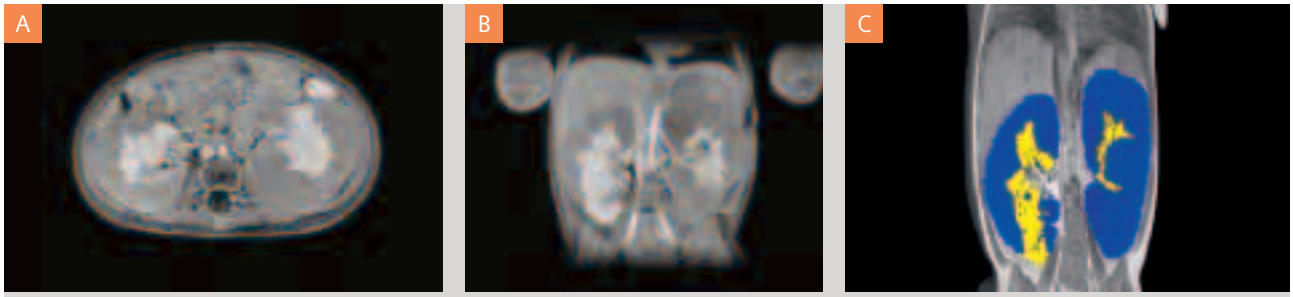

[Figure 3] *17-months-old girl with nephroblastomatosis of both kidneys. (A) Shows the original transversally acquired VIBE sequence post-contrast injection. The flip angle should be increased to pronounce the effect of contrast media. The resolution of this dataset was 1.2 x 1.2 x 1.2 mm³. (B) The coronally reconstructed isotropic VIBE dataset showed an excellent delineation between the tumor and surrounding organs. Also the abdominal vasculature and stretched arteries of the kidneys can be evaluated. (C) Based on the post-ce VIBE, a voxel based quantification of the nephroblastomatosis (blue; left: 400 ml, right: 200 ml) and tissue of kidney (yellow) is possible. This approach allows monitoring of tumor volumes during chemotherapy. Also, the increase in necrosis and decrease in viable tumor tissue can be quantified.*

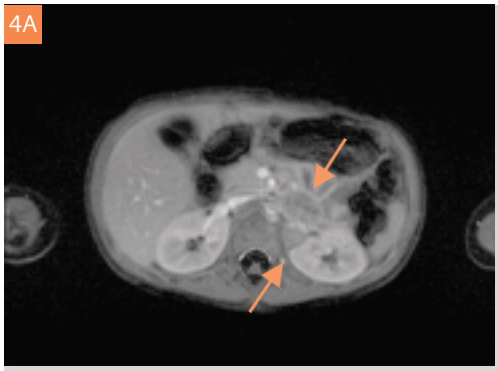

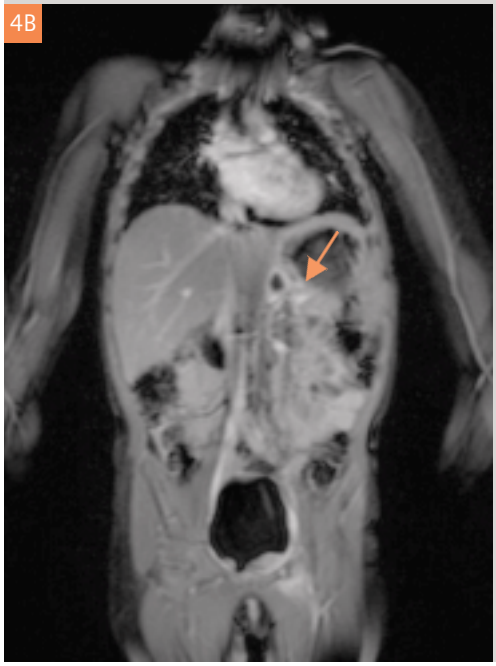

[Figure 4] *Same patient as shown in Fig. 2 with a neuroblastoma of the left adrenal gland. Transversal (A) and coronal (B) images of a T1-weighted TurboFLASH with fat saturation and respiratory gating (PACE). Due to respiratory gating the infradiaphragmal organs are visualized sharp and the tumor extent can be clearly seen (arrows).*

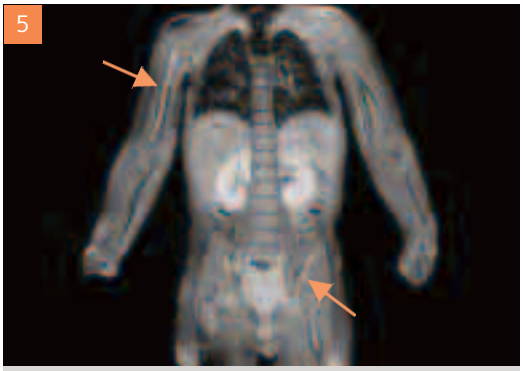

[Figure 5] *Same patient as in Fig. 2. This T1-weighted TSE with fat saturation (after contrast media) displays well the metastatic lesions due to the nephroblastoma (e.g. right humerus). While in T2-weighted TSE (Fig. 2) the whole pelvis seemed infiltrated, only a small area shows contrast enhancement. Therefore, this region is more likely to be a metastatic lesion, while the other T2-weighted hyperintensive regions are reactions to chemotherapy. While this sequence is less optimal for imaging the infradiaphragmatic regions, it shows better bone lesions than the T1-weighed TurboFLASH as shown in Fig. 4.*

For T1-weighted imaging, a volume interpolated breath-hold examination (VIBE) sequence is most favorable, because it allows isotropic image acquisition with subsequent multiplanar reconstruction (Fig. 3). However, since this technique is not available with respiratory gating, averaging (instead of breath-hold) has to be used. Good image quality is achieved for the lower abdomen/pelvis. The organs of upper abdomen may not be visualized well due to respiratory motion artifacts. Thus, a respiratory gated T1-weighted (Turbo-)FLASH has to be used in the upper abdomen (Fig. 4). For staging purposes we use a coronal T1-weighted TSE FS after contrast media (Fig. 5). In the future, isotropic imaging in one orientation and subsequent reconstruction will be increasingly used. The new SPACE technology provides ultra-high spatial resolution (down to 0.9 mm^3 isotropic) and provides exquisite images of the abdomen in children [4] (Fig. 6). The only drawback is a long acquisition time of 7 to 9 minutes, which is longer than applying two orientations of either a T2- or T1-weighed sequence. Therefore, it has to be evaluated if the increase in spatial resolution is worth the increase in imaging time. In our experience, isotropic resolution and making multiplanar reformats are the optimal way to help the operating surgeon to understand the spatial relationships between the tumor and its neighborhood. Furthermore, volume involution as well as the structural change of the tumor are criteria for the tumor response to chemotherapy. Following chemotherapy the inner structure of a tumor also changes with increase in necroses and tumor fragility.

3D morphological imaging can be used for a voxel-based tumor volumetric analysis by volume rendering. This is substantially more accurate than simply measuring diameters. The tumor volume determined by preoperative diagnostics can be important for the aggressiveness of the postoperative chemotherapy (therapy stratification). For instance, in a Wilms' tumor an involution of tumor volume below 500 ml by preoperative chemotherapy indicates a significantly better prognosis.

For optimal staging, a coronal examination of the head and thorax should be added to the abdominal examination. Especially in children this should be possible with only one table movement (50 cm field of view provided). As this is only intended to be a searching technique, a T2-weighted TIRM and T1-weighted TSE FS should be sufficient. This will extend the examination time by approximately 10 minutes but provides additional valuable information for the clinicians and makes other examinations either unnecessary or more tailored.

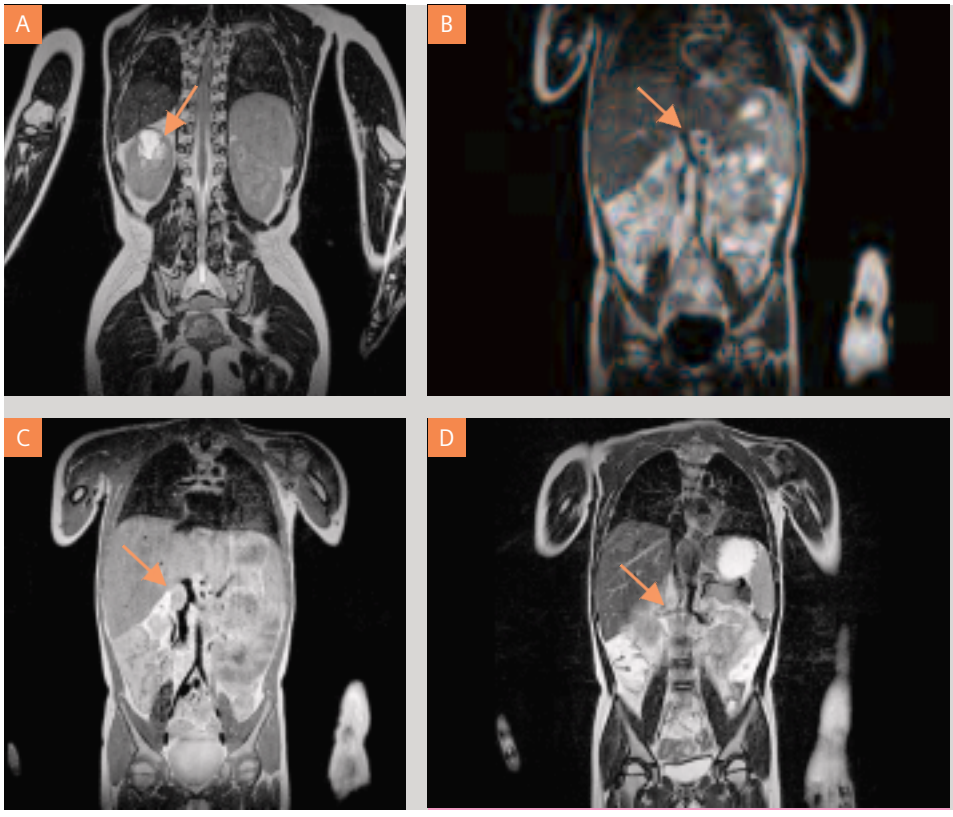

[Figure 6] *4-year-old girl with a Wilms' tumor of the right kidney (same patient as Fig. 1 A + B). (A) Shows the capability of the new SPACE technology (T2-weighted) for brilliant visualization of the primary tumor. The tumor induced a thrombotic formation in the inferior vena cava. Comparison between different sequences for visualization of the thrombus (B) SPACE T2-weighted (C) SPACE T1-weighted (D) T2-weighted TSE respiratory gated.*

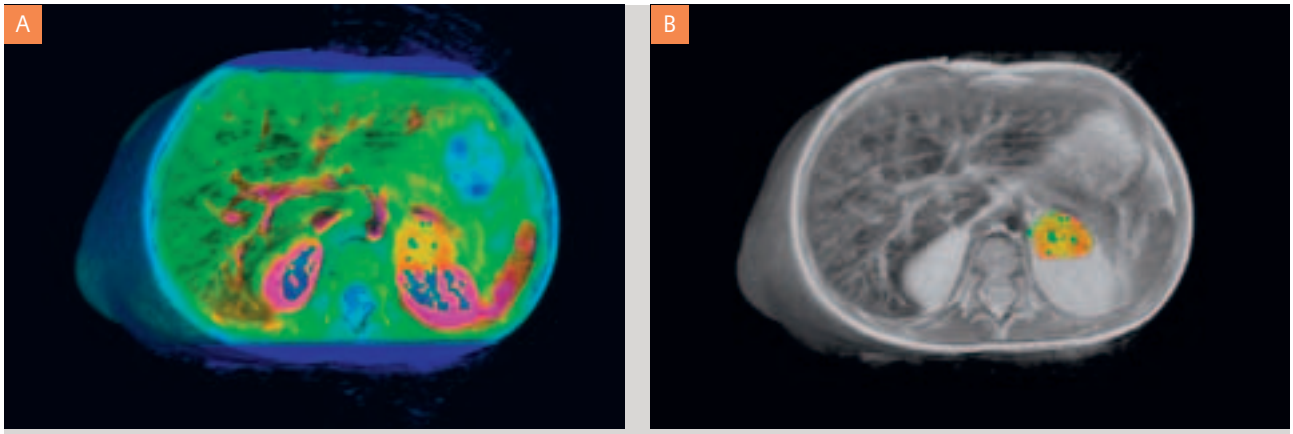

[Figure 7] *These images show the color-coded perfusion maps of the neuroblastoma of the left adrenal (see also Figs. 2, 4, 9A) following chemotherapy. While the parenchyma of the left kidney is well perfused (A), the tumor tissue is less perfused and shows central necrosis. These differences also allow to clearly separate the parenchyma of the kidney from the tumor (B).*

Time-resolved angiography and perfusion

Evaluation of arterial input and venous drainage of the abdominal organs and vessels is important to visualize. For this purpose a fast 3D FLASH sequence using Parallel Imaging Techniques (PAT) is optimal. Image acquisition time should be as fast as possible. Therefore, we use a temporal resolution of 2 to 3 seconds with a spatial resolution of 3 mm^3. The 3D volume should be acquired coronally and cover the whole abdomen. This will for example enable visualization of the hepatic arteries and portal veins and also help to detect a thrombotic occlusion of the inferior vena cava. Also venous outflow of the kidneys as indirect sign of obstruction can be displayed.

A second advantage of using a time-resolved angiography is that it is possible to calculate perfusion maps of the tumor. For the evaluation of the tumor perfusion as a function of time and intensity the dynamics of the contrast medium can be visualized, color-coded in 3D-parameter images (Fig. 7). Perfusion measurements of tumors have a long tradition in evaluation of brain tumors and are more and more implemented in the modern oncological concept in all other parts of the body. The background is that the basic tumor morphology does not necessarily reflect the biologic state of the lesion. Late post-contrast studies may not be sufficient, as contrast media may diffuse into necrotic areas and therefore give a false positive impression, that the lesion consists of more viable tissue than is actually the case. The precise analysis of the ratio between viable tumor and necrosis is used as an indicator of tumor fragility which is an important pre-surgical information or for planning biopsy [5].

High spatial resolution angiography

Visualization of the abdominal vessels is of utmost importance before surgery. In adults either a 3D FLASH or VIBE are used for contrast-enhanced (ce) MR-Angiography (MRA) of the abdomen (Fig. 8), but in children, they meet some specific problems: First, sedated children are not able to hold their breath, and motion artifacts reduce image quality markedly,

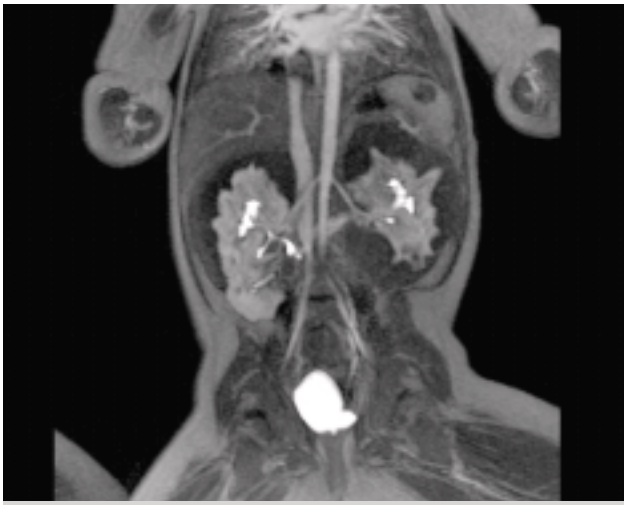

[Figure 8] *17-months-old girl with nephroblastomatosis of both kidneys (same patient as in Fig. 3). This is a maximum intensity projection (MIP) of a FLASH 3D angiography dataset (acquisition time of a 3D dataset 7 seconds). Due to the bilateral nephroblastomatosis both renal arteries are bent downwards but have no stenosis.*

even with acquisition times as short as 6 seconds per 3D dataset. Second, the small field of view leads to an increase in noise, sometimes making 3D reconstructions and clear delineation of vessels and tumor difficult.

Therefore, for acquisition of high spatial resolution 3D angiographic datasets sequences from the coronary artery examination protocols are best suited. As a prerequisite, the patient has to be equipped with an ECG before the examination (which is also useful for monitoring the patient). We use a T2 prepared 3D TrueFISP with respiratory gating to acquire images with an isotropic resolution of 1 – 1.2 mm^3 [6]. Due to the double gating technique (respiratory and cardiac) images present with excellent sharpness and without blurring artifacts (Fig. 9). They allow for exquisite reformation and anatomical evaluation of the anatomic relation of a tumor to the local vasculature. Also compression of vessels like vena cava inferior by large tumors can be evaluated. The precise location of a thrombus in the inferior vena cava or in rare cases to the right atrium can be visualized and presented to the surgeon. This will help in planning the type of resection and indicate whether, for example, cardio-thoracic surgeons need to be involved in the operation.

Conclusion

The combination of high spatial resolution imaging with respiratory gating allows examination of children with mild sedation. All aspects of clinical questions can be solved satisfactorily. The new, isotropic image acquisition techniques with subsequent multiplanar reconstructions in particular will reduce imaging time and further improve 3D visualization of the relation of pathologic tissue to normal organs.

Abbreviations

ceMRA	contrast enhanced MR Angiography
HASTE	Half-Fourier Acquisition Single-Shot Turbo SE. HASTE is used for sequential acquisition of high-resolution T2-weighted images.
FLASH	Fast Low Angle SHot
FS	Fat Saturation
PACE	Prospective Acquisition CorrEction
SPACE	Sampling Perfection with Application optimized Contrasts using different flip angle Evolutions
TIRM	Turbo Inversion Recovery Magnitude
TrueFISP	A gradient echo sequence that provides the highest signal of all steady state sequences.
TSE	Turbo Spin Echo. A fast multiecho sequence.
TurboFLASH	The entire raw data matrix is measured in one acquisition with an ultra-fast gradient echo sequence.
VIBE	Volume Interpolated Breathhold Examination. For reducing the acquisition time of 3D scans with a reduced number of slices using interpolation.

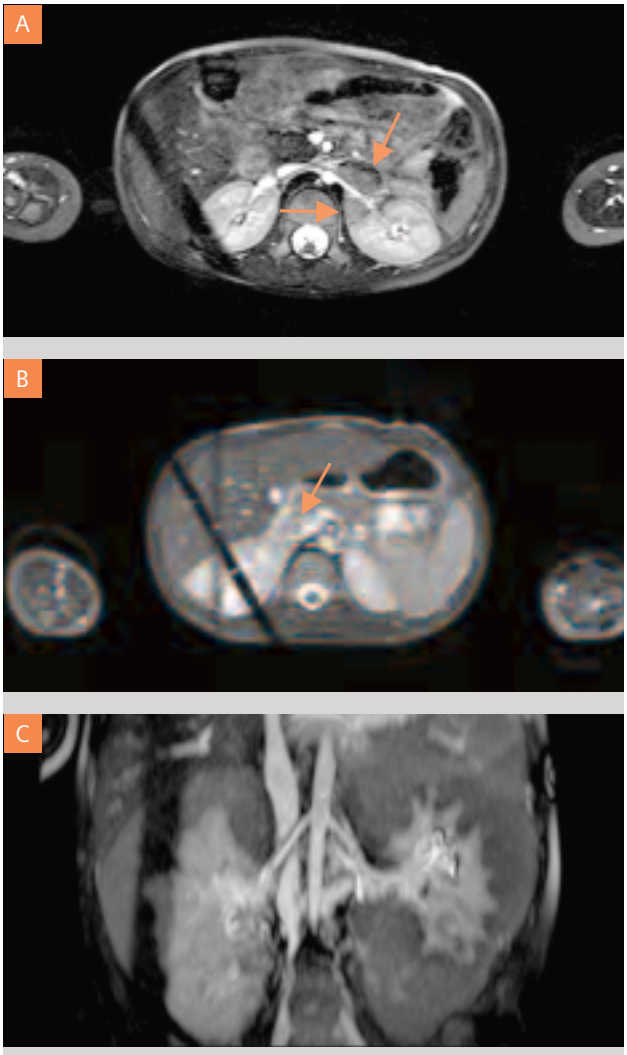

[Figure 9] *For non contrast enhanced angiography the use of T2 prepared 3D TrueFISP sequences show excellent results. (A) Transversal orientated image acquisition with exquisite delineation of the left renal artery with tumor formation dorsal and ventral to the artery (arrows) (same patient as Fig. 4). This information is of utmost importance to the surgeon before resection of the lesion. (B) Transversal orientated T2 prepared 3D TrueFISP in the same patient as in Fig. 6B showing the thrombus in inferior vena cava. (C) 17-months-old girl with nephroblastomatosis of both kidneys (same patient as in Figs. 3 and 8). Due to isotropic image acquisition reformats like this coronal one are possible without loss of information (coronal MIP). A higher spatial resolution is gained compared to contrast enhanced angiography (Fig. 8) allowing better evaluation of the small abdominal vasculature in children. (The dark bands indicate the location of the navigators.)*

Protocol

Name	TE	TR	FA	Orientation	FS	Respiratory compensation	Resolution	Distance factor in %	Base / Phase resolution in %	PAT	TA
Basic localizer	1.16	337	60	Tra/ Cor/Sag	No	No	2.4 x 1.6 x 8	300	256 / 66	2	0:10
TrueFISP	1.2	290	80	Tra	No	No	2 x 1.3 x 4	-50	256 / 65	2	0:37
TrueFISP	1.2	290	80	Cor	No	No	2.4 x 2 x 4	-50	256 / 81	2	0:29
TrueFISP	1.2	290	80	Sag	No	No	1.9 x 1.6 x 4	-50	256 / 80	2	0:39
HASTE	119	1100	150	cor	Yes	3x average	2.6 x 2.0 x 4	0	256 / 77	2	1:56
T2 TIRM (TSE)	100	3800	144	Tra	IR 150	PACE + 2x average	1.8 x 1.2 x 5	10	320 / 65	2	~ 2:27
T2 TIRM (TSE)	87	4500	150	Cor	IR 150	2x average	1.7 x 1.2 x 5	5	384 / 70	2	3:45
T2 TSE	96	1660	150	Tra	No	PACE	1.6 x 1.2 x 5	20	320 / 75	2	~ 1:13
T2 TSE	96	1670	150	Cor	No	PACE	1.6 x 1.2 x 5	0	320 / 75	2	~ 1:20
T1 TFL	4.08	600	15	Tra	No	PACE + 3x average	2.4 x 1.8 x 5	21	192 / 75	2	~ 2:44
T1 TFL	4.08	600	15	Cor	No	PACE + 3x average	3 x 2.2 x 4	21	192 / 75	2	~ 1:59
VIBE (FL3D)	1.54	3.47	12	Tra	No	3x average	1.2 x 1.2 x 1.2	20	256 / 100	2	1:51
FLASH 3D	0.73	2.42	20	Cor	No	No	3 x 3 x 3	20	128 / 100	2	0.03 (x 30)
T1 TFL	4.08	13500	15	Tra	IR 900	PACE + 3x average	2.4 x 1.8 x 5	21	192 / 75	2	~ 4:14
T1 TFL	4.08	1190	15	Cor	IR 900	PACE + 3x average	3 x 2.2 x 4	21	192 / 75	2	~ 2:47
VIBE	1.54	3.47	25	Tra	Yes	3x average	1.2 x 1.2 x 1.2	20	256 / 100	2	1:57
T2 prep 3D TrueFISP	1.51	500	90	Tra	Yes	Yes	0.9 x 0.9 x 1	15	384 / 100	2	6:30
T2 TIRM (whole-body)	87	4500	150	Cor	IR 150	No	1.7 x 1.2 x 5	5	384 / 70	2	3:45
T1 TSE (whole-body)	11	476	180	Cor	Yes	No	1.5 x 1.2 x 4	10	384 / 80	2	2:55
Sum											< 50 min

***FS** = Fat saturation; **TA** = Acquisition time; **IR**= inversion recovery; ~ = approximately*
This table summarizes the possibilities of sequences that can be applied. Some sequences can be used instead of another like HASTE and T2-weighted TIRM. Also the transversal VIBE can be used instead of T1-weighted TFL transversal. However, it is recommended to put them all together in one imaging protocol, as the image quality of a specific sequence can vary interindividually.

References
[1] Kleinerman RA (2006) Cancer risks following diagnostic and therapeutic radiation exposure in children. Pediatr Radiol 36 Suppl 14: 121–125.
[2] Graf N, Tournade MF, de Kraker J (2000) The role of preoperative chemotherapy in the management of Wilms' tumor. The SIOP studies. International Society of Pediatric Oncology. Urol Clin North Am 27: 443–454.
[3] Hoffer FA (2005) Magnetic resonance imaging of abdominal masses in the pediatric patient. Semin Ultrasound CT MR 26: 212–223.
[4] Scott KT, Schmeets SH (2005) SPACE: An Innovative Solution to Rapid, Low SAR, T2-Weighted Contrast in 3D Spin Echo Imaging. Magnetom Flash 2: 92–95.
[5] Cecchetto G, Mosseri V, De Bernardi B, Helardot P, Monclair T, Costa E, Horcher E, Neuenschwander S, Toma P, Rizzo A, Michon J, Holmes K (2005) Surgical risk factors in primary surgery for localized neuroblastoma: the LNESG1 study of the European International Society of Pediatric Oncology Neuroblastoma Group. J Clin Oncol 23: 8483–8489.
[6] McNeal GR (2006) Whole Heart MRI – Adopting the CT Approach. MAGNETOM Flash 1: 16–22.

Cardiovascular

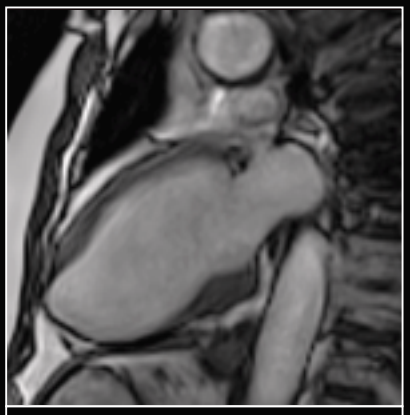

[1] ***MAGNETOM Trio, A Tim System:*** *Cardio / function / TrueFISP cine retro / 2 chamber view / GRAPPA 2 / infarct. / TR 42.8 ms / TE 1.3 ms / TA 6.09 s / SL 6 mm / slices 25 / matrix 192 / FoV 360 mm.*

Courtesy of University Hospital Tuebingen, Tuebingen, Germany

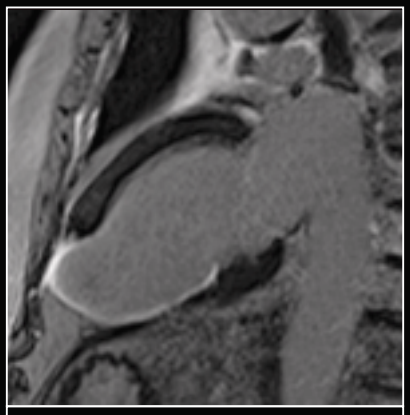

[2] ***MAGNETOM Trio, A Tim System:*** *Cardio / tissue characterization / Turbo FLASH Inversion Revovery / 2 chamber view / GRAPPA 2 / infarct. / TR 750 ms / TE 2 ms / TI 310 ms / TA 8.10 s / SL 8 mm / slices 1 / matrix 256 / FoV 370 mm.*

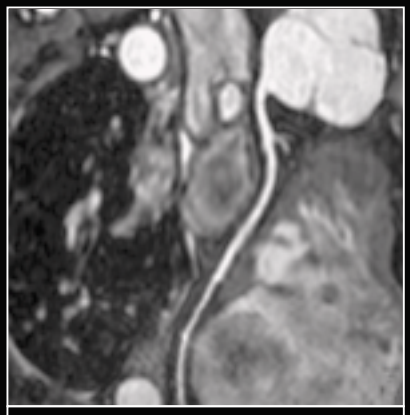

[3] ***MAGNETOM Avanto:*** *Cardio, coronary / 3D TrueFISP segmented / maximum intensity projection (MIP) / 9-year-old / situs inversus. TR 230.7 ms / TE 1.8 ms / TA 12:35 min / eff. SL 1.0 mm / partitions 104 / matrix 512 / FoV 240 mm.*

Courtesy of Olga Hospital, Stuttgart, Germany

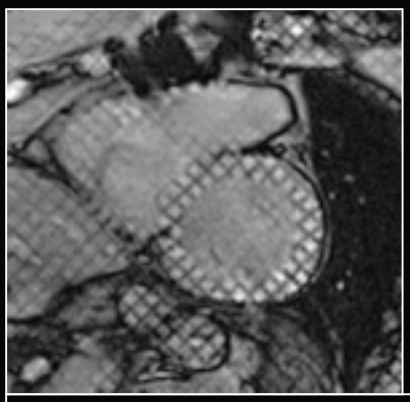

[4] ***MAGNETOM Trio, A Tim System:*** *Cardio / function / FLASH cine / tagging / short axis view / atrial septal defect (ASD). / TR 46 ms / TE 3.6 ms / TA 18.53 s / SL 6 mm / slices 18 / matrix 256 / FoV 320 mm.*

Courtesy of New York University, New York, USA

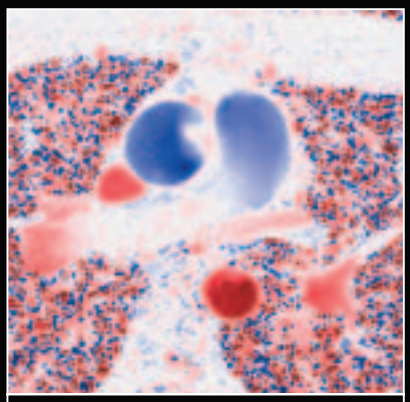

[5] ***MAGNETOM Symphony, A Tim System:*** *Cardio / flow / FLASH cine / coloured / transversal. / TR 46 ms / TE 3.8 ms / TA 3:04 min / SL 5 mm / slices 60 / matrix 256 / FoV 320 mm.*

Cardiovascular Whole-Body MR* with Parallel Acquisition Techniques (PAT) and Matrix Coils at 3 Tesla: Comparison to 1.5 Tesla

Harald Kramer M.D., Stefan O. Schoenberg M.D., Maximilian F. Reiser M.D.

Department of Clinical Radiology, University of Munich – Grosshadern Campus, Munich, Germany

Introduction

Cardiovascular disease is well known as systemic in nature and still ranks number one in mortality and morbidity statistics in the industrialized countries [1]. 70% of all patients suffering from peripheral vascular aneurysms also suffer from aortic aneurysms, 50% of patients suffering from peripheral arterial occlusive disease (PAOD) also suffer from coronary artery disease (CAD), and 40% also suffer from carotid artery stenosis (CAST) [2]. At the time point these diseases become symptomatic, an invasive treatment like dilatation and stenting of vessel segments or even surgery usually becomes necessary. Therefore an exam for early detection of initial, asymptomatic changes seems reasonable. Within the last few years it has been shown that whole-body cardiovascular MRI is feasible without compromises in image quality compared to organ-based MR exams [3-5]. MRI has become the new standard of reference for the evaluation of global cardiac function and perfusion, and magnetic resonance angiography (MRA) now replaces most diagnostic digital subtraction

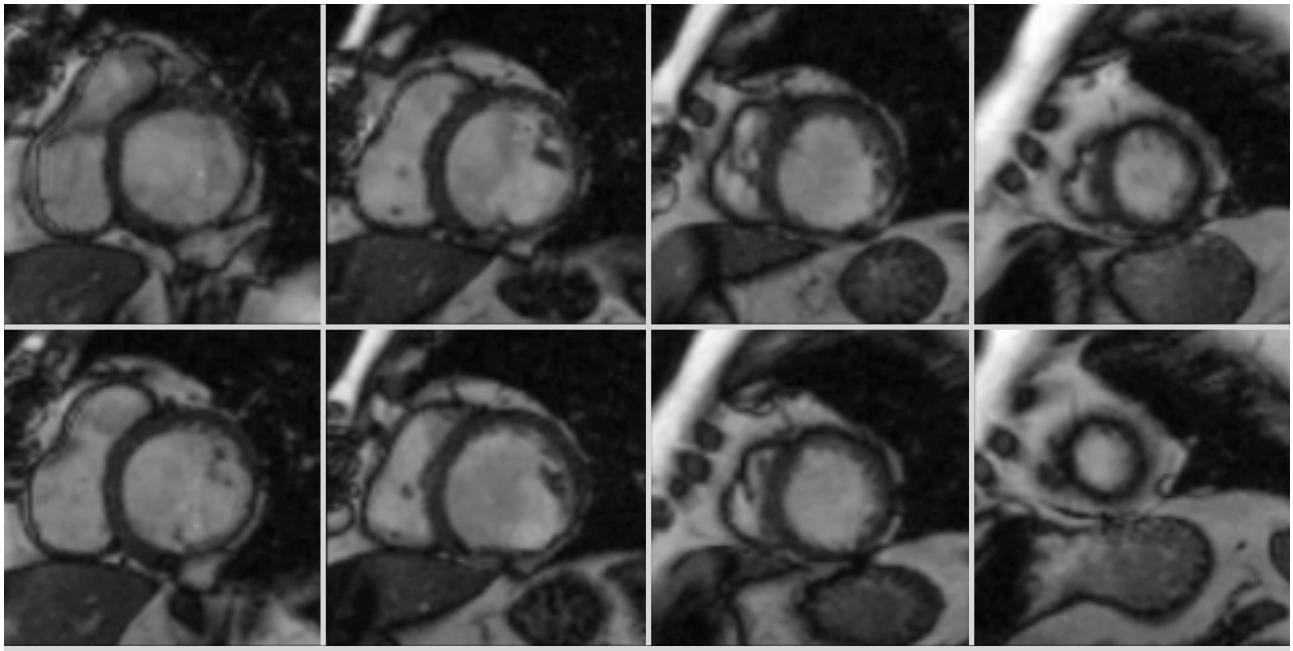

[Figure 1] *Functional cardiac imaging of up to 11 short axis slices with a PAT factor of 4 and a temporal resolution of 48 ms in only one breath-hold. Made possible by MAGNETOM Trio, A Tim System.*

angiography exams [6-10]. Latest developments in MR hardware have demonstrated the possibility of combining parallel acquisition techniques (PAT), matrix-coils (Tim, Siemens Medical Solutions) and high field strength to further increase image quality.

Material and methods

To date, more than 300 individuals taking part in their company's healthcare program have been examined at 1.5T and 3T respectively. The whole-body examination protocol was optimized over time when moving from a standard 1.5T MR system (MAGNETOM Sonata) to a dedicated 1.5T whole-body MR system (MAGNETOM Avanto) and then to 3.0T (MAGNETOM Trio, A Tim System). The existing and clinically approved cardiovascular MRI protocol including comprehensive cardiac imaging and whole-body MR-angiography (WB-MRA) was implemented trouble-free on the 3T 32-channel whole-body MR system (MAGNETOM Trio, Siemens Medical Solutions, Erlangen, Germany) [5, 11]. All participants were referred by their company's medical officer and underwent yearly conventional routine exams such as ECG, Doppler Ultrasound of the carotid arteries, ultrasound of the abdomen, chest x-ray etc. The combination of a matrix-coil system and high field strength allowed performing functional cardiac imaging of up to 11 short axis slices with a PAT acceleration factor of 4 and a temporal resolution of 48 ms in only one breath-hold (Fig. 1). Perfusion imaging at rest in 5 representative slices of the left ventricular myocardium was also performed with a PAT factor of 2 in one breath-hold. To complete the cardiac examination, tissue characterization imaging was performed 13–17 minutes after the last CA injection. WB-MRA was performed within 4 steps from the head down to the lower extremity in 85 seconds. Acquiring 4 to 5 consecutive steps from the head down to the feet for a whole-body MRA dataset will inevitably lead to venous enhancement in the abdominal station because the CA bolus moves

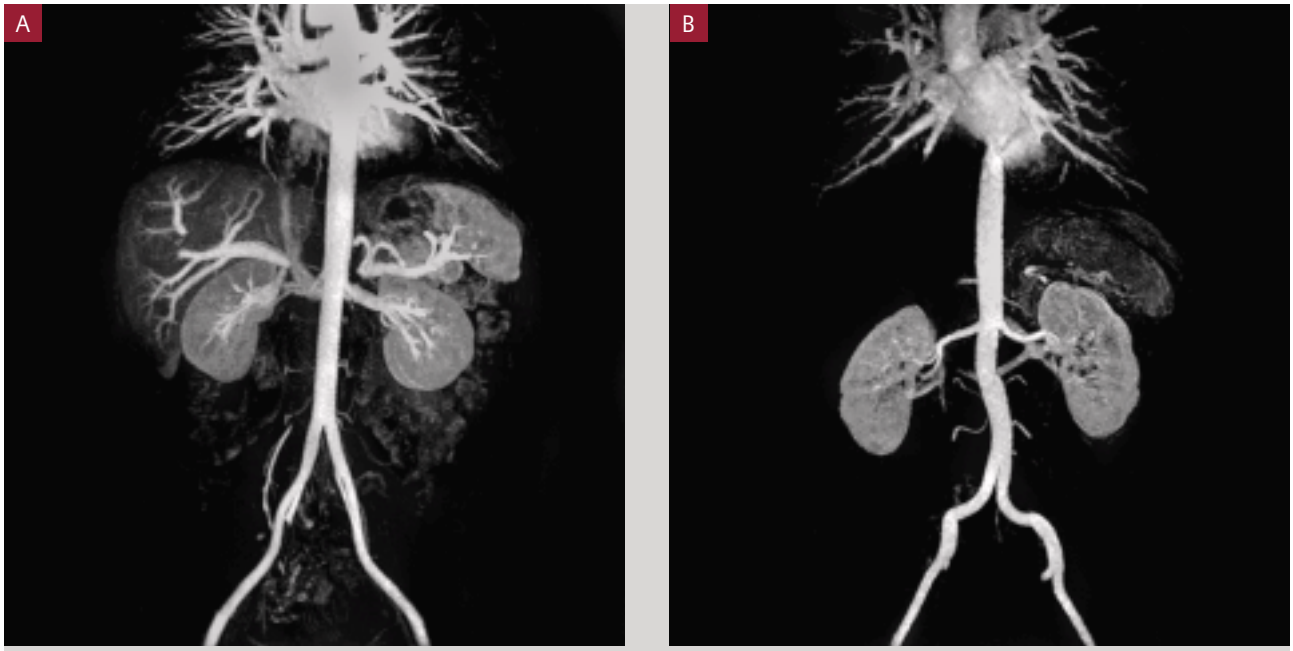

[Figure 2] *The special protocol used by the Department of Clinical Radiology at the University of Munich decreases the venous enhancement (B) compared to conventional whole-body MR Angiography protocols (A).*

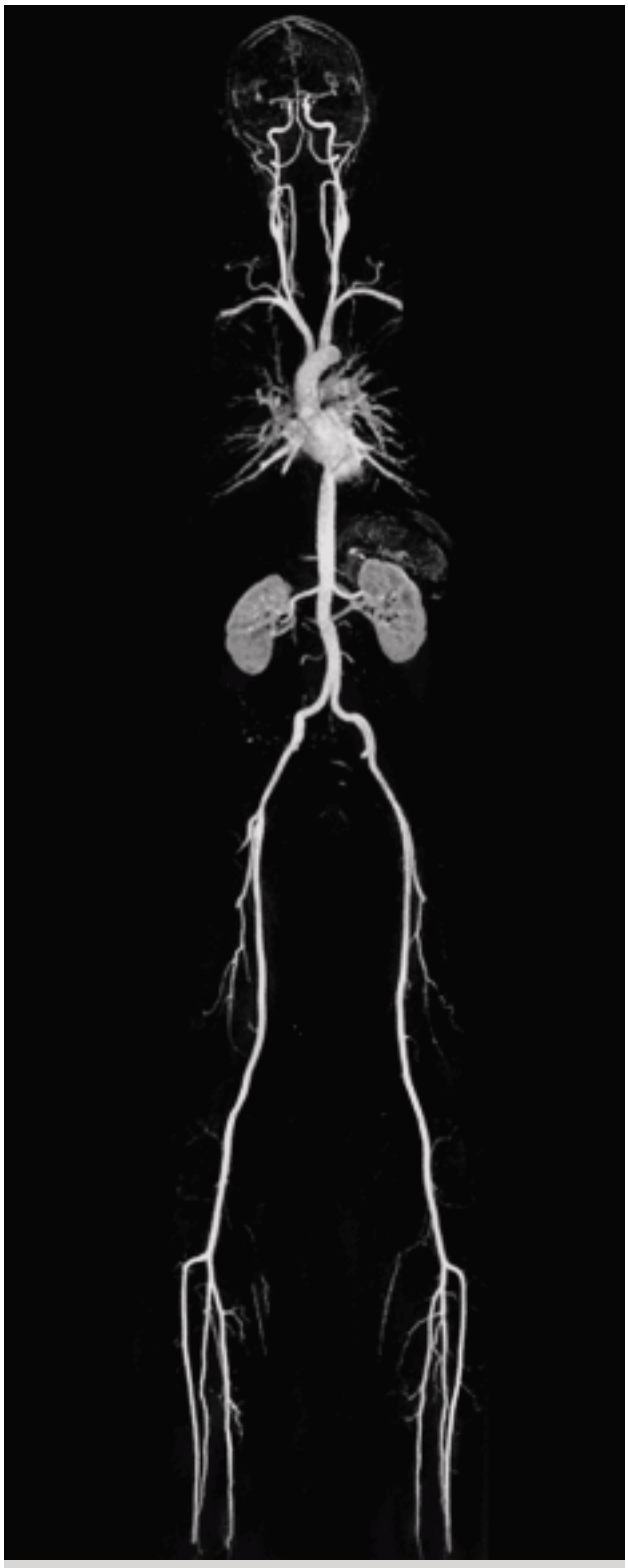

[Figure 3] *Whole-body MR Angiography with a spatial resolution of 1.4 x 1.1 x 1.2 mm³.*

to the lower body part while acquiring the first MRA station [12] (Fig. 2). To avoid this venous enhancement, a special MRA protocol was used. In this protocol first the carotid vessels and the lower extremity are imaged and then, in a second step, the abdominal and thigh vessels. After acquiring the carotid dataset, the large range of table movement enables the "overtaking" of the CA bolus and the acquisition of the calf station in a perfect arterial phase. The second CA injection allows for imaging of the abdominal vessels including the renal arteries in an arterial phase also without venous overlay (Fig. 3). Spatial resolution of WB-MRA was reduced to < 1.4 x 1.1 x 1.2 mm^3 in all steps (Table 1). In addition to high spatial resolution, dynamic MRA of the calves with an acceleration factor of 3, spatial resolution of 1.4 x 1.4 x 1.5 mm^3 and temporal resolution of 3.7 sec / frame was performed (Fig. 4). To complete the whole-body examination Time of Flight (TOF) MRA of the brain, T1- and T2-weighted, pre- and post-contrast imaging of brain, thorax and abdomen was performed with PAT (Fig. 5, Table 2). To evaluate image quality, MRA was divided into 26 vessel segments and judged by two blinded readers in terms of vessel conspicuity, artifacts and venous overlay on a three point scale. Results were compared to those from 1.5T WB-MRA. Inter-reader-agreement was calculated by the kappa statistics. Findings of conventional exams and the MRI exam were compared on a case-by-case level.

Results

The transition from 1.5T to 3.0T helped to obviously improve image quality. The increase in SNR and the dedicated matrix coil system were used to step up image quality and to accelerate image acquisition. Comprehensive cardiac imaging at rest could be performed within 3 breath-holds without any restrictions compared to cardiac based exams. Functional cardiac imaging with up to 11 short axis slices and a temporal resolution of less than 50 ms takes only one breath-hold. Similarly, perfusion at rest and tissue characterization imaging take only one breath-hold each. The quality of MRA increased in terms of image quality and higher spatial resolution compared to 1.5T exams. Due to the increase in SNR at high field strength it is possible to apply higher PAT acceleration factors and thus to shorten acquisition time and to increase spatial resolution. 88.46% of all vessel segments showed good vessel conspicuity; 89.86% showed no artifacts. Application of the improved injection protocol for whole-body MRA lead to 93.71% of vessel segments without any venous overlay. Inter-reader-agreement in rating image quality of MRA datasets was excellent, with kappa values between 0.84 and 0.95.

Table 1: Whole-body MR Angiography protocol

	CA dose @ flowrate	PAT factor	Scan-time	Resolution
Carodits	10 ml @ 1.5 ml/s	3	20 sec	1 x 1 x 1 mm^3
Calf & feet		2	26 sec	1 x 1 x 1 mm^3
Abdominal aorta	18 ml @ 1.5 ml/s	3	18 sec	1.4 x 1.1 x 1.2 mm^3
Thigh		2	21 sec	1.1 x 1.1 x 1.1 mm^3

Table 2: Whole-body examination protocol and Time of Flight (ToF) examination of the brain

min	CNS	HEART	THORAX	ABDOMEN	MRA
20	ToF, T2, Diff.				
			HASTE coronal & axial	HASTE, T2 fs	
		Function			
40		Perfusion			
					Carotids & Calf
	T1 + CA		VIBE + CA		
60		DCE			
					Abdomen & Thigh
				FLASH	

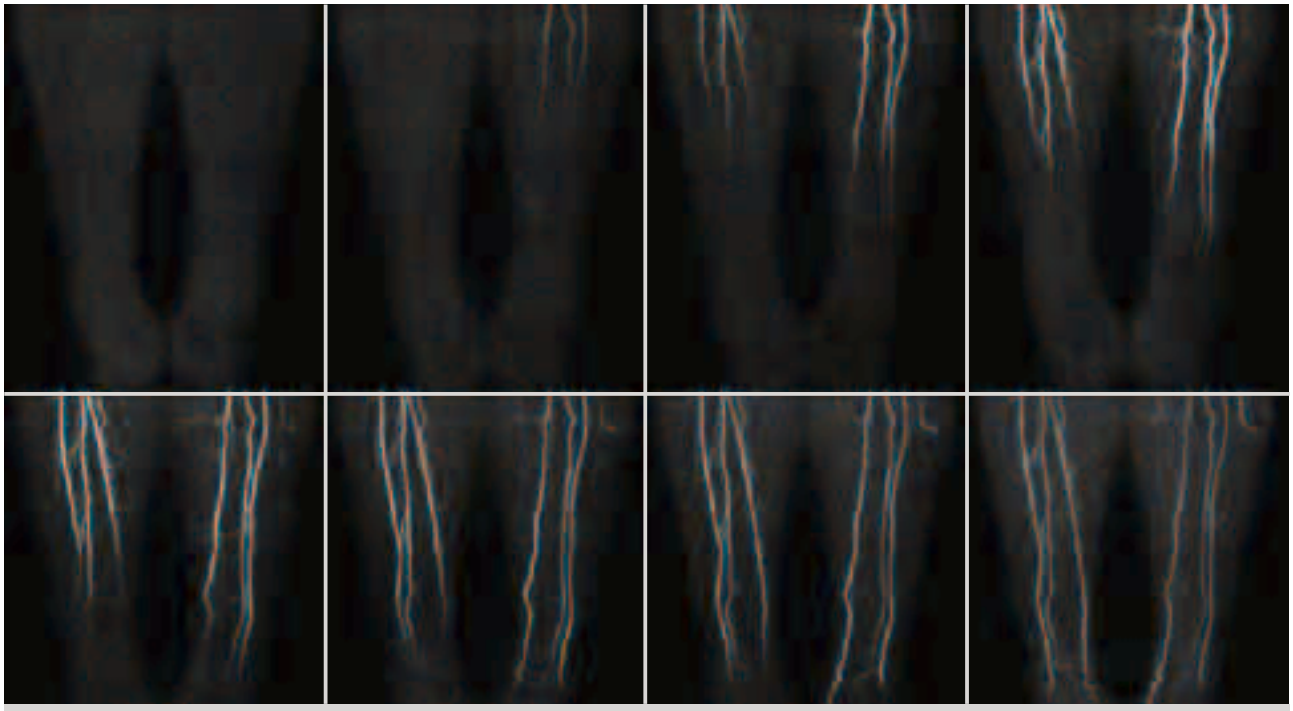

[Figure 4] *High spatial resolution (1.4 x 1.4 x 1.5 mm^3) and high temporal resolution (3.7 s/frame) MRA of the calf vessels is added to the routine protocol of whole-body MR Angiography.*

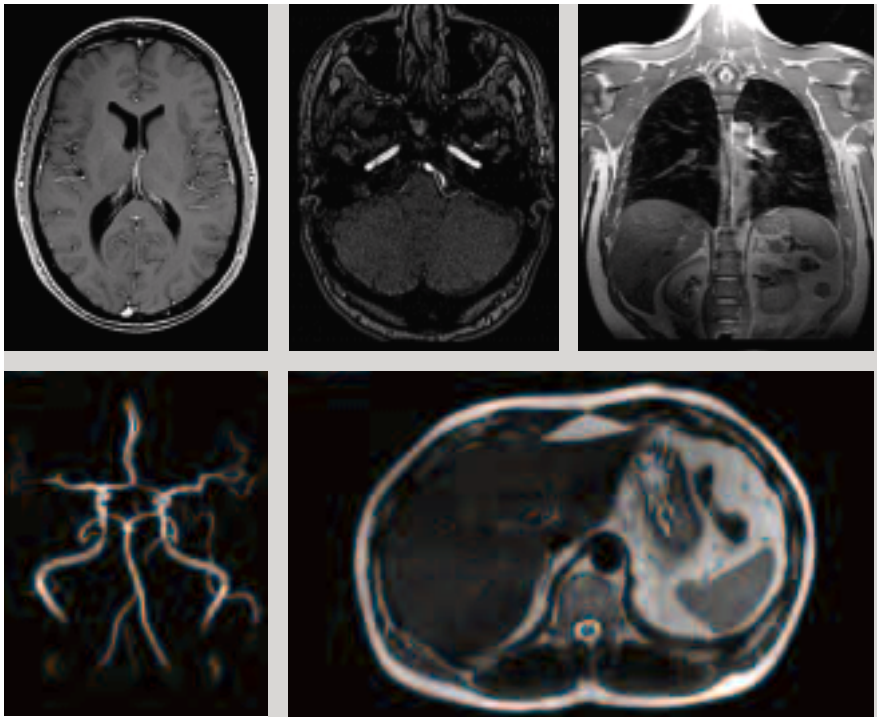

[Figure 5] *Whole-body examination and Time of Flight (ToF) of the brain.*

Conclusion

The recent technical improvements in MR hardware and cardiovascular imaging techniques enable a combination of different morphologic and functional techniques at 3T. A prerequisite for this kind of comprehensive exam is the same high image quality in every part of the exam as it is known from single station organ based exams. A matrix coil system together with PAT offers the chance of whole-body disease-specific imaging instead of organ-based imaging at high image quality and excellent spatial and temporal resolution within reasonable imaging time.

Acknowledgement

The authors also acknowledge the work of the entire cardiovascular team of the Department of Clinical Radiology, especially Dr. B. Wintersperger, Dr. S. Weckbach, Dr. H. Michaely and Dr. K. Nikolaou. This work was supported by the "Verein Magnetresonanz Forschung e.V."

*Works In Progress – The information about this product is preliminary. The product is under development. It is not commercially available in the US and its future availability cannot be assured.

References

[1] Sans, S., H. Kesteloot, and D. Kromhout, The burden of cardiovascular diseases mortality in Europe. Task Force of the European Society of Cardiology on Cardiovascular Mortality and Morbidity Statistics in Europe. Eur Heart J, 1997. 18(12): p. 1231–48.
[2] Cahan, M.A., et al., The prevalence of carotid artery stenosis in patients undergoing aortic reconstruction. Am J Surg, 1999. 178(3): p. 194–6.
[3] Goyen, M., et al., Detection of atherosclerosis: systemic imaging for systemic disease with whole-body three-dimensional MR angiography-initial experience. Radiology, 2003. 227(1): p. 277–82.
[4] Goyen, M., et al., Whole-body three-dimensional MR angiography with a rolling table platform: initial clinical experience. Radiology, 2002. 224(1): p. 270–7.
[5] Kramer, H., et al., Cardiovascular screening with parallel imaging techniques and a whole-body MR imager. Radiology, 2005. 236(1): p. 300–10.
[6] Alfakih, K., et al., Normal human left and right ventricular dimensions for MRI as assessed by turbo gradient echo and steady-state free precession imaging sequences. J Magn Reson Imaging, 2003. 17(3): p. 323–9.
[7] Barkhausen, J., et al., Assessment of ventricular function with single breath-hold real-time steady-state free precession cine MR imaging. AJR Am J Roentgenol, 2002. 178(3): p. 731–5.
[8] Kramer, H. Magnetic Resonance Angiography (MRA) of the Lower Extremities with Parallel Imaging and a Dedicated 36 Element Matrix-Coil at 3 Tesla. in ISMRM. 2006. Seattle.
[9] Meaney, J.F. and N. Sheehy, MR angiography of the peripheral arteries. Magn Reson Imaging Clin N Am, 2005. 13(1): p. 91–111, vi.
[10] Wintersperger, B.J., et al., Single breath-hold real-time cine MR imaging: improved temporal resolution using generalized autocalibrating partially parallel acquisition (GRAPPA) algorithm. Eur Radiol, 2003. 13(8): p. 1931–6.
[11] Kramer, H. Cardiovascular Whole-Body MRI with Parallel Acquisition Techniques (PAT) and Matrix-Coils at 3 Tesla: Comparison to 1.5 Tesla. in ISMRM. 2006. Seattle.
[12] Klessen, C., et al., [Whole-body MR angiography: comparison of two protocols for contrast media injection]. Rofo, 2006. 178(5): p. 484–90.

An Overview of Coronary MR Angiography* at 3.0 Tesla

Debiao Li, Ph.D.[1], Xiaoming Bi, Ph.D.[2]

[1] *Northwestern University, Chicago, IL, USA*
[2] *Siemens Medical Solutions, USA*

Abstract

In this article we review the current status of coronary imaging at 3.0T with its potential and limitations. We conclude that new 3T tailored strategies – rather than replications of 1.5T ones – and some further developments show promise in exploiting the potential of 3.0T in coronary imaging.

Since the first reports of visualizing the ostia of coronary arteries in the late 1980's [1, 2], tremendous progress has been made in coronary magnetic resonance angiography (MRA). With rapid development of imaging hardware as well as advanced fast imaging techniques, coronary MRA has become a very promising method for the noninvasive imaging of coronary arteries. However, to consistently acquire coronary artery images with diagnostic quality still remains challenging in routine clinical settings. Major limitations include the limited signal-to-noise ratio (SNR) and low spatial resolution of the image, respiratory and cardiac motion related artifacts, and relatively long imaging time.

Whole-body 3.0 Tesla imaging systems have recently been used more frequently clinically and gained great interest in cardiac imaging. Intuitively, the SNR gain from 1.5 Tesla to 3.0 Tesla can be directly traded to improve the spatial resolution of images and/or decrease the overall imaging time. Unfortunately, the improved SNR at higher field strength is usually

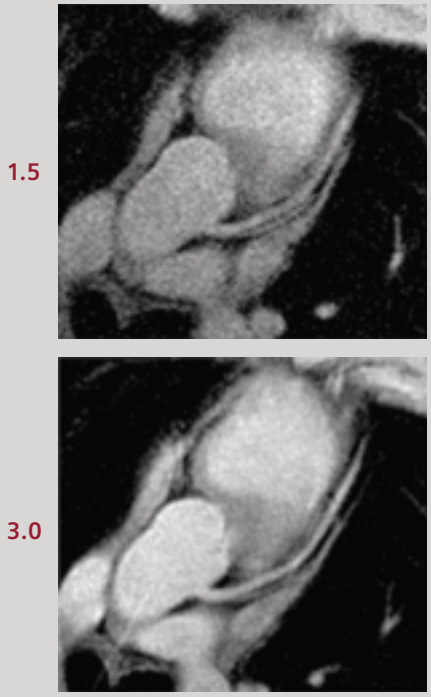

[Figure 1] *Exemplary images of the left anterior descending (LAD) coronary artery acquired from a healthy volunteer at 1.5 Tesla and 3.0 Tesla using FLASH and TrueFISP sequence, respectively. Note the SNR and vessel delineation are substantially improved at 3.0 Tesla using both sequences.*

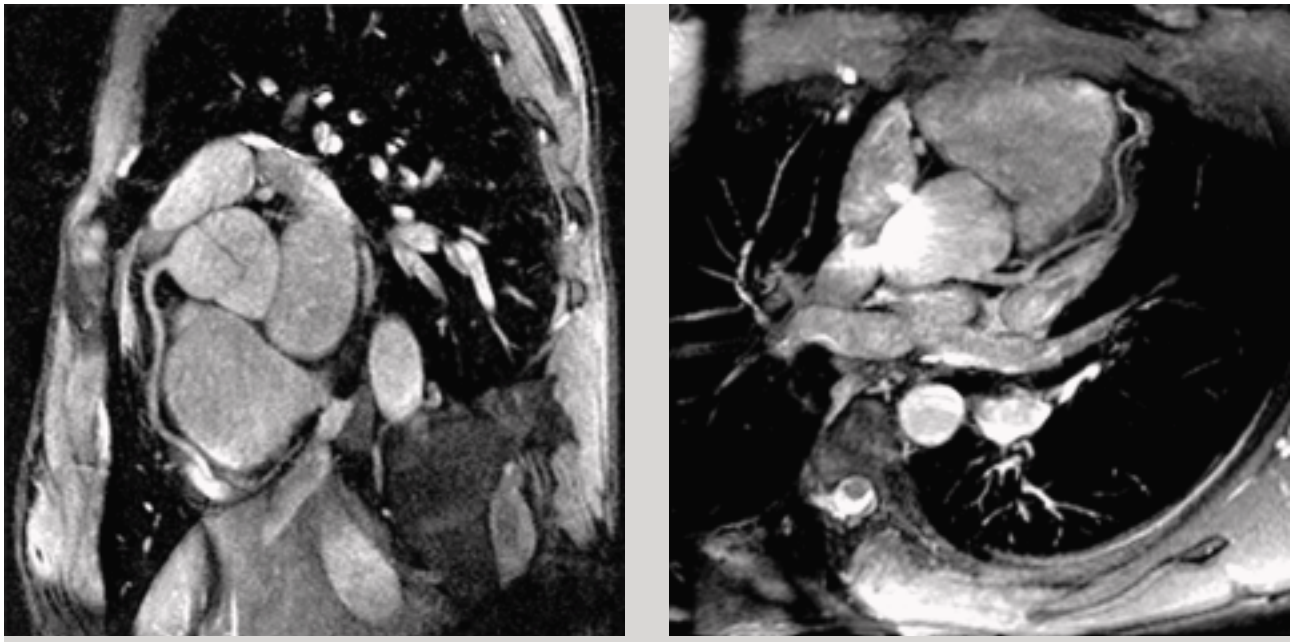

[Figure 2] *Example coronary artery images acquired at 3.0 Tesla using a TrueFISP sequence. Imaging parameters include: TR/TE = 3.2/1.3 msec; flip angle = 65°; spatial resolution 1.0 x 1.0 x 1.5 mm³. Data acquisition was gated by ECG and navigator-echo with slice following. The center frequency was shifted by 30 Hz in this case. Epicardial fat signal was suppressed by applying a spectral selective inversion pulse.*

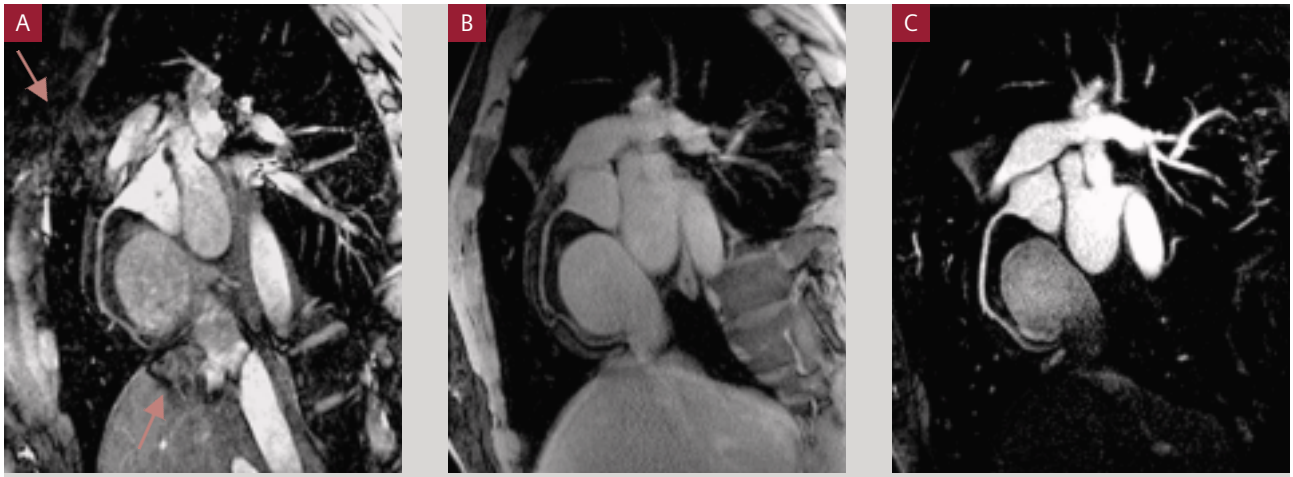

[Figure 3] *Maximum Intensity Projection (MIP) images of right coronary artery acquired from a healthy volunteer at 3.0 Tesla using TrueFISP (A), FLASH (B), and inversion recovery (IR) prepared FLASH sequence (C). Each 3D image set is acquired within a 24 heartbeat breath-hold. A: Note that high SNR is achieved using TrueFISP sequence. However, images were associated with off-resonance and flow artifacts as indicated by arrows. B: FLASH sequence yields artifact-free image with limited CNR. C: In combination with a T1-shortening contrast agent, IR-FLASH results in high SNR, CNR and good quality image. Background signal is well suppressed by applying a non-selective inversion pulse and the right coronary artery is sharply delineated.*

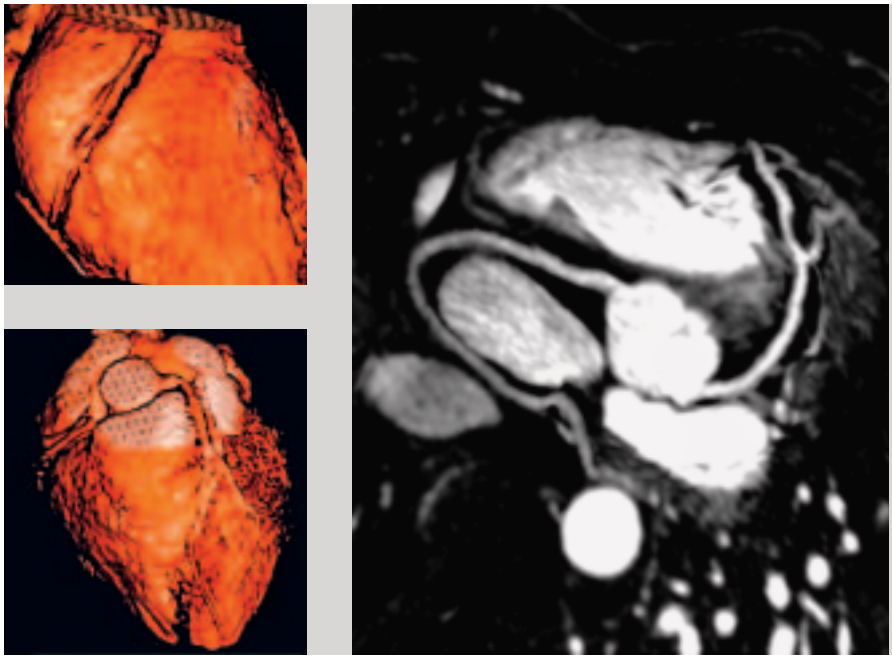

[Figure 4] *Whole-heart coronary MRA from a healthy volunteer at 3.0 Tesla with slow infusion of clinical contrast agent. Double dose of contrast agent was intravenously injected at a rate of 0.3 ml/sec. The total imaging time for collecting this data set was 5.5 minutes. Nearly isotropic spatial resolution was achieved: 0.65 x 0.70 x 0.75 mm³. A navigator-gated FLASH sequence was used for data acquisition with a non-selective inversion pulse for magnetization preparation (TI = 200 msec). Image acquisition was accelerated using PAT (GRAPPA) factor of 2 in the phase-encoding direction.*

accompanied by physical constraints, especially for balanced gradient-echo sequences such as TrueFISP, as the result of increased sensitivity to susceptibility changes, radio-frequency (RF) pulse distortion, dielectric resonance effects and eddy currents. The flip angle of the RF excitation pulses may also be limited as a consequence of limitations imposed by the SAR (Special Absorption Rate) monitor resulting in compromised image contrast which impacts on the theoretical gain in contrast-to-noise (CNR) at 3T.

TrueFISP imaging has gained great success in cardiac imaging at 1.5 Tesla due to its intrinsic high blood signal intensity and blood-myocardial contrast. The increased B1 field inhomogeneity, frequency offset from tissue susceptibility variation and energy deposition however, limit the consistency of TrueFISP in acquiring high quality coronary artery images at 3.0 Tesla. Images are sometimes contaminated by artifacts manifesting as dark "banding", ghosting of flow, or suboptimal fat saturation. Usually, adjusting the central frequency [3], applying localized shimming, maximizing the spectral width of the pass band by minimizing the repetition time (TR), and modifying the magnetization preparation [4] are helpful to alleviate such off-resonance imaging artifacts.

Compared to TrueFISP, spoiled gradient-echo sequences (e.g., FLASH) have better tolerance to the field inhomogeneity because phase errors are not accumulated from one RF cycle to another. SAR is no longer a major issue anymore due to the use of low flip angle RF pulses. A major drawback of using this approach for coronary MRA is that the blood-myocardial contrast is not as high. The combination of FLASH and a T1-shortening contrast agent has shown great potential at high field strength. Visualization of coronary arteries using this approach produces more consistently good image quality than the TrueFISP approach at 3T.

The elongation of myocardial T1 values warrants for a longer inversion recovery time than that at 1.5 Tesla for myocardium suppression, facilitating the recovery of blood longitudinal magnetization. However, because imaging data are typically acquired during the arterial phase of contrast agent, which is usually less than 30 seconds depending on the injection protocol, the resulting spatial resolution is low limited by the short available imaging time (e.g., a single breath-hold).

Recent developments in fast imaging techniques especially Parallel Imaging significantly increase the imaging speed. Whole-heart coronary MRA becomes feasible with reasonable imaging time [6]. Not only is the imaging procedure highly simplified compared to the conventional volume-targeted method, but the whole-heart data set provides greater flexibility in reformatting coronary artery images retrospectively in any desired orientation.

With improved SNR at 3.0 Tesla, it becomes possible to apply a lower dosage of contrast agent than that at 1.5 Tesla while still maintaining similar SNR level in contrast-enhanced coronary MRA. We have demonstrated the feasibility of high-resolution coronary MRA at 3.0 Tesla with a slow infusion of a clinical contrast agent. In combination with integrated Parallel Acquisition Techniques – or Parallel Imaging (iPAT), a whole-

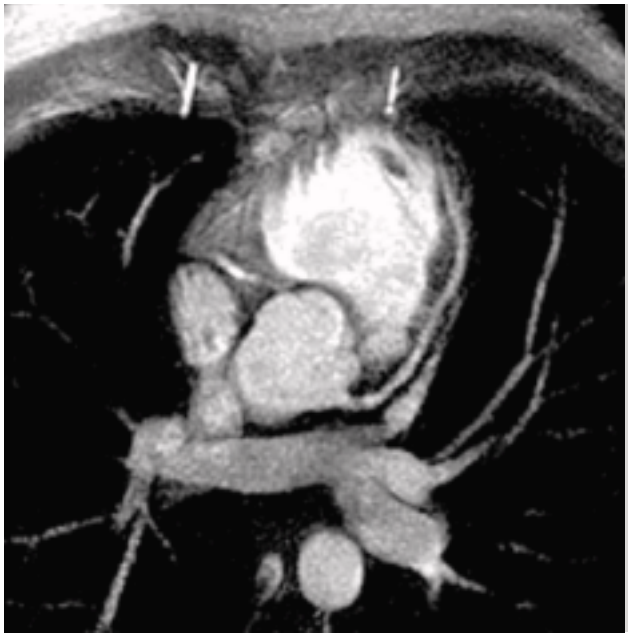

[Figure 5] *LAD coronary artery image acquired at 3.0 Tesla using cardiac phase-resolved 3D acquisition. The need for setting trigger delay time and data acquisition window is eliminated. Also, acquired 3D cine images offer great flexibility in post-processing. Images from multiple phases with minimal motion can be averaged to improve the SNR. Shown above is the averaged MIP image of three consecutive cardiac phases during mid-diastole. Image parameters included: TR/TE/flip angle = 4.6/2.3/22°; FOV = 200 mm; 22 cardiac phases; 6 acquired partitions interpolated to 12; spatial resolution 1.0 x 1.0 x 1.5 mm³; temporal resolution = 37 ms; radial acquisition in-plane and Fourier acquisition through-plane; SENSE reconstruction with sliding window factor of three.*

heart acquisition can be finished in about 5 minutes under free breathing using a navigator technique for respiratory motion compensation, assuming a 60 bpm heart rate and 50% navigator acceptance rate.

Cardiac motion has always been one of the major challenges for coronary MRA. To address this issue ECG gating is widely used to synchronize the data acquisition with the cardiac stasis. Typically a trigger delay time is added after detecting an R wave in the ECG signal. However, the optimal data acquisition window with reference to R-R interval varies from subject to subject. Even for the same subject, it varies with heart rate. A possible solution to this problem is to acquire cardiac phase-resolved coronary artery images which can potentially eliminate the need of predetermining the trigger delay time and data acquisition window. We have successfully implemented such cardiac motion-resolved 3D coronary MRA at 3.0 Tesla [5]. Background signals including myocardium and epicardial fat were suppressed by continuously applying RF pulses (22° to 30°) and spoilers. Blood signal intensity was maintained with intravenous administration of clinical contrast agent.

In summary, coronary MRA at 3.0 Tesla shows great promise using various techniques. The signal gain over 1.5 Tesla warrants further research to translate the SNR advantage of high field systems into a clear clinical benefit. These early studies demonstrate the possibility of exploiting the benefits of high field systems in coronary artery imaging by using alternative sequences and approaches to contrast optimization rather than simply replicating approaches used at 1.5T. Further technical developments are still required to take full advantage of 3.0 Tesla in coronary MRA.

*Works In Progress – The information about this product is preliminary. The product is under development. It is not commercially available in the US and its future availability cannot be assured.

References

[1] Lieberman JM, Botti RE, Nelson AD. Magnetic resonance imaging of the heart. Radiol Clin North Am 1984; 22: 847–858.

[2] Paulin S, von Schulthess GK, Fossel E, Krayenbuehl HP. MR imaging of the aortic root and proximal coronary arteries. AJR Am J Roentgenol 1987; 148: 665–670.

[3] Deshpande VS, Shea SM, Li D. Artifact reduction in true-FISP imaging of the coronary arteries by adjusting imaging frequency. Magn Reson Med 2003; 49: 803–809.

[4] Le Roux P. Simplified model and stabilization of SSFP sequences. J Magn Reson 2003; 163: 23–37.

[5] Bi X, Park J, Larson AC, Zhang Q, Simonetti O, Li D. Contrast-enhanced 4D radial coronary artery imaging at 3.0 T within a single breath-hold. Magn Reson Med 2005; 54: 470–475.

[6] Weber OM, Martin AJ, Higgins CB. Whole-heart steady-state free precession coronary artery magnetic resonance angiography. Magn Reson Med 2003; 50: 1223–1228.

Ultrafast Viability* Imaging in Less than 5 Minutes

James C. Carr M.D.

Northwestern University, Feinberg School of Medicine, Chicago, Illinois, USA

Introduction

Magnetic Resonance Imaging (MRI) is increasingly being recognized as the gold standard for assessing left ventricular myocardial viability [1, 2]. MRI has the advantage of being able to provide information about wall motion at the same time as demonstrating scar within the myocardium. The presence of scar occupying more than half of the wall thickness indicates lack of viability. This finding may determine whether a patient undergoes potentially risky surgical or endovascular intervention. Therefore, it is essential that any MRI protocol has sufficient spatial resolution so that transmural extent of enhancement can clearly be determined.

Conventional myocardial viability imaging protocols include segmented cine TrueFISP [3] and delayed enhanced inversion recovery (IR) TurboFLASH [4]. Viability studies using these techniques can last as long as 30-45 minutes and thus preclude the use of additional techniques such as coronary magnetic resonance angiography (MRA) or myocardial perfusion imaging, due to long overall imaging times. Rapid imaging techniques such as real-time cine TrueFISP [5] and single-shot inversion recovery TrueFISP [6, 7, 8] are now becoming more widely available. By using Parallel Imaging with these pulse sequences, it is possible to gain back some of the spatial and temporal resolution that had been sacrificed due to fast scan times. If these techniques could be used to accurately assess myocardial viability, exam times could be significantly reduced as a result of shorter acquisition times. Reducing the acquisition time would then allow use of other techniques simultaneously to study the coronary arteries and myocardial perfusion, without significantly lengthening the overall study time. Shorter scan times are also advantageous to achieve better patient compliance; avoid contrast change in the myocardium over time; and to shorten the examination time for a comprehensive examination of function, perfusion, and viability during one examination.

Our objective was to compare a new rapid viability imaging technique to the conventional viability protocol for assessment of myocardial viability.

Methods

All examinations were performed on a 1.5T Siemens MAGNETOM Avanto scanner. 22 patients, referred for assessment of left ventricular viability, underwent cardiac MRI

Table 1: Imaging parameters for the rapid viability technique.

	Real-Time Cine TrueFISP	Single-shot IR TrueFISP
TR/TE	2.6 / 1.0 msec	2.6 / 1.0 msec
Flip angle	65°	55°
Pixel size	3.5 x 1.9 mm^2	2.8 x 2.1 mm^2
Slice thickness	6 mm	6 mm
Frame time	60 msec	200 msec/slice
Parallel imaging	tSENSE x3	GRAPPA x2
Bandwidth	1300 Hz/px	1200 Hz/px

Table 2: Imaging parameters for the conventional viability technique.

	Segmented Cine TrueFISP	Segmented IR TurboFLASH
TR/TE	2.8 / 1.1 msec	8.0 / 4.0 msec
Flip angle	65°	30°
Pixel size	2.1 x 2.1 mm^2	2.8 x 2.1 mm^2
Slice thickness	6 mm	6 mm
Frame time	50 msec	8 – 10 sec/slice
Parallel Imaging	GRAPPA x2	None
Bandwidth	930 Hz/px	130 Hz/px

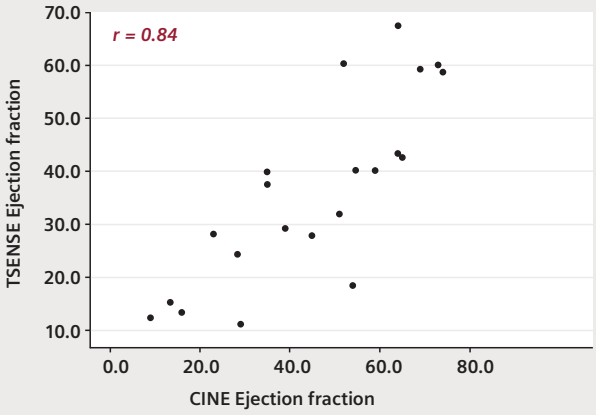

[Figure 1] *Quantitative analysis of ejection fraction between real time cine TrueFISP and segmented cine TrueFISP. Pearson's correlation (r) values are statistically significant at the 1% level.*

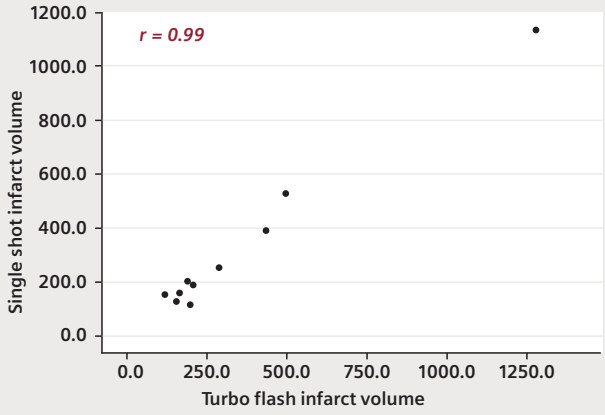

[Figure 2] *Quantitative analysis of infarct volume between single-shot IR TrueFISP and segmented IR TrueFISP with Pearson's correlation (r) values.*

using both the conventional viability imaging protocol and the rapid viability imaging protocol. Conventional viability imaging consisted of segmented cine TrueFISP and delayed enhanced IR TurboFLASH. Rapid viability imaging consisted of real-time cine TrueFISP with tSENSE and delayed enhanced single shot IR TrueFISP. The parameters for each of the pulse sequences are provided in tables 1 and 2.

The heart was imaged from base to apex in a short axis orientation. Segmented and real-time cine imaging were carried out first. CM was then injected intravenously via an 18G cannula placed in an antecubital vein. After a period of 10 minutes, segmented IR TurboFLASH and single shot IR TrueFISP imaging were carried out.

Ejection fraction was calculated from both the real-time and segmented cine techniques using the ARGUS (Siemens Medical Systems) post-processing tool. All images were randomized and assessed qualitatively for regional wall motion abnormalities. The presence or absence of enhancement and the transmural extent of enhancement was noted on both the segmented IR TurboFLASH and single shot IR TrueFISP. The infarct area was also measured quantitatively for both techniques.

Results

Total acquisition times were much shorter for real-time cine TrueFISP and single-shot IR TrueFISP (25 seconds and 58 seconds respectively) compared to conventional segmented cine TrueFISP and segmented IR TurboFLASH (4.49 minutes and 6.01 minutes respectively). There was excellent correlation between left ventricular ejection fraction calculated for both cine techniques (Fig. 1). Regional wall motion analysis also showed high correlation. All regions of enhancement detected using segmented IR TurboFLASH were also visualized using single-shot IR TrueFISP. Measurement of infarct area also showed high correlation for both techniques (Fig. 2).

Conclusion

The fast viability imaging protocol using real-time cine TrueFISP and single shot IR TrueFISP performs well compared to the conventional technique in a small group of patients. Total scan times for the rapid imaging approach are nearly 10 times faster. With faster imaging times, it is easier to more efficiently incorporate other techniques such as perfusion imaging or coronary MRA into a single study.

References

[1] Judd RM, Wagner A, Rehwald WG, Albert T, Kim RJ. Technology insight: assessment of myocardial viability by delayed-enhancement magnetic resonance imaging. Nat Clin Pract Cardiovasc Med. 2005 Mar; 2(3): 150–8. Review.

[2] Thomson LE, Kim RJ, Judd RM. Magnetic resonance imaging for the assessment of myocardial viability. J Magn Reson Imaging. 2004 Jun; 19(6): 771–88.

[3] James C. Carr, Orlando Simonetti, Jeff Bundy, Debiao Li, Scott Pereles, and J. Paul Finn. Cine MR Angiography of the Heart with Segmented True Fast Imaging with Steady-State Precession. Radiology 2001; 219: 828.

[4] Orlando P. Simonetti, Raymond J. Kim, David S. Fieno, Hanns B. Hillenbrand, Edwin Wu, Jeffrey M. Bundy, J. Paul Finn, and Robert M. Judd An Improved MR Imaging Technique for the Visualization of Myocardial Infarction. Radiology 2001; 218: 215.

[5] Zhang A, et al. ISMRM 2005.

[6] Carr JC, et al. ISMRM 2003.

[7] Li W, et al. J Magn Reson Imaging. 2004; 20: 327–30.

[8] Huber A, Schoenberg SO, Spannagl B, Rieber J, Erhard I, Klauss V, Reiser MF. Single-shot inversion recovery TrueFISP for assessment of myocardial infarction. AJR Am J Roentgenol. 2006 Mar; 186(3): 627–33.

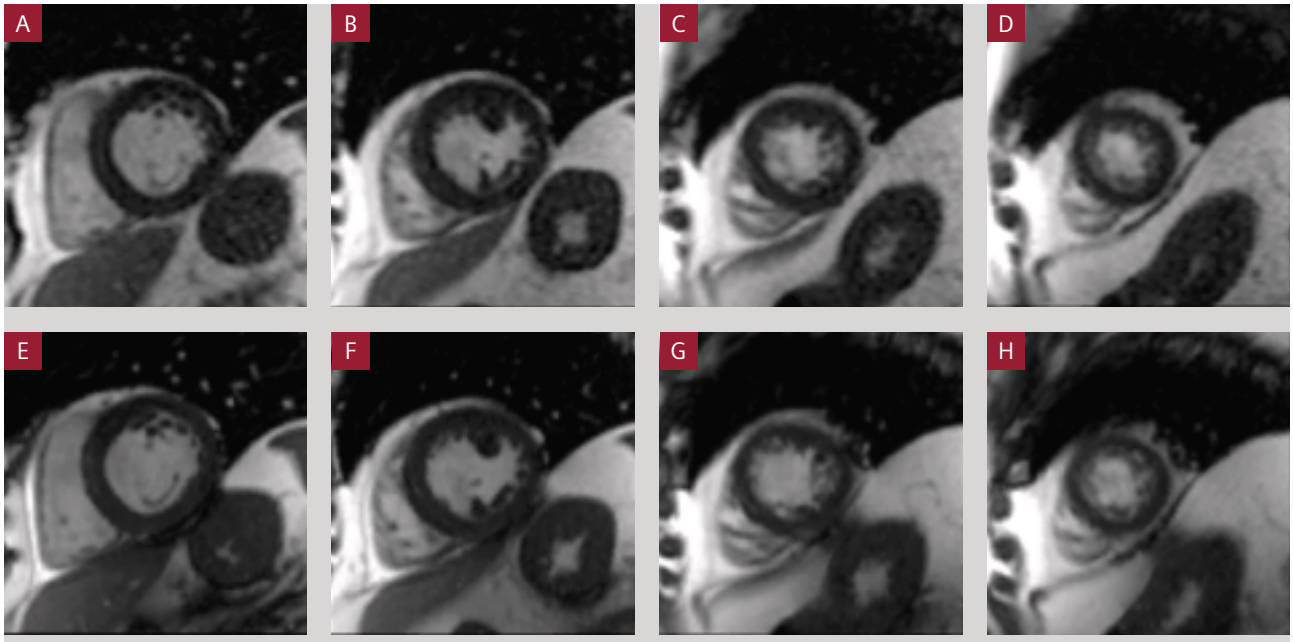

[Figure 3] *(A–D) Short axis real-time cine TrueFISP with tSENSE, acceleration factor of 3. (E–H) Short axis segmented cine TrueFISP with GRAPPA, acceleration factor of 2.*

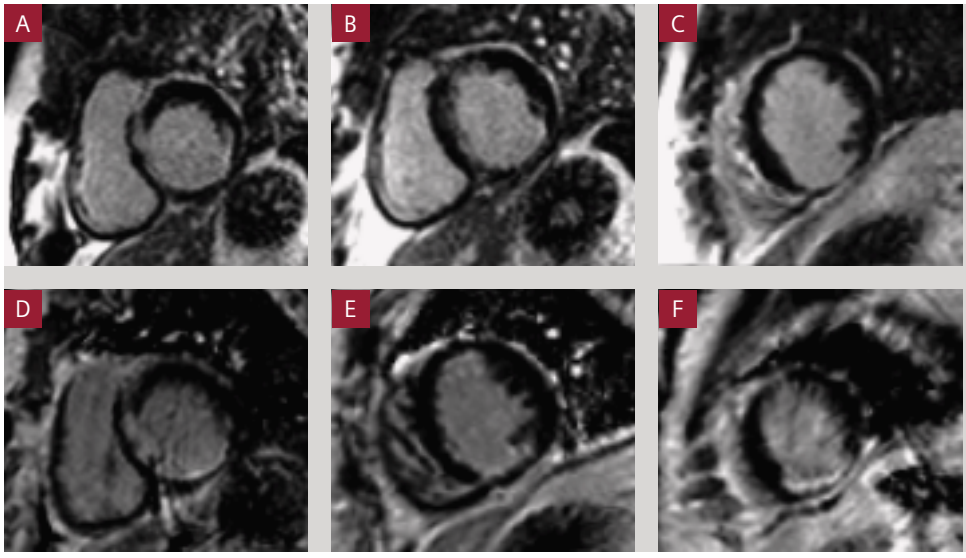

[Figure 4] *(A–C) Short axis single-shot IR TrueFISP with GRAPPA, acceleration factor of 2 and (D–F) short axis segmented IR Turbo-FLASH showing a subendocardial infarct in the inferior wall. The presence and transmural extent of the infarct is well seen with both techniques.*

*Works In Progress – The information about this product is preliminary. The product is under development. It is not commercially available in the US and its future availability cannot be assured.

syngo TWIST for Dynamic Time-Resolved MR Angiography

TWIST (**T**ime-resolved Angiography **Wi**th Interleaved **S**tochastic **T**rajectories)

Gerhard Laub, Ph.D.; Randall Kroeker, Ph.D.

Siemens Medical Solutions at University of California in Los Angeles, CA, USA

Introduction

Siemens, a leader in advanced engineering as well as applications development, has made 3D dynamic imaging available in the late 90s for the MAGNETOM Vision. The speed of dynamic imaging got an extra boost with the strong 40 mT/m gradients available with the MAGNETOM Sonata. Since then, dynamic imaging has gone through several changes and improvements, including the expansion of parallel imaging with the Tim (**T**otal **i**maging **m**atrix) technology, and more recently, the new k-space coverage now available with the *syngo* TWIST technique. *syngo* TWIST achieves significant improvements in temporal and spatial resolution and faster tracking of dynamic processes relative to the other versions of dynamic imaging introduced earlier.

syngo TWIST offers a practical, flexible, and elegant way to perform sub-second, time-sequential 3D measurements, both at 1.5T an 3T field strengths. This can be used in combination with contrast injection to provide dynamic clinical information, including the evaluation of abnormal vascular anatomy as well as vascular hemodynamics, and perfusion measurements. Common applications include examining a range of vascular pathologies as well as other dynamic processes such as vocal cord movement, speech formation/singing, swallowing, and other voluntary and involuntary movements in the body. In this paper we will present the underlying principles for *syngo* TWIST and we will present initial clinical applications related to dynamic, contrast-enhanced MR Angiography (MRA) as shown in Fig. 1. Following the intravenous injection of an MR contrast agent we will acquire a series of fast 3D imaging sequences. The necessary temporal resolution depends on the physiology of the contrast injection, and can be as fast as 1 second, or less, for intracranial structures, up to several seconds for slower processes in the peripheral vasculature.

syngo TWIST is available with software *syngo* MR B13 for all systems with Tim technology, and can be used in combination with an ultra-short TR supported by the gradient performance to achieve a high temporal resolution. *syngo* TWIST is fully compatible with parallel imaging (*syngo* GRAPPA or mSENSE) thus allowing subsecond 3D acquisitions with reasonable spatial resolution. The *syngo* TWIST acceleration can be up to 20 times compared to a standard, full k-space acquisition. Furthermore, *syngo* TWIST is compatible with the Inline angio card to allow fast processing similar to the standard angio sequences.

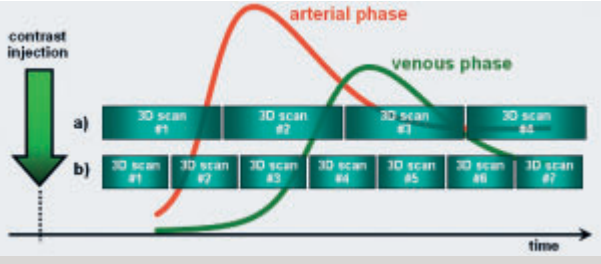

[Figure 1] *Basic idea of contrast-enhanced dynamic MRA. a) Conventional measurements with relatively poor temporal resolution. b) syngo TWIST reduces the time between subsequent 3D data sets to better distinguish between the arterial and venous phase.*

Methods

To shorten scan time in 3D imaging, one can use any or a combination of the following to achieve time-resolved dynamic imaging:

- Use a short TR
- Apply rectangular field-of-view (FoV)
- Use Partial Fourier
- Reduce spatial resolution
  - In-plane resolution
  - Slice resolution
- Use parallel imaging

To further increase the temporal resolution, one can manipulate the coverage of k-space during data acquisition. For

example, one does not have to cover k-space with a uniform rate at every point. This has been demonstrated many years ago in a MAGNETOM Vision system using a random phase encoding strategy where the low k-space lines are visited more frequently (CURE, MRM 33: 326-336, 1995). We have adopted this basic strategy in a straight forward fashion to a three-dimensional acquisition scheme.

In a first step, k-space is divided into two regions A and B as shown in Fig. 2.

Fig. 2 shows the data points in k-space divided into region A and B. A is the low frequency central region responsible for the overall image contrast. B is the higher frequencies outer k-space region responsible for image details. As is well-known, the number of k-space points depends on the spatial resolution and field-of-view (FOV) in the in-plane and through-plane phase encoding directions. A larger size of region "A" better defines the overall image contrast resolution, whereas a larger size of region "B" improves the spatial resolution in the image.

Region A contains a total number of $\mathbf{N}_A$ sampling points, and region B contains $\mathbf{N}_B$ sampling points. In the conventional scenario, all sampling points in A and B are sampled at a uniform rate as shown in Fig. 3.

In an effort to shorten the time between two subsequent A-regions the k-space points in the B-region are visited less frequently. This is indicated in Fig. 4 as shaded area in "B".

In Fig. 4, the time intervals between subsequent A regions are shorter than in the conventional approach, i.e., the apparent temporal resolution is increased. However, k-space is not completely scanned in one B interval. To fill in the missing points, data from several B intervals are copied into the raw data to calculate the 3D image data at time point t_i as shown in Fig. 6.

The remaining step in understanding *syngo* TWIST is to look at the k-space trajectory for regions A and B, respectively. In a first step, all sampling points that are to be measured will be sorted according to their radial distance in k-space, and the azimuthal angle (see Fig. 6).

The details of the *syngo* TWIST trajectory are shown in Fig. 7. The k-space trajectory in both region A and B is starting and ending at k_c. Specifically, the trajectory starts in region A at point 1 to take every other k-space point of the sorted k-space distribution until the center is reached at point 2. From here every other remaining k-space point is used outwards to point 3. In region B we use a bigger, variable stepping rate until point 3 is reached, and come back to the interface at point 4. Region A will be repeated similar to the first time (point 5 – 7) followed by region B with a different trajectory to fill the missing points of the first B trajectory. The key

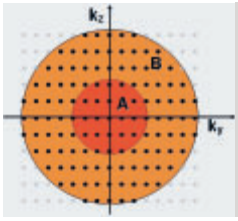

[Figure 2] *syngo TWIST uses regions A and B with different sampling properties to achieve faster update rates.*

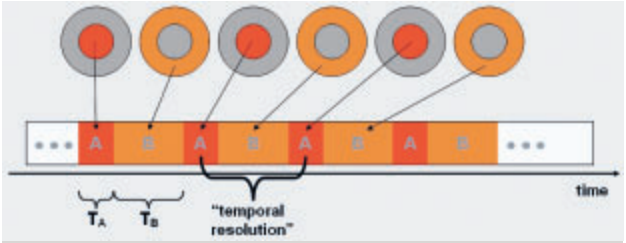

[Figure 3] *Full sampling of A and B, i.e. every point in k-space is sampled at the same rate. The temporal resolution depends on the total number of k-space points multiplied by TR.*

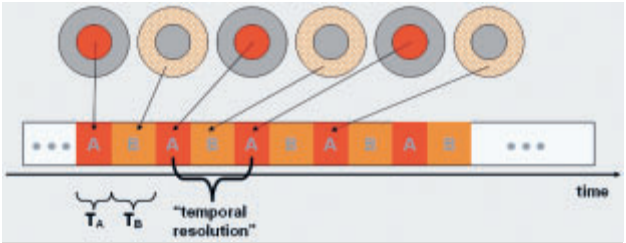

[Figure 4] *The temporal resolution is improved when k-space points in region B are visited less frequently than region A.*

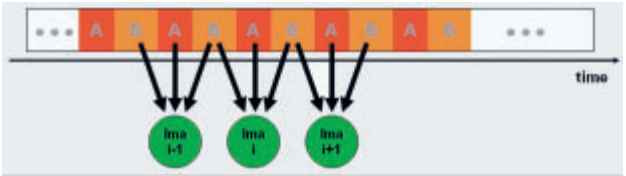

[Figure 5] *Data from several B intervals are copied into the raw data to calculate the three-dimensional image data at time interval t_i.*

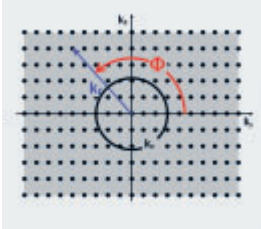

[Figure 6] *All k-space sampling points are sorted according to their radial distance in k-space and azimuthal angle relative to the in-plane phase encode axis.*

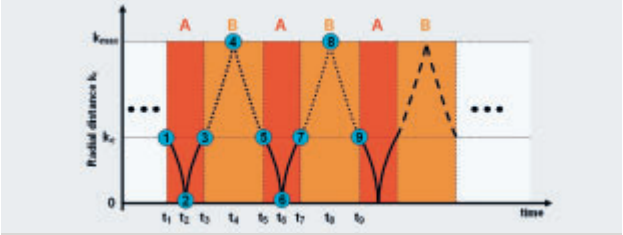

[Figure 7] *k-space trajectory for syngo TWIST.*

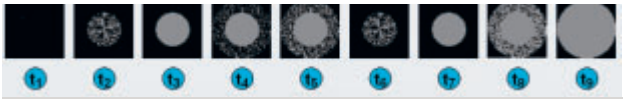

[Figure 8] *Snapshots of k-space filling at time points t_1 through t_9 from Fig. 7.*

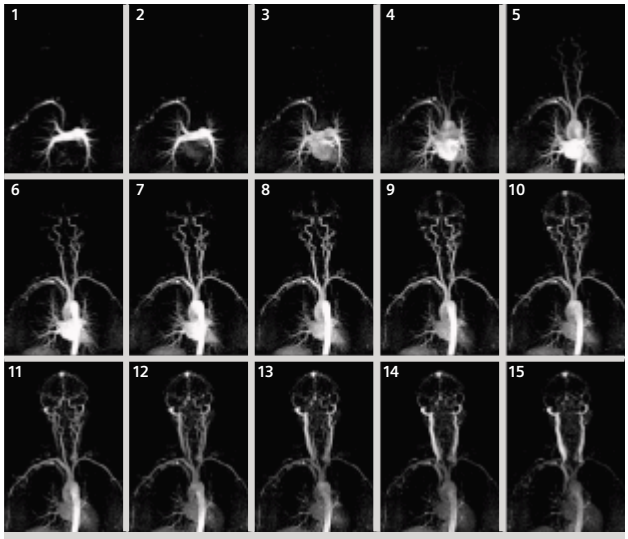

[Figure 9] *Time-resolved contrast-MRA study of the carotid artery in a normal volunteer. The syngo TWIST acceleration factor is 2.1 to provide a temporal resolution of 2 seconds.*

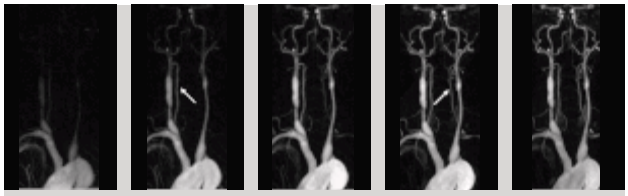

[Figure 10] *Time-resolved MRA using syngo TWIST in a patient with steal syndrome. Data are acquired on MAGNETOM Trio.*

Courtesy of Dr. J. Paul Finn, UCLA, Los Angeles, USA.

advantage of this technique is that a full range of k-space coverage from k=0 to k_{max} occurs for every repetition of the basic cycle. Thus, high-frequency information is updated at the same rate as the central region A.

To further illustrate the k-space sampling strategy of *syngo* TWIST, we take snapshots of k-space filling at the timepoints t_1 through t_9. These snapshots are shown in Fig. 8.

Overall, k-space is acquired in a random fashion even though there is a well-defined strategy behind every sampling point. This behavior explains the name of "stochastic trajectories" as part of the name of *syngo* TWIST (**T**ime-resolved Angiography **Wi**th **S**tochastic **T**rajectories).

Clinical Applications

There are many benefits of using dynamic *syngo* TWIST for clinical applications. These include:

- Better detection of vascular diseases such as in arteriovenous malformations (AVM) or shunts by providing the dynamic information.
- Better assessment of vascular diseases such as in peripheral obstructive artery disease (POAD) or steal phenomenon by visualizing the hemodynamics.
- Smaller amounts of contrast agent required for the contrast enhancement study.
- Complete elimination of venous contamination even in abnormal hemodynamic states.

Fig. 9 shows the series of maximum intensity projection (MIP) images of a normal volunteer. This data set was acquired on MAGNETOM Trio using a combination of the Head Matrix coil (12 elements), Neck Matrix coil (4 elements), and one row of the Body Matrix coil (3 elements), and the Spine Matrix coil (3 elements). The protocol uses a FoV of 500 mm with a readout matrix of 512, and a parallel acceleration factor of 3 to enable a spatial resolution of 1.2 mm x 1.0 mm x 4.0 mm. The *syngo* TWIST parameters are 30% for the size of region A, a 25% for the undersampling in B. Therefore, the *syngo* TWIST acceleration is 2.1, i.e. the *syngo* TWIST acquisition provides a 2.1-fold acceleration over a conventional acquisition using similar measurement parameters. Adding the values for parallel imaging and partial Fourier, the total acceleration corresponds to 9.8. In other words, the *syngo* TWIST acquisition is nearly 10 times faster than a standard, full k-space acquisition technique. This measurement is performed with a small amount of contrast agent, sufficient to create enough T1-shortening during the course of data acquisition. This is important for many clinical applications as it provides the visualization of the passage of a contrast bolus, and it also allows to repeat the measurement at several locations. Typically, the time-resolved MRA is fol-

lowed by a high-resolution scan. Due to the small amount of contrast agent necessary for the time-resolved MRA the high-resolution scan is not affected by the contrast which is already in the vascular system.

A clinical application of this technique is demonstrated in Fig. 10. The filling of the left vertebral artery is delayed (see arrow) due to a steal syndrome.

syngo TWIST can be applied in all vascular territories. Fig. 11 shows a series of MIPs in a patient with congenital vascular disease. The data were acquired on the MAGNETOM Avanto using two sets of Body Matrix coils, and the corresponding elements of the Spine Matrix coil. A total of 24 coil elements were used to acquire signal over a FoV of 500 mm with a parallel imaging factor of 2 in the left-right direction.

Finally, Fig. 12 shows the potential of *syngo* TWIST as a full 4-dimensional contrast-enhanced MRA technique. In this example we have used the following *syngo* TWIST parameters: size A = 15%, sampling rate B = 20%, providing a TWIST acceleration of 3.125, and a total acceleration of 14.6. The spatial resolution is 1.3 mm x 1.0 mm x 1.3 mm, and the time between individual 3 data sets is 2.5 seconds. In other words, the *syngo* TWIST measurement provided data that would otherwise take 36 seconds to acquire. Due to the short time between subsequent A regions only a small amount of contrast agent is necessary to provide a sufficiently large contrast bolus.

Summary

syngo TWIST is a versatile technique that can be adjusted to all imaging needs of time-resolved contrast-enhanced MRA. *syngo* TWIST is available o all MAGNETOM systems with Tim (Total imaging matrix) technology, and is a very powerful tool in the functional assessment of vascular disease.

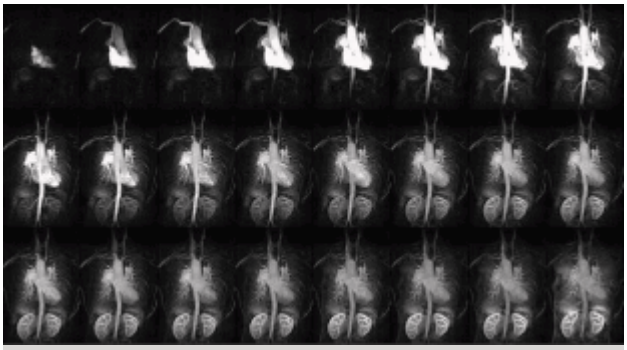

[Figure 11] *Time-resolved MRA using syngo TWIST in a patient with congenital vascular disease. Data are acquired on MAGNETOM Avanto.*
Courtesy of Dr. J. Paul Finn, UCLA, Los Angeles, USA.

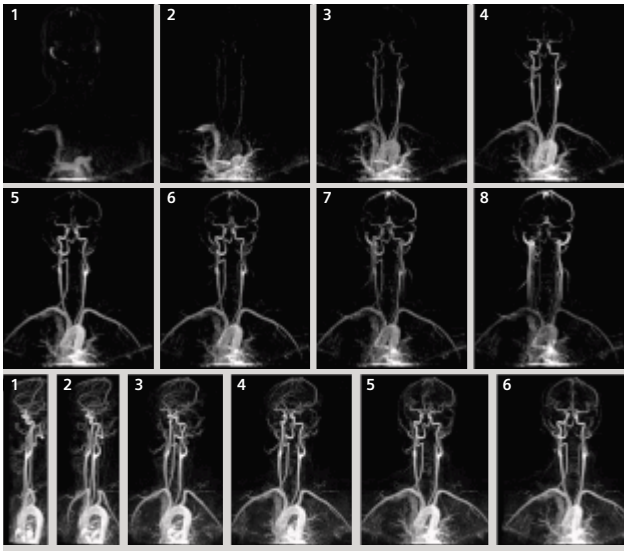

[Figure 12] *Top: Series of coronal MIPs in a 4D MRA study. Bottom: Series of MIPs at different projection angles of the arterial phase of the same 4 measurements.*

References

[1] Hennig J, Scheffler K, Laubenberger J, Strecker R. Time-resolved projection angiography after bolus injection of contrast agent. Magn Reson Med 1997; 37: 341–345.

[2] Finn JP, Baskaran V, Carr JC, et al. Thorax: low-dose contrast-enhanced three-dimensional MR angiography with subsecond temporal resolution: initial results. Radiology 2002; 224: 896–904.

[3] Korosec FR, Frayne R, Grist TM, Mistretta CA. Time-resolved contrast-enhanced 3D MR angiography. Magn Reson Med 1996; 36: 345–351.

[4] Riederer SJ, Bernstein MA, Breen JF, et al. Three-dimensional contrast-enhanced MR angiography with real-time fluoroscopic triggering: design specifications and technical reliability in 330 patient studies. Radiology 2000; 215: 584–593.

[5] Cashen TA, Carr JC, Shin W et al, Intracranial Time-Resolved Contrast-Enhanced MR Angiography at 3T. American Journal of Neuroradiology 2006; 27: 822–829.|

[6] Fink C, Puderbach M, Ley S, et al. Time-resolved echo-shared parallel MRA of the lung: observer preference study of image quality in comparison with non-echo-shared sequences. European Radiology 2005; 15(10) 2070–2074.

[7] Pinto C, Hickey R, et al. Time-resolved MR Angiography with Generalized Autocalibrating Partially Parallel Acquisition and Time-resolved Echo-sharing Angiographic Technique for Hemodialysis Arteriovenous Fistulas and Grafts. Journal of Vascular and Interventional Radiology2006; 17: 1003–1009.

We see a way to evaluate myocardial infarct and vascular disease within one exam without any patient repositioning

Tim won't let you miss a beat.

We see a way to determine regional ventricular function in real time allowing free-breathing using 12 matrix coil elements

Proven Outcomes in Cardiology with Tim® (Total imaging matrix technology).

Tim offers unmatched MRI capabilities for all cardiovascular exams without repositioning the patient. Ideal not only in diagnosing subendocardial infarct and congenital heart disease, but also systemic diseases like diabetes and atherosclerosis. With its 76 matrix coil elements and up to 32 RF channels, you enjoy revolutionary acquisition speed with virtually unlimited Parallel Imaging even in double oblique slice orientations. Tim transforms workflow from an exam limited by the dimensions of local RF-coils to one determined by the disease. Tim. Very heart smart.

www.siemens.com/Tim

SIEMENS
medical

MR-Z906-10-7600

Results may vary. Data on file.

Orthopedics

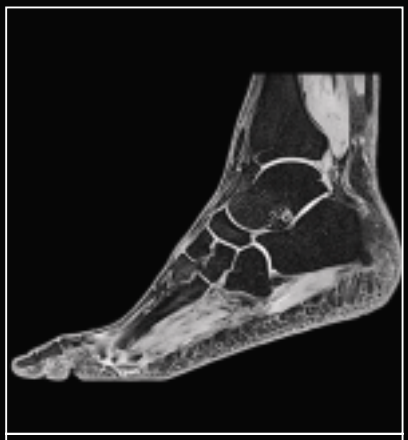

[1] ***MAGNETOM Avanto: Ankle, VIBE water exitation, sagittal, GRAPPA 2.***
TR 15.7 ms / TE 6.8 ms / eff. SL 1 mm / partitions 72 / matrix 576 / FoV 280 mm.

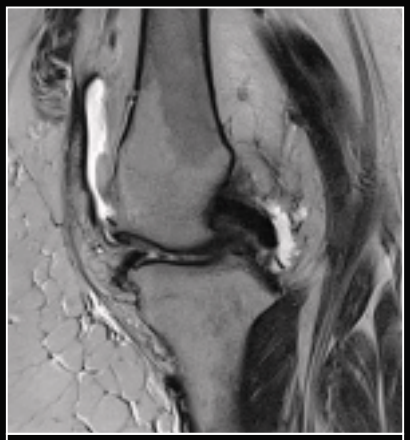

[2] ***MAGNETOM Espree: Knee, T2-weighted Turbo Spin Echo (TSE), GRAPPA 2, patient weighs 450 lbs, sagittal, meniscal tear.***
TR 4980 ms / TE 91 ms / SL 4 mm / slices 23 / matrix 256 / FoV 160 mm.
Courtesy of Cleveland Clinic Star Imaging, Columbus, Ohio, USA

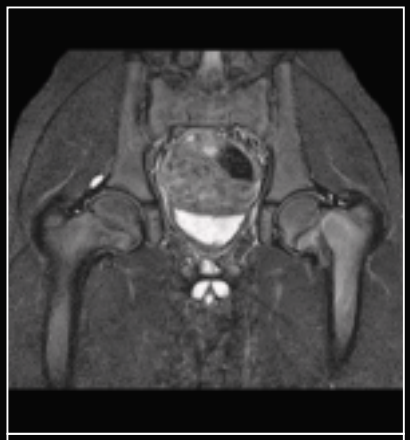

[3] ***MAGNETOM Espree: Hip, T2-weighted Turbo Inversion Recovery (TIR), 7-year-old male,*** *GRAPPA 2 / coronal / Morbus Perthes. / TR 5250 ms / TE 57 ms / TI 150 ms / SL 3.5 mm / slices 20 / FoV 280 mm.*
Courtesy of Alegent Gold Circle, Omaha, USA

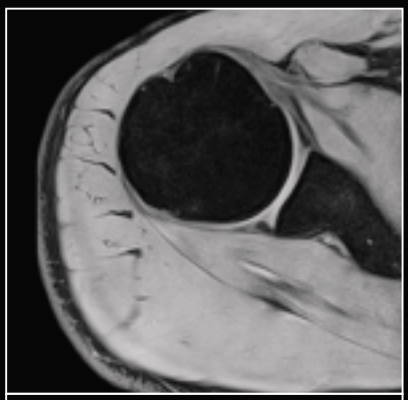

[4] ***MAGNETOM Trio: Shoulder, 3D MEDIC isotropic resolution, GRAPPA 2, transversal.***
TR 41 ms / TE 18 ms / eff. SL 1.5 mm / partitions 60 / matrix 320 / FoV 129 mm.
Courtesy of Chang Gung Memorial Hospital, Taiwan

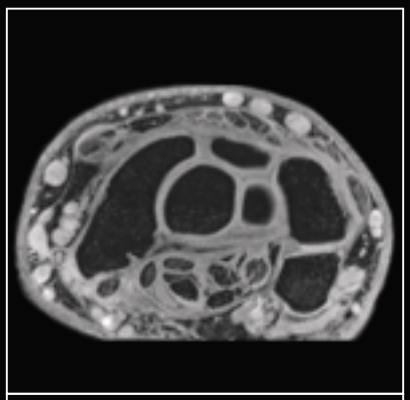

[5] ***MAGNETOM Trio: Wrist, T1-weighted VIBE 3D water excitation,*** *GRAPPA 2, multiplanar reconstruction (MPR) transversal, 8-channel wrist coil. TR 12 ms / TE 5.2 ms / eff. SL 0.3 mm / partitions 33 / matrix 320 / FoV 100 mm.*

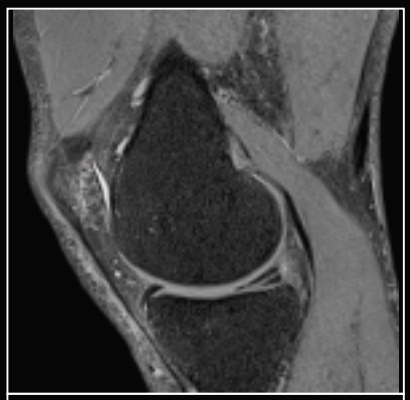

[6] ***MAGNETOM Avanto: Knee, proton density weighted SPACE, water excitation, sagittal, GRAPPA 2, meniscal tear.***
TR 1800 ms / TE 23 ms / eff. SL 0.6 mm / partitions 176 / matrix 256 / FoV 170 mm.
Courtesy of MRI Bremen Mitte, Bremen, Germany

MR Arthrography, a Minimally Invasive Diagnostic Intervention

Markus Braun, M.D.; Serban Mateiescu

Grönemeyer Institute of Microtherapy, Bochum, Germany

Introduction

An arthrography of the hip joint is a minimally invasive diagnostic intervention for patients with hip joint symptoms and the presumption of a labrum lesion. Under sonography, radiology or directly in the framework of the MRI, the hip joint is aspirated and diluted contrast medium (1:200) is injected intra-articularly thus enabling a better evaluation of the labrum. This diagnostic method has become an established element for the evaluation of the acetabular labrum.

Technique

The intervention is done in dorsal decubitus position. The flex-loop-large coil is positioned above the affected left hip and tightly fixed by belts on the patient table. A nitro capsule is stuck on to the patient's skin at the potential puncture spot of the needle. The nitro capsule shows a high signal in the MRI and serves as marker of orientation. The laser positioning line is placed on the nitro capsule respectively on to the thereby marked transversal slice. Subsequently, the patient is moved into the MR system.

Diagnostic imaging

For the anatomic representation, T2*-weighted gradient-echo-sequences are acquired in axial and sagittal slices – MEDIC (Multi Echo Data Image Combination), which show a high anatomic resolution. Due to the coil configuration (anterior: the flex-loop-large, and posterior: one to two elements of the spine-array), integrated Parallel Acquisition Techniques (iPAT, direction of the phase coding: anterior – posterior) can be used for the axial and sagittal measurements. This allows a high matrix (512) with relatively short acquisition time (about 2.5 minutes). Before and after the application of contrast agent, PD-weighted measurements are carried out in two spatial directions in order to guarantee a precise localization of the needle.

Planning and guidance of the arthrography

The nitro capsule is localized by quick measurements (Table 1, nos. 3, 4, 5, 6) and serves as reference point for the determination of the puncture point. Via the generated images (Fig. 1), the therapist defines the ideal access from the skin to

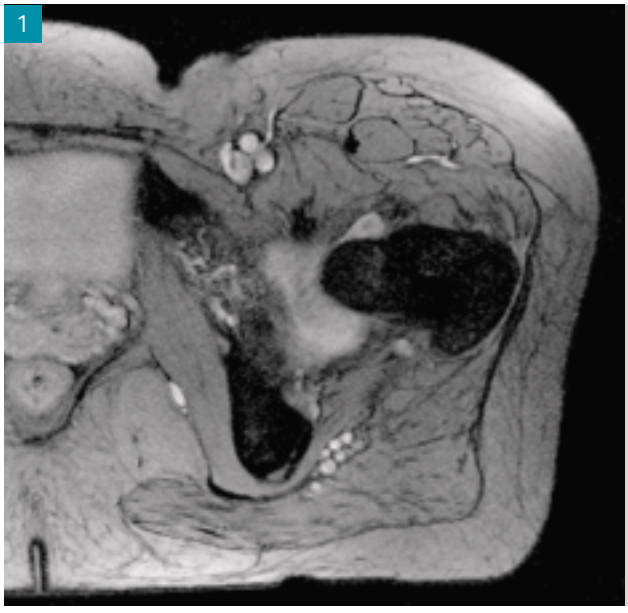

[Figure 1]
MEDIC axial.

[Figure 2]
MEDIC sagittal.

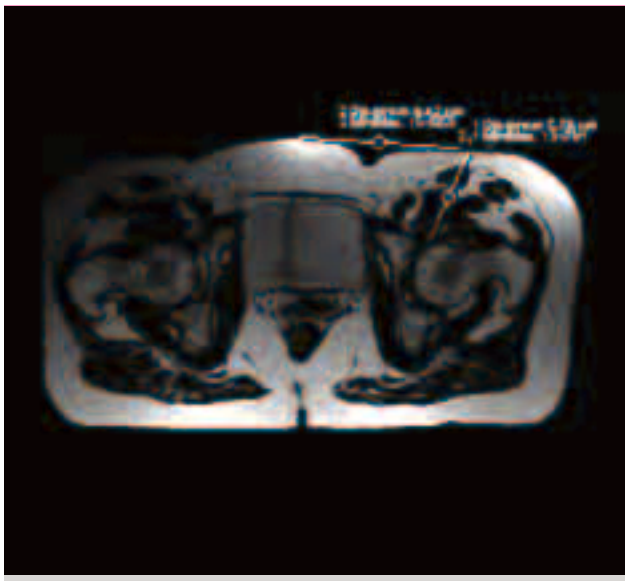

[Figure 3] *Planning of the intervention*

the joint (puncture and target point). The distance between the puncture point and the capsule on the skin surface in head-feet-direction is determined by the slice distances of the puncture slice (Fig. 3) and the slice with the nitro capsule. In right-left-direction the distance to the puncture point is measured from the patient centre (Fig. 3). Both distances allow the transfer of the puncture point to the patient's skin. An antero-lateral access under sterile conditions was found at the level of the transition from the femoral head to the femoral neck. A direct aspiration of the joint is done under local anesthesia without the risk of iatrogenic cartilage lesions of the femoral head by prick damages. The visualization and control of the determined access of the MRI-compatible needle made of titanium (in Vivo, formerly Daum, Schwerin) is done under local anesthesia and puncture via fast, HASTE, PD- and T2-weighted measurements (see Table 1, nos. 3, 4, 5, 6). If the needle is ideally positioned, it can be pushed forward to the hip joint under periarticular local anesthesia by Mepivacain 1%.

After the perforation of the joint capsule, the diluted gadolinum can be instilled into the recess. Afterwards, according to the prior MRI planning, images are acquired in the three standard orientations (sequences 1 and 2 from Table 1) for the evaluation of the glenoid labrum.

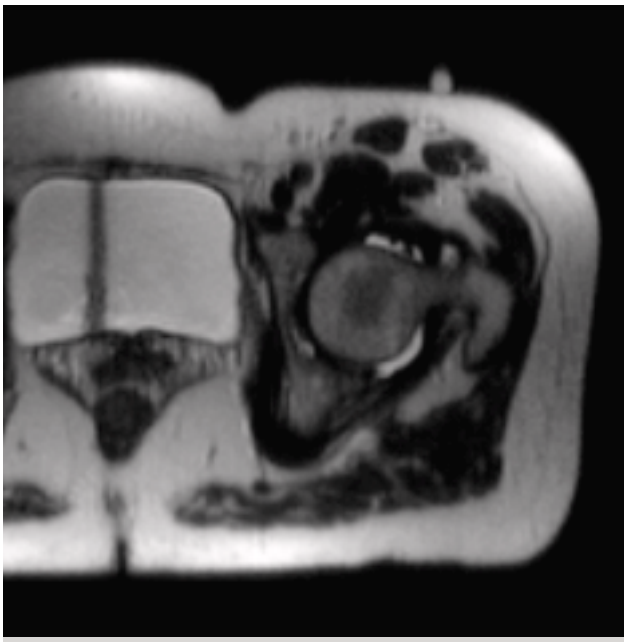

[Figure 4] *HASTE before administering fluid, already existing intraarticular effusion.*

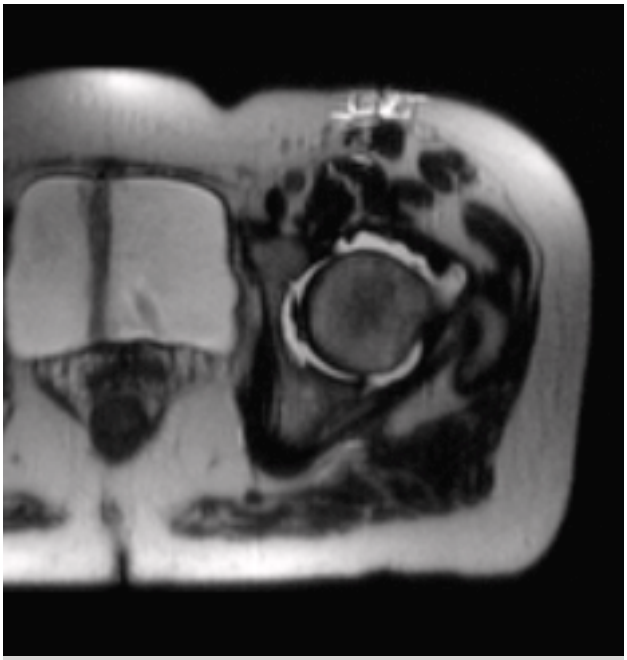

[Figure 5] *HASTE after the administration of fluid.*

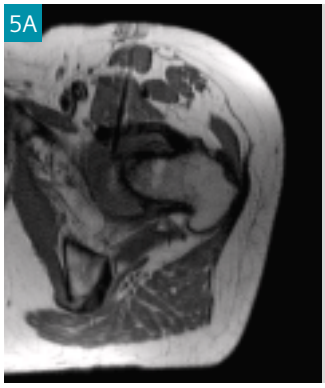

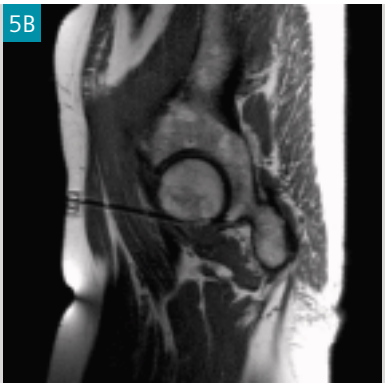

[Figure 5A] *PD-weighted axial image without contrast agent.*

[Figure 5B] *PD-weighted sagittal image without contrast agent.*

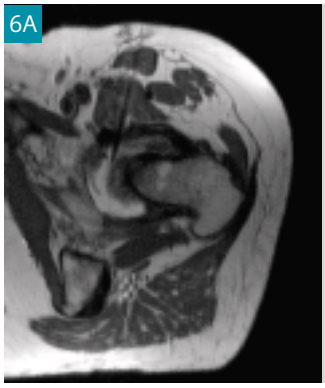

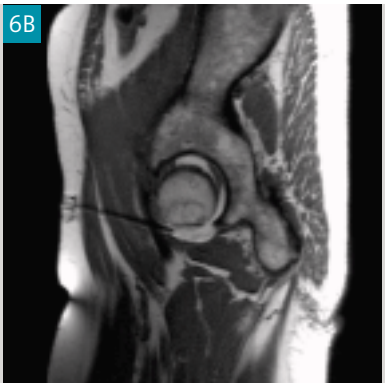

[Figure 6A] *PD-weighted axial image with contrast agent.*

[Figure 6B] *PD-weighted sagittal image with contrast agent.*

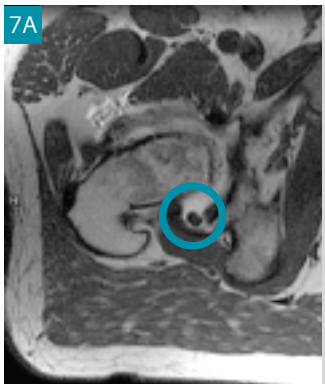

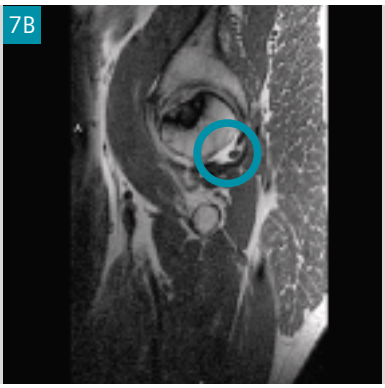

[Figure 7A] *T1-weighted axial. Proof of joint mice in the case of known dysplasia of the hip.*

[Figure 7B] *T1-weighted sagittal image.*

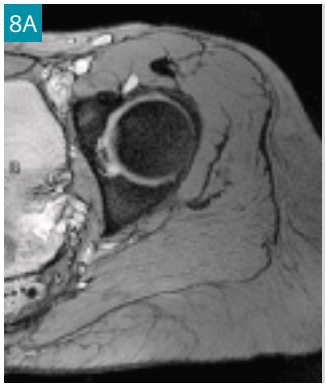

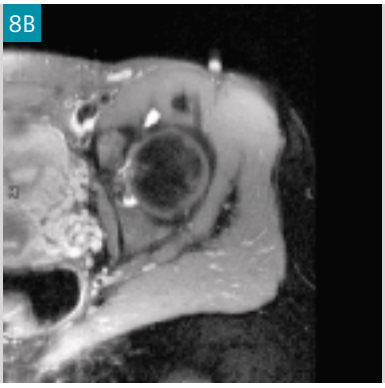

[Figure 8A] *MEDIC axial. Representation of paralabral cysts.*

[Figure 8B] *PD-weighted, fatsat, axial image.*

Table 1

	No.	TR/ms	TE/ms	Slices			FOV/mm	NEX	Flip angle	Matrix
				Number	thickness/mm	Dist. Factor/%				
T2-med-ax	1	700	27	15	3	30	219 x 350	1	40	320 x 512
T2-med-sag	2	780	27	19	3	30	238 x 380	1	40	480 x 768
PD-TSE-sag	3	1500	11	5	3	0	238 x 380	1	180	480 x 768
PD-TSE-ax	4	1870	11	5	3	0	219 x 350	1	180	480 x 768
HASTE-ax	5	1020	116	10	3	0	219 x 350	2	160	160 x 256
T2-TSE-ax	6	2500	122	10	3	20	213 x 350	1	150	156 x 256

	No.	Bandwith/Hz/Px	Turbo-factor	PAT			TA/min.
				PAT-Modus	Factor	Ref. lines	
T2-med-ax_pat	1	212	4 Echo	GRAPPA	2	50	2,3
T2-med-sag	2	213	4 Echo				2,1
PD-TSE-sag	3	170	17				0,4
PD-TSE-ax_pat	4	170	17	GRAPPA	2	120	0,4
HASTE-ax	5	227	160				0,2
T2-TSE-ax	6	199	29				0,3

Access: perforation of the hip joint capsule at the head-neck-transition (Figs. 5B, 6B). Dispersion of contrast medium in the joint cavity in the lower recess (Figs. 6A, 6B).

Fast measurements

The guiding of the needle from the puncture point to the hip joint and the control after administering the contrast medium is done via the above mentioned fast measurements (see Table 1, nos. 3, 4, 5, 6). There are high demands on the sequences:

1. For the planning of the therapy, good anatomic images are necessary.
2. In the sequences, the course and the tip of the needle have to be represented with a good contrast to the adjoining tissue in order to guarantee the precise positioning of the diluted contrast agent at the desired place.
3. The additional stress for the patient which is caused by a prolonged examination time has to be avoided. The longer the examination takes, the higher is the probability that the patient moves thus changing the positioning of the slices.

In order to answer these demands, different sequences are tested and they are modified and optimized according to the prerequisites. The HASTE-sequence (Half Fourier Acquired Single Shot Turbo Spin Echo) was used in order to see the fluid. The other anatomic structures are suppressed, in the images they appear dark and blurred.

Conclusion

The arthrography under MRI is a minimally invasive intervention for the diagnostic evaluation of the acetabular labrum of the hip joint. Furthermore, it is used for the evaluation of paralabral cysts, of joint mice and of an impingement of the ligament of the head of femur in the central fovea.

Scanner and software

The measurements were carried out on a 1.5 Tesla MAGNETOM Symphony system with Quantum gradient system (Siemens AG, Medical Solutions, Erlangen, Germany). The system is equipped with software version *syngo* MR 2004A.

Refurbished MRI Systems Now Available through the Proven Excellence Program

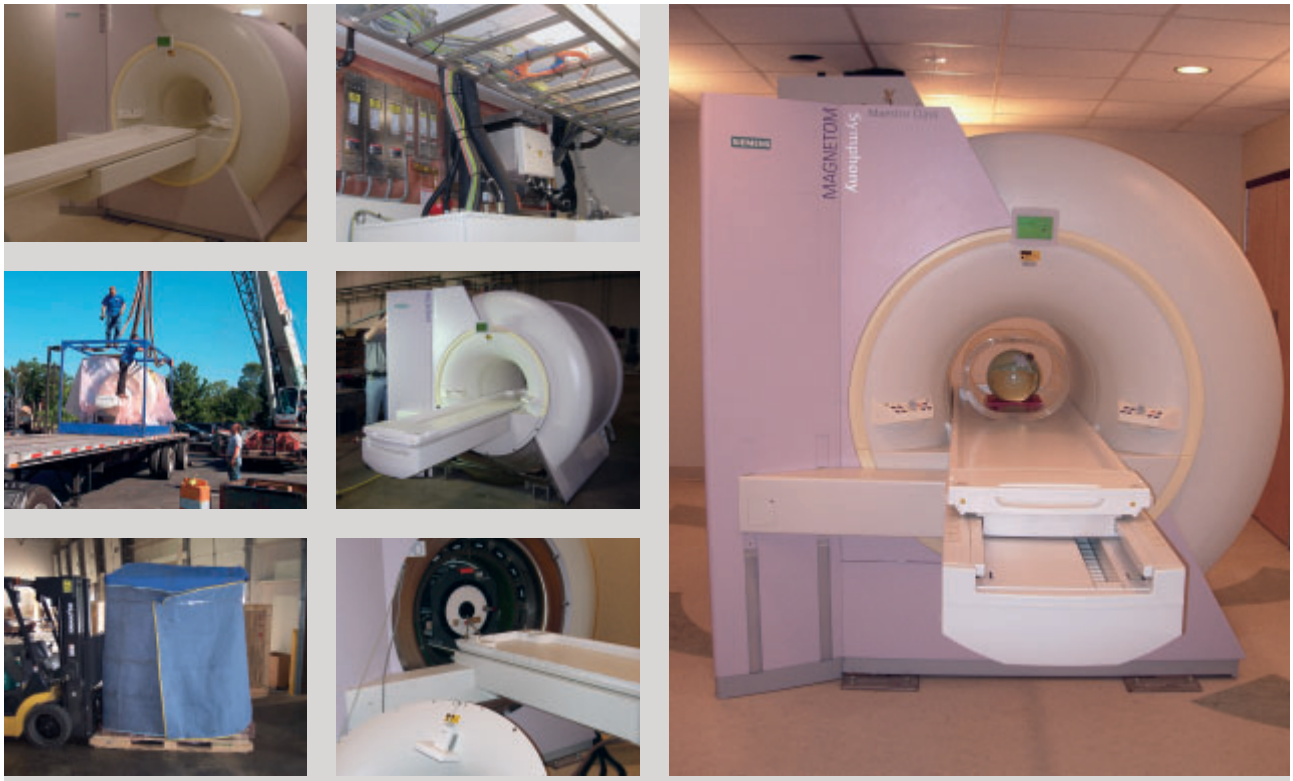

A MAGNETOM Symphony on its way through our refurbishing facility.

The Refurbished Systems division in the USA recently incorporated MRI into its Proven Excellence product portfolio. Proven Excellence (PE) is Siemens' multi-modality medical equipment refurbishment program. The MAGNETOM Symphony, Harmony, and Concerto are proven products from our MRI equipment portfolio that can meet your everyday clinical and technological demands. These systems are available at an affordable price point through our Proven Excellence Program.

The program starts with an initial inspection of each system, taking into consideration age, condition, service history, performance and upgradeability of software and hardware. After a professional de-installation and transportation to our Siemens Refurbished Systems facility, the system is thoroughly cleaned, disinfected and painted, worn parts are replaced with original spare parts and applicable software updates are performed. After passing a complete system check with original test equipment and procedures, the system is rewarded with our Proven Excellence quality seal. This seal represents the fulfillment of the strict specifications of relevant international norms and standards as well as security regulations.

After transportation to the customer site, the system is installed by our Siemens installation and service team of trained technicians.

With the Proven Excellence Program, Siemens Medical Solutions also offers its customers various flexible financing solutions and service contracts as well as a warranty typically equivalent to that of new systems. Moreover, spare parts are generally available for 5 years.

Fore more information please contact your local Siemens representative.

Experience *syngo* TimCT

Don’t miss the MAGNETOM Flash special issue on *syngo* TimCT. See the first clinical results from the Universities of Freiburg and Essen. Check out how the table moves during the measurement on the *syngo* TimCT mini CD.

TimCT Sonderheft:
A91MR-1000-17C-7600

Mini-CD: A91MR-1000-18E-7600

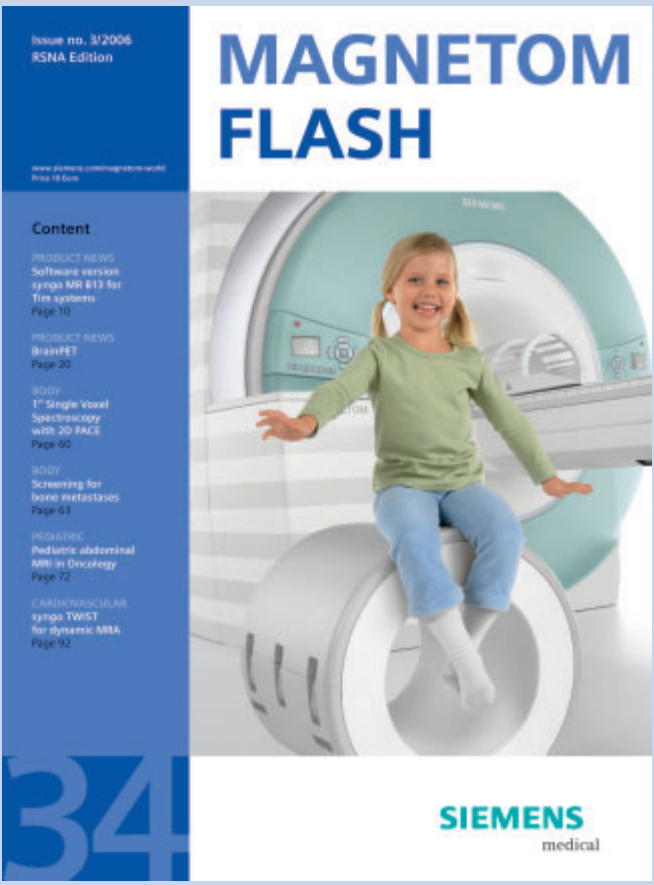

MAGNETOM FLASH offers product news, clinical methods, application tips, MR technology and information on Life.

MAGNETOM FLASH

Institution

Title

Name*

Street/P.O. Box*

Zip/Postal Code*

City*

State/Province*

Country*

E-mail

Please print clearly!

☐ Yes, I consent to the above information being used for future contact regarding product updates and other important news from Siemens MR.

Siemens AG
Medical Solutions
Magnetic Resonance
Marketing
P.O. Box 3260

D-91050 Erlangen
Germany

SUBSCRIBE NOW!

– and get your free copy of future MAGNETOM Flash! Interesting information from the world of magnetic resonance – gratis to your desk. Send us this postcard, or subscribe online at www.siemens.com/MAGNETOM-World

The information in this document contains general descriptions of the technical options available, which do not always have to be present in individual cases.

The required features should therefore be specified in each individual case at the time of closing the contract.

Siemens reserves the right to modify the design and specifications contained herein without prior notice. Please contact your local Siemens sales representative for the most current information.

Original images always lose a certain amount of detail when reproduced.

This brochure refers to both standard and optional features. Availability and packaging of options varies by country and is subject to change without notice. Some of the features described are not available for commercial distribution in the US.

Siemens AG
Wittelsbacherplatz 2
D-80333 Muenchen
Germany

Headquarters
Siemens AG, Medical Solutions
Henkestr. 127, D-91052 Erlangen
Germany
Telephone: +49 9131 84-0
www.siemens.com/medical

Contact Addresses

In the USA
Siemens Medical Solutions USA, Inc.
51 Valley Stream Parkway
Malvern, PA 19355
Telephone: +1 888-826-9702
Telephone: +1 610-448-4500
Telefax: +1 610-448-2254

In Japan
Siemens-Asahi
Medical Technologies Ltd.
Takanawa Park Tower 14F
20-14, Higashi-Gotanda 3-chome
Shinagawa-ku
Tokyo 141-8644
Telephone: +81 3 5423 8411

In Asia
Siemens Medical Solutions
Asia Pacific Headquarters
The Siemens Center
60 MacPherson Road
Singapore 348615
Telephone: +65 6490-6000
Telefax: +65 6490-6001

In Germany
Siemens AG, Medical Solutions
Magnetic Resonance
Henkestr. 127, D-91052 Erlangen
Germany
Telephone: +49 9131 84-0

Siemens **Medical Solutions** that help

Order No. A91MR-1000-16M-7600
Printed in Germany
CC MR 66214 WS 120620.